University of Leicester

Pharmacological Characterisation of Recombinant Nociceptin Receptors

Timothy Andrew Barnes B.Sc. M.Sc.

University Department of Cardiovascular Sciences
(Pharmacology and Therapeutics Group)
University of Leicester

Thesis Submitted for the Degree of Doctor of Philosophy
February 2005

ProQuest LLC
789 East Eisenhower Parkway
P.O. Box 1346
Ann Arbor, MI 48106-1346

Pharmacological Characterisation of Recombinant Nociceptin Receptors

Timothy Andrew Barnes

The heptadecapeptide Nociceptin/OrphaninFQ (N/OFQ) is the endogenous ligand for the G-protein coupled receptor, NOP, activation of which is involved in a plethora of physiological functions, including pain. Studies in man are hampered by a relative lack of suitable, well characterised ligands, especially antagonists and an understanding of the effects of prolonged receptor activation.

The N/OFQ sequence can be divided into a message domain, associated with receptor activation and an address domain, associated with receptor binding. In a series of biochemical assays, using Chinese Hamster Ovary (CHO) cells stably expressing human NOP, a number of ligands suitable for *in vivo* animal testing were characterised including a high affinity, high potency agonist ([(*p*F)Phe^4,Arg^{14},Lys^{15}]N/OFQ-NH_2), a high affinity antagonist ([Nphe^1,Arg^{14},Lys^{15}]N/OFQ-NH_2 or UFP-101) and several partial agonist molecules.

In a CHO cell line expressing NOP at a range of levels via the ecdysone inducible expression system, the behaviour of the partial agonist [F/G]N/OFQ(1-13)-NH_2 could be modulated to encompass full agonism and antagonism, using the previous assays, underscoring the need to assess activity in a range of models and steps in the signal transduction cascade.

Receptor desensitisation, by prolonged exposure of the inducible cells to N/OFQ, led to a decrease in NOP density, a reduction in N/OFQ stimulated GTPγ[^{35}S] binding with a reduction in functional potency and a reduction in potency of cAMP inhibition. More interestingly, a reduction in NOP mRNA was also observed.

Collectively this thesis has made a significant contribution to the N/OFQ-NOP field in that:

(1) several novel molecules have been characterised and are now available to other researchers;

(2) a system in which pharmacological behaviour can be accurately defined has been characterised;

(3) the first example of genomic desensitisation of NOP has been described.

The N/OFQ-NOP system is ready to leave the pre-clinical laboratory and full clinical evaluation is eagerly awaited.

For all the Firstborn

Every journey starts with a single step –

as long as you take that step!

Acknowledgements

As with most projects of this nature, this thing is more than the work and effort of one.

So, I commence by giving my thanks to Dave Lambert, without whom it wouldn't have happened this way anyway. Also to Prof. Rowbotham for enabling it to happen.

Next, the team at Leicester who have collaborated, put up with, helped, cajoled, sworn at and been there for me and supplied lots of times:
Christine, Ed, Jim, John 1, John 2, Kat, Lynn, M, Paul, 'Prof.' Hebbes, Wei and all the rest (apologies to any not singled out). Grateful thanks to Tiago Duarte for PCR advice.
A special thank you goes to Miss Trish – for putting up with me, more than just part of the team!

I should also like to extend my gratitude to Giro and all at Ferrara, as without them it would all be much less! Jack, don't forget – scienza è ..... fffffantastic!
Thanks also to the Japanese contingent – especially Masato, Hiro and Eiji (good sake!).

Family and friends always deserve a special mention and no exception in this case, so thanks Mum and Dad, Bruv & co, Sis & co, plus Gee and Stu (for sanity), Grm'n'Mand, Pat, Sylv & co and Dry'n'Jo.
Plus the football and social crowd here – long live international relations!

Others who contributed on the way –
Sue Pavord, who helped me back onto the path; all at the Dept. of Applied Biology and Biotechnology at DeMontfort Uni/Leicester Poly and TMB Etten-Leur; Colin Goodman, Mr. Holmes (who kind of knew) and Jeff Spencer ("he's finally where he should be") plus all the others I may have left out, however unintentionally, thanks.

Lastly, but not least, to Nicky, who's had a lot to cope with these couple of years.

CONTENTS

I List of Abbreviations

III-BTD – Ac-Arg-D-cyclohexyl-Ala-(3S,6S,9R)-2-Oxo-3-amino-7-thia-1-aza-bicyclo[4.3.0]nonane-9-carboxylic acid-D-Arg-*p*Chloro-D-Phe-NH_2
5-HT – 5-Hydroxy Tryptamine (Serotonin)
AC – Adenylyl Cyclase
ADP – Adenosine Diphosphate
ANOVA – Analysis of Variance
ATP – Adenosine Triphosphate
Bq – Becquerel (= 1 disintegration.s^{-1})
BSA – Bovine Serum Albumin
cAMP – Cyclic Adenosine Monophosphate
cGMP – Cyclic Guanosine Monophosphate
CHO – Chinese Hamster Ovary
Ci – Curie (= 3.7 x 10^{10} Bq)
CNS – Central Nervous System
CRE – cAMP Response Element
CREB – cAMP Response Element Binding Protein
CTx – Cholera Toxin (from *Vibrio cholerae*)
D_a – Dynorphin A
Da/kDa – Dalton/kiloDalton
DAMGO – [Tyr^1-D-Ala^2-Gly^3-N-methyl-Phe^4-Gly^5-ol]-enkephalin
D-MEM – Dulbecco's Modified Eagle Medium
DOP – Delta Opioid Receptor
DPDPE – [Tyr^1-D-Pen^2-Gly^3-Phe^4-D-Pen^5]-enkephalin
dpm – Disintegrations Per Minute
DPN - Diprenorphine
DTT - Dithiothreitol
EDTA – Ethylenediaminetetraacetic acid
EGTA – Ethyleneglycol-bis(2-aminoethylether)-N,N,N',N'-tetraacetic Acid
FBS – Foetal Bovine Serum
GABA – γ-aminobutyric Acid
GAPDH – Glyceraldehyde 3-Phosphate Dehydrogenase
GDP – Guanosine Diphosphate
GPCR – G-protein Coupled Receptor
G-protein – Guanine Nucleotide Binding Protein
GRK – G-protein Receptor Kinase
GTP – Guanosine Triphosphate
GTPγS - Guanosine 5'[γ-thio]trisphosphate
HEPES – N-(2-Hydroxyethyl)piperazine-N'-(2-ethanesulphonic acid)
IASP – International Association for the Study of Pain
IBMX – 3-Isobutyl-1-methylxanthine
IUPHAR – International Union of Pharmacology
J113397 (CompB) – 1-[(3R,4R)-1-cyclooctylmethyl-3-hydroxymethyl-4-piperidyl]-3-ethyl-1,3-dihydro-2H-benzimidazol-2-one
JTC-801 – [N-(4-amino-2-methylquinolin-6-yl)-2-(4-ethylphenoxymethyl) benzamide monohydrochloride]
KOP – Kappa Opioid Receptor
Leu-Enk – Leucyl Enkephalin
MEM – Minimal Essential Medium

Met-Enk – Methionyl/Met-enkephalin
MOP – Mu Opioid Receptor
N/OFQ – Nociceptin/OrphaninFQ
NalBzOH – Naloxone Benzoylhydrazone
NOP – Nociceptin Receptor
NRM – Nucleus Raphe Magna
NRPG – Nucleus Reticularis Paragigantocellularis
NSB – Non-Specific Binding
Nst – Nocistatin
PAG – Periaqueductal Grey (matter)
PBS – Phosphate Buffer, Saline
PEI – Polyethylenimine
PKA – Protein Kinase A
PKC – Protein Kinase C
PLC – Phospholipase C
ppN/OFQ – preproNociceptin/OrphaninFQ
PTx – Pertussis Toxin (from *Bordetella pertussis*)
RGS – Regulatory G-protein Signalling Protein
Ro64-6198 – (1*S*,3a*S*)-8-(2,3,3a,4,5,6-hexahydro-1*H*-phenalen-1yl)-1-phenyl-1,3,8-triaza-spiro[4.5]decan-4-one (Roche NOP agonist)
SA – Specific Activity
S.e.mean – Standard Error of the Mean
SG – Substantia Gelatinosa
SP – Substance P
Tris-HCl – Tris(hydroxymethyl)aminomethane Hydrochloride

II List of Figures

III List of Tables

1 General Introduction

1.1 Signalling in Higher Organisms

Transmission of signals between cells and organs in higher organisms may be achieved through chemical signals (hormones) in the vascular system or via electrochemical impulses. This latter type of signal is conducted in specialised cells called nerve cells or neurones. There are many such cells, forming a complex network from the periphery to the centre of the body, involved in both sensation and response. The central nervous system (CNS), comprising the brain and spinal cord, forms the regulatory core of neurones through which all impulses are routed.

1.2 Neuronal Structure

A typical nerve cell consists of the cell body (soma) containing the nucleus, organelles and most of the mitochondria, and elongated protrusions of the cytoplasm. These latter may be multiple, highly branched dendrites, responsible for bringing nerve impulses into the cell, or an axon, which is usually singular, unbranched, and conducts the resultant signal away from the soma to other sites which may be further neurones, muscle cells or other tissue. The axon of a cell may merely comprise the cell membrane or be sheathed in myelin-rich Schwann cells (Despopoulos *et al.*, 1986). The typical structure of a neurone is shown in Figure 1.1.

Within this loose description, neurones are further classified according to morphology and function. Under morphological classification, a neurone with several dendrites and one axon is termed multipolar, which is typical of those in the central nervous system (CNS), comprising the brain and spinal cord. Those with a single dendrite and one axon are bipolar neurones, commonly found in the eye, ear and nose. Unipolar neurones are those which have only one outgrowth, functioning as both axon and dendrite, in separate branches, these are located in the sensory ganglia (Tortora *et al.*, 1990).

Functionally, neurones are classified as either afferent, conveying sensory information to the CNS from the periphery, or efferent, transmitting instructions from the CNS to motor or effector cells. Within the CNS are interneurones, connecting the sensory input to effector output (Tortora *et al.*, 1990). At the junction of an axon with its destination is the synapse (forming the target site for most pharmacologically active compounds). A typical synapse is depicted in Figure 1.2.

SPECIAL NOTE

ITEM SCANNED AS SUPPLIED
PAGINATION IS AS SEEN

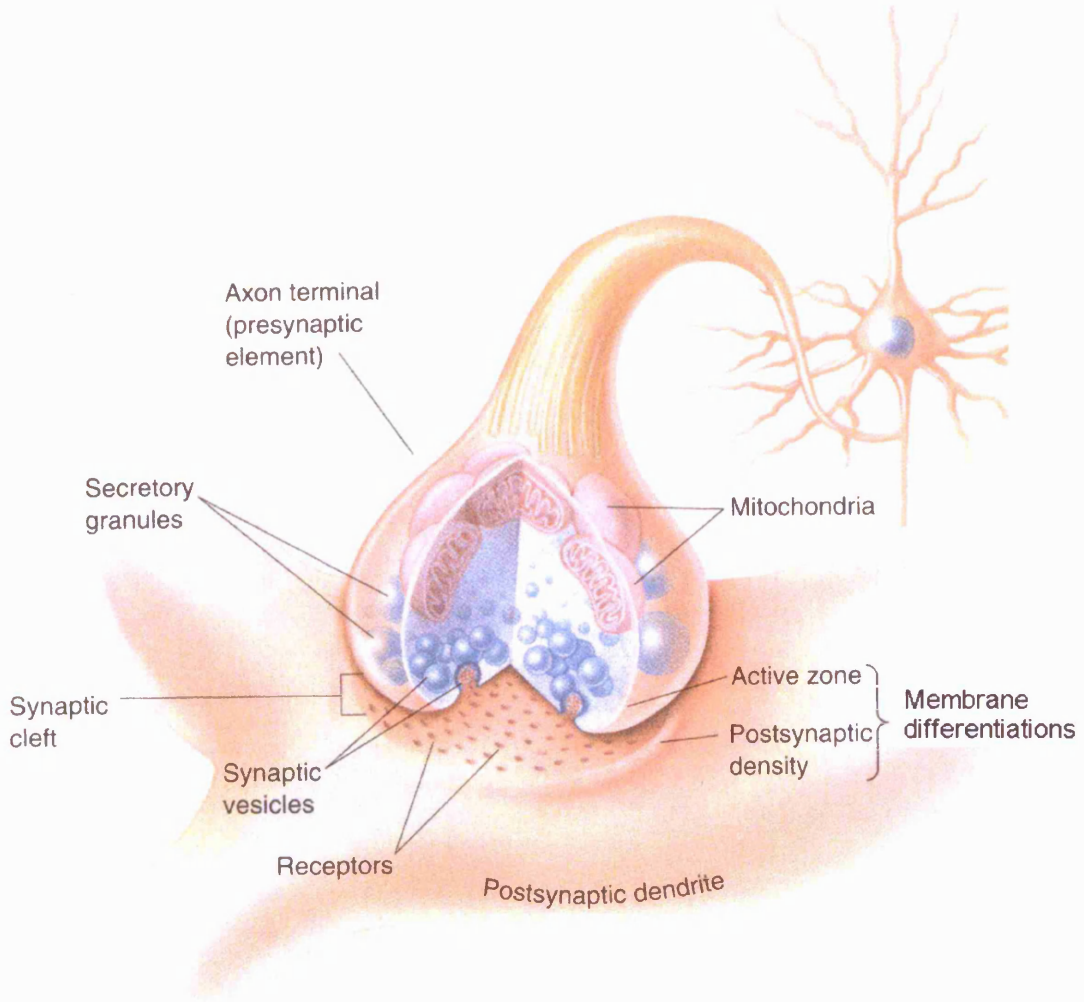

Figure 1.2 The terminal of an axon and its associated synapse.
The terminal bouton forms the end of the axon where the impulse is transmitted across the synapse by neurotransmitters. Upon stimulation by the incoming impulse, these chemicals are released by the synaptic vesicles and migrate across the synaptic cleft to effect a change in the ionic state of the postsynaptic dendrite. The principle of activation is the same for all classes of neurone. Secretory granules are responsible for storage and release of soluble transmitters such as the endorphins (Bear *et al.*, 2001).

In the CNS, the naming of the type of synapse depends upon where along the postsynaptic neurone the terminal bouton is attached. An axon terminating at the afferent or dendrite is termed axodendritic, one attached at the cell body is termed axosomatic and where the synapse is on the axon of the post synaptic cell, the term axoaxonic is used. There also occur dendrodendritic synapses, where a dendrite forms a synapse with another dendrite. Outside the CNS, the synapse between, for example, a motor neurone and a skeletal muscle is termed a neuromuscular junction. The structure of such a synapse is very similar to that of a synapse in the CNS (Bear *et al.*, 2001).

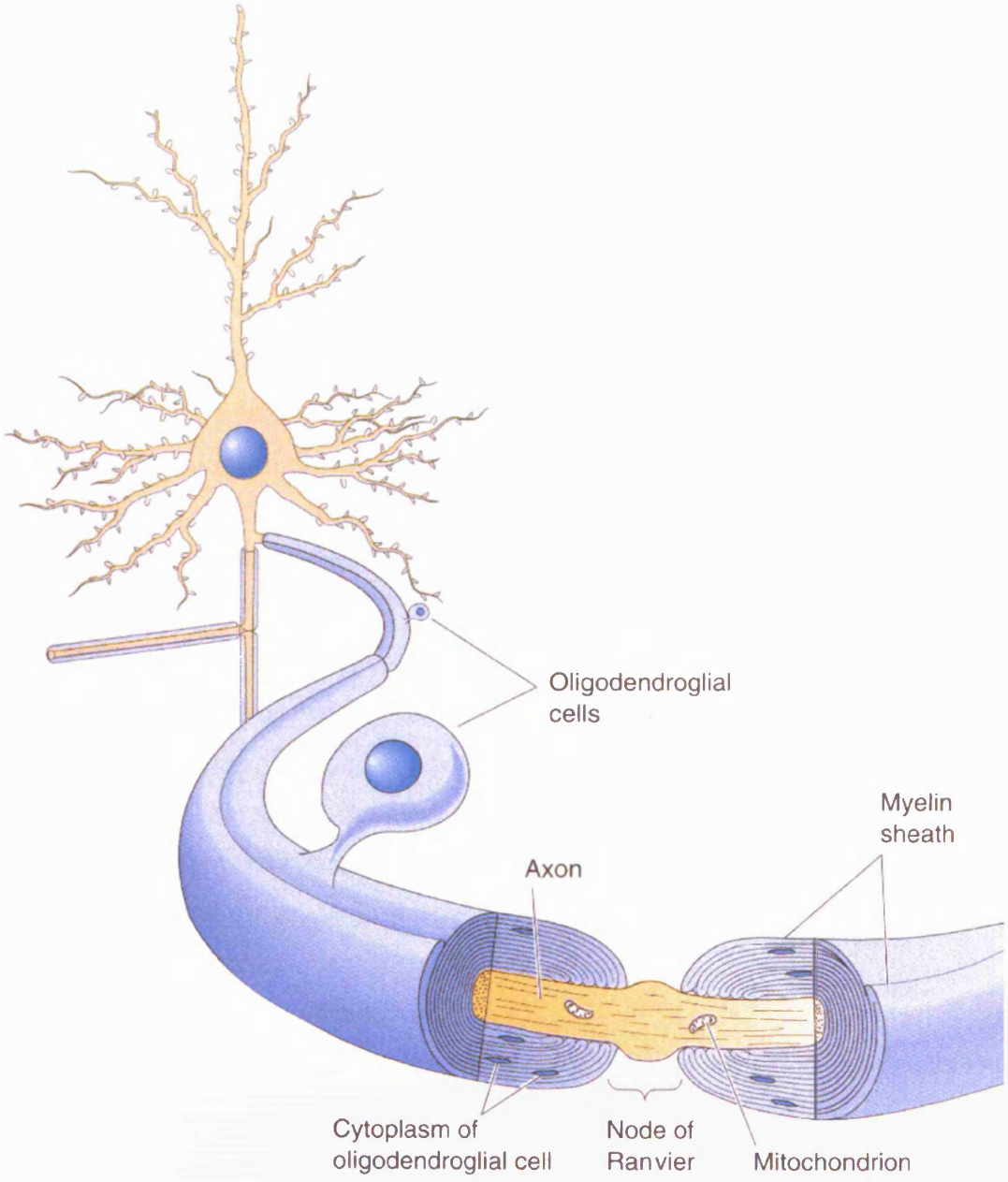

Figure 1.1 Structure of a typical neurone.
This representation shows oligodendroglial cells surrounding a neurone in the brain. These cells provide the same insulating and protective function as the Schwann cells in the periphery. All myelin sheaths are interrupted at regular intervals by nodes of Ranvier. These contractions in the myelin sheath allow the impulse of the signal to be enhanced by saltatory conduction. (Bear *et al.*, 2001).

1.3 The Nature of Pain

Pain is the unpleasant sensation derived from harmful or injurious occurrence, which is classified according to the nature of its cause. The sensation of pain is both physical and subjective, being influenced by the psychological state of the individual. This is the current definition according to the International Association for the Study of Pain (IASP) (Merskey, 1994).

The sensation of pain is classified according to two broad categories. Acute pain is caused by a large, harmful stimulus (capable of causing cell damage) and is generally perceived as an intense, unpleasant feeling (sensation). Chronic pain is defined as outlasting the initial stimulus and can be hyperalgesic (where the level of pain is much greater than the original stimulus), allodynic (where the pain sensation is derived from a non-harmful stimulus), or spontaneous pain with no apparent stimulus (Tortora *et al.*, 1990).

Whilst there are two components to this sensation, the biochemical mechanisms involved in the transmission of a pain signal and the afflicted individual's personal interpretation of this signal, the main concerns of this thesis are the biochemical aspects of pain. Whilst psychological state is of importance in this field, this aspect will not be dealt with here but the reader is directed to the book by Price (1999).

1.4 The Nervous System and Pain

The term nociception is used to describe the sensation of pain via the nervous system, with nociceptors forming the sensory apparatus. The relief from pain is termed analgesia when applied to humans, the absence of pain in animals being termed antinociception (Riedel *et al.*, 2001).

The transmission of a pain signal is conducted along specific nerve fibres from the site of injury to the sensory areas in the CNS. This signal begins when a harmful stimulus causes the release of chemical agents that act upon the terminals of nociceptive cells, in the affected area. These nociceptors generally take the form of nerve fibre endings embedded in tissue. When stimulated, they initiate an impulse that is propagated along afferent fibres to the dorsal horn of the spinal cord where the signal is perceived as pain

within the central nervous system (CNS) (Rang *et al.*, 1995). An outline of afferent pain transmission is shown in Figure 1.3.

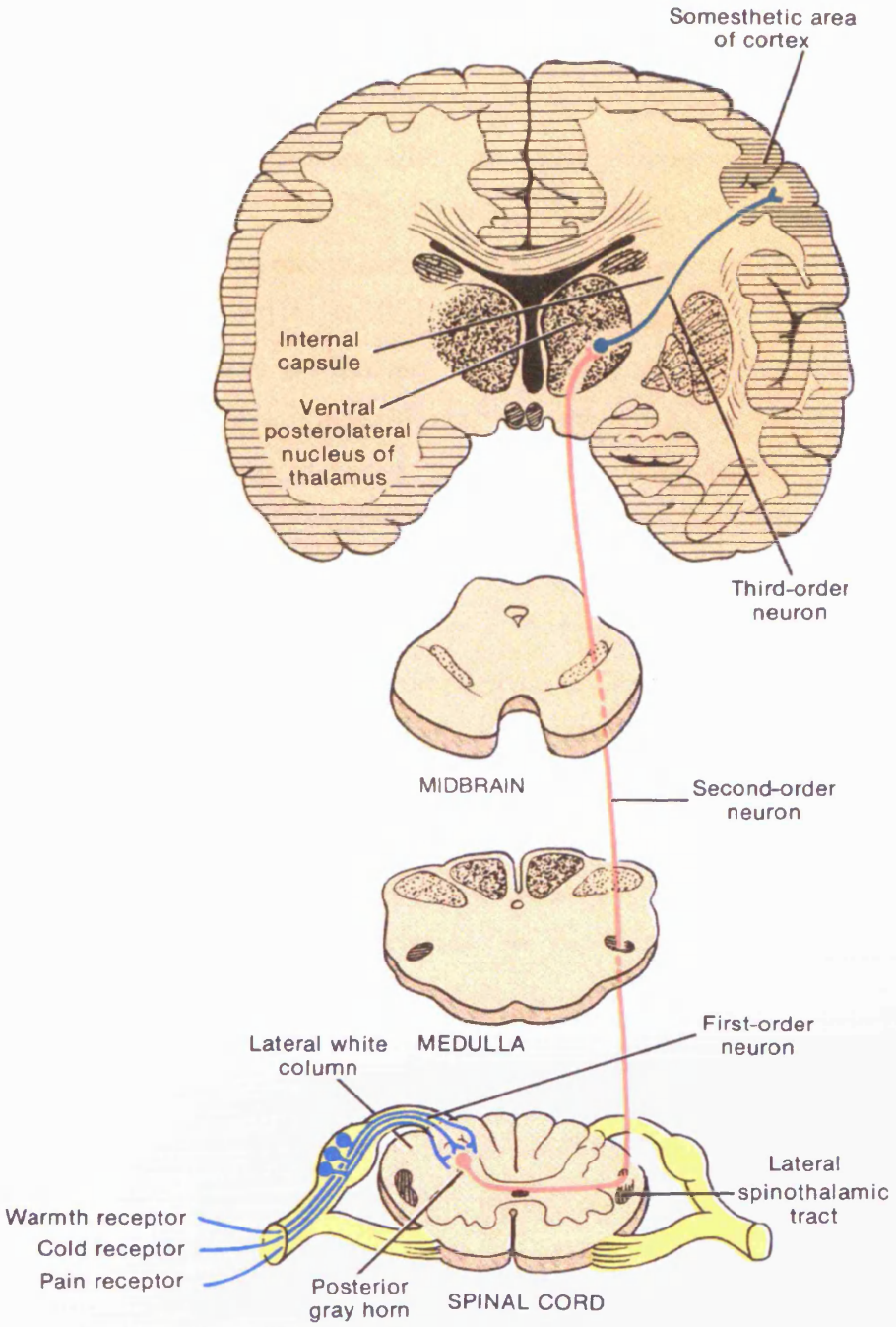

Figure 1.3 Route of a pain signal in nociception.
First order neurone connects the sensory site with the dorsal horn on the same side of the spinal cord and synapses with the second order neurone. The axon of the second order neurone crosses the spinal cord and follows the lateral spinothalamic tract up the spinal column to synapse with the third order neurone in the thalamus. Here pain is recognised but the source of the stimulus is not localised. The third order neurone carries the impulse from the thalamus to the cerebral cortex where the pain signal is quantitatively analysed. Temperature signals are also known to follow this pathway (Tortora *et al.*, 1990).

The nociceptive afferent pathway consists of two types of nerve fibre, A- and C-fibres. A-fibres are myelinated, comparatively large in diameter and have fast conduction velocity (typically $130m.s^{-1}$). They deliver a sharp, localised sensation and are mostly found where life and death situations provoke the stimulus, requiring rapid response. These are further divided into subtypes, of which Aβ and Aδ types are involved in nociception. Of these, Aδ are afferents, sensing noxious pain, whilst Aβ are more commonly associated with feedback from mechanoreceptors, giving positional information, but have a role in nociception via control pathways (Tortora *et al.*, 1990). Although they respond to similar stimuli in the periphery, C-fibres, known as C-polymodal nociceptors (PMN), are simpler in structure, unmyelinated and narrow compared with A-fibres. They are more numerous, with a wider distribution than the more complex A-fibres and have slow conduction (typically $0.5m.s^{-1}$), delivering a prolonged, dull, burning sensation (Rang *et al.*, 1995).

1.5 Neurotransmitters

The chemical signalling compounds involved in the transmission of nervous impulses are many and varied, but are grouped into three categories, namely amino acids, monoamines and peptides. Each may play a role in transmission, inhibition or modulation of signals. Acetylcholine is one of the most prevalent transmitters involved and is mostly excitatory, although in heart muscle it is inhibitory. It was discovered by Otto Loewi in 1921 and is responsible for rapid transduction at all neuromuscular junctions. Excitatory transmitters include the amino acids glutamate and aspartate, although inclusion of the latter is controversial (Patneau *et al.*, 1990).

Glutamate is ubiquitous and the most prevalent excitatory transmitter in the CNS. The biogenic amines are responsible mostly for neuromuscular excitation but may possibly also play a role in inhibition (Bear *et al.*, 2001). They include noradrenaline (norepinephrine), dopamine (in the midbrain, substantia nigra, usually inhibitory) and 5-HT (serotonin, causes excitation in the raphe nucleus). Dopamine is inhibitory in the brain as is gamma amino butyric acid (GABA), whilst glycine is inhibitory in the spinal cord. Many exogenous compounds also play a part in the pain process, either by mimicking the naturally occurring compounds or through interaction with the components of the system.

1.6 Receptors and Neuronal Transmission.

All neurotransmitters exert their influences via a binding site upon specific receptors located either on the surface of the target neurone or at the nucleus. The cell-surface receptors are classified according to their action upon effector proteins or ion channels, and the first to be classified pharmacologically were of the ionotropic type, also referred to as ligand gated ion channels (Watkins *et al.*, 1981). There are four categories of receptor, with examples from each, shown in Table 1.1.

Table 1.1 The Four Categories of Cellular Receptors (Rang, *et al*, 2003).

Receptor type	1	2	3	4
Name	Ligand-gated ion channels	G-protein coupled receptors	Kinase-linked receptors	Nuclear/steroid receptors
Cellular location	Surface membrane	Surface membrane	Surface membrane	Intracellular nuclear membrane
Structure	Several subunits forming a central pore	Single/double unit(s) with 7 transmembrane domains	Single unit with 1 transmembrane domain	Single unit with receptor and DNA-binding domains
Effect	Opening of ion channel	Channel or enzyme	Enzyme	Regulation of gene transcription
Effect mediated by	Directly	G-protein	Directly	DNA
Speed of response	Fast (milliseconds)	Moderate (seconds)	Slow (hours)	Slow (hours)
Duration	Short	Intermediate	Long	Long
Examples	nAChR, $GABA_A$	mAChR, opioid receptors, adrenoceptors	Insulin, tyrosine kinase, cytokine, growth factor receptors	Steroid, thyroid hormone receptors

Receptors of the second type in Table 1.1 act via a guanine nucleotide-binding regulatory protein (G-protein) and are termed G-protein coupled receptors (GPCR). These have seven transmembrane domains with extracellular and intracellular domains associated with cell signalling. Such receptors are divided into three main groups (Pierce *et al.*, 2002), each with differing numbers of subgroups, as outlined below.

A. the largest group, contains receptors activated by opioids and biogenic amines;
B. contains the calcitonin and glucagon receptors;
C. contains the glutamate and GABA receptors.

1.7 Signal Transduction

The G-proteins are themselves categorised according to their effect upon cell signalling via second messenger production. An outline of classification is shown in Table 1.2.

Table 1.2 The main groups of G-proteins, their effects and associated receptor agonists. CTx denotes sensitivity to cholera toxin, PTx denotes sensitivity to pertussis toxin.

G-protein	G_s	G_i	G_o	G_t	G_q
Effector enzyme	Adenylate Cyclase			cGMP Phosphodiesterase	Phospholipase C
Effect	↑cAMP	↓cAMP ↑K^+ efflux ↓Ca^{2+} influx	↓ cAMP	↑ Perception of light	↑Inositol(1,4,5)P_3 ↑ Diacylglycerol
Receptor Agonists	Glucagon, βadrenoceptor	Opiates, N/OFQ	Opiates N/OFQ?	Photons	Acetylcholine (via $M_{1/3/5}$)
Toxin sensitivity	CTx	PTx		CTx/PTx	-

The first group of G-proteins includes those stimulating second messenger production, termed G_s. Another group includes those inhibiting such production, termed G_i. Both of these affect cyclic adenosine monophosphate (cAMP) formation via the enzyme adenylyl cyclase (AC) (Sutherland *et al.*, 1958). A further group has been identified and termed G_o, for other effect, since its action is not fully understood, although an effect upon AC similar to that of G_i is observed. Also involved in the inhibition of second messenger formation and grouped with G_i and G_o are members of G_z. The transducins form a third group, which has a role in the sensation of light by activating cGMP phosphodiesterase. They are denoted G_t and are sub-divided into G_{t1} and G_{t2}, depending upon the light sensitive cell in which they are found (Lefkowitz, 1996). Another group, with a role in the activation of phosphatidylinositol 4,5 P_2-specific phospholipase C, includes G_q (Theilade *et al.*, 2001).

G-proteins may be composed of one unit (monomeric, e.g. RAS) or multiple subunits. Those associated with this type of receptor are heterotrimeric, meaning that they comprise three differing subunits, termed α, β and γ. Their approximate sizes are typically 39-45kDa, 35-37kDa and 8kDa respectively. In the inactive state, a guanosine diphosphate (GDP) molecule is bound to the α-subunit, all three subunits being

associated and loosely held to the cytoplasmic side of the membrane. The binding of an agonist causes a conformational change in the receptor that stimulates the G-protein into exchanging GDP for guanosine triphosphate (GTP) from the cytoplasm. The α-subunit dissociates and interacts with effector enzymes to bring about the downstream effects associated with the receptor-type (Birnbaumer, 1990). Conversion of GTP to GDP by inherent catalytic activity of the α-subunit causes the G-protein to re-associate and renew its interaction with the receptor, ready for further activation.

The other subunits remain as a β/γ dimer, only separable by denaturation and this dimer is itself known to have activity, including the decrease of intracellular calcium levels via voltage sensitive channels and closing inwardly rectifying potassium channels. Indirect action of this dimer may also be seen upon AC and phospholipase Cβ and it is postulated that the total number of actions may be even more numerous and widespread than those of the α-subunit (Clapham *et al.*, 1997). In the case of $G_{i/o}$, to which NOP is coupled, the GTP-bound α-subunit associates with AC which it down-regulates, causing an inhibition of cAMP formation (Hawes *et al.*, 2000). In a neurone, along with a decrease in voltage-sensitive calcium channel activity and an increase in potassium efflux, this may be inhibitory to the transmission of a nerve impulse (Harrison *et al.*, 2000a; Harrison *et al.*, 2000c).

1.8 Adenylyl Cyclase

In mammals, AC has at least 9 isoforms varying in size from just over 1000 amino acids to almost 1400. These show a range of interactions with the various G-protein subunits, increasing further the complexity of the system. Expression of these isoforms is varied throughout the body but all are expressed in the brain (Simonds, 1999). A schematic of the G_i-coupled receptor system and cellular pathway is shown in Figure 1.4.

Pertussis toxin (PTx), from the bacterium *Bordetella pertussis* responsible for whooping cough in humans, may be used to confirm the action of $G_{i/o}$-coupled GPCR, as this uncouples the GPCR and G-protein. The disabling of $G_{i/o}$ GPCR action by PTx is through ADP-ribosylation of the G-protein α-subunit, causing GDP to remain bound. Since the G-protein is unable to exchange GDP for GTP it remains inactive, association with AC cannot occur and thus cAMP formation is not inhibited (Katada *et al.*, 1981).

For confirmation of G_s-coupled and G_t GPCRs, cholera toxin (CTx) from *Vibrio cholerae*, the causative agent of cholera, may be used. The effect of this toxin is ribosylation of the α-subunit, reducing intrinsic GTPase activity and thereby remaining active, leading to an prolonged increase in AC activity and second messenger accumulation. This essentially forms a marker for G_s, since G_t is found exclusively in retinal cells (Pierce *et al.*, 2002).

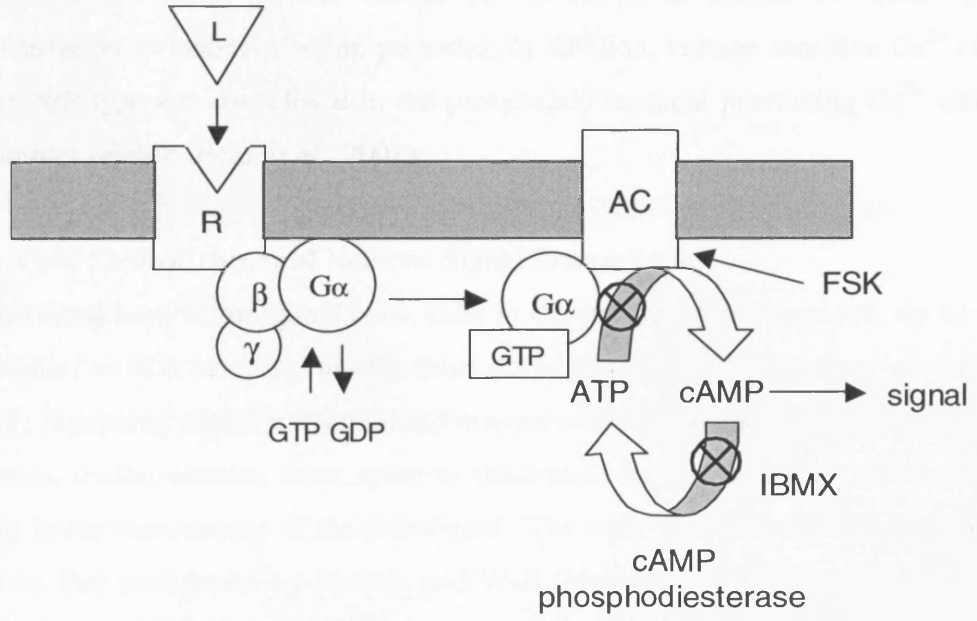

Figure 1.4 The signalling pathway of a Gi-coupled GPCR.
The ligand (L) binds to the receptor (R) and, if the ligand is an agonist, GDP is exchanged for GTP at the α-subunit of the G-protein. The GTP-bound α-subunit dissociates from the other two subunits and negatively affects production of cAMP by adenylate cyclase (AC). In a cyclic AMP assay, forskolin (Fsk) is used to increase AC activity in conjunction with IBMX, which prevents the degradation of cAMP formed.

1.9 Inhibition of Neuronal Transmission.

Synaptic transmission involves the movement of ions across membranes and whilst the consequences of this in some neurones may be excitatory (propagating a signal), other neurones can have inhibitory effects (suppressing a signal). The release of transmitters at one synapse, located along the axon of another, whilst not causing depolarisation of this second neurone, may cause hyperpolarisation, preventing any further conduction of a signal. Different neurotransmitters are involved in such inhibitory neurones, namely

GABA and glycine. Figure 1.5 shows the effect at a cell of a synapse inhibitory to an incoming pain signal (Bear *et al.*, 2001).

The role of neuroactive peptides in the inhibition of pain signal transmission may be mediated by the movement of either positively charged potassium ions out of the cytoplasm or negatively charged chloride ions into the neuronal cytoplasm (of a C- or Aδ fibre), each through specific ion channels. Activation of these channels causes hyperpolarisation of the neurone that prevents the incoming signal from propagating further, as the effect of the charge in the signal is unable to cause sufficient depolarisation to maintain action potential. In addition, voltage sensitive Ca^{2+} channels of the N/P type are also closed in the presynaptic terminal preventing Ca^{2+} influx and transmitter release (Bear *et al.*, 2001).

1.10 Gate Control Theory of Nervous Signal Transmission

In the dorsal horn of the spinal cord, cells in the second layer (lamina II, the substantia gelatinosa, or SG) comprise mostly short nerve terminals which project into laminae I and V, regulating signal transmission between nociceptive primary afferent fibres and the transmission neurons from spine to thalamus. In this way they act as inhibitory agents to the transmission of the pain signal. The term 'Gate Control Theory' originates from its first postulation by Melzak and Wall (Melzack *et al.*, 1965), who proposed a model in which pain signal transmission is regulated by the response of SG cells to both afferent fibres entering from the periphery and to fibres descending from the CNS, the descending inhibitory pathway. This area is known to be rich in opioid peptides and receptors, which may also be associated with nociceptive activity. Similar gate mechanisms are also thought to operate in the thalamus, implying that a series of 'gates' may be responsible for the complete pathway of pain signal transmission. The major transmitters involved at this site are glutamate and Substance P (Rang *et al.*, 1995).

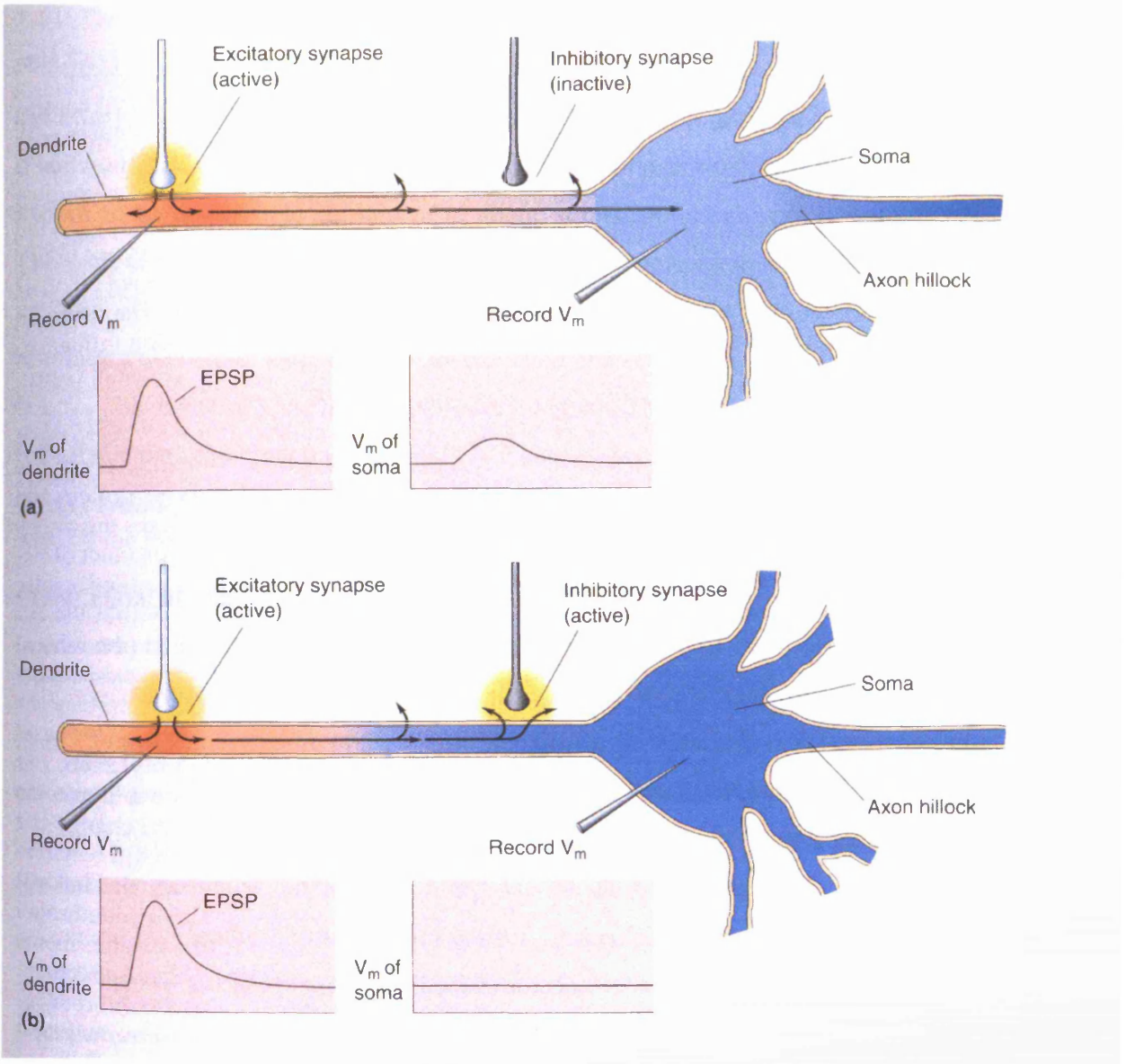

Figure 1.5 Presynaptic (shunting) inhibition of a nerve signal.
The incoming signal at the excitatory synapse causes depolarisation of the postsynaptic dendrite in the form of an excitatory post-synaptic potential (EPSP), with consequent propagation of the signal towards the soma of the postsynaptic neurone. With the inhibitory synapse inactive, the signal is propagated through the soma to create an output impulse in the axon of this second cell. Activation of the inhibitory synapse causes the influx of negatively charged chloride ions (equivalent to a net efflux of positive charge) serving to hyperpolarise this area of the postsynaptic neurone, preventing further depolarisation and effectively terminating the impulse generated by the excitatory neurone (Bear *et al.*, 2001).

1.11 Descending Inhibitory Control

Neurones involved in the suppression of pain signals acting via the descending inhibitory control pathways seem to be channelled via the periaqueductal grey (PAG) matter, an area of the midbrain receiving signals from many other areas of the brain and known to be responsible for analgesia when electrically stimulated (Reynolds, 1969). The path of inhibitory signals runs from the PAG to the nucleus raphe magnus (NRM), an area of the medulla close to the midline and connected to the dorsal horn. A regulatory feedback loop appears to act such that signals received at the thalamus control the level of descending inhibitory signal. This is mediated via the nucleus reticularis paragigantocellularis (NRPG) located adjacent and connected to the NRM (Bear *et al.*, 2001). A summary of this pathway is shown in Figure 1.6.

Modulation of this pathway leads to an attenuation of pain, or analgesia. Since its introduction, the Gate Control Theory has stood the test of time and is substantially unchanged from its original form (Dickenson, 2002). A schematic representation of the Gate Control Theory pathways is shown in Figure 1.7. Transmitters involved in this part of the pathway are predominantly noradrenaline (norepinephrine) and 5-hydroxytryptamine (5-HT, or serotonin). Opioids are known to act at several sites in this system, in particular having inhibitory effects at the dorsal horn synapse and at peripheral nociceptors. As shown in Figure 1.7, impulses from Aβ-fibres also affect this system. These are neurones from mechanoreceptors involved in conducting positional information to the CNS from skeletal muscle, and stimulate the SG into inhibiting the transmission of a pain impulse. This effect is seen in, say, flexing a limb to ease the feeling of pain by stretching or rubbing an affected area.

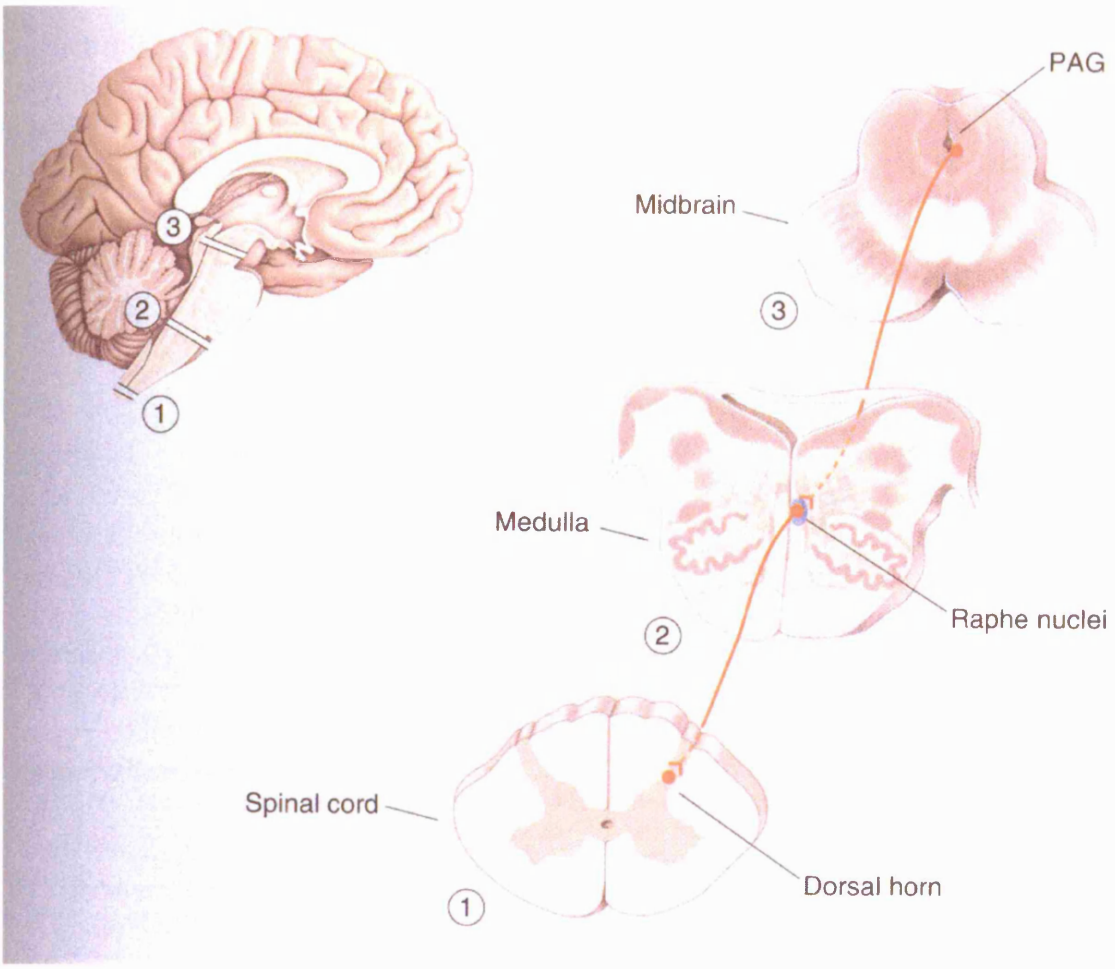

Figure 1.6 The descending inhibitory pathway.
Descending neurones, activated by opioids in the PAG, affect interneurones in the NRM which in turn influence the nociceptive afferents of the dorsal horn via the 'gate' of the Gate Control Theory (Bear *et al.*, 2001).

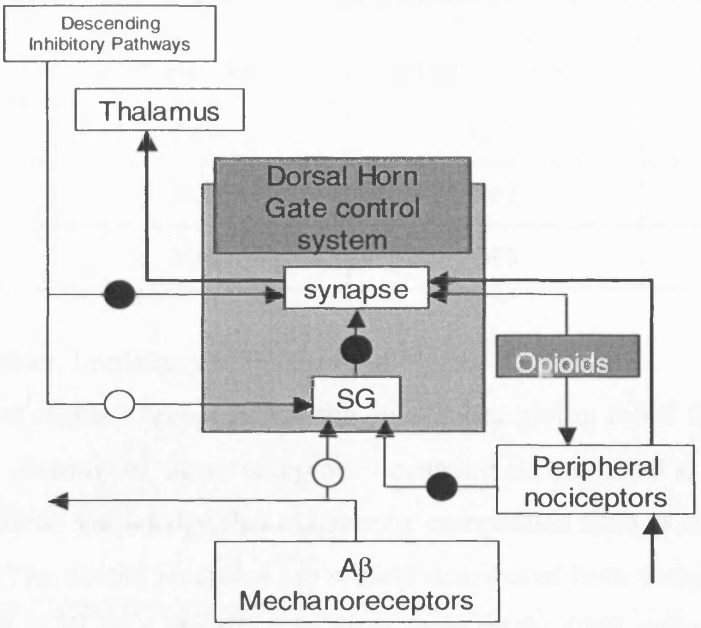

Figure 1.7 Gate control systems in nociception.
The first order neurone (shown as a thicker line) connects the peripheral nociceptor to the dorsal horn, where it synapses with the second order neurone (also shown thicker), which transmits the signal to the thalamus. Several control synapses are involved in regulating signal transmission, both from afferents and from descending neurones in the spinal cord. In the diagram, black circles indicate inhibitory effects, white circles indicate stimulatory effects.

1.12 Opioid Receptors

These receptors comprise a family of membrane-bound proteins acting via inhibitory G-proteins. The three classical opioid receptors have for many years been regarded as the classic mediators of analgesia, due to the effect of exogenous ligands such as morphine, the first to be recognised with activity at the mu (μ) receptor, which is named from it. The other two are delta (δ), named after vas deferens, the tissue from which it was first isolated and kappa (κ), from ketocyclazocine, the first ligand known to act upon it. In addition to the Greek notation, these receptors have also been known as OP1 (δ), OP2 (κ), and OP3 (μ) (Dhawan *et al.*, 1996), but are now officially classified as DOP, KOP and MOP respectively (Cox *et al.*, 2000) and this system will be adopted throughout this thesis. These changes in nomenclature are outlined in Table 1.3.

Table 1.3 Nomenclature of the opioid receptor family.
The later classifications are as unified by the International Union of Pharmacology (IUPHAR).

Pre-cloning	Post-cloning	IUPHAR 1996	IUPHAR 2000
δ	DOR	OP1	DOP
κ	KOR	OP2	KOP
μ	MOR	OP3	MOP

1.13 Classification, Location and Function of Opioid Receptors.

The discovery of distinct receptors for the substances giving relief from pain came in 1973, with the cloning of these receptors occurring in the 1990's, after almost two hundred years of the knowledge that exogenous compounds such as morphine could act to relieve pain. The opioid receptors are widely distributed both peripherally and in the CNS. The MOP, with sites identified in most areas of the CNS and peripherally in the gut and vas deferens. Both DOP and KOP are found in the CNS and peripherally, but shown greater variation with species (Harrison *et al.*, 2000a). By definition, the action of ligands at classical opioid receptors is sensitive to naloxone (Dhawan *et al.*, 1996).

1.14 Identification and distribution of an orphan receptor.

Investigation of DOP under conditions of low stringency revealed an opioid-like receptor for which no ligand was then known (Mollereau *et al.*, 1994). Despite having approximately 60% sequence homology with the MOP and KOP opioid receptors, the classic opioid ligands had little or no affinity for it and the receptor was recognised as an 'orphan'. The discovery of the human form of this receptor in 1994/5 and its identification in other species by several research groups led to some confusion over naming. Research groups involved in the discovery of the receptor and the names adopted by them are shown in Table 1.4. This receptor is highly conserved between species and is now officially known as NOP, in line with opioid receptor nomenclature, as shown in Table 1.5. In addition to the low affinity of the classical opioid ligands for NOP, any activity shown at NOP was not antagonised by naloxone, the definitive opioid receptor antagonist (Butour *et al.*, 1997).

Table 1.4 Early reported studies of the orphan receptor (Mogil *et al.*, 2001).

Species studied	Name of receptor	Reference
Mouse	KOR-3	(Pan *et al.*, 1995)
	MOR-C	(Nishi *et al.*, 1994)
Rat	LC132	(Bunzow *et al.*, 1994)
	XOR1	(Wang *et al.*, 1994) (Wick *et al.*, 1994)
	Ratxor1	(Chen *et al.*, 1994)
	C3	(Lachowicz *et al.*, 1995)
	ROR-C	(Fukuda *et al.*, 1994)
Pig		(Osinski *et al.*, 1999)
Human	ORL1	(Mollereau *et al.*, 1994)

NOP is found in many species although expression level varies both between species and according to the anatomical location within species. High levels of expression are seen in the CNS, where the highest include the dorsal horn of the spinal cord and the cerebral cortex. Lower expression is generally seen in peripheral sites such as vas deferens and this can lead to misleading assumptions being made about the properties of some ligands (Calo *et al.*, 1996), as discussed later in this thesis. Low expression is also seen in other peripheral tissue including ileum, liver and spleen. No expression is seen in skeletal muscle, oesophagus, kidney, adrenal gland or testes (Calo *et al.*, 2000c; Mogil *et al.*, 2001; Mollereau *et al.*, 2000).

The action of NOP is associated with a variety of effects including analgesia (the attenuation of pain signals in nerve fibres), hyperalgesia, antagonism of opioid-mediated analgesia and allodynia(Calo *et al.*, 2000c; Mogil *et al.*, 2001; Zeilhofer *et al.*, 2003). Effects upon feeding, anxiety, opiate tolerance, spatial awareness and reproductive behaviour have also been reported (Calo *et al.*, 1998; Calo *et al.*, 2000c; Mogil *et al.*, 2001). The receptor is also implicated in the blocking of excitatory nerve signals, for example the twitch response in mouse vas deferens, gut and renal pelvis tissue (Meunier *et al.*, 2000).

1.15 NOP and Opioid Receptors

In common with the opioid receptors, as illustrated in Figure 1.8, NOP is a membrane-bound, G-protein coupled receptor (GPCR) comprising an amino-terminus displayed on the extracellular side of the membrane, seven transmembrane domains linked by alternate extracellular and intracellular loops and an intracellular carboxy-terminus. Receptor activation is brought about by a conformational change when a ligand binds to the third, sixth and seventh transmembrane domains, which are closely associated. The third intracellular loop contains the G-protein binding domain. Human NOP comprises 370 amino acids, whilst the opioid receptors consist of 398 (MOP), 380 (DOP) and 372 (KOP) amino acids (Harrison *et al.*, 2000a). A comparison of the primary structures of the opioid receptors and NOP is shown in Figure 1.9.

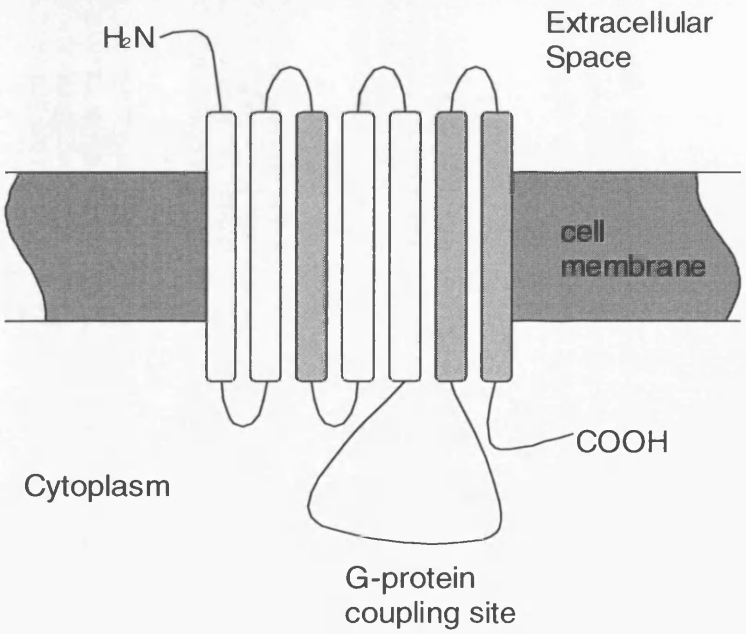

Figure 1.8 Structure of a typical G-protein coupled receptor.
The ligand binding transmembrane domains are shown highlighted and are more closely associated in the three dimensional structure. The larger, third intracellular loop is associated with G-protein coupling.

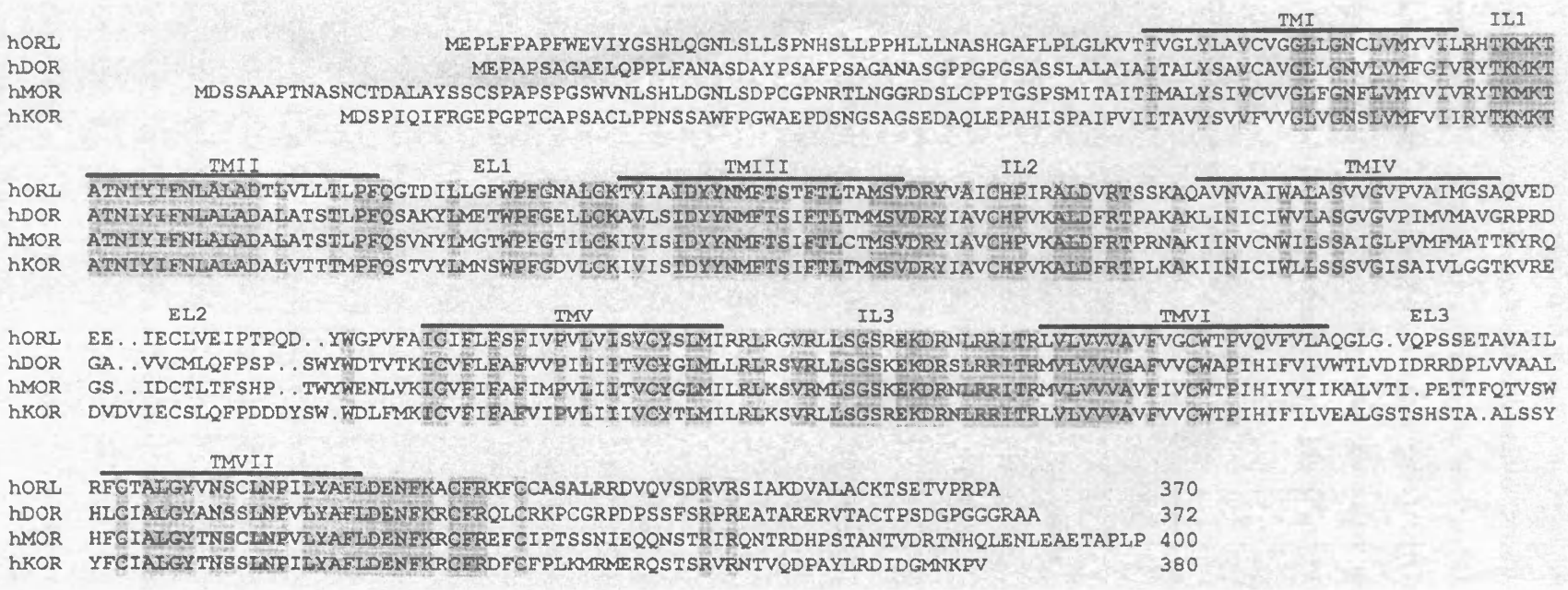

Figure 1.9 The primary structures of NOP and the opioid receptors in man.
Note that the older system of nomenclature is used, wherein ORL corresponds to NOP, DOR to DOP, MOR to MOP and KOR to KOP.
Prefix h indicates the human form of a receptor. Shaded areas indicate homologous amino acids.
The seven transmembrane domains (TM) and the intracellular and extracellular loops (IL and EL, respectively) are also indicated (Meunier, 1997).

Amongst the classic analgesic molecules are non-steroidal anti-inflammatory drugs such as aspirin, paracetamol and ibuprofen, local anaesthetics such as lidocaine and its analogues and the members of the opioid family, including morphine. The opioids act upon specific receptors, which are outlined in Table 1.5. In keeping with this nomenclature the nociceptin receptor, previously named OP4, is now termed NOP. It is interesting to note that endogenous opioid receptor ligands, such as the enkephalins, endorphins and dynorphins, were not identified until 1975.

Table 1.5 The opioid family of GPCR's.

Receptor	MOP	DOP	KOP	NOP
Endogenous agonists	Endomorphin	Enkephalin	Dynorphin	N/OFQ
Exogenous agonists	DAMGO	DPDPE	U40588, U69593 Nalorphine	Roche series (e.g. Ro64-6198)
Antagonists	CTOP	Naltrindole	NorBNI	[Nphe^1]N/OFQ UFP-101 J113397
Clinical agonists	Morphine	-	-	-
Effect of N/OFQ	None	None	Negligible	Activation

1.16 Identification of the NOP ligand and its distribution.

The discovery of a ligand for NOP occurred in 1995 and was accompanied by great interest in the role that this receptor system might play in the transmission of pain signals. Nociceptin and Orphanin FQ were the names adopted by two of the research groups which first isolated the compound. The ligand, a heptadecapeptide, was named nociceptin by one of these groups due to its perceived role in pain signal transmission, as it seemed to cause pain in some assays (Meunier *et al.*, 1995). The other group used the term orphanin FQ, derived from the 'orphan' nature of the receptor and the first and last amino acids of the elucidated sequence (Reinscheid *et al.*, 1995). These names were formally given equal weight by the International Union of Pharmacology (IUPHAR), hence the use of the term Nociceptin/OrphaninFQ (N/OFQ) in describing this compound (Cox *et al.*, 2000).

The ligand was discovered using the 'orphan receptor strategy', the procedure of which is outlined in Figure 1.10. In this process cells expressing an orphan receptor (one for which no ligand is known) are exposed to crude homogenates, any of which showing activity at the receptor are fractionated and subjected to further testing until a candidate ligand is isolated. Further testing, such as the use of synthesised versions of the potential ligand, may be used to confirm the activity at the receptor (Civelli *et al.*, 1998). An excerpt from one of the original papers showing the initial discovery of N/OFQ is shown in Figure 1.11.

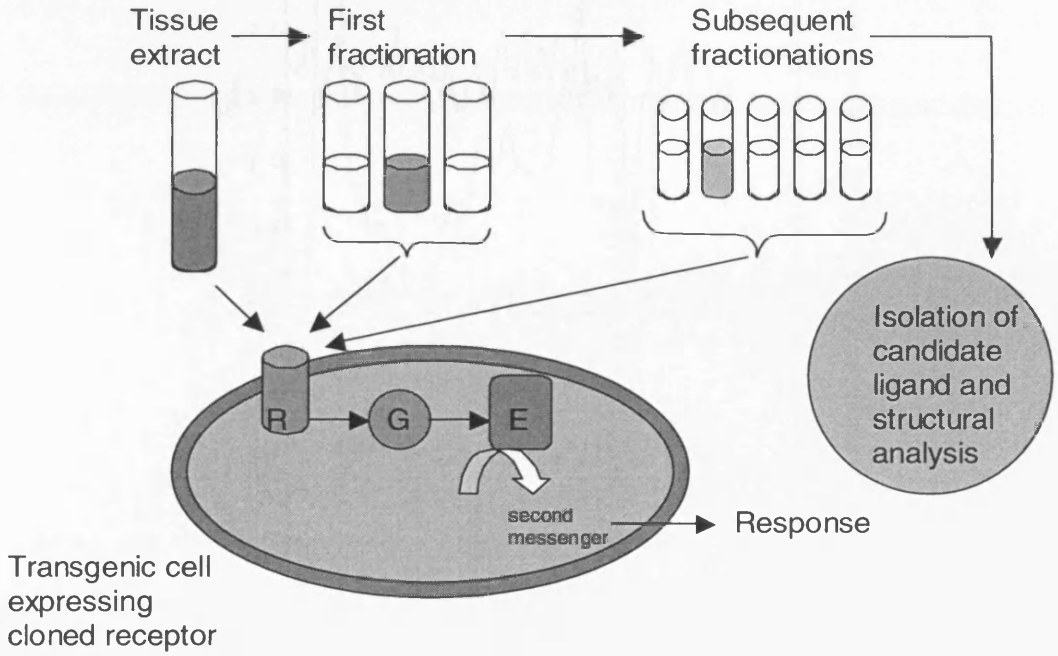

Figure 1.10 Outline of the orphan receptor strategy.
Grey shading of tissue extract and fractions indicates presence of candidate molecule. Crude homogenate (tissue extract) is applied to transgenic cells expressing the 'orphan' receptor (R) for which a ligand is sought. Any activity at the receptor will activate the G-protein (G) which in turn affects the effector enzyme (E) and the signal will indicate the presence of an agonist. The extract may then be fractionated and the assay repeated, fractions showing further activity being further fractionated until a potential ligand is isolated for analysis (adapted from (Civelli *et al.*, 1998)).

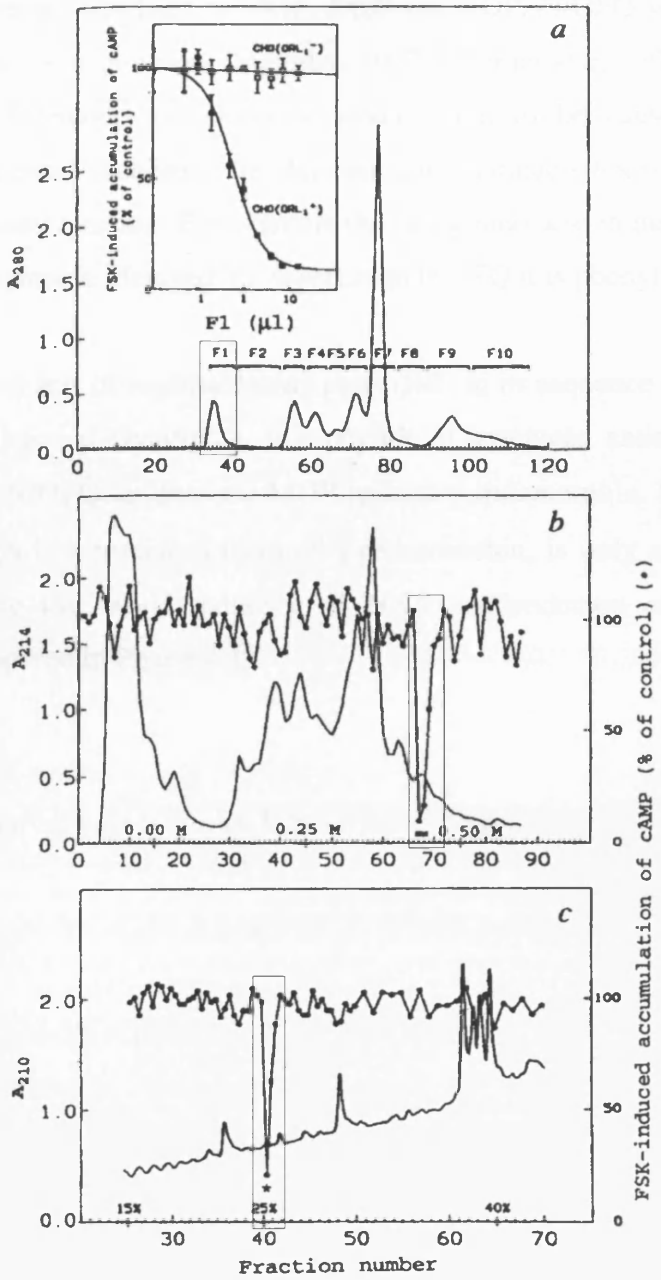

Figure 1.11 Original, step-wise purification of N/OFQ.

Shown are elution profiles from: a) size exclusion chromatography; b) cation exchange chromatography and c) reverse-phase HPLC, illustrating the discovery of N/OFQ.

a) Elution profile of protein from a fresh homogenate of rat brain applied to a size exclusion chromatography column, with analysis of fraction F1 (inset) showing inhibitory activity on cAMP formation in Chinese Hamster Ovary (CHO) cells expressing ORL1, as NOP was then known. This fraction corresponds to larger peptides from the homogenate and was applied to the second column. The traces in b) and c) are overlaid with cAMP inhibition data (shown as filled circle data points). The cation exchange trace (b) indicates the presence of a highly positively charged substance in a late-eluting fraction (outlined) with activity at the receptor shown by inhibition of cAMP formation. The reverse phase column trace (c) shows (outlined) a narrow band of fractions, around fraction 40, giving a marked inhibition of cAMP formation, corresponding to a hydrophilic protein of moderate size. This peptide is now known as N/OFQ (Meunier *et al.*, 1995).

Despite NOP showing homology to MOP, DOP and KOP, N/OFQ was found to have little or no action at these receptors (Meunier, 1997; Meunier *et al.*, 2000; Reinscheid *et al.*, 1998). This difference in behaviour would seem to be caused by small but fundamental differences between the determinant pharmacophores of the peptides having activity at each receptor. For example the first amino acid in the sequences of the opioid agonists is tyrosine (denoted Y), whereas in N/OFQ it is phenylalanine (F).

N/OFQ also has two sets of arginine lysine pairs (RK) in its sequence which the opioids do not. The KOP agonist Dynorphin, is a peptide of seventeen amino-acids, showing some similarity to N/OFQ, as does the MOP agonist γ-endomorphin. Met-enkephalin, a DOP agonist which is a truncated form of γ-endomorphin, is only a heptapeptide but shows similarity to the initial sequence of N/OFQ (Henderson *et al.*, 1997). The sequences are compared in Figure 1.12.

H_2N-F**GGF**TGAR**KS**AR**K**LA**NQ**-COOH	N/OFQ
H_2N-Y**GGF**LRRIRPKL**K**WD**NQ**-COOH	D_a
H_2N-Y**GGF**MTSE**KS**QTPLVTL-COOH	γ-end
H_2N-Y**GGF**M-COOH	Met-E

Figure 1.12 Sequences of nociceptin and the opioid agonists dynorphin A (D_a), γ-endomorphin (γ-end) and Met-enkephalin (Met-E).
Amino-acids homologous to N/OFQ are shown in bold. Note that the four N-terminal residues in the opioid agonists show 100% homology (endomorphin-1 YPWF-NH_2 is an exception but acts as a highly MOP-selective agonist).

1.17 Post-translational processing and N/OFQ-related peptides

The translation product from the N/OFQ gene, known as prepronociceptin (ppN/OFQ), contains two further peptides in addition to N/OFQ. These are named nocistatin (sometimes referred to as NST) and nociceptin II (NocII), identified from the presence of potential peptidase cut sites flanking the sequences and spliced out in post-translational processing. The enzymes responsible for this processing cut peptides at pairs of the cationic amino acids arginine (R) and lysine (K) (Mogil *et al.*, 2001; Okuda-Ashitaka *et al.*, 2000). The sequences of cow, human, mouse and rat ppN/OFQ are shown in Figure 1.13.

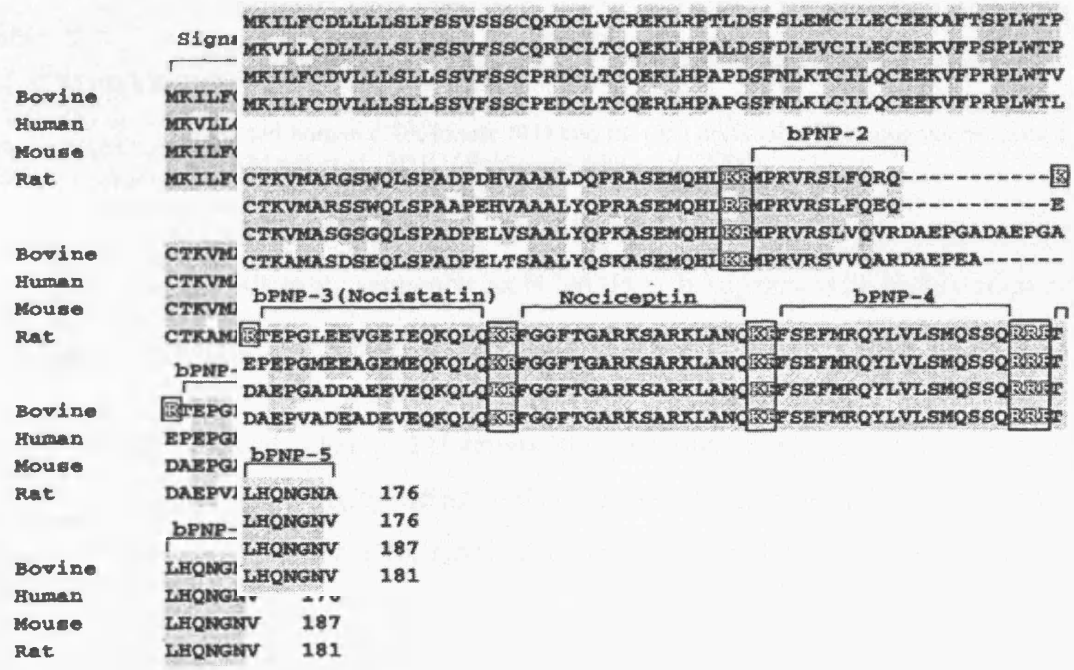

Figure 1.13 Comparison of the sequences for prepronociceptin (ppN/OFQ) in cow, man, mouse and rat. Homologous sequences are shaded and significant translation products are indicated. The sequences marked bPNP-3 (Nocistatin) and bPNP-4 are also known as NST and Noc-II, respectively (Okuda-Ashitaka *et al.*, 2000).

Despite showing little affinity for NOP, NST (coded for immediately upstream of N/OFQ) is so named since it acts as a functional antagonist of N/OFQ. From the high affinity binding shown in mouse spinal cord and brain membranes, is proposed that this action may be mediated allosterically and although NST is known to be expressed in the CNS, little is currently known of its action. Whereas N/OFQ does not seem to show species variation, NST shows considerable interspecies difference in length and content,

whilst maintaining some homology (Mogil *et al.*, 2001; Okuda-Ashitaka *et al.*, 2000). The sequences of NST in cow, human, mouse and rat are shown in Figure 1.14.

Cow

bPNP-2	bPNP-3 (nocistatin)
H_2N-**MPRVRS**LFQRQ-COOH	H_2N-T**EP**GLEEVG**EIEQKQLQ**-COOH

Human

H_2N-**MPRVRS**LFQEQEE_PEP _ _ _ _ _ _ _ _ _ _GMEEAG**EMEQKQLQ**-COOH

Mouse

H_2N-**MPRVRS**LVQVRDAEPGADAEPGADA**EP**GADDAE**EVEQKQLQ**-COOH

Rat

H_2N-**MPRVRS**VVQARDAEPEA_ _ _ _ _ _DA**EP**VADEAD**EVEQKQLQ**-COOH

Figure 1.14 Comparison of post-translational sequences of other peptides from ppN/OFQ.
Shown are bPNP-2 (11 residues) and bPNP-3 (nocistatin, 17 residues) in the cow and proposed human (30), mouse (41) and rat (35) nocistatin. Homologous residues are shown in bold (Mogil *et al.*, 2001; Okuda-Ashitaka *et al.*, 2000).

bPNP-4/NocII is a heptadecapeptide with phenylalanine and glutamine as the first and last amino acids in its sequence, as is N/OFQ. It appears to be highly conserved within mammalian species and its position in the gene product relative to N/OFQ is similar to that of the relative position of dynorphin B to dynorphin A in preprodynorphin. Dynorphin A is also a 17 amino acid peptide. NocII is reported to have some pharmacological activity when applied to the CNS and may have some physiological relevance. The sequence for NocII is shown in Figure 1.15 (Mogil *et al.*, 2001).

H_2N-FSEFMRQYLVLSMQSSQ-COOH

Figure 1.15 Sequence of NocII, identical for cow, human, rat and mouse (Mogil *et al.*, 2001).

1.18 Distribution of NOP and N/OFQ

Figures 1.16 and 1.17 show cDNA autoradiograms of NOP expression and distribution of the nociceptin precursor peptide, prepronociceptin (ppN/OFQ, see Section 1.16), in rat brain. From these it may be seen that some areas show high intensity relative to a background, with some of these areas (in particular the hippocampus, preoptic areas and the medial amygdala) showing both receptor and ligand precursors coexpressed at high levels. These areas are involved in the basic functioning of the CNS, such as pain signal transmission (Darland *et al.*, 1998).

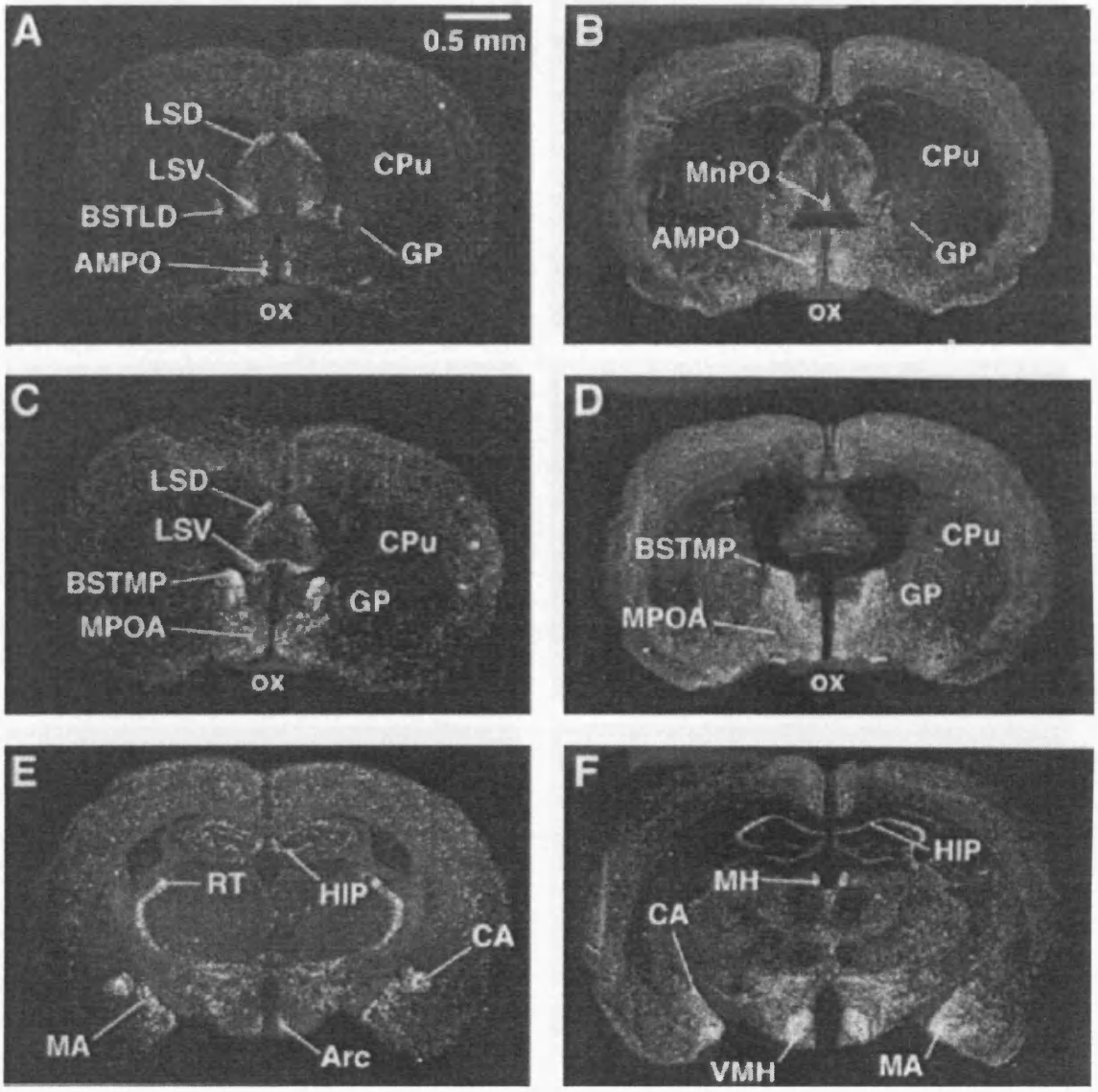

Figure 1.16 Rat cDNA probe radiograms showing distribution of ppN/OFQ (left) and NOP (right) mRNA in adult rat forebrain.

White zones show hybridisation. The sections A, C and E may be compared to sections B, D and F, respectively (Darland *et al.*, 1998). Arc = arcuate nucleus of hypothalamus; AMPO = anterior medial preoptic nucleus; BSTLD = bed nucleus of stria terminalis, dorsolateral division; BSTMP = bed nucleus of stria terminalis, medial posterior division; CA = central amygdala; CPu = caudate putamen; GP = globus pallidus; HIP = hippocampus; LSD = dorsolateral septal nucleus; LSV = ventrolateral septum; MA = medial amygdala; MH = medial habenula; MnPO = median preoptic nucleus; MPOA = medial preoptic area; ox = optic chiasm; RT = reticular thalamic nucleus; VMH = ventral medial hypothalamus

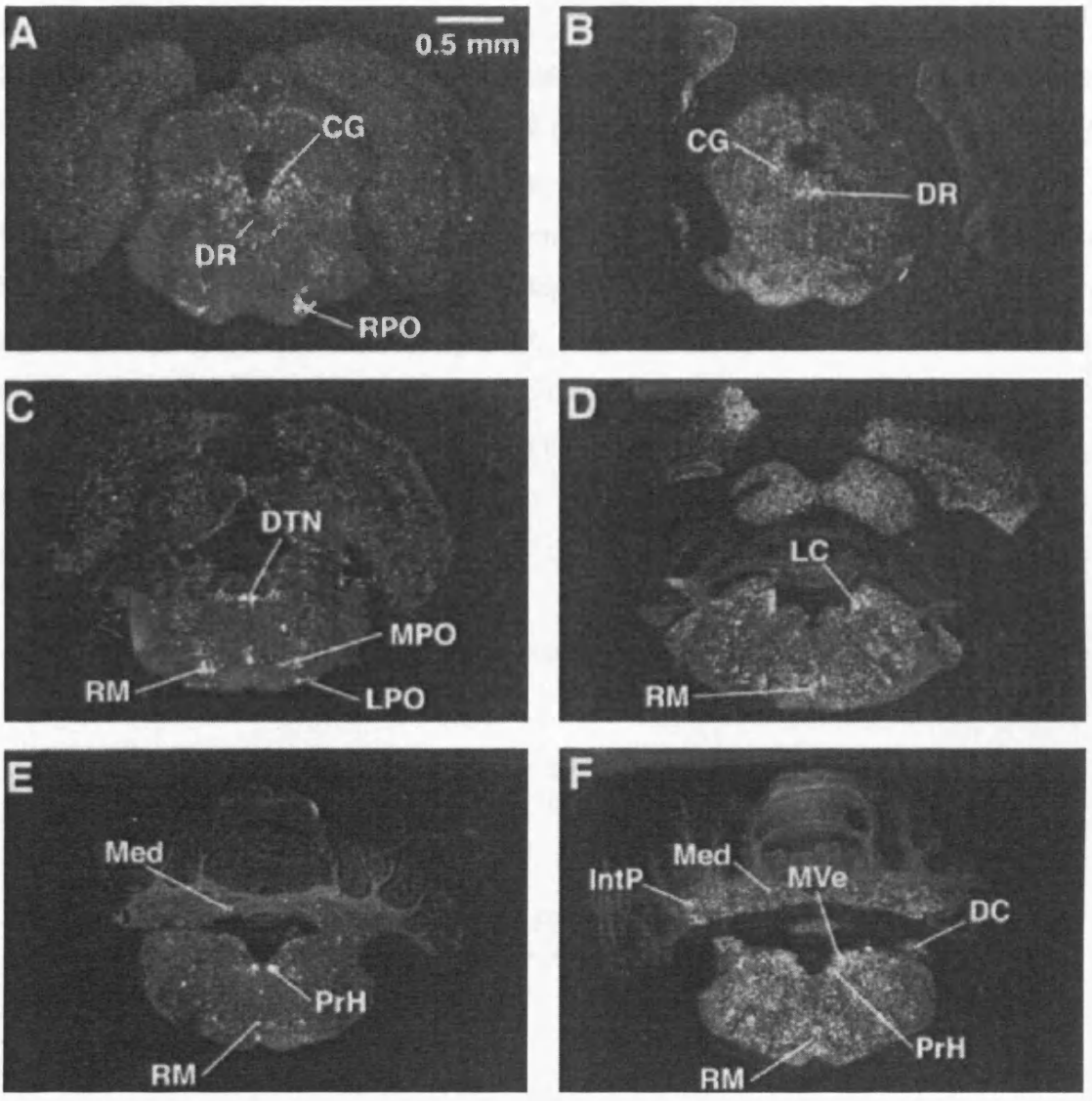

Figure 1.17 Rat cDNA probe radiograms showing distribution of ppN/OFQ (left) and NOP (right) mRNA in adult rat mesencephalon, pons and brainstem.
White zones show hybridisation. The sections A, C and E may be compared to sections B, D and F, respectively (Darland *et al.*, 1998)CG = central gray; DC = dorsal cochlear nucleus; DR = dorsal raphe; DTN = dorsal tegmental nucleus; IntP = interposed cerebellar nucleus; LC = locus coeruleus; LPO = lateral periolivary nucleus; Mve = medial vestibular; PrH = prepositus hypoglossi; RM = raphe magnus; RPO = rostral periolivary nucleus.

1.19 Metabolism of N/OFQ.

Inactivation of N/OFQ by the generation of smaller peptide fragments is mediated by further proteases such as aminopeptidase N (APN), endopeptidase 24.15 (EP24.15) and a further endopeptidase identified in rat hippocampus (Noble *et al.*, 1997; Sandin *et al.*, 1999). The loss of the first residue by action of APN negates all activity at NOP whilst endopeptidases (EP) are responsible for degradation of the peptide sequence through their action at basic residues (Dooley *et al.*, 1996; Montiel *et al.*, 1997). An outline of this process is shown in Figure 1.18. Note that the first degradation product of the EP from rat hippocampus is known as N/OFQ(1-13) and is the least sequence still retaining activity at NOP.

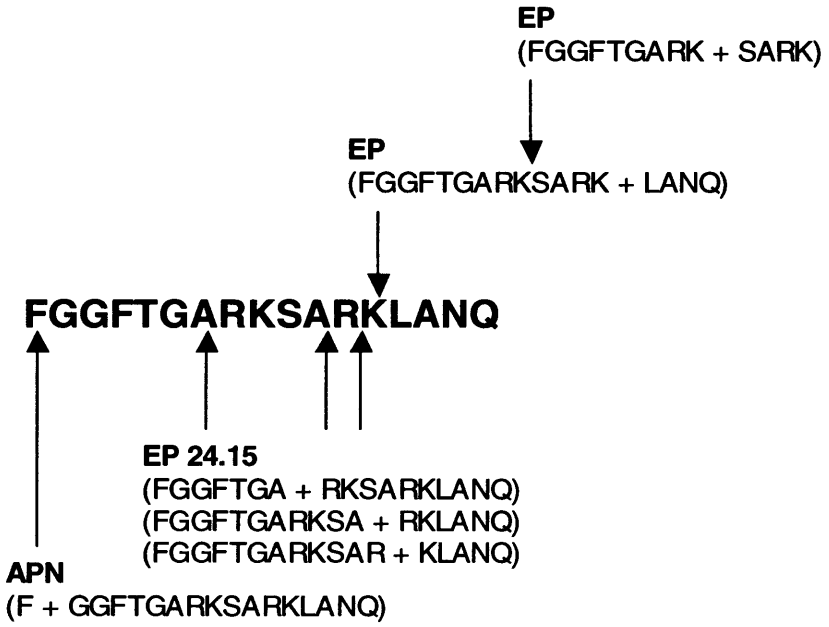

Figure 1.18 Peptidase metabolism of N/OFQ.
Native N/OFQ is shown in bold type. Sites of peptidase activity are indicated by arrows.
Peptidases shown are:
APN, Aminopeptidase N; EP 24.15, endopeptidase 24.15;
EP, endopeptidase identified in rat hippocampus.
Products of peptidase activity are shown in brackets. (Calo *et al.*, 2000c).

1.20 Duality of NOP in Pain Response.

N/OFQ may also elicit apparent stimulatory effects in the CNS. This would appear to depend upon the location of the receptors rather than any functional differences. Due to this seemingly contradictory nature of N/OFQ in eliciting analgesia when given spinally whilst evoking hyperalgesia supraspinally, an explanation of how these effects may come about was proposed in the bi-directional pain modulating theory (Pan *et al.*, 2000).

The descending inhibitory control pathway comprises two parts, primary cells, eliciting analgesia, which are known to be inhibited by one type of opioid and secondary cells, eliciting hyperalgesia, sensitive to another type of opioid and possibly having an inhibitory effect upon the primary cells. In the theory it is proposed that N/OFQ may act upon both types of cell to functionally antagonise the opioid effects. Upon the secondary cells, this disinhibition leads to the hyperalgesic effects, whilst direct action upon the primary cells elicits analgesia by a similar mechanism.

1.21 Clinical utility of Nociceptin.

The full role of the N/OFQ-NOP system remains unclear since there are actions implicated in both the suppression and enhancement of pain. This is seemingly dependent upon the anatomical site of the receptor in that antiopioid effects/hyperalgesia are seen supraspinally and analgesia spinally (Mogil *et al.*, 2001; Zeilhofer *et al.*, 2003). Since formal identification of N/OFQ there have been major advances in the design and evaluation of novel NOP ligands. Indeed, high potency/high efficacy agonists and high potency antagonists are now readily available for laboratory use. It has recently been shown that NOP antagonists delivered directly into the brain act as analgesics (Calo *et al.*, 2000b; Calo *et al.*, 2000c). In addition, there is industrial interest in this receptor system as a potential therapeutic target and several patents are registered (Calo *et al.*, 2000c; Gagliardi *et al.*, 2003; Mogil *et al.*, 2001; Smith *et al.*, 2001) (see also later sections of this thesis).

A summary of the available data from all currently published studies on measured concentrations of N/OFQ in humans is presented in Table 1.6. From this the question arises as to whether we are any nearer the clinic with this peptide-receptor system. Despite the perceived clinical importance of N/OFQ, there is a dearth of information

concerning circulating levels in man in both normal and disease states, such as pain (Anderberg *et al.*, 1998; Brooks *et al.*, 1998; Ertsey *et al.*, 2004; Hantos *et al.*, 2002; Horvath *et al.*, 2004; Ko *et al.*, 2002; Kumar *et al.*, 1999; Szalay *et al.*, 2004; Zeilhofer *et al.*, 2003).

Between the studies, a remarkable consistency may be seen in control ("non-diseased") plasma levels of around $10pg.ml^{-1}$, representing a circulating concentration of some 5pM. Does this represent an accurate assessment of the situation at the effect site, that is, at the receptor? As detailed above, NOP is found both peripherally and in the central nervous system, with effects upon organs such as the heart and kidney (Mogil *et al.*, 2001; Zeilhofer *et al.*, 2003). Accordingly, these data might reflect the concentration observed at the end organ, although no account for either metabolism or local release of the peptide, most probably from peripheral nerves, is made. In the CSF, however, the prevailing concentration appears to be much greater, in the order of $55pg.ml^{-1}$ (Brooks *et al.*, 1998), equivalent to 28pM. Indeed, this latter concentration approaches the value of 46pM in rat brain (Hashiba *et al.*, 2002) for effective binding between N/OFQ and NOP, although the same arguments concerning metabolism and local release still hold.

It seems reasonable to suggest that in pain states N/OFQ levels may change, based on an assumption that N/OFQ may be involved in setting pain thresholds. In experiments NOP antagonists given into the mouse brain produce an antinociceptive response (Calo *et al.*, 2000b; Calo *et al.*, 2000c). This would seem to imply that supraspinal N/OFQ-ergic tone is high, favouring "pain". Switching this off might reset the threshold to yield an apparently antinociceptive response. Therefore, in pain states, a supraspinal increase in N/OFQ could be postulated with a possible decrease in the spinal cord (as N/OFQ delivery to this site produces antinociception). The reported results are conflicting in that some pain states show raised levels compared to controls and others show lower levels.

Raised plasma levels, compared to controls, have been reported in both acute and chronic pain states (Ko *et al.*, 2002). A graded elevation of N/OFQ level was seen from control to chronic pain groups, through acute and subacute pain states. No difference due to sex was observed in the control group. It is important to note that in this study the pain was heterogeneous in nature.

In a study of fibromyalgia syndrome (FMS) patients (Anderberg *et al.*, 1998) a significant decrease in plasma N/OFQ levels was seen for all patients compared to non-FMS controls, although the actual levels measured were unclear. Interestingly, when levels in pre-menopausal subjects were analysed according to phase in the menstrual cycle, there was a significant difference only between sufferers and equivalent (non-FMS) controls for those in luteal phase.

In cluster headache patients (Ertsey *et al.*, 2004) decreased N/OFQ levels were also reported, compared to age- and sex-matched controls, with a post-episodic return to normal levels. This condition might be considered as something that would potentially release a range of neurotransmitters but no others were measured.

A recurring problem with these studies is how relevant the circulating level of N/OFQ in plasma is to the situation in the brain, especially if the clinical end point is pain? To address this problem, in as far as is practicable in a patient population, a study measured N/OFQ levels in both plasma and cerebrospinal fluid (CSF) for pregnant women presenting either for elective caesarean section or normal labour, requesting combined spinal epidural anaesthesia (CSE) (Brooks *et al.*, 1998). Whilst the latter would presumably be in a greater state of pain, it is of significance to note that there were no differences observed in either plasma or, more importantly, CSF N/OFQ levels. On balance the data from plasma/CSF measurements are too variable to reach any firm conclusions regarding pain at this time.

Hepatic disease such as hepatocellular carcinoma (HCC), primary biliary cirrhosis (PBC) and liver cirrhosis show elevated levels of N/OFQ in plasma, compared to age-matched healthy controls (Horvath *et al.*, 2004; Szalay *et al.*, 2004). In the case of the HCC patients, extremely high levels of N/OFQ were seen whether a patient was with or without pain. Increased levels are also seen for Wilson's disease, an hereditary disorder affecting copper metabolism with hepatotoxic effects. These studies may implicate a role for the liver in N/OFQ metabolism (Hantos *et al.*, 2002; Szalay *et al.*, 2004).

Whilst there are few studies detailing plasma levels there are currently even fewer detailing the targeting of this system in man. N/OFQ is currently unlicenced for use in man and, despite a clear pattern in animal behavioural studies (Calo *et al.*, 2000b; Calo

et al., 2000c), there is no correlation in humans between circulating levels and pain states.

In one of the first studies in man, healthy subjects were injected with N/OFQ into either the temporal muscle of the face or the trapezius muscle of the back (Mork *et al.*, 2002). The dosage was derived from both animal data and previous human studies conducted using other neuropeptides. Doses from 12.5 to 200pmol were used for temporal muscle injections and 200pmol injected into the trapezius muscle. Relating this to circulatory N/OFQ levels of 5pM (giving a total circulating mass of 20-25pmol), the implication is that the higher doses would occupy NOP with incipient effect. As might be anticipated, no pain was felt, indicating the actions of N/OFQ are more likely to be observed in the CNS (where N/OFQ was detected).

Two studies on urological patients (in detrusor hyperreflexia) (Lazzeri *et al.*, 2001; Lazzeri *et al.*, 2003) showed that administration of isotonic saline, containing 1μM N/OFQ, increased bladder capacity and volume threshold for voiding reflex compared to controls. A decrease in maximum bladder pressure was also noted, but this did not reach statistical significance. The studies show evidence for therapeutic use of N/OFQ (based on the identification of NOP on C-fibre afferents and their presence in the bladder) and, more importantly, an absence of adverse effects. Further studies are required to determine optimal dose and duration of action.

Use of a nociceptin cream to combat capsaicin-induced pain in healthy, human volunteers was reported to have produced no adverse effects. There was no lasting effect upon plasma N/OFQ levels ($57.1\pm16.6 pg.ml^{-1}$ before, $36.5\pm7.5 pg.ml^{-1}$ after; note that these are much higher than those reported in Table 1.6) and no change in pain response to capsaicin (Hashiba E, Hirota K, Calo' G, *et al.*, Effects of nociceptin/orphanin FQ cream on capsaicin cream-induced pain in human volunteers. Unpublished meeting abstract, 15/09/2003, Camerino, Italy).

It is clear that much further work is needed before any N/OFQ-containing or N/OFQ-like product is to be put into clinical practice. Is pain the most appropriate disease state, because until this is defined then the appropriate clinical trial cannot be designed.

Despite the plasma data described above and based on extensive small animal work, it may be predicted that pain at least represents a sensible starting point and that use of NOP antagonists might proceed to phase I studies, followed by "proof of concept" in an acute pain model. However, these hypothetical studies require the development of small non-peptide molecules with good oral bioavailability which are still awaited.

Table 1.6 N/OFQ levels in biological fluids of human origin.

Key: M - male; F - female; RIA - Radioimmunoassay; EIA – Enzyme-linked immunosorbent assay; n/d - not determined, below detectable limits; PBC – Primary Biliary Cirrhosis; HCC – Hepatocellular Carcinoma; FMS – Fibromyalgia Syndrome, NOP – nociceptin/orphanin FQ receptor.

Sample Source	Patient Group	Sample Size	N/OFQ level ($pg.ml^{-1}$)	Method	Notes	Study Author Date of Publication
Plasma	FMS	23 (F) 8cyclic/15non-	2.6/2.3	RIA	Luteal phase-FMS/Control 2.4/4.7	(Anderberg *et al.*, 1998)
	Control	17 (F) 8cyclic/9non-	4.0/2.5			
CSF	Elective Caesarean	10 (F)	52.49±34.25	RIA	Only study in CSF	(Brooks *et al.*, 1998)
	Labour/Epidural		63.39±33.26			
Plasma	Elective Caesarean		7.59±21.58			
	Labour/Epidural		13.73±23.79			
Synovial fluid	Knee surgery	10 (NOP, N/OFQ)	n/d	RIA	NOP density also measured	(Kumar *et al.*, 1999)
Synovial Tissue		11 (NOP)	n/d			
Plasma	Wilson Disease	20 (7F 13M)	13.98±2.44	RIA		(Hantos *et al.*, 2002)
	Control	25 (11F 14M)	9.18±1.63			
Serum	Acute Pain	30	16.65±8.01	RIA		(Ko *et al.*, 2002)
	Sub-acute Pain	20	20.66±8.98			
	Chronic Pain	20	24.44±13.60			
	Control	20 (10M, 10F)	10.65±5.58			
Plasma	Normal	5 (M)	5-16	EIA	Values are below detection range ($15\text{-}700pg.ml^{-1}$)	(Naito *et al.*, 2003)
Plasma	Cluster Headache	14 (3F, 11M)	4.91±1.96	RIA		(Ertsey *et al.*, 2004)
	Post-CH		8.60±1.47			
	Control	22	9.58±2.57			
Serum	HCC	single patient	172	RIA		(Horvath *et al.*, 2004)
	Baseline		9.20			
Plasma	Wilson Disease	26	14.0±2.7	RIA		(Szalay *et al.*, 2004)
	PBC	21	12.1±3.2			
	Liver Cirrhosis	15	12.8±4.0			
	Control	29	9.2±1.8			
	HCC	29	105.9±14.4			

1.22 Opioid Peptides, N/OFQ and the Message Address Concept

The structures of the opioid receptor ligands show diversity of composition but the peptide ligands may be said to follow a format of two domains (Guerrini *et al.*, 2000b; Harrison *et al.*, 2000a):

- A message domain, situated at the amino terminus in the native peptide, responsible for receptor activation in the case of agonists and partial/inverse agonists. This usually consists of (up to) four amino acid residues.
- An address domain, comprising the remainder of the residues (in number anywhere from none to thirty), responsible for receptor recognition and binding.

Each of these domains contains certain amino acids, termed determinant pharmacophores, essential to the function of the peptide at the receptor. These concepts, applied to the sequence of N/OFQ, are illustrated in Figure 1.19.

Figure 1.19 Sequence of native N/OFQ.
Determinant pharmacophores are shown in bold.

In the case of the classical opioid receptors, those termed MOP, DOP and KOP, the sequences, illustrating the two putative domains, for some typical endogenous compounds, along with that of N/OFQ, are illustrated in Figure 1.20.

One reason for the commonality of form and function is that there exists for each set of receptor ligands a common precursor: pro-opiomelanocortin for the endorphins; pro-enkephalin for the enkephalins and pro-dynorphin for the dynorphins (Calo *et al.*, 2000a); Corbett *et al.*, 1999). For exogenous peptides and synthetic ligands the case may be more complex as, although competitive binding must still occur at the same sites as the endogenous ligands, binding may be mediated differently. With the discovery of the opioid receptor-like receptor (ORL1, now referred to as NOP) and the subsequent isolation of its ligand, nociceptin or orphanin FQ (N/OFQ), it seemed a reasonable assumption that the message address concept would also apply to this receptor system. Structure activity studies show this not to be as rigorous in the case of

NOP as in the classical opioids and, in my opinion, this receptor system would appear to be the exception to the rule. The corresponding precursor is pro-nociceptin/orphaninFQ.

pro-nociceptin

N/OFQ	**F**G**GF**TGAR*K*SAR**K**LA**N**Q

pro-dynorphin

Dynorphin A (KOP)	**Y**G**GF**LRRI*R*PKL**K**WD**N**Q
Dynorphin B (KOP)	**Y**G**GF**LRRQFKVVT
α-neoendorphin (KOP)	**Y**G**GF**LRKYPK
β- neoendorphin (KOP)	**Y**G**GF**LRKYP

pro-enkephalin

Leu-enkephalin (DOP)	**Y**G**GF**L
Met-enkephalin (DOP)	**Y**G**GF**M
C-terminal extensions altering affinity	{ **Y**G**GF**MRF
- reduced at DOP, increased at MOP	{ **Y**G**GF**MRGL
Metorphamide (MOP)	**Y**G**GF**MRRV-NH_2

pro-opiomelanocortin

β-endorphin (MOP/DOP)	**Y**G**GF**MTSEKSQTPLVTLFKN-
	-AIIKNAYKKGE

Presumed precursor, as yet unidentified ('**pro-endomorphin**')

Endomorphin-1 ('MOP')	**YPW**F-NH_2
Endomorphin-2 ('MOP')	**YPF**F-NH_2

Figure 1.20 Precursors, names and sequences of N/OFQ and some typical endogenous mammalian ligands for the classical opioid receptors.
Precursors are in emboldened lower case. Note that the groupings illustrate the common precursors, receptor of greatest affinity is indicated, although some ligands are not greatly selective for one receptor over another.
Amino acids common to N/OFQ and the classical ligands are underlined, those showing similar chemistry at the same position are italicised.
Putative message sequences are shown in bold.

The endogenous opioid ligands may be of as little as four residues in length and exhibit activity at their receptors, whilst synthetic exogenous compounds of two residues or equivalent size are known to have full activity at MOP and DOP receptors (Hebbes, 2004).

It has been shown that truncation of the native sequence of N/OFQ reveals the shortest active peptide (with full agonist activity at NOP) comprises the first thirteen residues. Denoted N/OFQ(1-13), this is usually amidated at the carboxyl terminus to give N/OFQ(1-13)-NH_2, which protects from exopeptidase activity, maintaining agonist efficacy (Guerrini *et al.*, 1997).

Altering agonist affinity and potency are traditionally mediated via changes to the peptide backbone or the amino acid side chains, to introduce spatial constraints or alter chemical behaviour of the molecule. Such alterations include changes to the bonds or the sequence causing conformational changes and the substitution or addition of electronegative groups or ionising side chains.

1.23 Use of Transgenic Cells to Investigate the N/OFQ-NOP Receptor System

The study of receptor interactions *in vivo* may be complicated by interactions with other receptor systems and also by the varying levels of expression seen both in tissue from different species and from different anatomical locations within an organism. In order to study the effects of particular ligands upon a receptor it is convenient to use a transgenic system in which the receptor is expressed in cells where it would not normally be found. This enables isolation of the receptor from the complexity of the endogenous situation and the comparatively easy culturing of many cells for use in assays. A disadvantage of this method is that the receptor is often expressed at much higher levels than would be seen *in vivo*. Additionally, the receptor may be placed in a non-native environment with respect to signalling proteins, so the choice of host cell must be considered with care.

For this study, two transgenic Chinese Hamster Ovary cell lines were used. These are cells that are easily propagated and do not endogenously express NOP. The first of these cell lines, used for the studies reported in Chapter 2, stably expresses NOP at a high density. The second line, used in the remainder of the work, employs an inducible expression system, enabling the controlled variation of receptor density.

1.24 General Aims

The aims of this thesis were to test the following hypotheses:

1. Simple alterations to the structure and sequence of the nociceptin molecule produce radical changes in the effects upon the NOP receptor system.
2. Observed effects of a NOP ligand depend upon the receptor expression level of the cells in which it is tested.
3. Prolonged exposure of NOP to N/OFQ provokes changes in both the levels of receptors expressed and the response of the receptor system and may have effects at a genomic level upon the transcription of NOP mRNA.

The first of these hypotheses was tested, using a variety of biochemical assays, to pharmacologically characterise a range of NOP ligands using variations upon three templates:

Agonist – Both the native sequence of N/OFQ and that with amidation at the carboxyl terminus, the structure of which is shown in Figure 1.21.

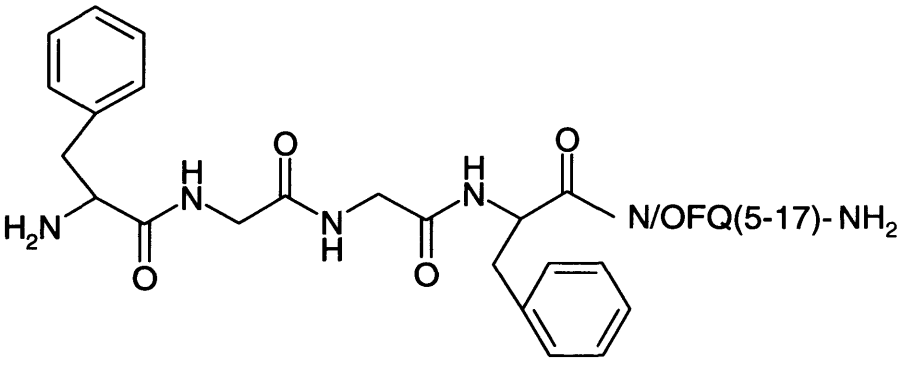

Figure 1.21 Structure of message sequence in the agonist template, amidated N/OFQ. Difference from native peptide shown in red.

Partial agonist – Alteration of the first peptide bond to incorporate a methylene group in the sequence of N/OFQ produces the partial agonist [Phe$^1\psi$Gly^2(CH_2-NH)]N/OFQ-NH_2, denoted [F/G], as depicted in Figure 1.22.

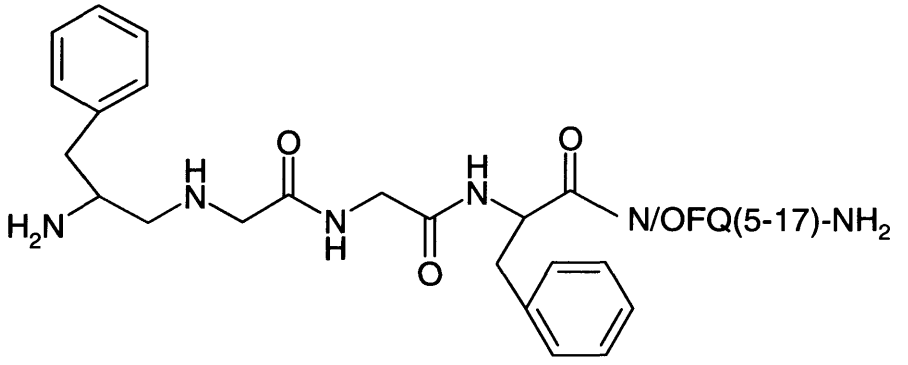

Figure 1.22 Structure of message sequence in the partial agonist template [F/G]. Difference from agonist template shown in red.

Antagonist – Modification in the initial phenylalanine residue, locating the side chain not on the alpha-carbon but at the terminal nitrogen removes all activity of the peptide, producing the antagonist [Nphe^1]N/OFQ(1-13)-NH_2. This is illustrated in Figure 1.23, with the alpha-carbon indicated.

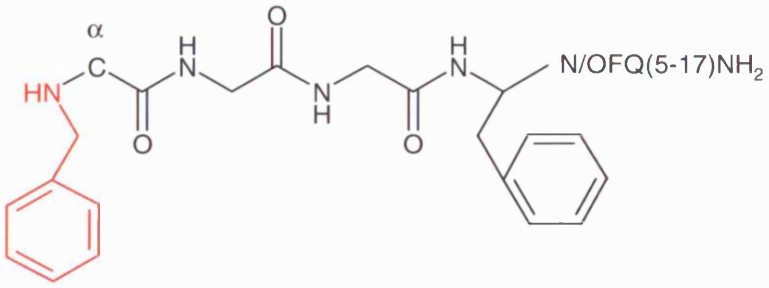

Figure 1.23 Structure of message sequence in the antagonist template [Nphe^1]N/OFQ-NH_2. Difference from agonist template shown in red.

The second hypothesis was tested using the same assays to characterise a cell line expressing human NOP in an inducible expression system and then use this system to investigate the role of receptor density in the perceived activity of the partial agonist [F/G] measured by these assays.

The third hypothesis was tested in the same inducible expression system by examining the effect of prolonged exposure to N/OFQ upon receptor expression and activity. The assays used for the previous chapters were again employed, with further investigation into the effect of desensitisation at a genomic level using Quantitative Real Time Polymerase Chain Reaction (Q-RT PCR).

2 Structure Activity Relationship Studies

2.1 Introduction

2.1.1 NOP, N/OFQ and the Message Address Concept.

As mentioned in the previous Chapter, the sequence of N/OFQ may be thought of in two domains – a message domain, responsible for receptor activation, containing the first four amino acids and an address domain, comprising the remaining amino acids, responsible for receptor recognition.

Deletion of the first residue in N/OFQ, phenylalanine (F) - denoted Phe^1, completely removes activity of the peptide (Dooley *et al.*, 1996). If arginine (R) is added to the N-terminus ([Arg^0]N/OFQ), affinity at NOP is not lost but an increase in KOP affinity is seen to the extent that a 150-fold decrease in selectivity occurs (Bobrova *et al.*, 2003). It would be presumed that the effect caused by this introduction would produce interference with hydrophobic interaction between the receptor binding site and the two phenylalanine residues (Phe^1 and Phe^4), but this would not seem to be the case.

The second and third positions are also sensitive to change in N/OFQ, as the substitution of arginine for the glycine (G) in position 3 causes a reduction in affinity of 8000 times. The substitution of the neutral amino acid asparagine (N) into this position renders the peptide inactive at NOP. Alteration of the sequence in N/OFQ shows some peculiar effects, for example the substitution of electronegative groups onto either of the phenylalanine residues at positions 1 and 4 (in the message sequence) may enhance the activity or remove it completely. Table 2.1 shows the effects of some alterations to these residues.

Table 2.1 Effects of alterations in the message sequence of N/OFQ(1-13)-NH_2.
Data are from CHO_{hNOP} cells, except: ($_m$) binding to mouse forebrain membranes (Bigoni *et al.*, 2002; Calo *et al.*, 2000a; Guerrini *et al.*, 2000a).

Ligand	Binding affinity pK_i		GTPγS stimulation pEC_{50}	cAMP inhibition pEC_{50}	Mouse vas deferens	Antagonist pA_2
N/OFQ(1-13)-NH_2	10.11	9.1_m	9.24	9.49	-	-
[Tyr^1]	-	8.3_m	-	-	7.6	-
[$Nphe^1$]	8.39	-	antagonist	antagonist	-	6.12
[(*p*F)Phe^4]	10.81	-	9.99	9.80	-	-
[Tyr^4]	8.45	-	6.61	6.87	-	-

It should be noted that the tyrosine (Y) substitution, as in [Tyr^1] and [Tyr^4]N/OFQ(1-13)-NH_2, is equivalent to *para*-hydroxy phenylalanine. When applied to the first position, this substitution results in a message domain common to the classical opioid ligands and produces a non-selective agonist with decreased activity at NOP (Calo *et al.*, 2000c; Guerrini *et al.*, 2001b). The results for the substitutions at residue four would appear to be contradictory in the first instance, as both fluorine and oxygen are electronegative elements and increase the hydrophilicity compared to the benzyl side chain of phenylalanine. So why should one enhance the agonist effect and the other decrease it? The answer might be the bulk of the atom concerned, both are much larger than hydrogen, but fluorine is not significantly different than oxygen, the two being adjacent in the periodic table. Also, the side chain of tyrosine is similar to phenol, which possesses acidic properties and this may explain the reason for the lack of activity.

The distance between the phenylalanine residues at positions 1 and 4 has been shown to be critical, as has the nature of any residues occupying the region between. For instance, alterations to the bonds in this part of the peptide, or the insertion of phenylalanine at either of positions 2 or 3 renders the peptide either inactive or with a significant decrease in activity (Calo *et al.*, 1998). The most radical example of altering ligand behaviour occurs in transferring the side chain from the α-carbon to the N-terminus in the first phenylalanine residue of the minimal agonist template. This produces an antagonist, denoted [Nphe^1]N/OFQ(1-13)NH_2, the nature of which would seem to reinforce the message/address concept as the total loss of activity derives solely from a change in the 'message' domain (Guerrini *et al.*, 2000a).

Alterations to the supposed address domain should only affect the affinity of a ligand. Making use of this effect by adding the basic amino acids arginine and lysine (K) to the end of the peptide, the analogue [Arg^{14},Lys^{15}]N/OFQ-NH_2 is created. This enhances ligand binding with a resulting increase in affinity and efficacy of agonists employing this modification (Rizzi *et al.*, 2002). The rationale of this is that a further repeat of arginine/lysine (these residues are seen at positions 8 and 9 and at positions 12 and 13) will enhance the effect of these basic amino acids. Combining the ideas of antagonist creation and enhanced receptor binding affinity led to the production of the commercially available antagonist known as UFP-101 which has the structure

[Nphe^1,Arg^{14},Lys^{15}]N/OFQ-NH_2. In this analogue both 'message' and 'address' domains are altered.

Alterations to the bonds within the peptide backbone lead to changes in activity of ligands and partial agonists may be produced by such modification. One such modification is a change of the initial peptide bond from the carbonyl to a methylene group to give [Phe$^1\psi$(CH_2-NH)Gly^2]N/OFQ(1-13)-NH_2, denoted [F/G] (Guerrini *et al.*, 1998; Okawa *et al.*, 1999). This effect may well be mediated by the introduction of either flexion or straightening at this bond due to a reduction in constraint by the oxygen atom of the peptide bond.

2.1.2 Dooley peptides

The so called 'Dooley peptides' comprise six residues with activity at NOP (Dooley *et al.*, 1997), the normal amino- and carboxyl-termini reversed for protection from exopeptidases. The sequences of these peptides are shown, together with data from assays for comparison with N/OFQ in Table 2.2. Although there is similarity to the address sequence, none of the residues corresponds to those in the message sequence of N/OFQ and yet these peptides show high potency, partial agonist activity with nanomolar affinity at NOP.

Table 2.2 Saturation binding, GTPγ[^{35}S] binding and cAMP inhibition data for the Dooley peptides. Data are for CHO cells transfected with mouse receptor (CHO_{mNOP}) for binding affinity and GTPγ[^{35}S] assays; rat receptor (CHO_{rNOP}) for cAMP assays (Dooley *et al.*, 1997).

Peptide	Binding affinity	GTPγ[^{35}S] binding		cAMP inhibition	
	pK_i	pEC_{50}	% max	pEC_{50}	% max
N/OFQ	9.37	8.40	100	8.84	84
Ac-RYYRWR-NH_2	9.22	8.66	52	9.28	75
Ac-RYYRWK-NH_2	9.15	8.68	57	9.28	58
Ac-RYYRIK-NH_2	8.82	8.29	30	8.94	62
Ac-RYYKWR-NH_2	8.83	8.11	49	8.71	68
Ac-RYYKWK-NH_2	9.14	8.17	52	9.01	66

Of these peptides, those showing greatest affinity and activity at NOP have arginine (R), tryptophan (W) or lysine (K) as the last three residues. Interestingly, those showing low affinity and potency are still capable of quite significant inhibition in the cAMP assay. Activity with isoleucine (I), an amino acid with a hydrophobic side chain, in the fifth position of one peptide may seem unexpected, although such properties may be similar to tryptophan (Berger *et al.*, 2000a). Tryptophan (W) is a bulky residue, the side chain

containing a hetero-cyclic carbon ring, not present in N/OFQ and not commonly seen in the classical opioid peptides. It is therefore puzzling as to what role (if any) it plays in these sequences – an unforseen effect which would not necessarily be inferred from traditional deductive chemistry and presents an advantage of the use of peptide libraries in screening large numbers of permutations of peptides. The sequences of the three sequences with highest activity at NOP are compared with N/OFQ in Figure 2.1.

UFP-101: H_2N-(Nphe)-GGFTG**ARK**SA**RKRK**-NH_2

Dooley peptide:
Ac-RYYRWR-NH_2
Ac-RYYRWK-NH_2
Ac-RYYRIK-NH_2

Figure 2.1 Comparison of UFP-101 and Dooley peptides.
Arginine/lysine pairs, thought to be responsible for receptor recognition and binding, in the address sequence of UFP-101 are indicated in bold. The same residues in the Dooley peptide sequences are underlined. Note that none of the Dooley peptides has a pair of these adjacent amino acids.

The lack of a terminal phenylalanine should render the Dooley peptides inactive according to strict interpretation of the message address concept. The fact that there is agonist activity would seem to indicate that the site of activation is elsewhere than the interaction site for the first four residues in the native peptide.

2.1.3 Synthetic/non-peptide ligands.

Morphine, the naturally occurring opioid that MOP is named after, is regarded as only a partial agonist by some but traditionally thought of as a full agonist as it shows the development of tolerance with chronic usage. This compound is plant-derived, not a peptide and is infamous for both its inherent potency and ability to produce tolerance (Connor, 2004). The structure of morphine contains hydroxyl, methyl and ether groups, which show similarity to the functional groups of the endogenous peptide MOP ligands, the endomorphins and enkephalins. Naloxone, an analogue of morphine is an antagonist at the three classical receptors and ineffective at NOP. Naloxone Benzoylhydrazone, a further analogue of naloxone, acts as a partial agonist at all, including NOP (Bigoni *et al.*, 2002).

Taking the similarity of structure as a basis for activity, what properties of the non-peptide N/OFQ ligands might be envisaged as the pharmacophores? Lack of effect of

the opioid antagonist naloxone is used as a defining characteristic of N/OFQ and the structure of this compound has similarities to morphine. In N/OFQ, the substitution [Tyr^1] gives a peptide that is active at the opioid receptors as well as retaining some activity at NOP, so what may be the site of action of naloxone in the opioids? The use of an analogy/model to enable visualisation of concepts, such as the function of a compound (in this case a peptide) may be very useful in the first instance but care and flexibility of thought must be exercised in the extrapolation of this as an idea to the actual situation in the case of newly discovered compounds. In general, the message address concept works well for the classical opioid receptors and their ligands but becomes confounded with the application of this concept to N/OFQ.

Thus the message/address concept, as applied to N/OFQ, forces the question – can potency and affinity be separated?

Under any circumstances, there cannot be potency without affinity but the affinity of a compound may not necessarily be an indication of its potency (or lack of), as seen for competitive antagonists. For agonists however, the separation of the two aspects of the pharmacology may not always be clear cut.

In terms of the receptor itself, the great similarity to the opioid receptors, whilst undeniable, can in large part be due to the majority of the structure involved in the transmembrane domains (Meunier, 1997). Small but significant differences in composition account for marked differences in behaviour whilst only contributing a small effect upon homology with other receptors. Perhaps more importantly, the extracellular ligand binding domain, a small part of the whole sequence, is crucial for the specificity of the receptor, whilst the intracellular G-protein associated domain may be relatively conserved between receptor types. The NOP-N/OFQ receptor system has already shown itself to be the 'awkward child' of the opioid receptor family, so why should it not continue to be 'awkward' in other aspects of its behaviour?

2.1.4 Experimental Rationale

The sequence of native N/OFQ, comprising seventeen amino acids, was used as a template to study the relationship between peptide structure and function. As detailed earlier in this thesis, the modification of residues can produce analogues with a variety

of affinities to and radically different activity at the receptor. Modifications to bonds of the peptide backbone can produce compounds with effects intermediate to those of full agonists and antagonists, often showing sub-maximal effects (decreased E_{max}) and/or lower potency (higher EC_{50}) compared to full agonists such as N/OFQ. Relocation of the sidechain of the initial phenylalanine (Phe^1) from the α-carbon to the terminal nitrogen produces an antagonist ([$Nphe^1$]N/OFQ(1-13)-NH_2) (Guerrini *et al.*, 2001a) that may be used as the template for further modification.

Adding electronegative elements, such as fluorine to the phenylalanine at position four (as in [(*p*F)Phe^4]N/OFQ-NH_2) results in enhanced potency. The incorporation of a further arginine/lysine (R/K) repeat at positions fourteen and fifteen ([Arg^{14}, Lys^{15}]N/OFQ-NH_2) can increase the binding affinity (Calo *et al.*, 2000a). For protection against metabolic degradation, amidation at the carboxyl terminus and the incorporation of amino acids able to form disulphide bonds within the sequence may be useful. In this chapter, amidation and truncation are dealt with first, then modification of the message motif, followed by alterations to the address motif and then combinations of the two.

2.2 Aims

The aims of this chapter are to examine the effects of the modifications to the message and address domains in:

- Full agonist template – N/OFQ
- Partial agonist template – [F/G]N/OFQ
- Antagonist template – [$Nphe^1$]N/OFQ

In particular, the use of [(*p*F)Phe^4] in the message and [Arg^{14},Lys^{15}] in the address sequences.

The amendments to the structures of these latter modifications, compared to the native sequence, are shown in Figures 2.13 and 2.16, in the appropriate sections.

2.3 Materials and Methods

In this thesis, common methodologies are described here with those more specific to a chapter described within that chapter.

2.3.1 Reagents

Materials were obtained from suppliers as follows:

General reagents

BSA, Calcium chloride, DTT, EDTA, EGTA, GDP, Glucose, GTP, GTPγS, HEPES, Hydrochloric acid, Magnesium sulphate, PEI, Pertussis toxin (PTx), Potassium chloride, Potassium dihydrogen phosphate, Sodium chloride, Sodium hydroxide, Tris-HCl – SIGMA-ALDRICH Co. Ltd, Poole, Dorset, UK or Fisher Scientific UK Ltd, Loughborough, Leicester, UK.

Cyclic Adenosine Monophosphate (cAMP) assay reagents

CyclicAMP, Forskolin, 3-isobutyl-1-methyl xanthine (IBMX) – SIGMA-ALDRICH Co. Ltd, Poole, Dorset, UK.

Activated charcoal – BDH, Poole, Dorset, UK.

Peptidase inhibitors

Amastatin, Bestatin, Captopril, Phosphoramidon – SIGMA-ALDRICH Co. Ltd, Poole, Dorset, UK.

Protease inhibitor

Bacitracin – SIGMA-ALDRICH Co. Ltd, Poole, Dorset, UK.

Radiolabelled Compounds

GTPγ[^{35}S] kBq.ml^{-1} (Ci.mmol^{-1}); Adenosine 3',5'-cyclic phosphate, ammonium salt, [2,8-^{3}H], 37MBq.ml^{-1} (29-32Ci.mmol^{-1}) – PerkinElmer Life Sciences Inc. Boston, MA, USA.

[*leucyl*-^{3}H]N/OFQ, 740kBq.ml^{-1} (145-155Ci.mmol^{-1}) – Amersham Pharmacia Biotech UK Ltd, Buckinghamshire, UK.

Scintillation fluids

'HiSafe3', OptiPhase Safe – Fisher Scientific UK Ltd, Loughborough, Leicester, UK.

Cell culture media

Dulbecco's MEM, Foetal bovine serum (FBS), Fungizone, Geneticin (G418), HAM-F12, Hygromycin B, Penicillin/streptomycin, Trypsin/EDTA – Invitrogen Ltd, Paisley, Scotland, UK.

Cell culture flasks and assay plates – Nalgene Nunc International, Denmark or Greiner, Germany.

Ligands used were either peptides synthesised and supplied by The University of Ferrara, Italy, or non-peptide compounds supplied by The University of Ferrara, Roche or SIGMA-ALDRICH Co. Ltd, Poole, Dorset, UK.

The Chinese hamster ovary cell line, expressing human NOP (CHO_{hNOP}), was kindly supplied by GlaxoSmithKline, Stevenage, Hertfordshire, UK.

2.3.2 Buffer Composition

Harvest Buffer – 154mM NaCl, 10mM HEPES, 1.71mM EDTA, to pH7.4 with NaOH

Receptor Binding Assay

Wash Buffer - 50mM Tris-HCl, 5mM $MgSO_4$, to pH7.4 with KOH.

Assay Buffer – 1% w/v BSA in Wash Buffer.

Stimulated GTPγ[^{35}S] Binding Assay

Radiolabel Reconstitution Buffer - 50mM Tris-HCl, 10mM DTT, to pH7.4 with NaOH.

Homogenisation Buffer - 50mM Tris-HCl, 200μM EGTA, to pH7.4 with NaOH.

Assay Buffer - 100mM NaCl, 50mM Tris-HCl, 1mM $MgCl_2$, 200μM EGTA, to pH7.4 with NaOH.

cAMP Assay

Krebs'/HEPES Wash Buffer – 143mM NaCl, 10mM HEPES, 12mM Glucose, 4.7mM KH_2PO_4, 1.2mM KCl, 2.6mM $CaCl_2$, 1.2mM $MgSO_4$, to pH7.4 with NaOH

Suspension Assay Buffer - 0.5% BSA in Krebs/HEPES as above.

cAMP Assay Buffer - 50mM Tris-HCl, 4mM EDTA, to pH7.4 with NaOH.

Charcoal Suspension - 250mg activated charcoal, 100mg BSA in 25ml cAMP assay buffer.

cAMP Binding protein

Stock extract prepared from bovine adrenal glands obtained from a local slaughterhouse.

Working solution - 0.5ml stock extract in 9.5ml cAMP assay buffer,

2.3.3 Culture media

CHO_{hNOP} cells were cultured in F-12/Dulbecco's MEM (50:50) supplemented with 5% FBS, Penicillin/Streptomycin ($100U.ml^{-1}$) and Fungizone ($2.5\mu g.ml^{-1}$). Stock culture flasks contained media as detailed above, supplemented with selection agents Geneticin G418 ($200\mu g.ml^{-1}$), to maintain the NOP-containing plasmid and Hygromycin B ($200\mu g.ml^{-1}$) to maintain a reporter gene plasmid not used in this study.

2.3.4 Cell culture

For general propagation of cells and seeding of flasks for experimental purposes, after removal of spent medium, confluent cultures were treated with trypsin/EDTA (trypsinised) to detach the cells from culture vessel surface. Once cells were detached, the trypsin was neutralised by addition of fresh medium (see section 2.2.3) and the resulting suspension centrifuged at 437xg for 2 min (Heraeus Instruments Labofuge 400R). The supernatant was decanted, the cell pellet resuspended in fresh medium and appropriate volumes of suspension pipetted into flasks of fresh medium. Cell cultures were incubated at 37°C in 5% CO_2, humidified air.

2.3.5 Saturation Binding Assay

Theory

An initial step in the investigation of the interaction of a ligand and its receptor is to determine the affinity between the two. This may be accomplished using a saturation binding assay in which increasing levels of a radiolabelled ligand are added to a suspension of cell membrane until saturation is reached. By calculating the radioactivity bound to receptors as a fraction of that added, a binding profile may be established from which the maximum binding (indicating receptor density) and the affinity of the ligand for the receptor can be determined (Bylund *et al.*, 1993; Keen, 1997).

The assay results yield disintegrations per minute for total bound and non-specific binding (NSB) of labelled ligand. Total binding is the result of the ligand binding to all possible sites present and includes non-specific binding to sites other than the receptor of interest. Within the limits of the assay, NSB is non-saturable and increases linearly with ligand concentration. Values for NSB are subtracted from total binding to determine specific binding to the receptor. Typically, results are plotted as ligand bound vs ligand concentration and take the form of Langmuir isotherms. A stylised profile for a saturation binding assay, showing total, NSB and specific binding isotherms, is shown in Figure 2.2.

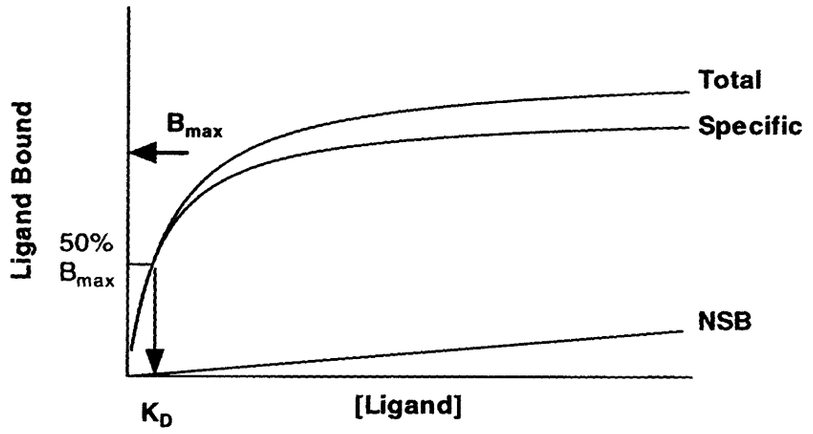

Figure 2.2 Saturation plot of disintegrations per minute (dpm) bound vs ligand concentration.
Graph shows total binding, non-specific (NSB) and specific binding (= Total - NSB). Specific binding saturates when all receptors of interest are occupied, giving an approximation for maximal binding, B_{max}. NSB follows a straight line.

The values for labelled ligand bound (dpm) may be expressed as a measure of receptor density using a conversion factor based upon the specific activity (s.a.) of the labelled

ligand. From the amount of protein added to each tube of the assay, a further calculation gives the receptor density as a fraction of total protein.

i) Conversion of s.a. to $dpm.nM^{-1}$

$$\frac{\text{radiolabel s.a.} \times 3.7 \times 10^{10} \times 60 \times 10^{-6} \times \text{assay vol.}}{1000} = \text{dpm.nM}^{-1}$$

Note on units: s.a. in $Ci.mmol^{-1}$; assay volume in ml.

ii) Expression of receptor density as a fraction of total protein.

$$\frac{\text{dpm bound} \times 1000 \times \text{assay vol.} \times 1000}{(\text{dpm.nM}^{-1}) \times (\mu\text{g protein.tube}^{-1})} = \text{fmol/mg protein}$$

Note: assay volume in ml.

Maximum specific binding, B_{max}, gives an indication of the receptor density in the membranes. The value for B_{max} derived from a plot such as that in Figure 2.2 is not reliable as the maximum is only approached asymptotically. By transforming the ligand concentration into logarithmic form a sigmoid curve of specific binding is produced, from which B_{max} is derived. This is shown in figure 2.3. This analysis is used throughout this thesis.

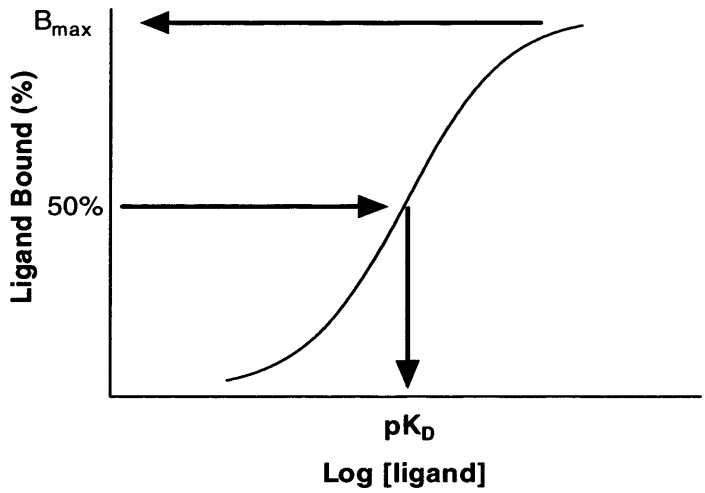

Figure 2.3 Sigmoid plot of receptor density vs log ligand concentration.
Maximum binding may be determined from this curve, as may the pK_D and thus the K_D.

The equilibrium dissociation constant, K_D, is the concentration of ligand occupying 50% of the receptors available (half B_{max}) and can be derived from a Langmuir plot or, more accurately, as a pK_D from a semi-logarithmic plot as in Figure 2.3. With reference to this value, properties of other, non-labelled ligands may be determined in a displacement assay, described later.

Method

Confluent cell cultures were treated with harvest buffer to detach cells, spun once to clean and membrane suspension prepared by resuspending cell pellet in wash buffer, homogenising (Ultra-turrax) and centrifuging (20375xg, 10min, 4°C). The homogenisation process was repeated twice and the pellet resuspended in a minimal volume of wash buffer, the protein content was then determined using Folin phenol reagent (Lowry *et al.*, 1951). The suspension was diluted with assay buffer to an appropriate concentration and a cocktail of peptidase inhibitors (amastatin, bestatin, captopril and phosphoramidon – 10μM each) was then added to prevent degradation of peptide ligands. Volumes of 100μl suspension (corresponding to 20μg protein.tube^{-1}) were incubated (1hr, room temperature) with a doubling dilution series of radiolabelled nociceptin (1pM-2nM). Non-specific binding was determined in the presence of 1μM unlabelled nociceptin. The contents of the assay tubes are shown in Table 2.3.

Table 2.3 Contents of Tubes for Saturation Binding Assay.
All volumes are μl.

Tube	Binding Buffer	NSB (1μM N/OFQ)	[*leucyl*-^{3}H]N/OFQ (1pM-2nM)	Membrane suspension
Total	300	-	100	100
NSB	200	100	100	100

Reaction was terminated by rapid vacuum filtration through glassfibre filters (Whatman GF/B), pre-soaked in 0.5% PEI to reduce non-specific binding, using a Brandel vacuum harvester, trapping bound radioactivity. Filter discs were transferred to polypropylene vials, 4.5ml Optiphase safe scintillation fluid added, allowed to extract for 8h and radioactivity counted (3min) in a scintillation counter (Packard 1900TR).

2.3.6 Displacement (Competition) Binding Assay

Theory

A variation on the binding assay enables the relative affinities of two compounds (one radiolabelled) to be compared and is known as a displacement or competition binding assay. Since not all ligands are available in labelled form and cannot therefore be used in a simple saturation assay, the displacement assay enables the affinity of an unlabelled ligand to be inferred from its ability to displace a labelled ligand. This unlabelled ligand is termed the displacer or competitor (Bylund *et al.*, 1993; Keen, 1997).

The two ligands are used simultaneously, the labelled at a fixed concentration and the other at increasing concentrations, such that the labelled ligand is displaced from the receptor. The results may be plotted as percent radioactivity bound against free radiolabel added, provided that the amount bound is no more than 10% of that added, and give a decreasing sigmoid curve, shown in Figure 2.4.

When the results are plotted as percent displacement versus logarithm of ligand concentration the result is a sigmoid curve, whose position along the x-axis varies with affinity of displacer and affinity and concentration of radiolabelled ligand. A typical displacement curve is shown in Figure 2.5.

iii) Derivation of percentage displacement for a competitive binding experiment.

$$\% \text{ Displacement} = \frac{\text{Total}_{(\text{Specific})} - \text{Displacer}_{(\text{Specific})}}{\text{Total}_{(\text{Specific})}} \times 100$$

From the results of such an experiment, a value for the concentration at which 50% of the radiolabel is displaced (IC_{50}) can be determined which depends upon the concentration of radiolabel used. The inhibition constant for a ligand may be calculated from the Cheng-Prusoff equation, shown below (Cheng *et al.*, 1973). This is an estimate of the affinity for the receptor and is an absolute number for that compound. This value is termed K_i and represents the concentration of ligand at which half of the receptors would be occupied in the absence of radioligand.

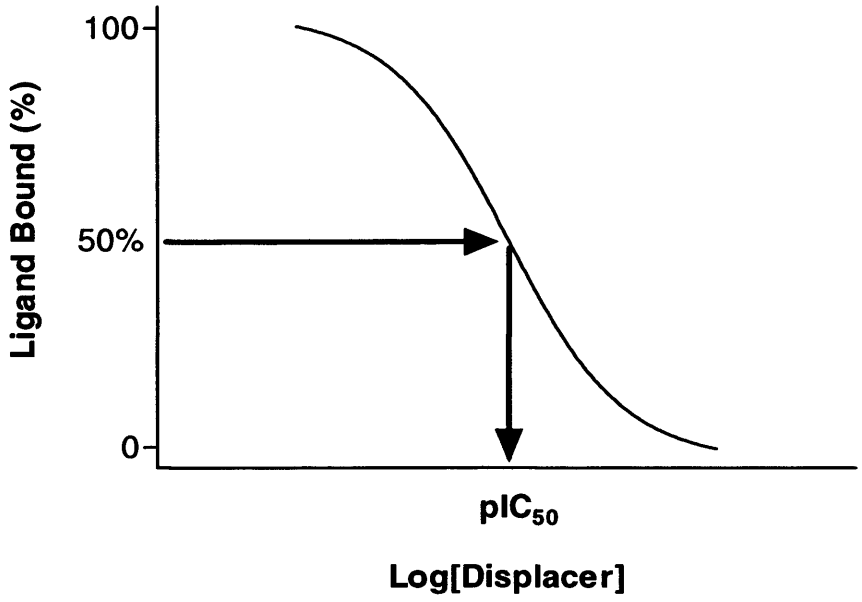

Figure 2.4 Sigmoid plot of ligand bound vs ligand concentration for displacement assay.
Note that bound ligand decreases with increase in displacer concentration. The data may be transformed to give the plot shown in Figure 2.7.

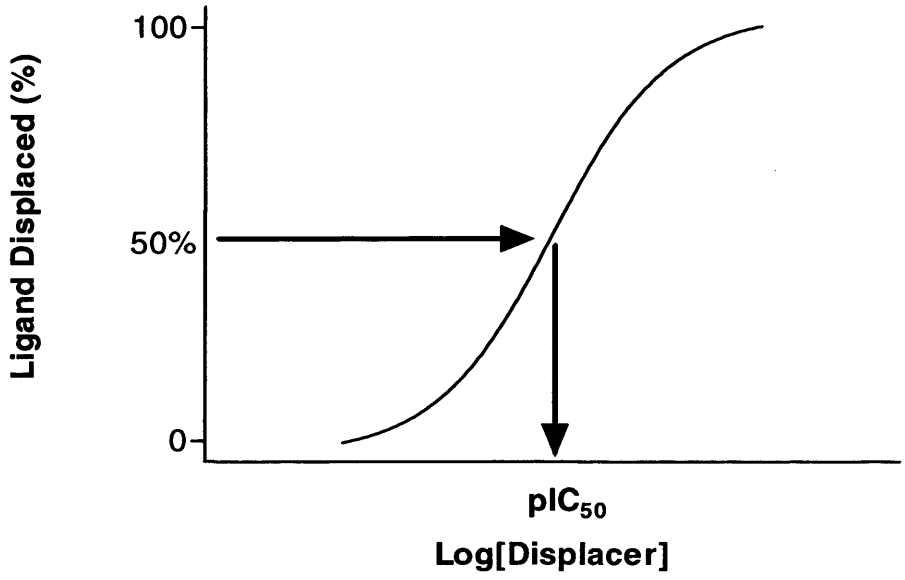

Figure 2.5 Sigmoid plot of % displacement vs ligand concentration for displacement assay.
Note that as the concentration of radioligand increases, the displacement curve would shift rightwards. Therefore, IC_{50} derived from this graph depends upon the radiolabelled ligand concentration and may be converted to the K_i using the Cheng-Prusoff equation.

iv) Cheng-Prusoff equation.

$$K_i = \frac{IC_{50}}{1 + \left(\frac{[L]}{K_D}\right)}$$

Where: IC_{50} is the concentration of ligand at which 50% of the specific binding is displaced; $[L]$ represents the free radioligand concentration added to the assay; K_D is the dissociation constant of the radioligand, determined from saturation binding studies.

Method

Membrane suspension was prepared as for the saturation assay and incubated (1h, room temperature) with a fixed concentration of labelled N/OFQ (≈ 0.2nM) and a dilution series of unlabelled ligand as displacer (10fM-10μM, as appropriate). NSB was determined in the presence of 1μM unlabelled N/OFQ. Protein content of membrane suspension added (≈ 20μg.tube^{-1}) was determined in the same manner as for saturation binding studies. The contents of reaction tubes are shown in Table 2.4.

Table 2.4 Contents of Tubes for Displacement Binding Assay.
All volumes are μl.

Tube	Binding Buffer	NSB (1μM N/OFQ)	Displacer	[*leucyl*-^{3}H]N/OFQ (200pM)	Membrane suspension
Total	300	-	-	100	100
NSB	200	100	-	100	100
Displacer	200	-	100	100	100

Incubation, harvesting and scintillation counting were as for saturation binding studies.

2.3.7 GTPγ[^{35}S] Binding Assay

Theory

A further step in the investigation of GPCRs from saturation binding may be taken by studying the activation of the coupled G-protein by the receptor. As this assay involves the functional aspects of the system, it enables distinction to be made between agonists and antagonists, whereas binding assays usually only give data on affinity of ligands for the receptor, regardless of their effect upon it (Berger *et al.*, 2000b; Lazareno, 1997).

This assay concentrates upon the step immediately downstream from the receptor and analyses the level of activation of the G-protein by the agonist-bound receptor. The α-

subunit of the G-protein exchanges GDP for GTP, provoking dissociation of this trimeric protein into the GTP-bound α-subunit and a dimer comprising the β- and γ-subunits. The principle behind this assay is that substition of a non-hydrolysable analogue of GTP, such as the sulphur-containing GTPγS prevents the intrinsic catalytic activity of the α-subunit from converting the GTP back to GDP, thus remaining in the 'active' state. By incorporating radiolabelled sulphur in this analogue, the accumulation of GTPγS bound to the G-protein α-subunit may be quantified by measuring the bound radioactivity after a set time period. Figure 2.6 shows a representation of GTP and its analogue GTPγS.

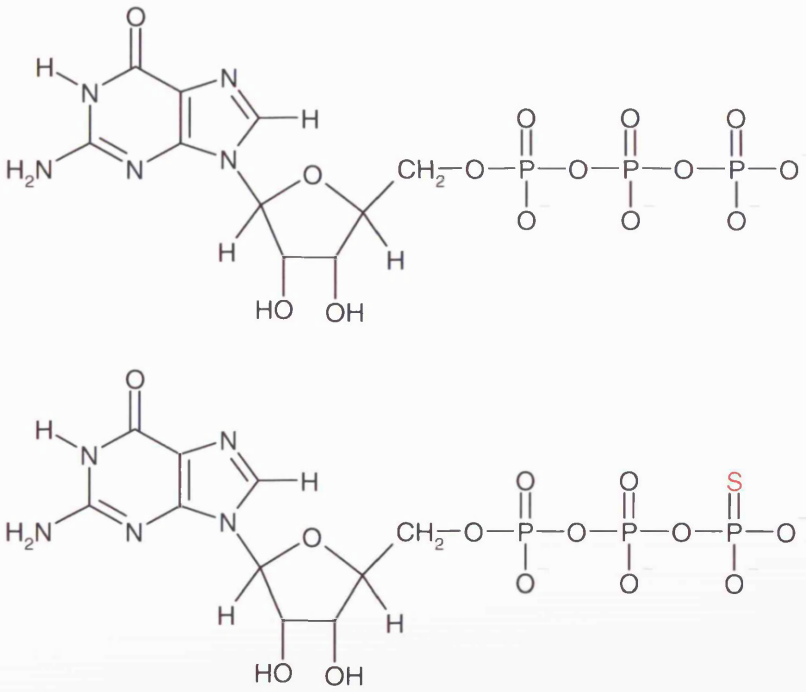

Figure 2.6 The structures of GTP (above) and its stable analogue GTPγS (below).
The difference between the two compounds, the thio-group, is highlighted and this would be the location of the radiolabel in GTPγ[^{35}S].

The results of an experiment are collected as dpm for bound radioactivity. These are then expressed as stimulation factor via the calculation shown below.

v) Stimulation Factor calculation.

$$StimulationFactor = \frac{dpm(Sample) - dpm(NSB)}{dpm(Total) - dpm(NSB)}$$

The stimulation factors for each run of tubes are then graphed and a sigmoid dose-response curve should result as shown in Figure 2.7. From this may be calculated the maximum stimulation, or efficacy (E_{max}) and the potency (pEC_{50}) for that ligand.

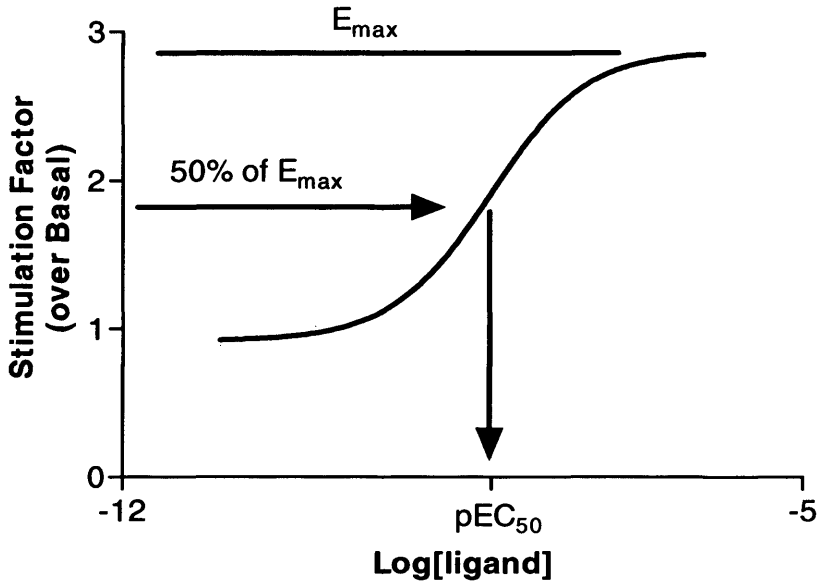

Figure 2.7 Stimulation factor vs ligand concentration for stimulated GTPγ[^{35}S] binding.

Method

As described previously, confluent cell cultures were detached from their substrate using harvest buffer and centrifuged (430xg, 2min) to clean them of media and debris. Membrane homogenate was then prepared and the final pellet resuspended in GTPγ[^{35}S] assay buffer (≈ 2ml, without BSA). Protein was determined as previously described and where appropriate the membrane suspension was further diluted with GTPγ[^{35}S] assay buffer to give a final protein level of approximately 200μg.ml^{-1}, equating to 20μg per tube in the assay. Homogenates were incubated with serial ten-fold dilutions of ligand, in the presence of radio-labelled GTPγ[^{35}S], with 0.1% BSA, 100μM GDP, 10μM peptidase inhibitor cocktail (as described previously) and 150μM bacitracin. Non-specific binding was determined in the presence of 10μM GTPγS. Membrane suspension was added last of all to start the assay. Contents of tubes are detailed in Table 2.5.

Tubes were incubated at 30°C, with gentle agitation, for 1h before harvesting by vacuum filtration through dry Whatman GF/B filters. Bound radiolabel was determined, after 8h extraction in Optiphase safe, by scintillation counting and results expressed as binding stimulation above basal. Antagonist potency may be derived from a competitive assay in which a constant amount of antagonist is used to displace a varying concentration of agonist. The contents of tubes for such an assay is shown in Table 2.6.

Table 2.5 Contents of tubes for GTPγ[^{35}S] binding assay.

Content (µl)	Assay buffer	BSA	Bacitracin	PI	GDP	GTPγ[^{35}S]	GTPγS (10µM)	Ligand	Membrane suspension
Total	220	20	20	20	20	100	-	-	100
NSB	200	20	20	20	20	100	20	-	100
Ligand	200	20	20	20	20	100	-	20	100

Table 2.6 Contents of tubes for GTPγ[^{35}S] binding antagonist competition assay.

Content (µl)		Assay buffer	BSA	Bacitracin	PI	GDP	GTPγ[^{35}S]	GTPγS (10µM)	Ligand	Antagonist	Membrane suspension
Control	Total	220	20	20	20	20	100	-	-	-	100
	NSB	200	20	20	20	20	100	20	-	-	100
	Ligand	200	20	20	20	20	100	-	20	-	100
Antagonist	Total	200	20	20	20	20	100	-	-	20	100
	NSB	180	20	20	20	20	100	20	-	20	100
	Ligand	180	20	20	20	20	100	-	20	20	100

2.3.8 Adenylyl Cyclase Inhibition - cAMP Assay

Theory

A second messenger affected by the N/OFQ-NOP system is cAMP (see General Introduction), the formation of which may easily be assayed. The assays described previously require the preparation of cell membrane suspensions before use, whereas assay of cAMP formation may be made using whole cells in a two-step process. First, a suspension of live cells is allowed to accumulate cAMP whilst being exposed to a varying concentration of ligand in the presence of forskolin. Forskolin stimulates adenylate cyclase to produce cAMP, which may be inhibited by the action of a NOP ligand of interest. Enzymatic degradation of cAMP is prevented by use of 3-isobutyl-1-methyl xanthine (IBMX). Synthesis of cAMP is stopped and the cells lysed after incubation. A competitive binding assay is then performed between the cAMP formed by the cells and a fixed amount of radiolabelled cAMP. This measures the level of cAMP formed compared to a standard curve and the inhibition of cAMP formation may then be calculated using the formula shown below.

vi) Calculation of cAMP Inhibition.

$$Percentage\ Inhibition = \frac{\left(cAMP_{Forskolin} - cAMP_{Sample}\right)}{\left(cAMP_{Forskolin} - cAMP_{Basal}\right)} \times 100$$

From these results, the effect of a ligand upon the formation of cAMP may be determined as potency (pEC_{50}), the negative logarithm of the ligand concentration giving half maximal inhibition and efficacy (E_{max}).

Method

Confluent cell cultures were removed from flasks with harvest buffer and centrifuged (437xg, 2min, room temperature) to clean cells. After discarding the supernatant, the pellet was resuspended in Krebs/HEPES wash buffer and spun again. This was repeated and the pellet finally resuspended in 2.2ml assay buffer, from a 75cm^2 flask, per assay set. In each assay tube, 200µl cell suspension, in a total volume of 300µl, was incubated (37°C, 15min, with gentle agitation) in presence of 1mM IBMX (dissolved in wash buffer, no BSA, at 50°C prior to use). For agonist assays, the effect of 1µM forskolin with a dilution series of the ligand of interest (all in assay buffer) was examined.

Peptidase inhibitors are known to be unnecessary in this assay (Hashimoto *et al.*, 2000). Details of the contents of the assay tubes are shown in Table 2.7.

Table 2.7 Contents of tubes for cAMP inhibition assay.
All volumes in µl.

Tube label	Assay buffer	Forskolin (1µM)	Agonist (0.1pM-10µM)	IBMX (1mM)	Cells
Basal	60	-	-	40	200
Forskolin	40	20	-	40	200
Agonist	20	20	20	40	200

Accumulation of cAMP was stopped by addition of 20µl 10M HCl, then neutralised with 20µl 10M NaOH and buffered to pH7.4 with 200µl 1M Tris-HCl. Tubes were vortexed between each step. Reaction tubes were then spun (5min, 16100xg, room temperature) to clear cellular debris. At this point the assay can either be continued or the samples frozen (-20°C) for assay at a later time.

To continue, 50µl supernatant was incubated (4°C, >2.5h) with 100µl [^{3}H]cAMP (in ratio of 1µl stock to 2.5ml assay buffer) and 150µl binding protein in a competitive binding assay, with previously prepared cAMP standards (0-10pmol.50µl^{-1}, plus NSB at 250pmol.50µl^{-1}, all in cAMP assay buffer) used to establish a calibration curve for bound cAMP. A typical calibration curve is shown in Figure 2.8. Where necessary, samples were pre-diluted with cAMP assay buffer, to ensure bound radiolabel lay within the standard curve.

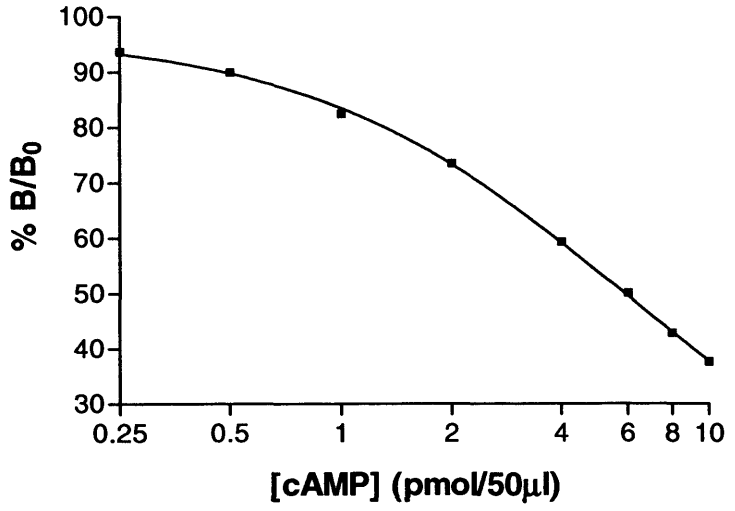

Figure 2.8 Calibration curve for cAMP competitive binding assay.
Plot shows "% B/B_0" (dpm bound ÷ dpm bound in absence of cAMP x 100) vs log cAMP concentration, expressed as pmol/50µl.

After incubation, 250µl charcoal suspension was added, the tubes allowed to stand (1min) then centrifuged (1min, 16100xg, room temperature) to remove unbound cAMP. Bound radioactivity was measured by removal of 200µl supernatant to which 1ml "HiSafe3" scintillation fluid was added and mixed. Bound radioactivity was counted (3 $min.tube^{-1}$) by scintillation counter (Packard 1900TR) and the results interpreted via an internal program (Riasmart).

Antagonist assays

To further determine the relative affinity of an antagonist in a functional assay, either a single or a series of dilutions of the ligand may be made and used as antagonist in a functional assay such as cAMP. If a single ligand concentration is used, the value arrived at is known as the pK_B for that compound and is derived using the Gaddum equation.

vii) Derivation of Antagonist Dissociation Constant – Gaddum Equation.

$$pK_B = \log(CR - 1) - \log[\text{antagonist}]$$

Where:
CR, the concentration ratio, is the concentration of agonist producing a 50% response in the presence of antagonist divided by the concentration of agonist producing the same response in the absence of antagonist. [antagonist] is the concentration of antagonist used in the assay.
For this method, it is assumed that the slope of the regression line is unity.

For a purely competitive antagonist, a plot of log(concentration ratio-1) vs log(ligand concentration) at several concentrations of antagonist, known as a Schild plot (Lazareno *et al.*, 1993), will result in a straight line with slope of unity, the x-intercept giving a value known as the pA_2 for that compound. This is the concentration of antagonist producing a two-fold rightward shift in the concentration-response curve. This value is theoretically equal to the pK_D for the ligand, and should also be equal to the pK_i. Competitive antagonism assays were performed using both NOP-selective and non-selective antagonists, giving an indication of relative affinity of ligands for NOP. In these cases, the volume of assay buffer was reduced to compensate for the volume of antagonist added. This is illustrated in Table 2.8.

Table 2.8 Contents of tubes for competitive antagonist assay.
All volumes are µl. Control assay (without antagonist) allows shift to be determined.

Tube	Assay buffer	Forskolin (1µM)	Agonist (0.1pM-10µM)	Antagonist (100nM-1µM)	IBMX (1mM)	Cells
Basal	60	-	-	-	40	200
Forskolin	40	20	-	-	40	200
Agonist	20	20	20	-	40	200
Basal + Antagonist	40	-	-	20	40	200
Forskolin + Antagonist	20	20	-	20	40	200
Agonist + Antagonist	-	20	20	20	40	200

Assays with Pertussis Toxin (PTx)

To confirm the coupling of the receptors to G_i-proteins, 100ng/ml PTx (see Introduction) was added to cell culture media 20 hours prior to assay. It is known that PTx inhibits activity of both G_i and G_o coupled receptors by ribosylation of the α–subunit (Katada *et al.*, 1981) and we have used this concentration and duration as previously reported to abolish $G_{i/o}$ mediated events (Okawa *et al.*, 1999).

2.3.9 Data Analysis

Unless otherwise stated, all data are mean±s.e.mean for (n) experiments.

Saturation and Displacement Binding Assays

Results were processed by spreadsheet (MS Excel) and analysed using graphical software (Graphpad Prism v3.0, San Diego, CA, USA) to show saturation curves and sigmoid binding curve (variable slope) for each ligand. From these the values for B_{max} and K_D were derived. In displacement curves, IC_{50} values were corrected according to Cheng and Prusoff to yield K_i, as described earlier.

GTPγ[^{35}S] Binding Assays

Results were processed by spreadsheet (MS Excel) and analysed using graphical software (Graphpad Prism v3.0, San Diego, CA, USA) to produce a sigmoid plot of stimulated binding over basal. Results were expressed as maximal stimulation of binding (E_{max}) and potency (pEC_{50}).

cAMP Assays

Results were processed by spreadsheet (MS Excel) to determine percent inhibition of forskolin-stimulated cAMP formation, after deduction of basal, then analysed using graphical software (Graphpad Prism v3.0, San Diego, CA, USA) to give a sigmoid plot (variable slope) of cAMP inhibition vs ligand concentration. From this the values for maximal effect (E_{max}) and negative logarithm of ligand concentration at half-maximal effect (pEC_{50}) were derived.

Where an assay of competitive antagonism was made with only one concentration of antagonist a value for pK_B was obtained, assuming a slope of unity. For functional assays, following Schild analysis, calculation of values for slope and pA_2 were made using linear regression (Graphpad Prism v3.0, San Diego, CA, USA). Data were analysed statistically using analysis of variance (ANOVA) followed by t-tests with Bonferroni correction or simple t-tests, paired or unpaired, as appropriate. Whilst power calculations were not performed for the experiments described in this thesis, such evaluation may have been useful based on the relatively low number of repeats performed in some experimental paradigms. This would strengthen any "negative" conclusions made that could have occurred due to low sample size.

2.4 Results

2.4.1 Saturation studies of N/OFQ binding to CHO_{hNOP} membranes

The binding of [*leucyl*-^{3}H]N/OFQ to CHO_{hNOP} membranes is concentration-dependent and saturable. The laboratory "standard values" (B_{max}=1913fmol.mg^{-1} protein, pK_D=10.15) are used throughout this chapter in Cheng-Prusoff estimations of displacer affinity (Hashiba *et al.*, 2002).

2.4.2 Basic Amidation and Truncation

The substitution of an amide group in place of the terminal carboxyl group would be predicted to protect this part of the molecule from degradation (Calo *et al.*, 1996). The binding of N/OFQ, and N/OFQ-NH_2 produced a concentration-dependent displacement of [*leucyl*-^{3}H]N/OFQ binding to CHO_{hNOP} membranes, Figure 2.9, yielding pK_i values as shown in Table 2.9. As can be seen there was a two-fold increase in binding affinity, maintained with truncation to N/OFQ(1-13)-NH_2 and this is consistent with the published literature (Guerrini *et al.*, 1997).

In assays of functional potency using CHO_{hNOP} there was no appreciable change in efficacy following amidation or truncation. A slight decrease in potency was seen for the truncated compound in cAMP assays, but this remained a full agonist. Results of cAMP inhibition assays are shown in Figure 2.10.

Table 2.9 Displacement and GTPγ[^{35}S] binding at CHO_{hNOP} membranes and cAMP inhibition in whole CHO_{hNOP} cells for N/OFQ, N/OFQ-NH_2 and N/OFQ(1-13)-NH_2.
Where ANOVA test ($p<0.05$) indicated, *denotes significant difference from reference compound, N/OFQ-NH_2, using Bonferroni correction.
Data are mean±s.e.mean for (n) experiments. (Data in italics courtesy J. McDonald).

Ligand	Displacement Binding	GTPγ[^{35}S] Binding		cAMP Inhibition	
	pK_i	pEC_{50}	Maximum stimulation, E_{max}	pEC_{50}	Maximum Inhibition, E_{max} (%)
N/OFQ	9.91±0.04	*8.75±0.11*	*10.20±0.79*	9.86±0.13 (4)	103.0±0.6
N/OFQ-NH_2	10.31±0.04*	*8.98±0.08*	*10.98±1.30*	9.94±0.04 (4)	103.0±1.4
N/OFQ(1-13)-NH_2	10.24±0.09*	*8.94±0.01*	*11.19±0.48*	9.96±0.07 (3)	102.8±1.0

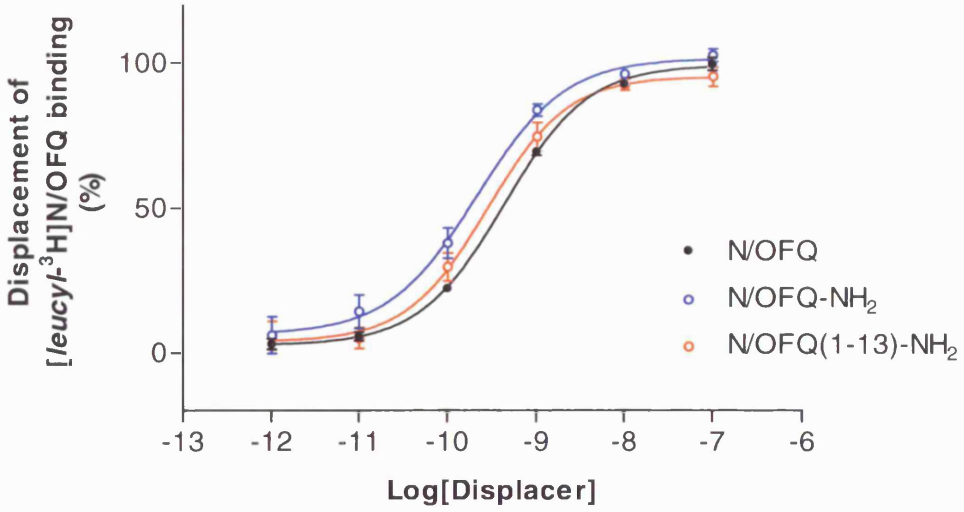

Figure 2.9 Displacement binding curves for N/OFQ, N/OFQ-NH_2 and N/OFQ(1-13)-NH_2 against [*leucyl*-^{3}H]N/OFQ in CHO_{hNOP} membranes.
Data are from n=4 experiments, except N/OFQ(1-13)-NH_2 (n=3).

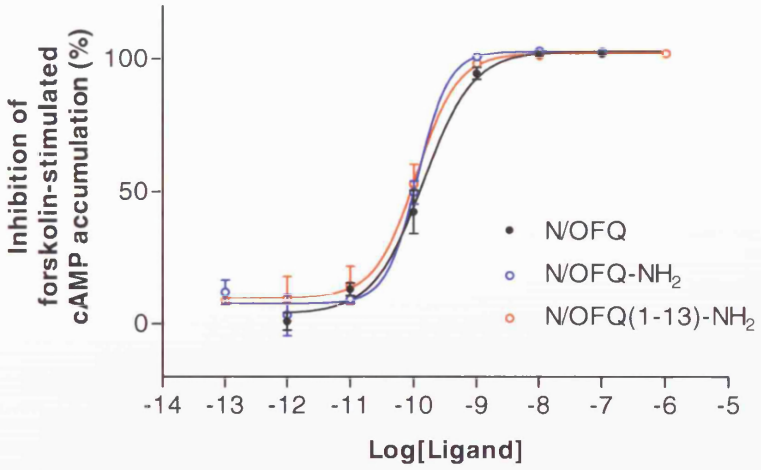

Figure 2.10 cAMP Inhibition curves for N/OFQ, N/OFQ-NH_2 and N/OFQ(1-13)-NH_2 in whole CHO_{hNOP} cells.
Data are from n=4 experiments, except N/OFQ(1-13)-NH_2 (n=3).

2.4.3 Alterations to the Message Motif – Creating Partial Agonists and Antagonists

The results for assays performed upon templates bearing these modifications are shown in Table 2.10, with displacement binding and cAMP inhibition curves shown in Figures 2.11 and 2.12. All peptides displaced labelled N/OFQ in a competitive and saturable manner. There was a progressive loss of binding affinity following [F/G] and [Nphe^1] alterations. In GTPγ[^{35}S] binding and cAMP inhibition studies there was a corresponding loss of functional potency following [F/G] and [Nphe^1] substitution. In addition, in the upstream GTPγ[^{35}S] binding assay both full and truncated [F/G] derivatives behaved as partial agonists with maximal stimulation values of approximately 4.6 and 7.8, respectively. However, in the amplified cAMP assay all peptides behaved as full agonists with the exception of the [Nphe^1] analogue.

Table 2.10 Displacement and GTPγ[^{35}S] binding at CHO_{hNOP} membranes and cAMP inhibition in whole CHO_{hNOP} cells for full and truncated sequences in agonist, partial agonist and antagonist templates.
Data are mean ± s.e.mean from (n) experiments (data in italics courtesy J..McDonald).
Where ANOVA test ($p<0.05$) indicated, *denotes significant difference from reference compound, N/OFQ-NH_2, using Bonferroni correction.
Data for cAMP assays with [Nphe^1]N/OFQ(1-13)-NH_2 from (Calo *et al.*, 2000b).

Ligand	Displacement Binding	GTPγ[^{35}S] Binding		cAMP Inhibition	
	pK_i	pEC_{50}	Maximum stimulation, E_{max}	pEC_{50}	Maximum Inhibition, E_{max} (%)
N/OFQ-NH_2	10.31±0.04	*8.98±0.08*	*10.98±1.30*	9.94±0.04 (4)	103.0±1.4
[F/G]N/OFQ-NH_2	9.89±0.08*	*8.28±0.57**	*4.58±0.52**	9.12±0.06*(4)	97.0±8.6
N/OFQ(1-13)-NH_2	10.24±0.09	*8.94±0.22*	*11.19±0.48*	9.96 ±0.07 (3)	102.8±1.0
[F/G]N/OFQ (1-13)-NH_2	9.27±0.06*	8.05±0.21*	7.75±1.02*	8.90±0.24*(5)	97.5±2.6
[Nphe^1]N/OFQ (1-13)-NH_2	8.08±0.07*	*Inactive*	*Inactive*	pA_2=5.96	Inactive

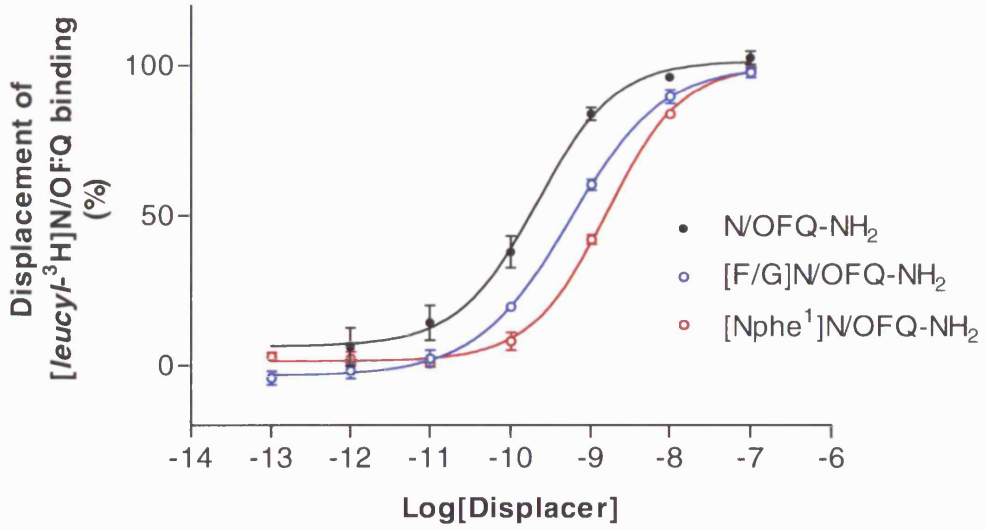

Figure 2.11 Displacement binding curves for agonist, partial agonist and antagonist templates with C-terminal amidation against [*leucyl*-^{3}H]N/OFQ in CHO_{hNOP} membranes.
Data are from n=4 experiments.

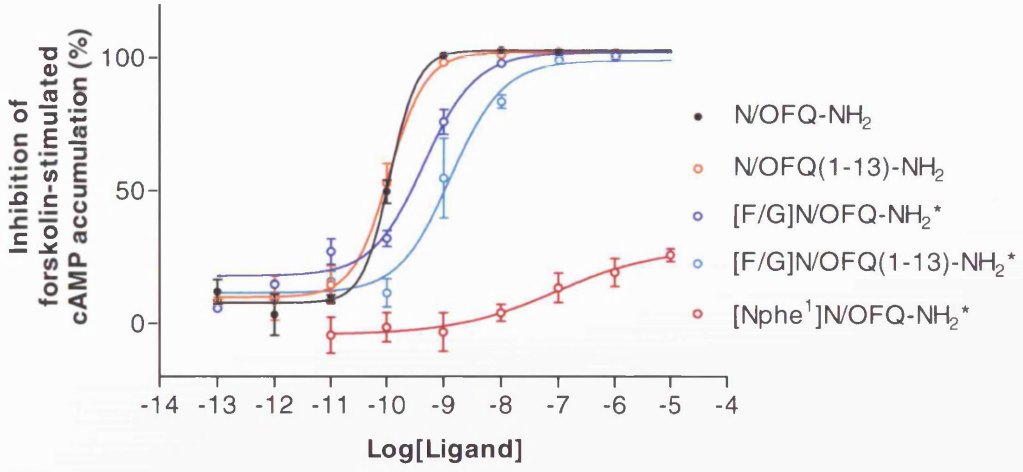

Figure 2.12 Inhibition of cAMP in whole CHO_{hNOP} cells for agonist and partial agonist templates with amidation and truncation.
Data are from n=4 experiments, except N/OFQ(1-13)-NH_2 (n=3) and [F/G](1-13)-NH_2 (n=5).
* denotes significant difference ($p<0.05$) from N/OFQ-NH_2.

2.4.4 *Modification of message motif*

From previous studies in isolated tissues, the introduction of the electronegative element fluorine in the *para*-position on the benzyl ring of phenylalanine at position four (Phe^4) gave the most potent of this type of modification (Guerrini *et al.*, 2001b). Data for analogues with this alteration are presented here. Denoted (pF)Phe^4, as it is situated in the message motif, this modification may be anticipated to increase potency and may also be combined with both amidation and truncation to form a high potency agonist. The structure of this analogue is illustrated in Figure 2.13.

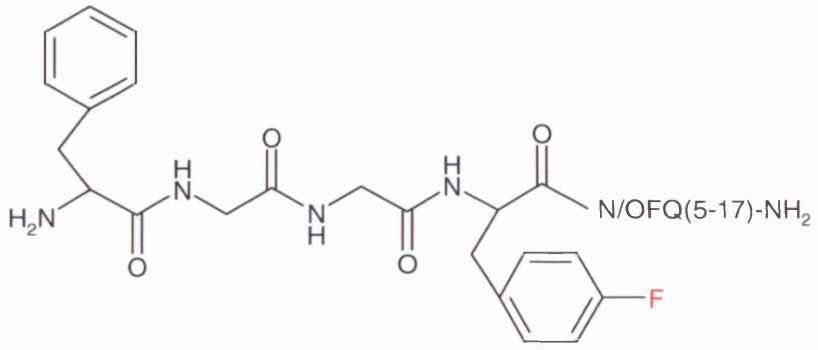

Figure 2.13 Structure of [(pF)Phe^4]N/OFQ-NH_2 modification in the N/OFQ agonist template.
Difference from agonist template shown in red.
This modification is the same in the partial agonist and antagonist templates.

The results for assays performed upon templates bearing this modification are shown in Table 2.11, with displacement binding and cAMP inhibition curves shown in Figures 2.14 and 2.15. Addition of [(pF)Phe^4] produced a small increase in binding affinity but this failed to reach statistical significance. In agreement with previous data, the [$Nphe^1$] substitution in combination with [(pF)Phe^4] produced a loss in binding affinity relative to N/OFQ-NH_2.

In functional assays incorporation of [(pF)Phe^4] into the N/OFQ sequence produced an agonist with increased functional potency, behaving as a full agonist. In the partial agonist template the [(pF)Phe^4] analogue still behaved as a partial agonist in GTPγ[^{35}S] binding assays but, as predicted for this amplified system, was a full agonist in cAMP inhibition assays. Combination of [(pF)Phe^4] and [$Nphe^1$] modifications produced a low potency, low efficacy, partial agonist in both assay systems.

Table 2.11 Displacement and GTPγ[^{35}S] binding at CHO_{hNOP} membranes and cAMP inhibition in whole CHO_{hNOP} cells for *para*-fluoro substitution in agonist, partial agonist and antagonist templates. Data are mean±s.e.mean from (n) experiments (data in italics courtesy J..McDonald). Where ANOVA test ($p<0.05$) indicated, *denotes significant difference from reference compound, N/OFQ-NH_2, using Bonferroni correction.

Ligand	Displacement Binding	GTPγ[^{35}S] Binding		cAMP Inhibition	
	pK_i	pEC_{50}	Maximum stimulation, E_{max}	pEC_{50}	Maximum Inhibition, E_{max} (%)
N/OFQ-NH_2	10.31±0.04	*8.98±0.08*	*10.98±1.30*	9.94±0.04 (4)	103.0±1.4
[(*p*F)Phe^4] N/OFQ-NH_2	10.66±0.09	9.51±0.04*	11.42±0.72	10.18±0.19*(4)	100.9±1.3
[F/G,(*p*F)Phe^4] N/OFQ-NH_2	10.32±0.04	*9.09±0.29*	*4.30±0.28**	9.32±0.52 (4)	104.0±4.1
[Nphe^1,(*p*F)Phe^4] N/OFQ-NH_2	9.62±0.02*	*8.23±0.30**	*1.36±0.11**	7.26±0.61*(3)	28.1±9.9*

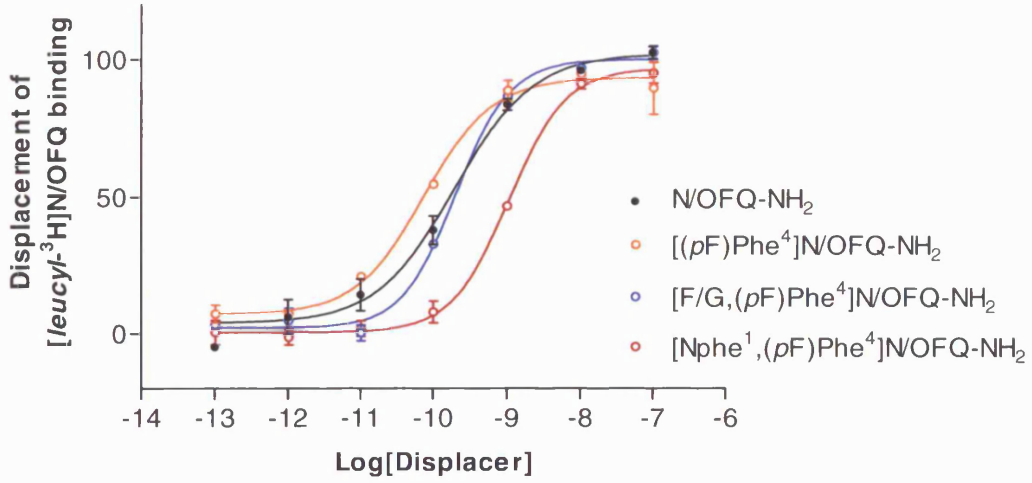

Figure 2.14 Displacement binding curves against [*leucyl*-^{3}H]N/OFQ at CHO_{hNOP} membranes for agonist, partial agonist and antagonist templates with amidation and [(*p*F)Phe^4] modification.
N/OFQ-NH_2 is included for comparison.
Data are from n=4 experiments.

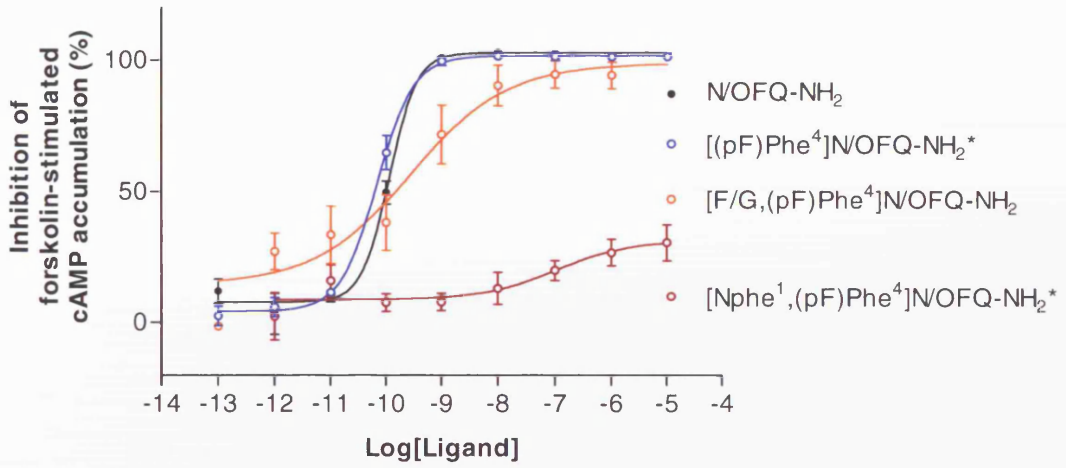

Figure 2.15 cAMP inhibition curves in whole CHO_{hNOP} cells for [(*p*F)Phe^4] modification to agonist, partial agonist and antagonist templates.
N/OFQ-NH_2 is included for comparison.
Data are from n=4 experiments except [Nphe^1,(*p*F)Phe^4]N/OFQ-NH_2 (n=3).
* denotes significant difference ($p<0.05$) from N/OFQ-NH_2.

2.4.5 Modification of address motif.

Further modification may be made in the C-terminal (address) region of the sequence by the addition of an arginine/lysine (R/K) repeat at positions fourteen and fifteen (Arg^{14},Lys^{15}), which may also be combined with the modifications previously described (Rizzi *et al.*, 2002). The structure of this analogue is illustrated in Figure 2.16.

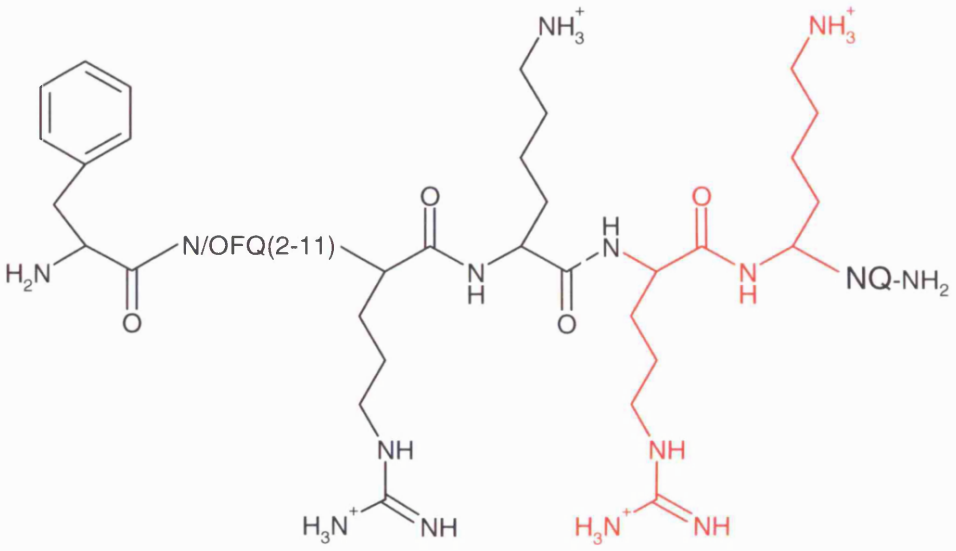

Figure 2.16 Structure of [Arg^{14},Lys^{15}]N/OFQ-NH_2 modification in the N/OFQ agonist template.
Difference from agonist template shown in red.
This modification is the same in the partial agonist and antagonist templates.

Table 2.12 shows results for assays using this modification in the address sequence of the template analogues. Figures 2.17 and 2.18 show, respectively, the displacement binding and cAMP inhibition curves for these modifications. Addition of the [Arg^{14},Lys^{15}] repeat in the agonist template increased binding affinity by ~3-fold.

In functional assays, GTPγ[^{35}S] binding showed [Arg^{14},Lys^{15}] modification of partial agonist template to have similar potency but lower efficacy compared to the reference agonist (N/OFQ-NH_2). However, this corresponded to an increase in potency with no change in efficacy compared to [F/G]. In cAMP assays there was a small reduction (<3-fold) in potency, although this peptide behaved as a full agonist. In the antagonist template, producing the commercially available compound UFP-101, this analogue was inactive in GTPγ[^{35}S] assays *per se* but reversed the effects of N/OFQ in a competitive manner with a pA_2 of 8.85. In original studies in cAMP assays, UFP-101 was also

inactive *per se*, but reversed the effects of N/OFQ with a pA_2 of 7.11 (Calo *et al.*, 2002). It is of importance to note that some batches of UFP-101 showed residual agonist activity in cAMP inhibition assays and where data is specified in this thesis for this analogue, the source is the original paper reporting this compound. In addition, where used in further experiments only batches with no agonist activity were used.

Table 2.12 Displacement and GTPγ[^{35}S] binding at CHO_{hNOP} membranes and cAMP inhibition in whole CHO_{hNOP} cells for [Arg^{14},Lys^{15}] modification in agonist, partial agonist and antagonist templates.
Data are mean±s.e.mean for (n) experiments (data in italics courtesy J. McDonald).
Where ANOVA test ($p<0.05$) indicated, *denotes significant difference from reference compound, N/OFQ-NH_2, using Bonferroni correction.

Ligand	Displacement Binding	GTPγ[^{35}S] Binding		cAMP Inhibition	
	pK_i	pEC_{50}	Maximum stimulation, E_{max}	pEC_{50}	Maximum Inhibition, E_{max} (%)
N/OFQ-NH_2	10.31±0.04	*8.98±0.08*	*10.98±1.30*	9.94±0.04 (4)	103.0±1.4
[Arg^{14},Lys^{15}] N/OFQ-NH_2	11.16±0.05*	9.85±0.11	9.70±0.69*	10.00±0.10 (4)	102.3±1.0
[F/G,Arg^{14},Lys^{15}] N/OFQ-NH_2	10.50±0.03	*9.03±0.09*	*5.29±0.27**	9.62±0.33* (4)	89.0±9.4
[Nphe^1,Arg^{14},Lys^{15}] N/OFQ-NH_2 (UFP-101)	9.89±0.09	*pA_2=8.85±0.12*	*Inactive*	pA_2=7.11 (3)	Inactive

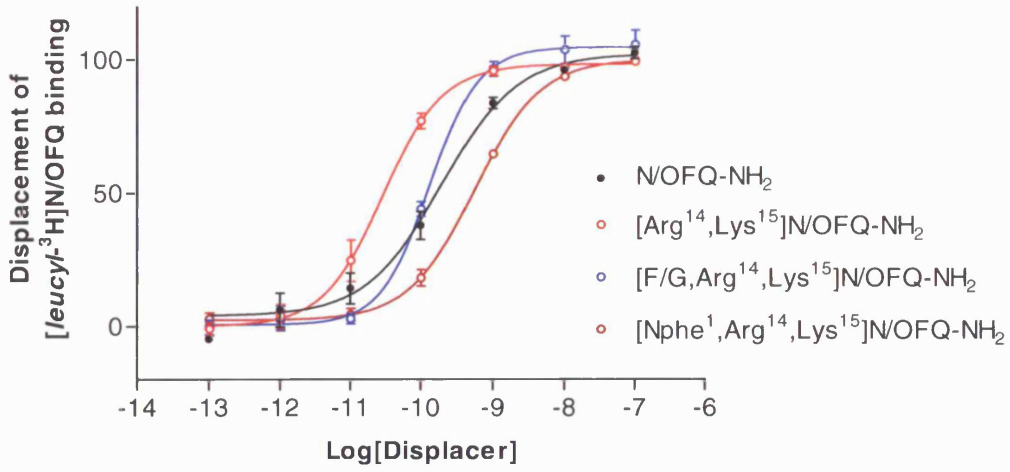

Figure 2.17 Displacement binding curves against [*leucyl*-^{3}H]N/OFQ at CHO_{hNOP} membranes for agonist, partial agonist and antagonist templates with amidation and [Arg^{14},Lys^{15}] modification. N/OFQ-NH_2 is included for comparison.
Data are from n ≥ 3 experiments.

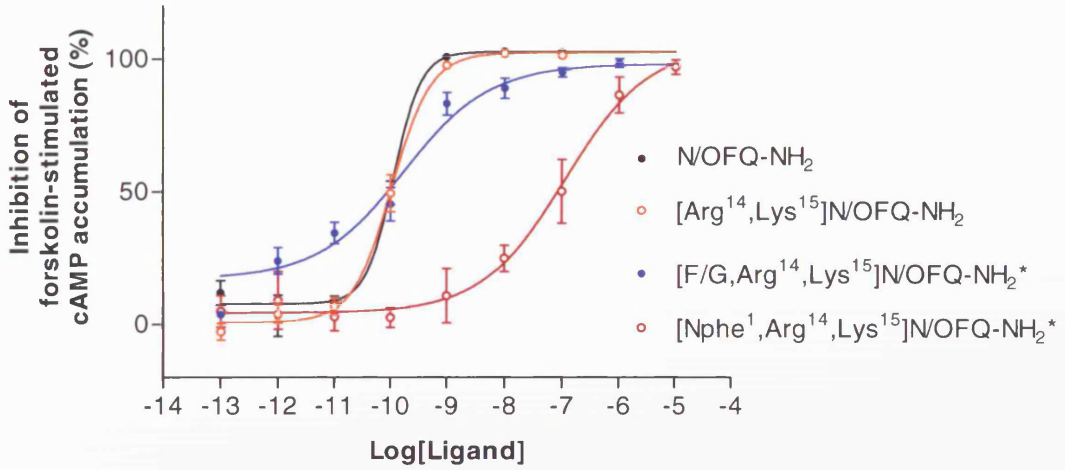

Figure 2.18 cAMP inhibition curves in whole CHO_{hNOP} cells for amidated agonist, partial agonist and antagonist templates with [Arg^{14},Lys^{15}] modification.
N/OFQ-NH_2 is included for comparison.
Data are from n=4 experiments, except [$Nphe^1$,Arg^{14},Lys^{15}]N/OFQ-NH_2, n=3.
* indicates significant difference ($p<0.05$) from N/OFQ-NH_2.

2.4.6 *Combination of Modifications to both Message and Address Motifs*

Both [(*p*F)Phe^4] and [Arg^{14},Lys^{15}] may be simultaneously applied to the agonist, partial agonist and antagonist templates described above. The results for the combination of these two modifications in the peptide sequence are shown in Table 2.13 with displacement binding and cAMP inhibition curves shown in Figures 2.19 and 2.20, respectively. Combination of the two modifications in the agonist template further increased the binding affinity (pK_i=11.32). As seen for [Arg^{14},Lys^{15}] alone, the combination increased functional potency in GTPγ[^{35}S] assays in the agonist template (pEC_{50}=10.12) and this improved potency was carried through to the partial agonist template but still with a significant loss of efficacy (E_{max}=4.20). In the cAMP assay the full and partial agonist templates behaved as full agonists with no appreciable change in potency. For the antagonist template, this modification displayed agonist activity in both assays. In GTPγ[^{35}S] the peptide was a partial agonist with increased efficacy compared to the [(*p*F)Phe^4] modification alone in this template. In the cAMP assay, as may be predicted, this peptide was a full agonist.

Table 2.13 Displacement and GTPγ[^{35}S] binding at CHO_{hNOP} membranes and cAMP inhibition in CHO_{hNOP} cells for [(*p*F)Phe^4,Arg^{14},Lys^{15}] modification in agonist, partial agonist and antagonist templates.
Data are mean±s.e.mean from (n) experiments (data in italics courtesy J..McDonald).
Where ANOVA test ($p<0.05$) indicated, *denotes significant difference from reference compound, N/OFQ-NH_2, using Bonferroni correction.

Ligand	Displacement Binding	GTPγ[^{35}S] Binding		cAMP Inhibition	
	pK_i	pEC_{50}	Maximum stimulation, E_{max}	pEC_{50}	Maximum Inhibition, E_{max} (%)
N/OFQ-NH_2	10.31±0.04	*8.98±0.08*	*10.98±1.30*	9.94±0.04 (4)	102.7±1.4
[(*p*F)Phe^4,Arg^{14},Lys^{15}] N/OFQ-NH_2	11.32±0.08*	*10.12±0.04**	*12.26±0.39*	10.17±0.09 (4)	103.8±1.1
[F/G,(*p*F)Phe^4, Arg^{14},Lys^{15}]N/OFQ-NH_2	10.70±0.03	*9.68±0.10**	*4.20±0.07**	9.52±0.44* (3)	92.0±7.3
[Nphe^1,(*p*F)Phe^4, Arg^{14},Lys^{15}]N/OFQ-NH_2	10.60±0.10	*9.39±0.20*	*2.03±0.01**	8.31±0.15* (4)	91.3±9.6

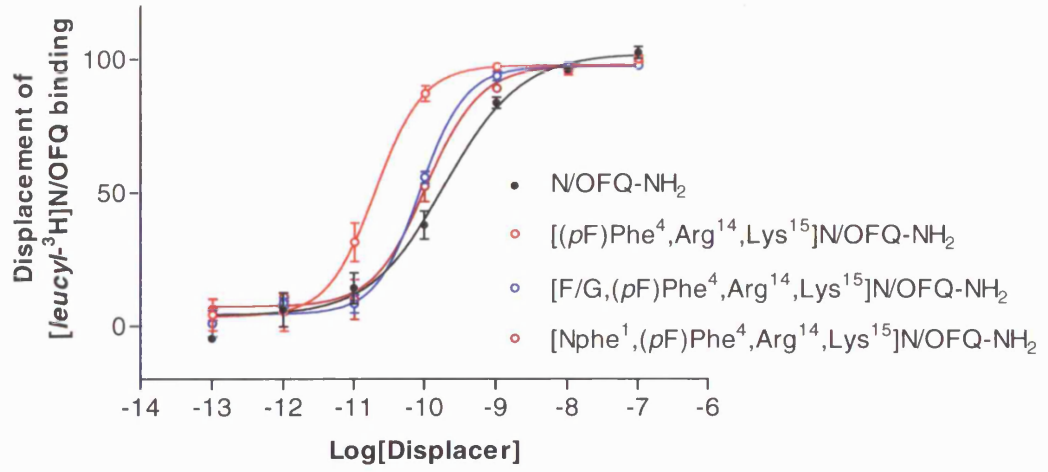

Figure 2.19 Displacement binding curves against [*leucyl*-^{3}H]N/OFQ at CHO_{hNOP} membranes for amidated agonist, partial agonist and antagonist templates with both [(*p*F)Phe^4] and [Arg^{14},Lys^{15}] modifications.
N/OFQ-NH_2 included for comparison.
Data are from n=4 experiments.

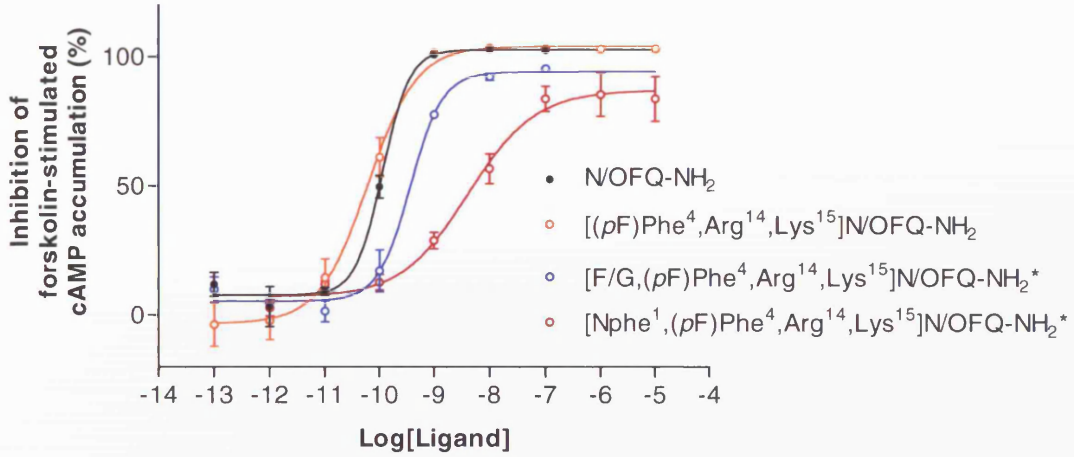

Figure 2.20 cAMP inhibition curves for for amidated agonist, partial agonist and antagonist templates with both [(*p*F)Phe^4] and [Arg^{14},Lys^{15}] modifications.
N/OFQ-NH_2 included for comparison.
Data are from n=4 experiments except [F/G,(*p*F)Phe^4,Arg^{14},Lys^{15}]N/OFQ-NH_2 (n=3).
* denotes significant difference ($p<0.05$) from N/OFQ-NH_2.

2.4.7 *Further investigation of Partial Agonists*

A further modification based upon the peptide bond alteration in [F/G] is the replacement of the amide group adjacent to the methylene substitution of [F/G] with oxygen, giving an ether link (Guerrini *et al.*, 2003). This compound, used in the truncated form of the peptide and denoted [F/G-O](1-13)-NH_2 ([F/G-O]), was seen to be a partial agonist with properties between those of the truncated versions of the agonist and partial agonist templates.

Data for [F/G-O], tested against both N/OFQ(1-13)-NH_2 and [F/G](1-13)-NH_2, are shown in Table 2.14 with displacement binding and cAMP inhibition curves shown in Figures 2.21 and 2.22 respectively. In displacement binding assays, [F/G-O] displayed lower affinity (pK_i=9.52) than N/OFQ(1-13)-NH_2, but this was significantly higher than that for [F/G](1-13)-NH_2. In GTPγ[^{35}S] assays, the loss of efficacy (compared to N/OFQ(1-13)-NH_2) seen for [F/G](1-13)-NH_2 was also seen to a lesser extent for [F/G-O] (E_{max}=10.17) along with a smaller reduction in functional potency (pEC_{50}=8.56). In the cAMP assay both [F/G](1-13)-NH_2 and [F/G-O] behaved identically, with lower potency than N/OFQ(1-13)-NH_2, but as full agonists.

Table 2.14 Displacement and GTPγ[^{35}S] binding in CHO_{hNOP} membranes and cAMP inhibition in whole CHO_{hNOP} cells for N/OFQ(1-13)-NH_2, [F/G]N/OFQ(1-13)-NH_2 and [F/G-O]N/OFQ(1-13)-NH_2.
Statistically significant difference ($p<0.05$) indicated by:
* compared to N/OFQ(1-13)-NH_2;
**, compared to both [F/G]N/OFQ(1-13)-NH_2 and N/OFQ(1-13)-NH_2.
Data are mean±s.e.mean from n=4 experiments.

Ligand	Displacement Binding	GTPγ[^{35}S] Binding		cAMP Inhibition	
	pK_i	pEC_{50}	Stimulation Factor E_{max}	pEC_{50}	Maximal inhibition E_{max} (%)
N/OFQ(1-13)-NH_2	10.22±0.09	8.94±0.22	11.13±0.48	10.18±0.05	100.4±0.9
[F/G] N/OFQ(1-13)-NH_2	9.27±0.06*	8.05±0.21*	7.75±1.02*	8.94±0.11*	101.3±0.4
[F/G-O] N/OFQ(1-13)-NH_2	9.52±0.09**	8.56±0.17**	10.17±1.88**	8.96±0.18**	103.1±2.3

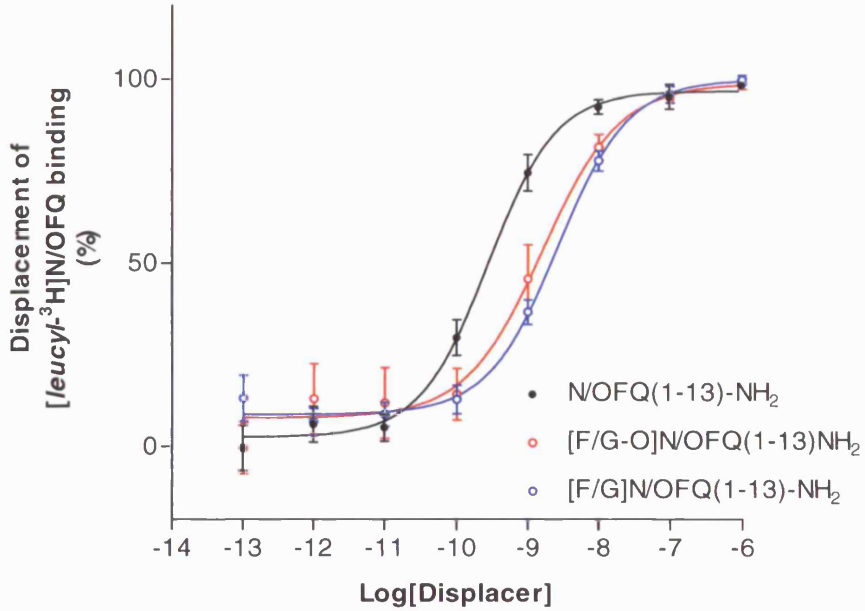

Figure 2.21 Displacement binding curves against [*leucyl*-^{3}H]N/OFQ at CHO_{hNOP} membranes for truncated agonist and partial agonist templates and [F/G-O]N/OFQ(1-13)-NH_2.
Data are from n=4 experiments.

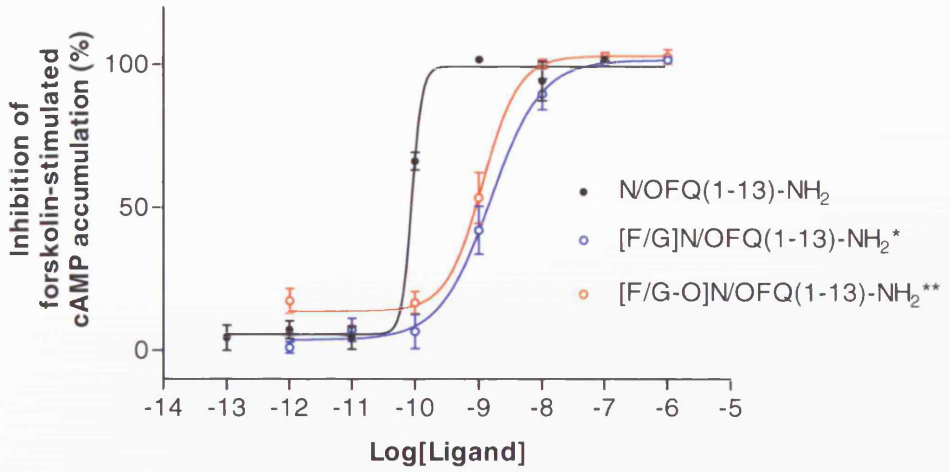

Figure 2.22 cAMP inhibition curves in whole CHO_{hNOP} cells for N/OFQ(1-13)-NH_2, [F/G]N/OFQ(1-13)-NH_2 and [F/G-O]N/OFQ(1-13)-NH_2.
Data are from n=4 experiments.
Statistically significant difference ($p<0.05$) indicated by:
* compared to N/OFQ(1-13)-NH_2,
** compared to both [F/G]N/OFQ(1-13)-NH_2 and N/OFQ(1-13)-NH_2.

2.4.8 Non-peptide Antagonists

JTC-801

The synthetic, non-peptide NOP antagonist JTC-801 (Yamada *et al.*, 2002) was used in a series of experiments where this compound was pre-incubated with cells prior to being tested for potency in competition assays with N/OFQ. The structure of this compound is shown in Figure 2.23.

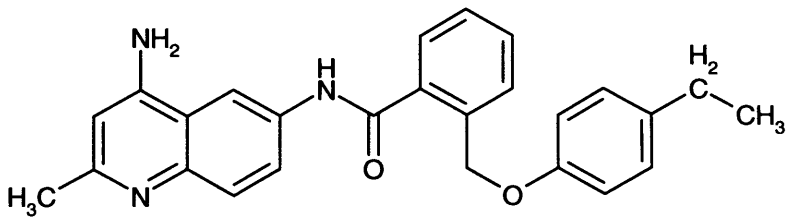

Figure 2.23 Structure of the non-peptide NOP antagonist, JTC-801.

When tested for any agonist activity, JTC-801 did not *per se* affect forskolin-stimulated cAMP formation (data not shown) but was able to reverse the effect of N/OFQ. This antagonism was time- and concentration-dependent as, when co-applied with N/OFQ (no pre-incubation, Figure 2.24), only 10μM caused a rightward displacement of the N/OFQ control concentration response curve (estimated $pK_B \approx 7.0$). The N/OFQ concentration-response curves at this antagonist concentration and for the control were parallel and reached similar maximal effects. With pre-incubation of JTC-801 for 40 min (Figure 2.25) and 90 min (Figure 2.26), a time dependent increase in pK_B was seen (estimated using the highest concentration of JTC-801). With the longer incubations, an inhibition became clear at lower concentrations (1μM). The effects of pre-incubation are summarised in Table 2.15. It was possible to perform a Schild regression upon the data for 90 min pre-incubation, giving a pA_2 of ≈ 6.5, but the slope (1.75) indicated that equilibrium was not achieved, even following this long pre-incubation period. This analysis is shown in Figure 2.27.

Table 2.15 Effects of pre-incubation time on pK_B values for the antagonist JTC-801 in cAMP Inhibition assays.
Analysis utilizes the Gaddum-Schild equation data are mean±s.e.mean from n=3 experiments.

Concentration of JTC-801 (μM)	JTC-801 pK_B		
	Without pre-incubation	40min pre-incubation	90min pre-incubation
0.1	inactive	inactive	inactive
1.0	inactive	6.46±0.21	6.70±0.15
10	6.97±0.19	7.49±0.10	7.77±0.19

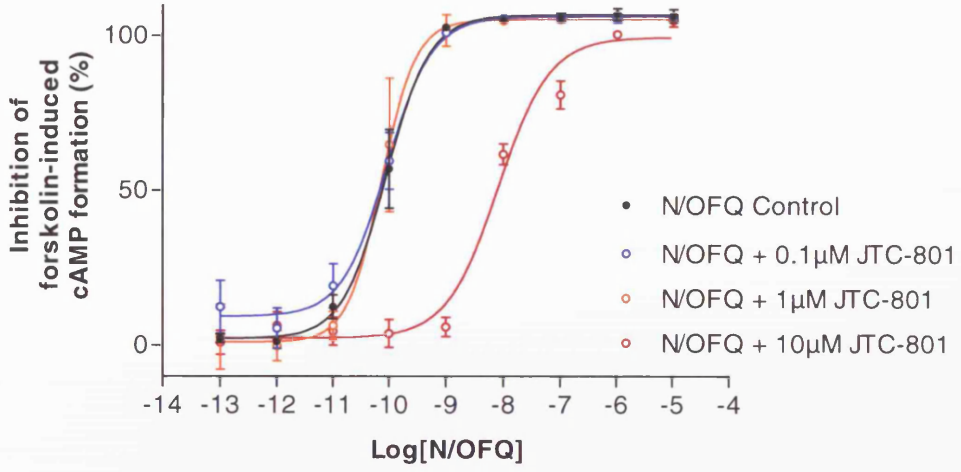

Figure 2.24 Effect of JTC-801 (0.1-10μM) upon N/OFQ inhibition of forskolin-stimulated cAMP accumulation in CHO_{hNOP} cells measured without pre-incubation of JTC-801.
Data are from n=3 experiments.

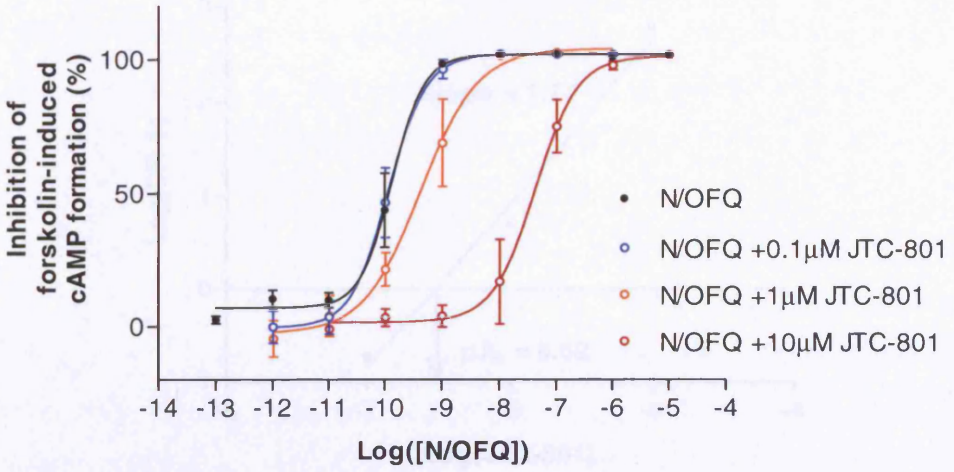

Figure 2.25 Effect of JTC-801 (0.1-10μM) upon N/OFQ inhibition of forskolin-stimulated cAMP accumulation in CHO_{hNOP} cells measured with 40min pre-incubation time for JTC-801. Data are from n=3 experiments.

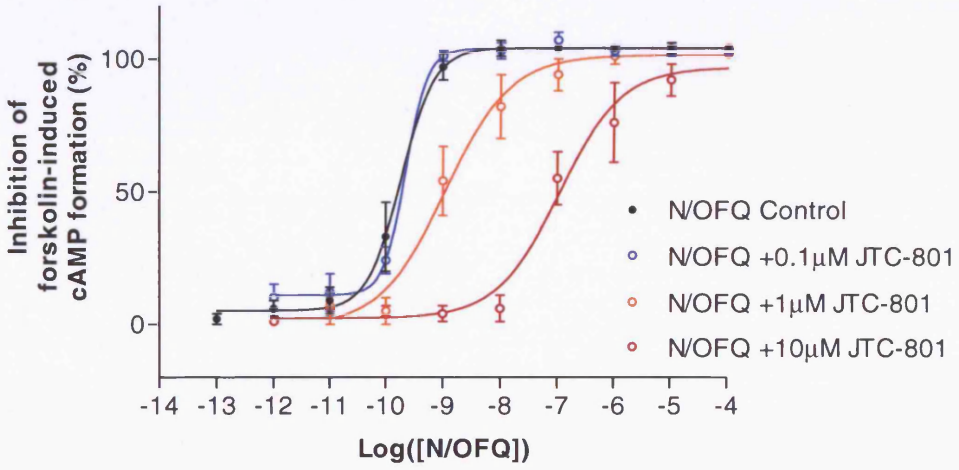

Figure 2.26 Effect of JTC-801 (0.1-10μM) upon N/OFQ inhibition of forskolin-stimulated cAMP accumulation in CHO_{hNOP} cells measured with 90min pre-incubation time for JTC-801. Data are from n=3 experiments.

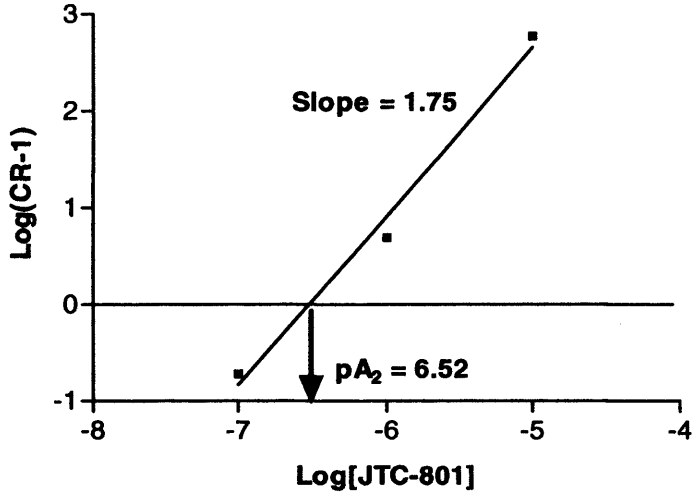

Figure 2.27 Schild regression analysis for average of 90min pre-incubation data for JTC-801. Data are from n=3 experiments.

J113397

The synthetic NOP-selective antagonist developed by the Banyu Corporation in Japan, J113397 (Kawamoto *et al.*, 1999), was assayed for antagonist potency at NOP by Schild analysis. The structure of this compound is shown in Figure 2.28.

J113397 was used at three fixed concentrations to antagonise the inhibition of adenylyl cyclase activity by N/OFQ. The resultant cAMP inhibition curves are shown in Figure 2.29. As can be seen, J113397 produced a parallel and concentration-dependent rightward shift in the concentration response curve to N/OFQ, consistent with competitive antagonism. Schild analysis of J113397, obtaining a value for pA_2 of 7.98±0.50, with a slope of 1.13±0.25 indicative of equilibrium, is shown in Figure 2.30.

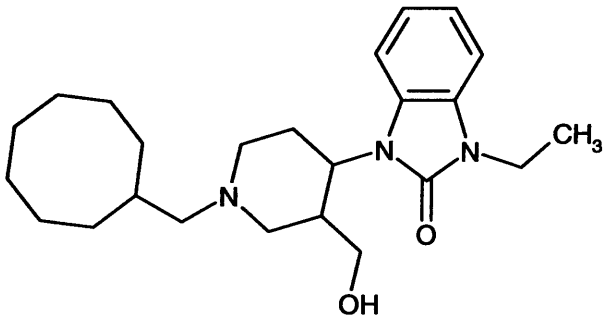

Figure 2.28 Structure of the non-peptide NOP antagonist, J113397.

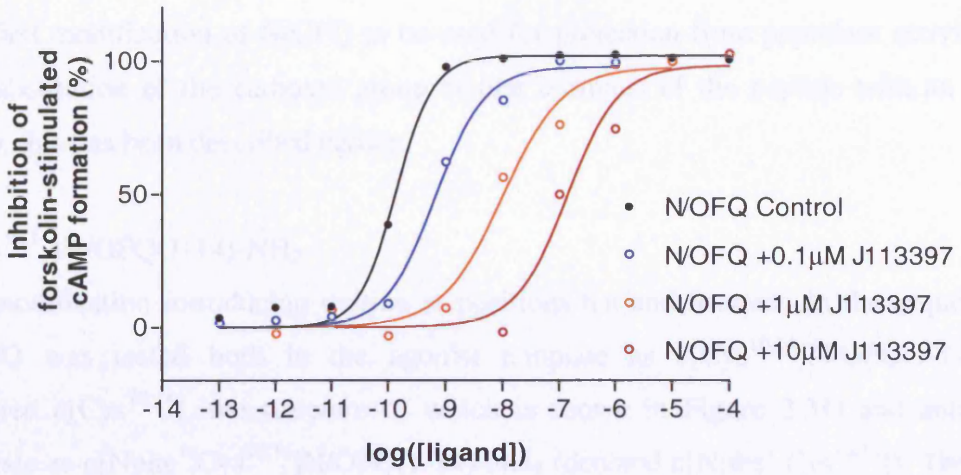

Figure 2.29 cAMP inhibition curves for N/OFQ in antagonist assay with J113397.
Specimen data from n=3.

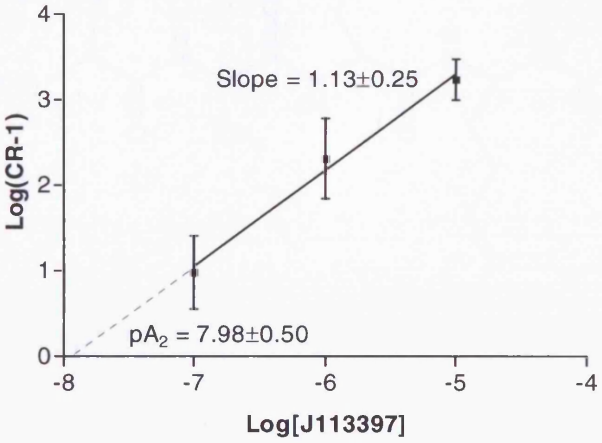

Figure 2.30 Schild analysis for J113397.
Data are from n=3 experiments.

2.4.9 *Modification of Peptides for Metabolic Protection*

Amidation

The first modification of N/OFQ to be used for protection from peptidase activity was the substitution of the carboxyl group at that terminus of the peptide with an amino group, this has been described earlier.

c[Cys^{10,14}]N/OFQ(1-14)-NH_2.

The modification introducing cystine at positions ten and fourteen in the sequence of N/OFQ was tested both in the agonist template as c[Cys^{10,14}]N/OFQ(1-14)-NH_2 (denoted c[Cys^{10,14}], the structure of which is shown in Figure 2.31) and antagonist template as c[Nphe^1,Cys^{10,14}]N/OFQ(1-14)-NH_2 (denoted c[Nphe^1,Cys^{10,14}]). The *para*-substitution of fluorine at [Phe^4] was not used for this compound.

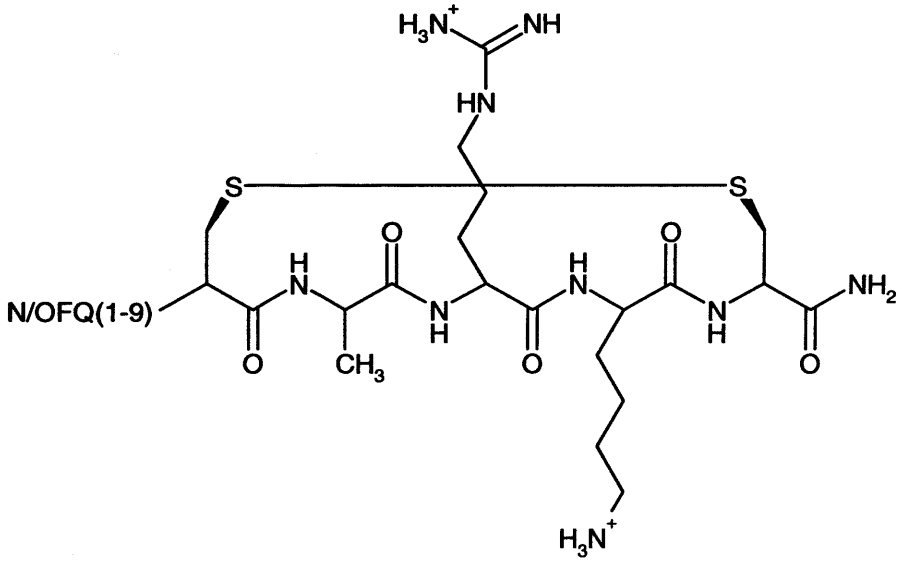

Figure 2.31 Structure of c[Cys^{10,14}]N/OFQ(1-14)-NH_2.

Results for these assays are shown in Table 2.16 with cAMP inhibition curves illustrated in Figure 2.32. In displacement binding assays cyclisation and [Nphe^1] substitution progressively reduced binding affinity. In GTPγ[^{35}S] binding assays c[Cys^{10,14}] was a full agonist with reduced potency and c[Nphe^1,Cys^{10,14}] was inactive as an agonist *per se* but reversed the effects of N/OFQ in a competitive manner (pK_B=7.05). The agonists N/OFQ(1-13)NH_2 and c[Cys^{10,14}] produced a concentration dependent inhibition of forskolin-stimulated cAMP formation. In this assay, the following rank order potency was observed:

N/OFQ(1-13)NH_2 > N/OFQ > c[Cys^{10,14}]

In contrast to the GTPγ[^{35}S] studies described above, c[Nphe^{1},Cys^{10,14}] also produced a marked inhibition of cAMP formation. However, due to the low potency of the peptide it was not possible to complete the concentration response curve to this peptide which exhibited 80% inhibition at 10μM.

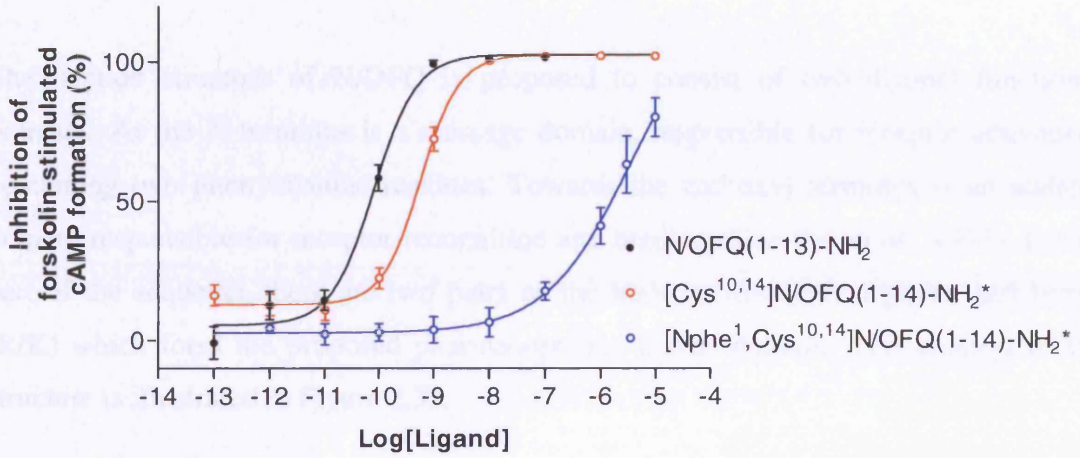

Figure 2.32 cAMP inhibition curves for agonist profile of c[Cys^{10,14}]N/OFQ(1-14)-NH_2 and c[Nphe^{1},Cys^{10,14}]N/OFQ(1-14)-NH_2.
Data are from n=7 experiments. * indicates significant difference from N/OFQ(1-13)-NH_2.

Table 2.16 Data for c[Cys^{10,14}] derivatives of N/OFQ-NH_2.
N/OFQ(1-13)-NH_2 is included both for comparison and was used as reference agonist in GTPγ[^{35}S] antagonist assay.
Data are mean±s.e.mean from n=7 experiments.
* denotes significant difference from N/OFQ(1-13)-NH_2.
[a] Data would appear to show this to be a partial agonist, but maximal stimulation was achieved at a concentration of 1μM. Concentration response curve was lowered by 22% loss of stimulation at 10μM.

Ligand	Displacement Binding	GTPγ[^{35}S] Binding		cAMP Inhibition	
	pK_i	pEC_{50}	Stimulation Factor E_{max}	pEC_{50}	Maximal inhibition E_{max} (%)
N/OFQ(1-13)-NH_2	10.26±0.20	8.57±0.09	6.37±0.61	10.16±0.07	103.0±1.25
c[Cys^{10,14}] N/OFQ(1-14)-NH_2	9.68±0.27	8.29±0.08*	5.67±0.46*[a]	9.29±0.05*	102.4±0.8
c[Nphe^{1},Cys^{10,14}] N/OFQ(1-14)-NH_2	7.92±0.23*	pK_B=7.05±0.05	Inactive	5.97±0.21*	80 (at 10μM)

2.5 Discussion

In a study of the pharmacology of the nociceptin receptor, its native ligand, nociceptin (N/OFQ), and analogues, a number of modifications to the agonist template may be made which affect the interaction of receptor and ligand. Using functional and binding assays to probe this interaction, a variation in effect from full agonism via partial agonism to pure antagonism may be seen, caused by minor changes to the chemical structure of the ligand.

The peptide structure of N/OFQ is proposed to consist of two distinct functional domains. At the N-terminus is a message domain, responsible for receptor activation, containing two phenylalanine residues. Towards the carboxyl terminus is an address domain responsible for receptor recognition and binding (Guerrini *et al.*, 1997). In this part of the sequence there are two pairs of the basic amino acids arginine and lysine (R/K) which form the proposed pharmacophores in this domain. This concept of the structure is illustrated in Figure 2.33.

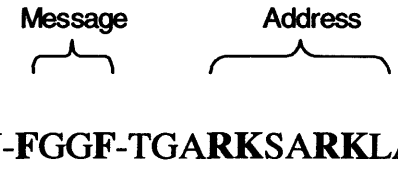

Figure 2.33 Message/address concept in the structure of N/OFQ.

2.5.1 Agonists

All agonist compounds showed full inhibition of forskolin-stimulated cAMP formation at NOP in a concentration-dependent and saturable manner. Use of amidation to protect the carboxyl terminus of N/OFQ from exopeptidase activity resulted in no loss in efficacy and a slight increase in potency (Guerrini *et al.*, 1997). This enabled the use of this modification as an agonist template for further studies.

Truncating N/OFQ to thirteen residues, in combination with amidation, resulted in no loss of potency or efficacy compared to the template. The use of amidation is especially important in the truncated peptide since the second of the arginine/lysine repeats proposed to be involved in receptor recognition is exposed at one terminus of this

compound, thus amidation offers protection at this site (Calo *et al.*, 1997). This is illustrated in Figure 2.34.

H_2N-**FGGFTGARKSARK**-NH_2

1 13

Figure 2.34 The position of the first and last amino acids in truncated N/OFQ.

Incorporation of an additional arginine/lysine repeat into the address sequence of the template, at positions 14 and 15, has been shown to increase affinity for the receptor and result in an increase in potency (Okada *et al.*, 2000). These positions are normally occupied by leucine and alanine, hydrophobic amino acids, not normally associated with receptor interaction.

Although the results for the cAMP inhibition assays showed no significant increase in potency, the displacement assays did show an increase in affinity with this modification. The reason for this may be in the nature of binding as measures of affinity of a ligand for the receptor are made via the address domain, where the modification has been made. The functional assay for cAMP inhibition measures the downstream effect following receptor recognition, activation and second messenger generation, during which the initial signal is subjected to several amplification steps. So in this instance, an increase in affinity had only a small effect upon potency.

Amidation, truncation and introduction of the arginine/lysine repeat are modifications applied to the address domain. Also associated with this area is the introduction of cystine residues, able to cyclise the peptide for protection against possible peptidase degradation. Whereas the previous modifications are available in combination, the introduction of these latter residues and the additional arginine/lysine repeat are mutually exclusive.

In the message domain, the addition of electronegative groups onto the sidechain of the fourth amino acid, phenylalanine, was shown to enhance the potency of N/OFQ. This is thought to be a result of the electron withdrawing properties of the substituted group, giving a more polar nature to the aromatic sidechain of this amino acid, thereby

enhancing ligand/receptor interaction (Guerrini *et al.*, 2001b). Initial studies in this region showed the largest effect with fluorine as the substituent. This is the most electronegative of the elements and was used for the studies in this thesis.

In the cyclase inhibition assay, the rank order of potency was seen to be:

$$[(pF)Phe^4,Arg^{14},Lys^{15}]N/OFQ\text{-}NH_2 > [Arg^{14},Lys^{15}]N/OFQ\text{-}NH_2 >$$
$$[(pF)Phe^4]N/OFQ(1\text{-}13)\text{-}NH_2 > N/OFQ\text{-}NH_2 > N/OFQ$$

The addition of fluorine to the phenylalanine at position four of the truncated version gave an approximately four-fold increase in potency over the truncated agonist template, although again this was not a statistically significant increase in the cyclase inhibition assay. The use of this modification in addition to the arginine/lysine repeat further enhanced the potency of N/OFQ.

In this study it has been demonstrated that $[(pF)Phe^4]N/OFQ(1\text{-}13)\text{-}NH_2$ stimulated the binding of GTPγ[^{35}S] and inhibited forskolin-stimulated cAMP formation in Chinese hamster ovary cells expressing human NOP. In both of these assay systems $[(pF)Phe^4]N/OFQ(1\text{-}13)\text{-}NH_2$ was ≈ 4 times more potent than the agonist template, $N/OFQ\text{-}NH_2$. The actions of this peptide were PTx sensitive and competitively inhibited by the NOP-selective antagonist J-113397 (GTPγ[^{35}S], pA_2= 8.53±0.06; cAMP, pK_B=7.96±0.05) and the non-selective antagonist III-BTD (GTPγ[^{35}S], pA_2=7.89±0.17; cAMP, pK_B=7.27±0.15) (McDonald *et al.*, 2002).

2.5.2 Rationale behind the use of [(pF)Phe^4]N/OFQ-NH$_2$

Several analogues of the N/OFQ sequence that act as full agonists at NOP and display 3-5 fold higher potency than the naturally occurring peptide have been reported. These involve replacing the hydrogen atom in the *para*-position of Phe^4 with a variety of substituents. The results support suggestions that Phe^4 is crucial in N/OFQ for the occupation and activation of NOP, a role similar to Tyr^1 in the classical opioids (Guerrini *et al.*, 2001b; Salvadori *et al.*, 1999). The pharmacological profiles of two particular agonists, with (*p*F) and (pNO_2) substitutions, were thought to be of particular use *in vivo* due to enhanced potency and high selectivity. In these studies, (*p*F) and

($p$$NO_2$) were consistently found to be more potent than N/OFQ and N/OFQ(1-13)NH_2 in experiments performed with recombinant hNOP expressed in CHO cells, native functional sites in the mouse vas deferens and colon, in isolated tissues of the rat and the guinea-pig and in rat cerebral cortex. In all assays the order of potency/affinity of the *para*-substitution series of compounds was:

$$F = NO_2 \geq CN \geq N/OFQ = N/OFQ(1\text{-}13)NH_2 = Cl \geq Br > I = CH_3 > OH = NH_2$$

There was strong correlation ($r \geq 0.92$) between data obtained in different assays, further indicating that the same receptor site is present in the various preparations. This suggestion was further supported by data obtained with the selective NOP antagonist [Nphe^1]N/OFQ(1-13)NH_2 (Calo *et al.*, 2000b), found to prevent the effects of N/OFQ in all preparations, with similar values ($pK_B \approx 6$).

In addition to its potency, the selectivity of any useful new receptor ligand is important. The (pF) and ($p$$NO_2$) substitutions were seen to be highly selective for NOP as, in CHO cells expressing the classical opioid receptors, these derivatives were either inactive at concentrations up to 10 μM or displayed micromolar EC_{50} values, with potency in CHO_{hNOP} cells below nanomolar. This data suggested a selectivity ratio for NOP of > 3000 over classical opioid receptors. The effects of (pF) and ($p$$NO_2$) were not antagonised by naloxone in endogenously expressed NOP in isolated tissues from a variety of species, also expressing classical opioid receptors (Guerrini *et al.*, 2001b). [Nphe^1]N/OFQ(1-13)NH_2 antagonized these effects with pK_B values very close to those reported for N/OFQ and N/OFQ(1-13)NH_2 (Calo *et al.*, 2000b). In membranes from rat cerebral cortex, a discrepancy was observed where the stimulatory effect of ($p$$NO_2$) on GTPγ[^{35}S] binding was antagonized by [Nphe^1]N/OFQ(1-13)NH_2 with a value (pK_B=7.67) very close to that obtained against N/OFQ (7.70, (Berger *et al.*, 2000b)) but 30-fold higher than for other assays/preparations.

Several reasons were proposed to explain these increased potencies:

- resistance to enzymatic degradation;
- higher efficacy;
- higher affinity.

An attempt was made to assess resistance to metabolism using peptidase inhibitors in a preparation from rat vas deferens, shown to increase potency of N/OFQ. A similar increase in potency (6-fold) was seen for both [(*p*NO_2)Phe^4]N/OFQ and N/OFQ (Calo *et al.*, 2000c), indicating that both compounds show similar liability to enzymatic degradation. This suggested it was unlikely that a resistance to degradation resulting in increased potency was the case.

In all functional assays maximal effects were seen for (*p*F) and (*p*NO_2), similar to the natural peptide, not only in those where N/OFQ is inhibitory, such as cAMP and electrically stimulated tissues (where saturation of effect could prevent true estimation of maximal inhibition), but also in those where N/OFQ is stimulatory, such as GTPγ[^{35}S] binding and mouse colon. This lack of difference between maxima elicited by these *para*-substituted derivatives and natural peptides implies equal efficacy. It would seem that the increased potencies of (*p*F) and (*p*NO_2) result from increases in affinity, supported by similar increases in potency obtained from both functional and binding assays, possibly due to an increase in the duration of binding to the receptor, this was supported by the results obtained from *in vivo* assays (Calo *et al.*, 2000c).

These are not the only analogues to show higher potency than the natural ligand. The analogue [Arg^{14},Lys^{15}]N/OFQ-NH_2 displayed 17-fold higher potency than N/OFQ in the GTPγ[^{35}S] assay performed in HEK_{293} cells expressing human NOP (Okada *et al.*, 2000). With the exception of one, all *para*-Phe^4 substituted analogues generated behaved as full agonists at NOP. The (*p*OH) substituted analogue acted as a full agonist in cAMP assays and in mouse colon, as a partial agonist in the GTPγ[^{35}S] binding assay (both CHO_{hNOP} and rat cerebral cortex) and as an antagonist (with residual agonist activity) in the mouse vas deferens and guinea pig ileum. This pharmacological behaviour closely resembles that of [F/G]N/OFQ(1-13)NH_2, which has been shown to act as a full agonist in the mouse colon (Rizzi *et al.*, 1999) and here in the cAMP assay (also (Okawa *et al.*, 1999), as a partial agonist in the GTPγS assay under certain experimental conditions (and (Berger *et al.*, 2000a)) and as an antagonist in the mouse vas deferens and guinea pig ileum (Guerrini *et al.*, 1998). The pharmacological profiles of (*p*OH) and [F/G]N/OFQ(1-13)NH_2 appear essentially identical and can therefore be interpreted if it is assumed that these ligands are actually low efficacy partial agonists,

the effects strongly depending upon the efficiency of stimulus/response coupling for the preparation under study (Calo *et al.*, 2000c). Collectively, these findings confirm a crucial role in the occupation and activation of NOP for the Phe^4 residue of N/OFQ, yielding a novel, highly potent and selective agonist analogue with the (*p*F) substitution. In all assays and preparations tested, this analogue mimicked the effects of N/OFQ and N/OFQ(1-13)NH_2 but with significantly higher potency. When combined with data from *in vivo* studies, the pharmacological profile in vitro for the (*p*F) substitution indicated potential for investigation of the N/OFQ-NOP system. In summary, [(*p*F)Phe^4]N/OFQ(1-13)-NH_2 is a highly potent agonist of NOP that will prove a useful tool in elucidating the pharmacology of the N/OFQ-NOP system.

2.5.3 Antagonists

Relocating the sidechain of the phenylalanine in position one of the sequence from the α-carbon to the terminal nitrogen atom produces a competitive antagonist that may be used as an antagonist template(Guerrini *et al.*, 2000a). The implication of this is that the position of the N-terminal sidechain is essential for receptor activation.

As for the agonist series, introduction of an extra arginine/lysine repeat at positions 14 and 15 (resulting in the antagonist, UFP-101) (Calo *et al.*, 2002) enhanced the effects in the antagonist series. In the antagonist template, it is worth noting that residual agonist activity was shown in most cases in the cAMP assay, implying that the translocation of the phenyl sidechain does not entirely abolish agonist activity where a large number of receptors are present on the cells.

Whilst fluoridation of the phenylalanine at position four enhances agonist activity (Guerrini *et al.*, 2001b), it gave no advantage in the antagonist template when used in this series. Combined with the additional arginine/lysine repeat this modification was seen to confer high residual agonist activity. This may be due to the modification, located in the (proposed) message domain, having some synergistic effect in combination with the arginine/lysine repeat in the (proposed) address domain, thereby overcoming the positional change in the sidechain of the terminal phenylalanine.

Rank order potency for these compounds was seen to be:

$$[Nphe^1,(pF)Phe^4,Arg^{14},Lys^{15}]N/OFQ\text{-}NH_2 > [Nphe^1,Arg^{14},Lys^{15}]N/OFQ\text{-}NH_2 > [Nphe^1,(pF)Phe^4]N/OFQ\text{-}NH_2 > [Nphe^1]N/OFQ\text{-}NH_2.$$

In this context, UFP-101 is worthy of further mention. As a highly potent (nM), competitive antagonist, it may form the basis of further research into the interaction of ligands with NOP. It is highly selective, having >1,000-fold selectivity over KOP and no activity at MOP and DOP the pA_2 *in vitro* is similar to that *ex vivo* and so should lend itself well to radiolabelling (Calo *et al.*, 2002).

2.5.4 Partial agonists

Altering the peptide bond in the message sequence of the template backbone, produces the peptoid [Phe$^1\psi$(CH_2-NH)Gly^2]N/OFQ-NH_2 ([F/G]), a partial agonist with potency between that of agonist and antagonist (Calo *et al.*, 1998). The change in conformational freedom caused by altering the bond between the first two amino acids obviously affects receptor activation but not to the extent seen in [Nphe^1]N/OFQ, where relocation of the sidechain has a dramatic effect upon activity. The modifications applied to other templates may also be applied to this series of compounds to give a variety of levels of activity.

The results showed that this series had rank order of potency:

[F/G,(*p*F)Phe^4,Arg^{14},Lys^{15}] > [F/G,Arg^{14},Lys^{15}] > [F/G,(*p*F)Phe^4] > [F/G].

Altering the peptide bond between Phe^1 and Gly^2 of the agonist template creates the partial agonists [F/G] and [F/G-O]. This modification affected radioligand binding affinity, potency and intrinsic activity compared to N/OFQ. Efficacy appeared to be dependent upon the assay system (compare GTPγ[^{35}S] binding with cAMP formation). The conformational freedom of the N-terminal portion of [F/G] and [F/G-O] generated by Phe^1-Gly^2 bond substitution may affect the relative orientation of the Phe^1 and Phe^4 pharmacophores, crucial for receptor occupation and activation. Compared to that of [F/G], the increased affinity and intrinsic activity of [F/G-O] indicated that the methoxy-bond produces a ligand in which Phe^1 and Phe^4 probably adopt a more favourable bioactive conformation for NOP activation (Meunier *et al.*, 2000).

It has been reported that [F/G] acts as a simple competitive antagonist with no residual agonist activity in the electrically stimulated mouse vas deferens, an N/OFQ sensitive preparation. However, in this preparation, [F/G-O] acts as an agonist with only 3-fold

reduction in potency and 81% relative intrinsic activity compared to N/OFQ(1-13)NH_2 (Guerrini *et al.*, 2003)).

In cAMP studies, all [F/G]-based ligands inhibited forskolin-stimulated cAMP formation to 100% and are classed as full agonists in this assay, in contrast to the situation in the GTPγ[^{35}S] binding assays. In a system where there is amplification between receptor, G-protein and effector the increased "downstream relative intrinsic activity" is common and has been described by several authors as a coupling reserve (Berger *et al.*, 2000a; Kenakin, 2002b). In the system used for this study there is a high level of receptor expression, a high degree of amplification and, hence, such a coupling reserve is inevitable. Whilst a system with a large dynamic response range (such as cAMP inhibition) is desirable, there is clearly a trade-off in terms of measured relative intrinsic activity and caution must be exercised when defining the pharmacological properties of drugs in a single cellular system.

In summary, [F/G-O] may represent a novel partial agonist at NOP with high relative intrinsic activity. Whilst this molecule has yet to be investigated *in vivo*, based on previous studies it may be predicted that central nervous system actions typical of N/OFQ (supraspinal pronociceptive and spinal antinociceptive actions, anxiolysis and a hyperphagic response) will be seen (Calo *et al.*, 2000c; Mogil *et al.*, 2001) albeit with a longer duration of action.

2.5.5 Cyclised Analogues

This study has shown that c[Cys^{10,14}] and c[Nphe^{1},Cys^{10,14}] bind to hNOP expressed in CHO cells, with a pronounced loss of affinity for the c[Nphe^{1},Cys^{10,14}] modification. Both peptides display high selectivity over classical opioid receptors (MOP/DOP/KOP) (Kitayama *et al.*, 2003). In GTPγ[^{35}S] and cAMP inhibition assays c[Cys^{10,14}] displayed full agonist activity. Both analogues bind to native NOP expressed in mouse and rat cerebrocortex and in mouse vas deferens (mVD) assays c[Cys^{10,14}] displayed agonist activity. In the GTPγ[^{35}S] assay, c[Nphe^{1},Cys^{10,14}] behaved as a competitive antagonist and this is also the case in mVD. However, in cAMP assays, where high amplification of signal occurs, the latter peptide behaved as an agonist (albeit with reduced potency, pEC_{50}). Considering tissue and assay differences c[Nphe^{1},Cys^{10,14}] was concluded to be

a partial agonist. The initial premise for this series was that cyclisation could produce a peptide with improved metabolic stability that would be of greater utility *in vivo*. In a series of crude metabolic stability studies, however, these cyclised analogues provided no increased protection compared to the equivalent amidated compound, N/OFQ-NH_2 (Kitayama *et al.*, 2003).

In radioligand binding studies c[$Cys^{10,14}$] showed a high degree of selectivity over MOP/DOP/KOP and this was confirmed by isolated tissue studies. In the mVD the effects of c[$Cys^{10,14}$] and N/OFQ(1-13)NH_2 were unaffected by the classical opioid receptor antagonist naloxone but competitively antagonised by the selective NOP antagonist, UFP-101 with a pK_B value (7.3) consistent with that reported previously (Calo *et al.*, 2002) thus demonstrating that the actions of both peptides are exclusively due to NOP activation.

A small reduction in binding affinity at NOP is seen for c[$Cys^{10,14}$], likely to result from modification of the address domain of the peptide, responsible for receptor binding (Guerrini *et al.*, 1997). Here the cyclic portion encompasses Arg^{11} and Lys^{12}, confirmed as essential residues for receptor binding in studies demonstrating N/OFQ(1-13)NH_2 as the shortest fragment that retains full biological activity. The creation of the first peptide with greater potency/affinity than N/OFQ, containing a triple Arg-Lys repeat motif (Okada *et al.*, 2000) further confirms this. This strategy was also used to design UFP-101 (Calo *et al.*, 2002). There was a reduction in efficacy at high concentration for the cyclic compound in the GTPγ[^{35}S] assay but not in cAMP inhibition.

These data are largely consistent with a paper where c[$Cys^{10,14}$] was evaluated using NOP in HEK-293 cells (Ambo *et al.*, 2001), where a small increase in binding affinity was seen, relative to N/OFQ(1-13)NH_2 and the linear version of the cyclic peptide [$Cys^{10,14}$]N/OFQ(1-14)NH_2. In GTPγ[^{35}S] assays there was a small reduction in functional potency but all analogues were full agonists.

It has been reported previously that [$Nphe^1$] substitution in both the N/OFQ(1-13)NH_2 and [Arg^{14},Lys^{15}]N/OFQ-NH_2 analogues results in highly selective NOP antagonists with the latter displaying improved affinity (Calo *et al.*, 2000b; McDonald *et al.*, 2003b). As for the cyclised agonist, it was hoped to make a more metabolically stable

cyclised antagonist, c[Nphe^{1},Cys^{10,14}]. In GTPγ[^{35}S] and mVD studies, clear competitive antagonism was observed but of relatively low affinity. Despite no indication of residual agonist activity with c[Nphe^{1},Cys^{10,14}] in GTPγ[^{35}S] (and mVD) assays, in cAMP assays this peptide behaved as an agonist. At the highest concentration tested (10μM) there was 80% inhibition of the forskolin- stimulated response, with a crudely estimated agonist potency of 5.76 (based on a theoretical 100% maximum inhibition).

When applied to the linear templates, [Nphe^{1}] modification produces pure antagonists (Calo *et al.*, 2000b) but when applied to the cyclised template, antagonism is observed in GTPγ[^{35}S] and mVD assays and agonist activity is seen in cAMP assays where signal is measured after amplification (present data). This difference is not easy to interpret although the address domain of N/OFQ can assume an alpha helix structure (Zhang *et al.*, 2002), likely to be important for NOP binding. In particular, the second extra-cellular loop of the receptor contains several acidic residues (Topham *et al.*, 1998) reminiscent of the binding site for dynorphin at KOP (Paterlini *et al.*, 1997). Cyclisation of the 10-14 region of the N/OFQ sequence may interfere with the ability to assume an alpha helix conformation and this, in turn, may affect the relative orientation between the address and the message domains, the latter where [Phe^{1}] (or the [Nphe^{1}] modification) are located. These changes may be negligible for agonist activity while they may limit the ability of the [Nphe^{1}] modification to reduce efficacy thereby generating a partial agonist.

The initial premise of the cyclization study was to generate a peptide with improved metabolic stability. In a crude attempt to assess metabolic stability c[Cys^{10,14}] was exposed to rat cerebrocortical membranes (as a potential source of peptidases) for increasing times. Peptide remaining in the supernatant was assessed using a simple competition binding "bioassay". There was a time dependent metabolism of N/OFQ which was reduced by amidation but cyclisation offered no additional protection. Reducing buffer pH to 3.0 was able to prevent c[Cys^{10,14}] metabolism (Kitayama *et al.*, 2003).

In essence, in this system the peptide did not have improved metabolic stability. There are several potential problems with this series of experiments in that N/OFQ(1-14)NH_2 or a linear version of c[Cys^{10,14}] have not been used as reference standards. but it is

perhaps unlikely that this will make a significant difference. However, potentially of more concern is the source of metabolic "activity" in rat brain homogenate if this is a representative example of *in vivo* peptide metabolism. Certainly in most *in vivo* studies direct i.c.v injection is used, so in this respect this is a representative model. However, it might be useful to perform future studies with plasma as a representation of i.v. administration, although the real test would be simple *in vivo* administration at both i.c.v and i.v. sites.

In summary, cyclisation at positions 10 and 14 produced an agonist with slightly reduced potency (pEC_{50}) in GTPγ[^{35}S] and mVD assays and [Nphe^{1}] substitution in this agonist, giving c[Nphe^{1},Cys^{10,14}], produced an antagonist in GTPγ[^{35}S] and mVD assays and an agonist in cAMP assays. With uncertainty regarding metabolic activity, *in vivo* studies are clearly warranted.

2.5.6 Synthetic compounds

Non-peptide compounds, both agonists and antagonists with varying degrees of selectivity for NOP, are generally more metabolically stable and less immunogenic than peptides and may therefore prove to be useful in clinical applications.

Studies of the pharmacology of the N/OFQ-NOP system have been hampered by the relative lack of ligands (both peptide and non-peptide) with which to make detailed *in vitro* and, more importantly, *in vivo* studies. For a molecule to be of interest in the therapeutic arena it needs to be highly selective and preferably non-peptide in nature. Several such molecules have been described and these include the Roche agonist (Ro64-6198) which displays an impressive anxiolytic profile (Dautzenberg *et al.*, 2001; Jenck *et al.*, 2000) and the antagonist of Banyu, J-113397 (Kawamoto *et al.*, 1999; Ozaki *et al.*, 2000). Several other ligands have been described in the literature with varying degrees of selectivity, such as JTC-801 (Shinkai *et al.*, 2000; Yamada *et al.*, 2002) and III-BTD (Becker *et al.*, 1999). In general these molecules have some activity at classical opioid (MOP/DOP/KOP) receptors.

It is important to confirm that any novel molecule activates the receptor of interest (NOP in this case), utilises the appropriate transduction machinery and displays selectivity. Two antagonists (J-113397 and III-BTD) have competitively reversed the effects of both [(*p*F)Phe^{4}] and N/OFQ(1-13)NH_2 with pA_2/pK_B similar to those obtained

against N/OFQ (Hashiba *et al.*, 2001; Hashiba *et al.*, 2002) and to those reported in the literature by other groups and in different preparations (Becker *et al.*, 1999; Kawamoto *et al.*, 1999). At this point it is worth reiteration that estimated antagonist potency in the GTPγ[^{35}S] assay is higher than that in the cAMP assay (Berger *et al.*, 2000a; Hashiba *et al.*, 2001). The Roche compounds comprise a series of synthetic agonists, of which Ro64-6198 has high selectivity for NOP over the opioid receptors, as compared with Ro65-6570 which has poor MOP selectivity (Hashiba *et al.*, 2001). Schild analysis of J113397, a synthetic antagonist selective for NOP, showed that its behaviour at NOP is competitive and highly potent (pA_2=7.48), with no intrinsic agonist activity. J113397 showed equi-potency at NOP (pK_B=7.52) with the non-selective opioid antagonist III-BTD (pK_B=7.49). This potency and its non-peptide nature, in combination with high selectivity (>300-fold) over human opioid receptors, mean that J113397 represents the most effective of the synthetic antagonists currently available (Chiou *et al.*, 2002).

Presently, a few studies (Marti *et al.*, 2003; Shinkai *et al.*, 2000; Yamada *et al.*, 2002) have reported the antagonist properties of JTC-801 at NOP. These show that, when co-applied with N/OFQ, 10μM JTC-801 antagonized both the binding of N/OFQ to recombinant human NOP and the inhibition of forskolin-stimulated cAMP accumulation by N/OFQ in HeLa cells. Without pre-treatment, 10μM JTC-801 antagonises the action of N/OFQ on cAMP formation in CHO_{hNOP} cells and is ineffective at lower concentrations. The results suggest that JTC-801 is not in equilibrium, similar to recently published findings by a Japanese group (Yamada *et al.*, 2002). Following a minimum 40min pre-incubation, the potency (pK_B) of JTC-801 at 1μM increased from zero to 6.46 and at 10μM increased from 6.97 to 7.49. Although these values serve only as indicators due to the conditions, the conclusion is that the equilibrium and, therefore, potency of JTC-801 is time-dependent. Evidence that the binding of non-peptide antagonists is slower than peptide antagonists is seen in some cases such as NK_2 tachykinin (Emonds-Alt *et al.*, 1992) and B_2 bradykinin receptors (Camarda *et al.*, 2002). Selective non-peptide NOP agonists, such as Ro 64-6198, also display different kinetics including slow on-time and pseudo-irreversible effects compared to N/OFQ (Rizzi *et al.*, 2001). Values of pK_B for 1 and 10μM JTC-801 were also different after 90min pre-incubation. This finding may be related to a similar, mixed nature of the compound (Yamada *et al.*, 2002).

3 Pharmacological characterisation of hNOP in an inducible expression system

3.1 Introduction

To date a variety of mammalian cell lines, including CHO and HEK-293, have been used to express hNOP (Dautzenberg *et al.*, 2001; Guerrini *et al.*, 2000b). In these cases expression is either transient, leading to relatively unpredictable levels of expression, or stable clones are generated, usually resulting in very high receptor density, unrepresentative of expression *in vivo*. To date, there have been no detailed studies on hNOP at differing levels of expression in one cell type. This dependence of activity upon the expression system used points to the need for a uniform cellular background that allows this variation to be eliminated, avoiding any background effects due to the expression system. It would be advantageous to have a single cell line available able to express differing levels of receptor, in a controllable manner, dependent upon the concentration of an induction agent.

The ecdysone-inducible expression system has the potential to fulfil these criteria and is available as a CHO cell line transfected with hNOP. This presents a relatively simple method for production of cultures with differing expression levels of the receptor using the same cellular background. In this system, addition of a hormone analogue to the incubation medium induces transcriptional activity of the receptor gene, resulting in receptor expression dependent upon the concentration of induction agent. The system has already been used to express such receptors as sst2 (Cole *et al.*, 2001), 5-HT (h5-HT 1B, 1F, 4B) (Van Craenenbroeck *et al.*, 2001) and DOP (Law *et al.*, 2000b).

3.1.1 The Ecdysone-Inducible Mammalian Expression System

The basis of this system is the hormonal control of ecdysis, the process of moulting in insects, specifically that of the model organism for genetic studies, species of the fruit fly genus *Drosophila*. When added to the incubation medium, Ponasterone A (Pon A), a plant-derived analogue of the steroid moulting hormone ecdysone, activates a chimæric variant of the ecdysone receptor. This activated receptor induces transcription of the gene for the receptor of interest, in this case hNOP, resulting in cell-surface levels of receptor density controllable in a manner dependent upon the concentration of Pon A used. Induction of expression levels to greater than 200 times basal have been reported for Muristerone A, another analogue of ecdysone (No *et al.*, 1996), with Pon A reported

to have comparable effect (Nakanishi, 1992). The chemical structure of Pon A is shown in Figure 3.1.

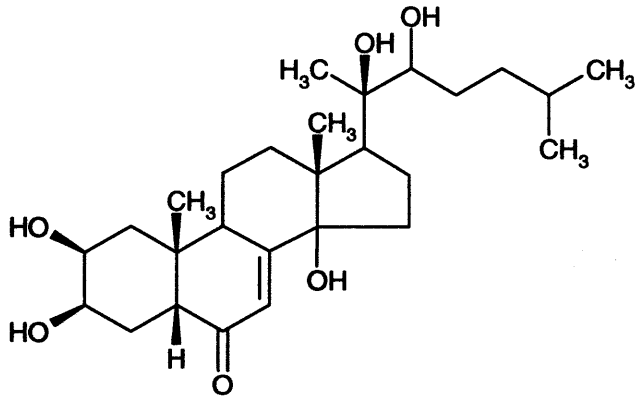

Figure 3.1 The structure of Pon A.
The induction agent for the ecdysone-inducible expression system used in this work.

To express the gene of interest (hNOP, in this case) cells are transfected with two plasmids. The first (pVgRXR) codes for the heterodimeric ecdysone receptor subunits and the second (pIND) contains the gene for hNOP. In stock cultures, the VgRXR plasmid is maintained by the selection agent zeocin and Geneticin (G418) is used to maintain pIND. For the structures of these two plasmids, see Figures 3.2 and 3.3.
The chimæric nuclear receptor employed by this system consists of a heterodimer comprising the ecdysone receptor from *D. melanogaster*, fused with a transactivation domain from Herpes simplex virus (VgEcR/VP16) and the retinoid X receptor (RXR), a mammalian homologue of ultraspiracle (USP) the native partner of VgEcR in *Drosophila.*

In the presence of Pon A, these subunits associate and the receptor binds to a hybrid response element (E/GRE, on pIND) comprising the natural ecdysone response element (5'-AGTGCA-3') and one half of the mammalian glucocorticoid response element (5'-AGAACA-3'). This response element lies upstream of a minimal heat shock promoter, activation of which is induced by the ecdysone receptor binding to the response element and leads to transcription of the hNOP gene (No *et al.*, 1996). The use of a hybrid response element reduces interaction with any endogenous receptors in the cells. A schematic illustration of the induction process is shown in Figure 3.4.

Figure 3.2 The pVgRXR plasmid used for the transfection of the hybrid receptor in the ecdysone-inducible expression system.
This plasmid carries the genes for the hybrid receptor used for the induction of hNOP. Features are: PCMV, cytomegalovirus immediate early enhancer-promoter; VgEcR, VP16/ecdysone receptor fusion protein sequence; TKpA, thymidylate kinase polyadenylation sequence; PRSV, Rous sarcoma virus promoter; RXR, retinoid X receptor sequence; BGHpA, bovine growth hormone polyadenylation sequence; f1 ori, origin of replication in mammalian cells; SV40 and EM-7, promoters for expression of zeocin resistance gene in mammalian cells and *E. coli*, respectively; SV40 pA, SV40 polyadenylation sequence; ColE1, origin of replication in *E. coli* (Invitrogen Life Technologies).

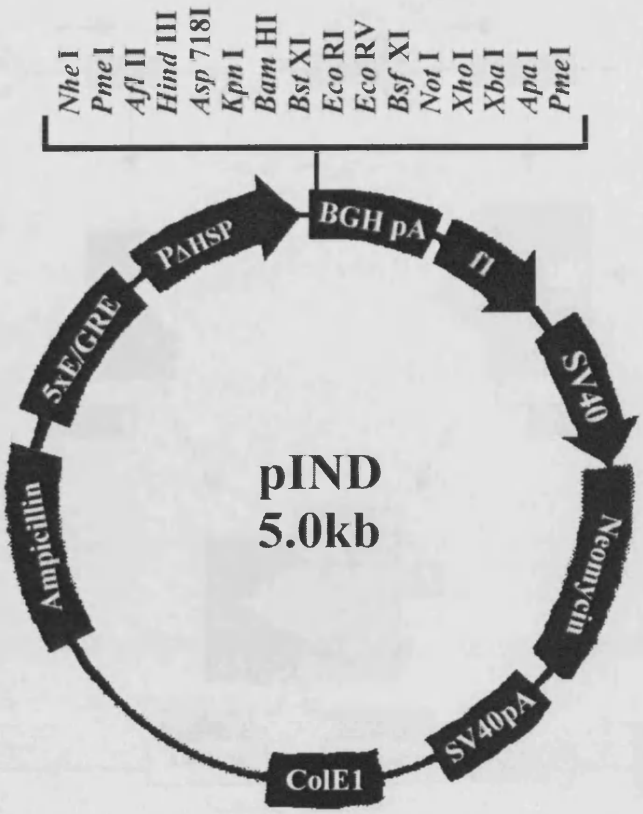

Figure 3.3 The pIND plasmid used for the transfection of hNOP in the ecdysone-inducible expression system.

The products of the VgRXR plasmid induce the transcription of the NOP gene from this plasmid. The gene of interest is ligated into the plasmid at the insertion site, marked by the restriction enzyme sites (top). For the cells used in this thesis the human NOP gene was inserted. Features are: 5xE/GRE, five repeats of the modified ecdysone/glucocorticoid response element; PΔHSP, promoter for minimal heat shock protein; BGHpA, bovine growth hormone polyadenylation sequence; f1, origin of replication in mammalian cells; SV40, promoter for neomycin selection resistance in mammalian cells; Neomycin, neomycin resistance gene sequence; SV40pA, SV40 polyadenylation sequence; ColE1, origin of replication in *E. coli*; Ampicillin, resistance gene for maintenance in *E. coli* (Invitrogen Life Technologies).

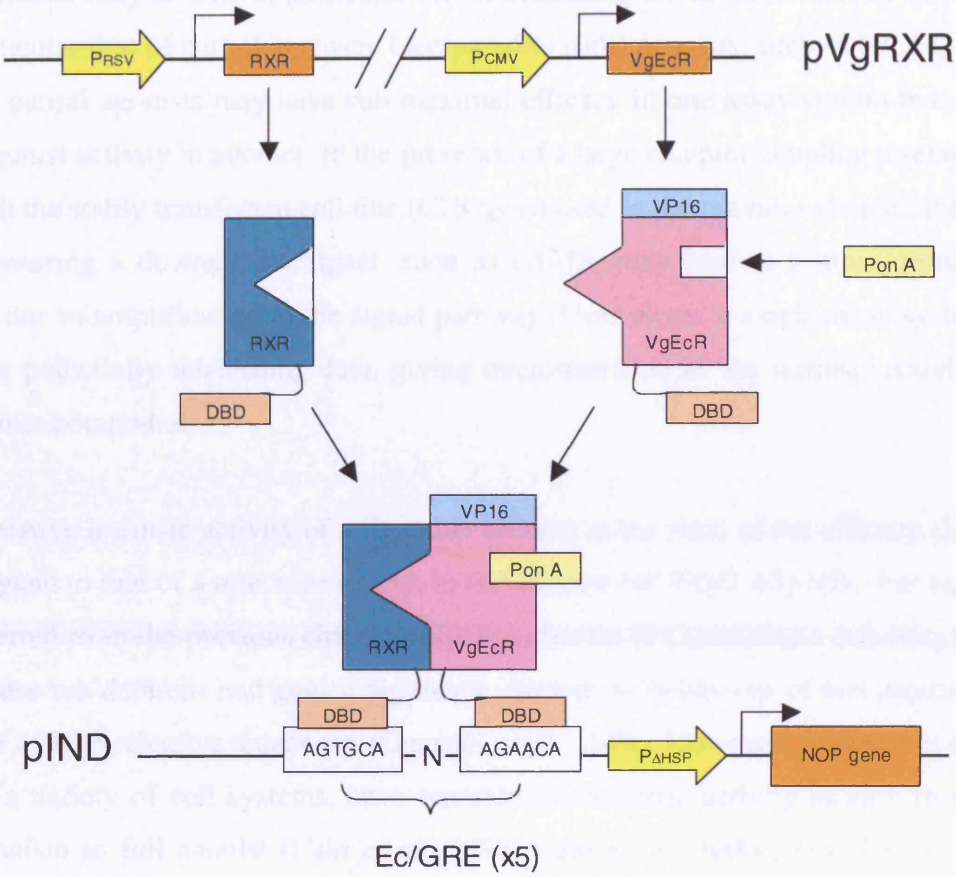

Figure 3.4 Schematic showing the induction pathway for the expression of human NOP in the ecdysone-inducible expression system, using the two plasmids – pVgRXR and pIND.
PRSV, Rous sarcoma virus promoter; PCMV, cytomegalovirus immediate early enhancer-promoter; RXR, retinoid X receptor; VgEcR, ecdysone receptor; VP16, VP16 transactivation domain; DBD, DNA binding domain; Pon A, Ponasterone A; Ec/GRE, modified ecdysone/glucocorticoid response element; N, single nucleotide spacer between two half-sites; PΔHSP, minimal heat shock protein promoter; NOP gene, DNA coding region for human NOP.

This system may also be of particular use in evaluating the intrinsic activity of ligands, in particular that of partial agonists. Compared to (full) agonists, such as N/OFQ in this work, partial agonists may have sub-maximal efficacy in one assay system but display full agonist activity in another. In the presence of a large receptor/coupling reserve, such as with the stably transfected cell line (CHO_{hNOP}) used in the previous chapter, the result of measuring a downstream signal, such as cAMP, may lead to a more pronounced effect due to amplification in the signal pathway. Used alone, a single assay system can deliver potentially misleading data, giving overestimation of the intrinsic activity of a particular compound.

The relative intrinsic activity of a ligand is defined as the ratio of the efficacy (E_{max}) of that ligand to that of a reference ligand, in this chapter N/OFQ(1-13)-NH_2. For example, as referred to in the previous chapter, initial studies on [F/G]N/OFQ(1-13)-NH_2 ([F/G]) in mouse vas deferens and guinea pig ileum showed the behaviour of this peptoid to be that of a NOP-selective antagonist (Guerrini *et al.*, 1998). However, subsequent studies, using a variety of cell systems, have reported the intrinsic activity to vary from pure antagonism to full agonist (Calo *et al.*, 1998; Calo *et al.*, 2000c; Grisel *et al.*, 1998; Mason *et al.*, 2001; Meis *et al.*, 1998; Menzies *et al.*, 1999; Okawa *et al.*, 1999).

3.2 Aims

The aims of this chapter are:

- To characterise the ecdysone-inducible expression system for the expression of hNOP in a CHO cell line ($CHO_{INDhNOP}$) to produce a reliable model for the study of the pharmacology of hNOP over a range of controllable levels of receptor density.
- Subsequent pharmacological characterisation of hNOP expressed at levels similar to those typically obtained from saturation binding studies in membranes prepared from rat cerebral cortex.
- To investigate the effects of receptor density upon the measured intrinsic activity of the NOP partial agonist [F/G].

3.3 Materials & Methods

3.3.1 Sources of Materials

All materials used for this section of the work are as noted in Section 2.2, with the following exceptions:

Chinese hamster ovary cells expressing human NOP using the ecdysone-inducible expression system ($CHO_{INDhNOP}$) were kindly provided by Dr F. Marshall and Mrs N. Bevan of GSK (Stevenage, Herts, UK).

Cell culture

Ponasterone A (Pon A), zeocin – InvitroGen, Paisley, Scotland, UK.

3.3.2 Cell Culture and induction

Cells expressing human NOP in the ecdysone-inducible system ($CHO_{INDhNOP}$) were cultured in HAMS F12 media, supplemented with 10% foetal bovine serum, penicillin ($100IU.ml^{-1}$), streptomycin ($100\mu g.ml^{-1}$) and fungizone ($2.5\mu g.ml^{-1}$). Some experimental cultures for cAMP assays were grown in media on 24-well plates. Stock media was further supplemented with zeocin ($250\mu g.ml^{-1}$) and geneticin ($1mg.ml^{-1}$) to maintain pVgRXR and pIND, respectively. All cultures were maintained at 37°C with 5% carbon dioxide, humidified air and sub-cultured as required using trypsin/EDTA. As they approached confluence, $CHO_{INDhNOP}$ cells were induced with Pon A, at concentrations of 1, 2, 5, 10 or 20μM, for 20h. Non-induced $CHO_{INDhNOP}$ cultures were used as negative controls in which the medium was replaced 20h prior to use. In studies using pertussis toxin (PTx), $100ng.ml^{-1}$ was added to media at the time of induction as described in Chapter 2.

3.3.3 Membrane Preparation

For saturation and displacement binding assays, membranes were prepared from freshly harvested $CHO_{INDhNOP}$ cells, 20h post-media change/induction. Membranes were prepared as described in Section 2.2.5, final concentration adjusted as required for the experimental procedure.

3.3.4 Saturation Binding

Membrane suspension (protein 15-350μg.tube^{-1}, depending upon induction level) was incubated (1h, room temperature) in 0.5ml volumes containing assay buffer, 10μM peptidase inhibitor cocktail (amastatin, bestatin, captopril and phosphoramidon) and various concentrations of [*leucyl*-^{3}H]N/OFQ (≈ 2nM to 0.002pM). Non-specific binding (NSB) was defined in the presence of 1μM unlabelled N/OFQ. Reactions were terminated by vacuum filtration through Whatman GF/B filters, soaked in 0.5% polyethylenimine (PEI), using a Brandel harvester.

3.3.5 Displacement Binding

Membrane suspension (protein 35-70μg.tube^{-1}) was incubated (1h, room temperature) in assay buffer, containing a fixed concentration of [*leucyl*-^{3}H]N/OFQ (≈ 200pM) and varying concentrations of a range of displacers. NSB was determined in the presence of 1μM unlabelled N/OFQ. Reactions were terminated via filtration through 0.5% PEI-soaked, Whatman GF/B filters using a Brandel harvester.

In all cases, bound radioactivity was determined following filter extraction (8 hours, Optiphase Safe, Wallac) using liquid scintillation counting.

3.3.6 Inhibition of forskolin-stimulated cAMP formation

Inhibition of forskolin-stimulated cAMP formation was measured using whole cells, induced at 1, 2, 5 and 10 and 20μM Pon A or non-induced control. Confluent, adherent cell cultures grown in 24-well tissue culture trays were incubated as described in Section 2.2.8. Ligands were included in various combinations and at different concentrations. Reactions were terminated as described previously. For plate assays, after ligand challenge reactions were terminated in the wells with 10M HCl for 30min, on ice, then neutralised and buffered. Lysates were then transferred to tubes for the remainder of the assay, as described previously. In all cases, concentration of cAMP formed was measured as described in Section 2.2.8.

3.4 Results

3.4.1 Saturation binding assays

Incubation of $CHO_{INDhNOP}$ cells with Pon A induced concentration-dependent expression of hNOP, as measured by the binding of [*leucyl*-^{3}H]N/OFQ. A representative plot of relative binding at the different Pon A inductions used is shown in Figure 3.5. The results for these assays are shown in Table 3.1.

Specific binding of [*leucyl*-^{3}H]N/OFQ increased from 24 to 1101 fmol.mg^{-1} protein as the concentration of Pon A was increased from 1 to 10μM. In non-induced cultures there was no significant specific binding despite the use of a high mass of membrane protein (350μg.tube^{-1}). Interestingly, the relationship between induction and expression appeared to be bell-shaped, such that an apparent maximum was obtained at 10μM Pon A, above which (20μM Pon A) binding decreased. In a simple series of trypan blue exclusion experiments (n=6, data not shown), induction of cells at 20μM Pon A did not show any evidence of cytotoxicity.

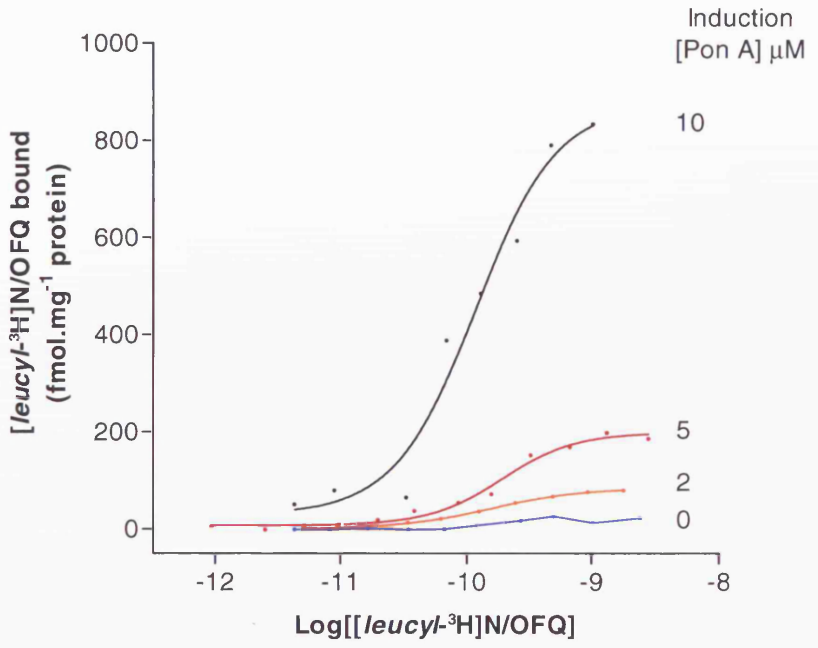

Figure 3.5 Representative [*leucyl*-^{3}H]N/OFQ saturation binding curves for membranes from $CHO_{INDhNOP}$ cells induced at various concentrations of Pon A.
Note that the 1μM Pon A induction has been omitted for clarity.

Table 3.1 Saturation binding in the ecdysone-inducible expression system.
The binding of [*leucyl*-^{3}H]N/OFQ to $CHO_{INDhNOP}$ membranes was Pon A dependent. Saturation analysis of log-transformed data was used to estimate B_{max} and pK_D.
Data are mean±SEM for n=5 experiments.

[Pon A] (μM)	pK_D	K_D (pM)	B_{max} (fmol.mg^{-1} protein)
0	-	-	-
1	9.91±0.04	123	23.5±4.4
2	9.83±0.09	148	68.3±9.7
5	10.22±0.15	60	190.6±25.5
10	9.89±0.14	129	1101.0±145.3
20	9.89±0.13	129	191.2±33.9

Expression of NOP at 5μM Pon A induction (≈ 200fmol.mg^{-1} protein) is similar to that measured in brain tissues (rat cerebral cortex membranes, 130-180fmol.mg^{-1} protein) (Hashiba *et al.*, 2002; Okawa *et al.*, 1998), so this level of induction was used in a series of displacement binding, GTPγ[^{35}S] binding and cAMP inhibition studies to detail the pharmacology of the inducible system for hNOP (GTPγ[^{35}S] binding data courtesy of J. McDonald).

3.4.2 Displacement binding assays

After determination of the expression profile for this cell system from the saturation binding experiments, displacement binding assays were conducted. This enables direct comparison of the affinities for NOP of non-labelled ligands with some of the modifications detailed in the previous chapter. Especially important is the effect on binding affinity of modifications resulting in partial agonists such as [F/G]. The effect of the NOP selective, non-peptide antagonist J-113397 was also evaluated in this system.

The binding of a fixed concentration of [*leucyl*-^{3}H]N/OFQ to membranes, prepared from $CHO_{INDhNOP}$ cells induced at 5μM Pon A, was displaced in a concentration-dependent and saturable manner by a range of peptide and non-peptide NOP ligands. Values of pK_i for these data are summarised in Table 3.2.

Table 3.2 Displacement assays measured in $CHO_{INDhNOP}$ membranes for a range of NOP ligands.
Cells were induced at 5μM Pon A. Values of pK_i from CHO_{hNOP} membranes are included from Chapter 2 for comparison. Data in $CHO_{INDhNOP}$ for Naloxone Benzoylhydrazone (NalBzOH) from J. McDonald; that in CHO_{hNOP} for NalBzOH from (Bigoni *et al.*, 2002) and for J113397 from (Hashiba *et al.*, 2001).
Values calculated using Cheng and Prusoff equation with K_D for [*leucyl*-^{3}H]N/OFQ of 60.3pM, measured in saturation experiments at same induction level (see Table 3.1).
Data are mean±s.e.mean (n=4). Nature of ligand: P, peptide; *P*, peptoid; S, synthetic.

Type of ligand	Ligand	pK_i	pK_i (CHO_{hNOP})	Nature of ligand
Agonists	N/OFQ	9.93±0.08	9.91±0.04	P
	N/OFQ-NH_2	10.37±0.04	10.31±0.04	P
	N/OFQ(1-13)-NH_2	10.35±0.04	10.24±0.09	P
Presumed partial agonists	NalBzOH	7.10±0.02	*7.26±0.02*	S
	[F/G]	9.60±0.1	9.89±0.08	*P*
Antagonist	J-113397	9.09±0.11	8.82±0.02	S

The rank order for pK_i was:

$$N/OFQ\text{-}NH_2 = N/OFQ(1\text{-}13)\text{-}NH_2 > N/OFQ >$$
$$[F/G]N/OFQ(1\text{-}13)\text{-}NH_2 > J\text{-}113397 > NalBzOH$$

3.4.3 GTPγ[^{35}S] functional studies

In membranes prepared from $CHO_{INDhNOP}$ cells incubated with 1, 2, 5 and 10μM Pon A both N/OFQ(1-13)-NH_2 and [F/G] stimulated the binding of GTPγ[^{35}S] in a concentration dependent and saturable manner. As the induction concentration of Pon A was increased the E_{max} (stimulation factor) of N/OFQ(1-13)-NH_2 increased, from 1.28 (1μM) to 6.95 (10μM). The E_{max} of [F/G] also increased as a function of the induction concentration, from 0.98 (effectively basal) at 1μM Pon A to 3.21 at 10μM Pon A. These results are shown in Table 3.3.

However, the relative intrinsic activity of [F/G] (relative to N/OFQ(1-13)-NH_2) remained similar at 0.37 – 0.55 for all induction levels.

Table 3.3 Effects of N/OFQ(1-13)-NH_2 and [F/G] upon stimulation of GTPγ[^{35}S] binding in $CHO_{INDhNOP}$ membranes.
pEC_{50} for N/OFQ(1-13)-NH_2 and [F/G] did not differ ($p>0.05$, ANOVA).
Pon A concentration-dependent increase in E_{max} for N/OFQ(1-13)-NH_2 and [F/G] ($p<0.05$ ANOVA). Data courtesy J. McDonald.

[Pon A] μM	N/OFQ(1-13)-NH_2		[F/G]		Relative Intrinsic Activity
	pEC_{50}	E_{max} Stimulation Factor	pEC_{50}	E_{max} Stimulation Factor	
10	8.60±0.07	6.95±1.05	7.72±0.06	3.21±0.38	0.37
5	8.52±0.06	4.33±0.80	7.68±0.10	2.01±0.23	0.30
2	8.68±0.11	1.93±0.20	7.23±0.38	1.51±0.15	0.55
1	8.12±0.32	1.28±0.03	Not analysable	Not analysable	-

The antagonist activity of [F/G] was also tested in GTPγ[^{35}S] binding experiments, performed at the lowest induction level (1μM), using full sequence N/OFQ as the reference agonist. From this a value of pK_B for [F/G] was derived. A comparison was also made with J113397. The results are shown in Table 3.4.

Table 3.4 Effects of N/OFQ, N/OFQ-NH_2, [F/G] and J113397 upon GTPγ[^{35}S] binding in membranes from $CHO_{INDhNOP}$ cells.
For partial agonist, cells were induced at low Pon A concentration for antagonist assays against N/OFQ and N/OFQ-NH_2.
Data are mean±s.e.mean for n=3 experiments. Data courtesy J. McDonald.

Ligand	[Pon A] (μM)	pEC_{50}	E_{max} (stimulation factor)	pK_B
N/OFQ	5μM	8.26±0.01	3.72±1.01	-
N/OFQ-NH_2	5μM	8.92±0.05	4.13±0.62	-
[F/G]	1μM	Inactive	Inactive	7.62±0.08
J113397	5μM	Inactive	Inactive	8.45

3.4.4 cAMP functional studies

Control Studies

Some initial studies were made to confirm that the action of any ligands was mediated via NOP in this system. The effect of N/OFQ upon cells induced at 5μM Pon A and non-induced (control) cells from the same passage number was tested. The results showed that there was no activity of N/OFQ in the non-induced cells, whilst inhibition of cAMP formation was seen in cells induced at 5μM Pon A (pEC_{50}=10.18±0.09, E_{max}=73.9±3.5). Results are shown in Figure 3.6.

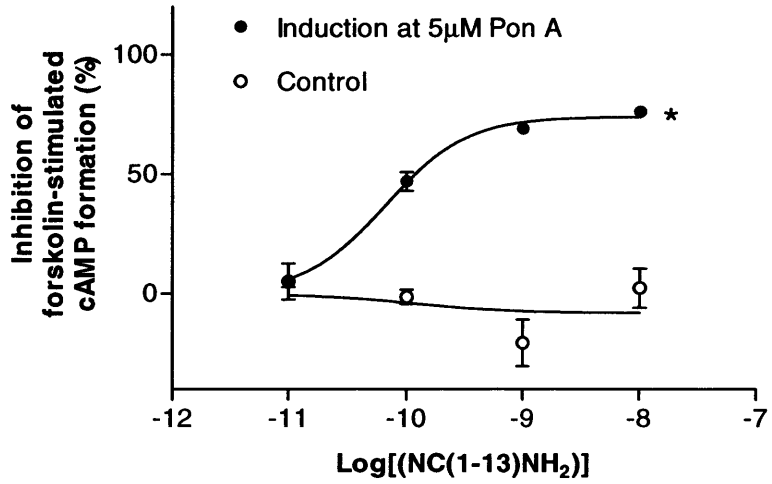

Figure 3.6 Concentration-response curves for $CHO_{INDhNOP}$ cells in cAMP assays with and without induction at 5μM Pon A.
Data are for n=3 experiments, * indicates significant difference from non-induced control.

The effect of amidation upon N/OFQ activity was also tested to ensure that this modification had no effect upon response. As also shown in Chapter 2 (SAR Studies), there was no difference between native N/OFQ (pEC_{50}=9.38±0.07, E_{max}=70.4±3.1) and N/OFQ-NH_2 (pEC_{50}=9.66±0.04, E_{max}=66.9±2.4), demonstrating similar pharmacology for NOP in this expression system. Results of these assays are shown in Figure 3.7.

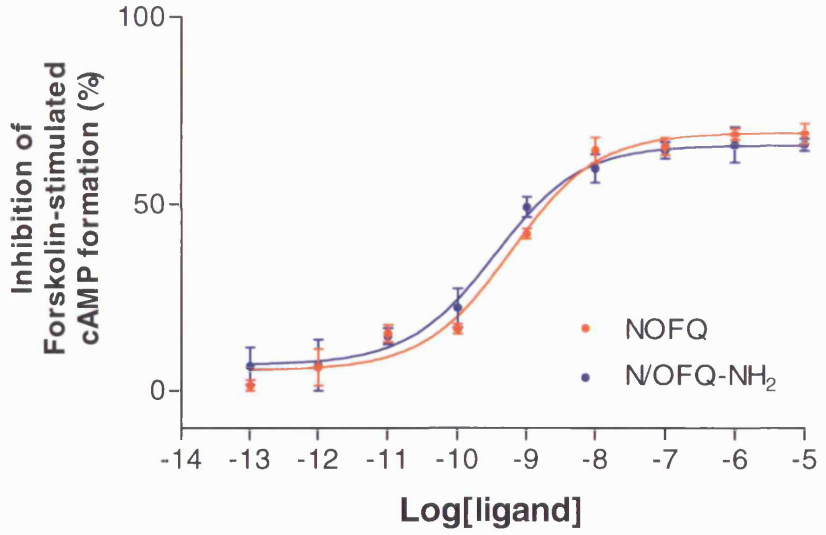

Figure 3.7 Effect of amidation upon N/OFQ inhibition of cAMP formation in $CHO_{INDhNOP}$ cells induced at 5μM Pon A.
Data are for n=3 experiments. Cells were cultured and induced in 24-well trays.

Comparison of N/OFQ with [F/G]

In cAMP inhibition studies, maximum inhibition (E_{max}) varied with induction concentration for both compounds. Values ranged from 41% to 86% for N/OFQ(1-13)-NH_2 and 20% to 83% for [F/G] at low and high Pon A induction respectively. Concentration response curves for these ligands are shown in Figure 3.8.

The relative intrinsic activity of [F/G] varied from 0.48 to 0.97 indicating that, at 10μM Pon A, this molecule, in this assay, behaved as a full agonist. At the lower 1μM Pon A induction, due to low expression of hNOP and sensitivity of this assay, data for cAMP studies could not be reliably analysed. Data for these experiments are shown in Table 3.5. Due to the high relative efficacy of [F/G] in cAMP assays, experiments were not performed using this compound as an antagonist of N/OFQ.

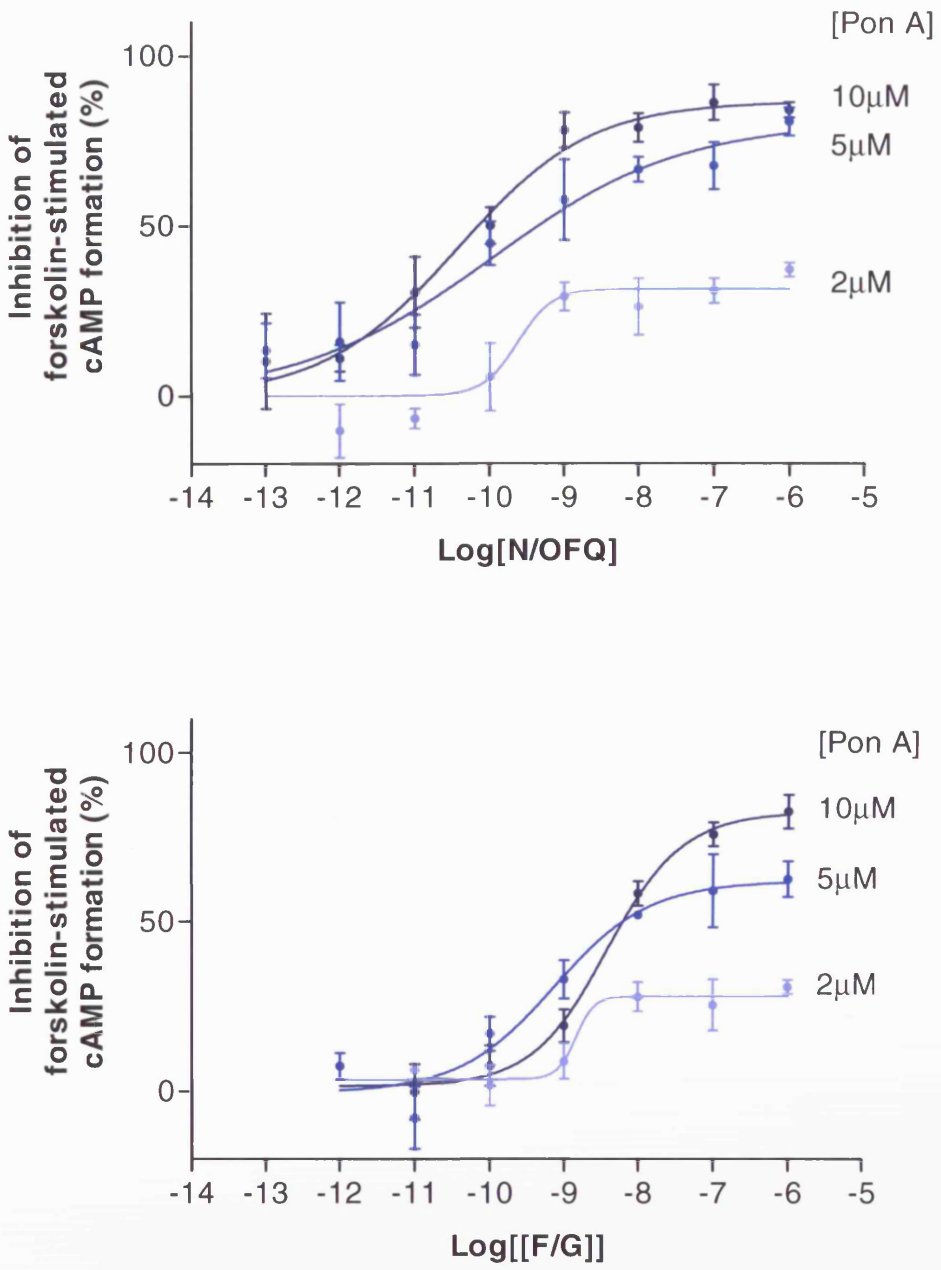

Figure 3.8 Inhibition of forskolin-stimulated cAMP formation by N/OFQ(1-13)-NH_2 (Upper) and [F/G] (Lower) in whole $CHO_{INDhNOP}$ cells induced at 2, 5 and 10μM Pon A.
Data are for n=4 experiments. Cells were cultured and induced in 24-well trays.

Table 3.5 Effect of inducing concentration of Pon A upon N/OFQ(1-13)-NH_2 and [F/G] inhibition of cAMP formation in whole $CHO_{INDhNOP}$ cells.
Data are mean±s.e.mean for n=4 experiments. Cells were cultured and induced in 24-well trays.
* indicates significant difference ($p<0.05$) from N/OFQ(1-13)-NH_2;
** indicates significant difference ($p<0.001$) from 10μM and 5μM induction.

[Pon A] (μM)	Ligand	pEC_{50}	EC_{50} nM	Max. inhibition (%)	Relative Intrinsic Activity
10	N/OFQ(1-13)-NH_2	10.35±0.22	0.04	86.0±3.7	-
	[F/G]	8.32±0.13	4.79	83.2±4.0	0.97
5	N/OFQ(1-13)-NH_2	9.72±0.40	0.19	79.5±4.1	-
	[F/G]	8.99±0.18	1.02	59.4±5.8*	0.75
2	N/OFQ(1-13)-NH_2	9.42±0.49	0.38	40.9±2.2**	-
	[F/G]	8.26±0.87	5.50	19.6±4.8**	0.48

3.4.5 Pertussis toxin (PTx) sensitivity

To confirm $G_{i/o}$ coupling for this receptor, $CHO_{INDhNOP}$ cells were induced (5μM Pon A, 20h, incubation conditions as before) in the absence and presence of PTx (100ng.ml^{-1}). Membrane fragments or whole cells were then tested for ability to stimulate binding of GTPγ[^{35}S] (data courtesy J. McDonald) or inhibition of cAMP formation by N/OFQ, N/OFQ(1-13)-NH_2 and [F/G]. Results for these assays are shown in Table 3.6.

Whilst, in this series of experiments, the degrees of stimulation of GTPγ[^{35}S] binding and inhibition of cAMP formation were slightly reduced, PTx treatment clearly prevented agonist-stimulated GTPγ[^{35}S] binding by N/OFQ, N/OFQ(1-13)-NH_2 and [F/G] confirming the action of NOP via $G_{i/o}$ in this cell system.

Table 3.6 PTx sensitivity of agonist stimulated GTPγ[^{35}S] binding and cAMP inhibition for $CHO_{INDhNOP}$ membranes and cells respectively.
Cells were induced at 5μM Pon A for 20h in culture flasks.
Ligands were included at 10μM (GTPγ[^{35}S]) and 100nM (cAMP).
Data are mean±s.e.mean for n=3 experiments.
* indicates values significantly reduced compared with control ($p<0.05$, unpaired t-test).

Ligand	GTPγ[^{35}S] binding (stimulation factor)		cAMP inhibition (%)	
	Control	+PTx	Control	+PTx
N/OFQ	2.45±0.34	1.01±0.16*	43.1±8.9	0.0±9.6*
N/OFQ(1-13)-NH_2	2.49±0.38	1.17±0.13*	50.3±8.8	1.7±7.0*
[F/G]	1.48±0.13	0.74±0.20*	45.5±16.7	3.4±15.3*

3.5 Discussion

The ecdysone-inducible expression system described here has been characterised for the expression of hNOP in CHO cells at a range of induction concentrations. Saturation binding studies showed a range of receptor density dependent upon the inducing concentration of Pon A used.

When induced at 20μM Pon A the cells showed decreased binding of [*leucyl*-^{3}H]N/OFQ compared to 10μM, indicating a comparative loss in receptors. There was no significant evidence of cytotoxic effects in the trypan blue exclusion experiments performed to investigate this phenomenon, indicating that a cause other than possible toxicity of the Pon A solution was responsible for the decrease in binding. Trypan blue exclusion determines cell viability and depends upon membrane permeability, a property that will be affected by alcohol. The solvent for Pon A is absolute ethanol and at this induction level (20μM Pon A) the effective concentration of ethanol in the medium was 2% by volume. As there was no evidence of cytotoxicity at this concentration, it may be concluded that the ethanol was not having an effect and that there should be no effect at the lower concentrations used in the later experiments. Further, all experiments involving induction have Pon A (and therefore ethanol) at the same level in cases of equal induction, so if the ethanol has any effect it should be seen in all, which was not the case.

In these experiments, 10μM Pon A produced the highest receptor densities (≈ 1pmol.mg^{-1} protein). This approaches many commonly used stable transfection cell systems such as the CHO_{hNOP} also used here - 1.9pmol.mg^{-1} protein (Hashiba *et al.*, 2002), HEK293 - 1.2pmol.mg^{-1} protein (Dautzenberg *et al.*, 2001) and CHO_{hNOP} - 0.9pmol.mg^{-1} protein (Mason *et al.*, 2001). The receptor density induced by 5μM Pon A (≈ 200fmol.mg^{-1} protein) was similar to that reported in rat central tissue (rat cortex, 236fmol.mg^{-1} protein, (Berger *et al.*, 2000b); rat frontal cortex, 246fmol.mg^{-1} protein, (Mason *et al.*, 2001) and rat cerebral cortex, 180fmol.mg^{-1} protein (Okawa *et al.*, 1998) and represented a pseudo-physiological level of receptor expression. Competition binding assays at this receptor density indicated pharmacology consistent with that reported in the literature.

At 5μM Pon A induction, both N/OFQ and N/OFQ-NH_2 acted as full agonists with pEC_{50} values of 8.26 and 8.92, respectively, in GTPγ[^{35}S] binding assays and 9.38 and 9.66, respectively, in cAMP inhibition assays. Furthermore, in GTPγ[^{35}S] assays at this induction concentration, the effects of N/OFQ(1-13)-NH_2 were antagonised by J-113397 ($pK_B \approx 8.45$). In all assays agonist effects were PTx-sensitive confirming the $G_{i/o}$ coupling expected for this system.

In GTPγ[^{35}S] binding, N/OFQ(1-13)-NH_2 acted as a full agonist at all expression levels, whilst [F/G] produced sub-maximal stimulation, possessing little or no response at 1μM Pon A induction. In cAMP measurements, N/OFQ(1-13)-NH_2 again acted as a full agonist in all preparations. However [F/G] displayed full agonist activity at 10μM Pon A induction, with maximum percentage inhibition similar to that reported for the stable expression in CHO_{hNOP} transfects (Okawa *et al.*, 1999), but partial agonist behaviour at all lower levels of expression. This effect is typically due to amplification of response seen when measuring a downstream effector such as cAMP, in that saturation of response becomes more likely with measurement further down a stimulus-response chain (Kenakin, 2002b; Kenakin, 1997). In GTPγ[^{35}S] assays at the lowest induction concentration (1μM Pon A) [F/G] and NalBzOH acted as competitive antagonists with pK_B values 7.62 and 7.02, respectively, similar to their pEC_{50} values of 7.68 and 7.00, respectively (Bigoni *et al.*, 2002).

For partial agonists, estimates of intrinsic activity will be dependent upon level of receptor density as opposed to pure antagonists that should be devoid of activity. Conflicting data from different groups using both similar and differing preparations report agonism, partial agonism and antagonism for [F/G]. This has also been reported for Ac-RYYRIK-NH_2, Ac-RYYRWK-NH_2 and NalBzOH (Berger *et al.*, 2000a; Calo *et al.*, 2000c; Mason *et al.*, 2001). Experiments upon [F/G] *in vitro* indicate a full agonist both for inhibition of cAMP formation in CHO_{hNOP} cells and of glutamate release from brain slices (Okawa *et al.*, 1999). Following i.c.v. injection in rats, [F/G] causes a decrease in heart rate, mean arterial pressure, urinary sodium excretion and a marked increase in urine flow, similar to the effects of N/OFQ, but of longer duration. Partial agonism was also reported for the stimulation of GTPγ[^{35}S] binding in mouse N1E-115 cells (Olianas *et al.*, 1999).

A detailed review of the actions of [F/G] has been published (Calo *et al.*, 2000c). This difference in signalling between central and peripheral NOP may be explained by perceiving [F/G] as being a partial agonist with strong coupling in central tissue and high expressing transfected systems and weak coupling in peripheral tissue and low expression systems (Okawa *et al.*, 1999). To date the variable pharmacology of these partial agonists has not been carefully examined in a single expression system.

To discriminate between antagonists and partial agonists a method based upon decreasing the GDP concentration in GTPγ[^{35}S] binding studies has been described (Berger *et al.*, 2000a). High GDP concentration (100μM, or more) can mask the low activity of partial agonists by shifting the equilibrium of GDP/GTP exchange at the G-protein. It has been shown previously that stimulation of GTPγ[^{35}S] binding by the partial agonist NalBzOH was dependent upon the GDP concentration (Bigoni *et al.*, 2002). This effect has now been described for [F/G] and Ac-RYYRWK-NH_2 (J. McDonald, unpublished data). A decrease in concentration of GDP to 5μM produces a net increase in stimulation of GTPγ[^{35}S] binding.

The intrinsic activity of the partial agonists [F/G] and Ac-RYYRWK-NH_2 relative to N/OFQ and N/OFQ(1-13)-NH_2, in both systems ($CHO_{INDhNOP}$ at 5μM Pon A and CHO_{hNOP}) increased. This change in intrinsic activity for these two partial agonists may suggest that full and partial agonists differ in their dependence upon GDP concentration. Few groups have addressed this problem, using either cells transfected with different levels of NOP or peripheral or central tissue. A recent paper by Mason and colleagues showed differences in the relative intrinsic activities of [F/G], Ac-RYYRIK-NH_2, and Ac-RYYRWK-NH_2 using transfected cells, central preparations and peripheral tissue (Mason *et al.*, 2001).

Differences in coupling efficiency are just one variable seen between different tissue preparations and native and recombinant NOP that can affect values of relative intrinsic activity. Hence, differences in relative intrinsic activity may not be the result of changes in receptor number but due to changes in coupling efficiency or other local cellular factors such GDP concentration. Recent suggestions and data have shown that

agonists differ in their efficacy for different cellular responses or subtypes of downstream effector (Berg *et al.*, 1998; Cordeaux *et al.*, 2000). Indeed N/OFQ can stimulate PLC activity, with differential potency via a $G_{\alpha 14}$ mediated PTx insensitive pathway (in $G_{\alpha 14}$ transfected cells, EC_{50} 5nM (Yung *et al.*, 1999)) and via a $G_{\alpha i}$ PTx sensitive pathway (Ec_{50} 0.4nM (Reinscheid *et al.*, 1995)). Therefore different subtypes of effector or cellular pathways leading to a given response, between different cell types or tissue preparations could give rise to differential efficacy/potency and hence make conclusions about relative activities of a ligand awkward, i.e. differences in relative efficacy of a ligand between tissues may not be due to receptor density alone.

As noted, it has been suggested that the variable activity reported for the actions of [F/G] (agonist, partial agonist and antagonist) were the result of different expression of NOP at those sites assayed. Since we were able to control the expression of hNOP by changing the inducing concentration of Pon A, the effect this had on the intrinsic activity of both N/OFQ(1-13)-NH_2 and [F/G]N/OFQ(1-13)-NH_2 in two functional assays could be measured. The efficacy of N/OFQ(1-13)-NH_2 with respect to ability to stimulate GTPγ[^{35}S] binding and inhibit adenylyl cyclase activity was that of a full agonist at all expression levels. However, the relative intrinsic activity of [F/G] varied at different expression levels and between assays. In cAMP measurements [F/G] was a full agonist at 10μM Pon A and partial agonist at all other induction concentrations.

An increased receptor reserve at 10μM Pon A induction, along with amplification steps in the pathway leading to the inhibition of adenylyl cyclase, may explain this finding. However, it may be apt to suggest a coupling reserve, that is only a small proportion of the activated G-proteins are required to generate a full response, since no change in relative intrinsic activity is seen in GTPγ[^{35}S] binding, suggesting that there is no receptor reserve. At expression levels greater than that induced by 1μM Pon A i.e. ≈ 30fmol.mg^{-1}, [F/G] was a partial agonist in GTPγ[^{35}S] measurements. Below this expression [F/G] produced no response. This is due to the very low density of hNOP and [F/G] reduced efficacy for the receptor. Indeed it is tempting to suggest that in previous studies where [F/G] behaved as an antagonist this is due to similar low expression to that shown here, although as mentioned previously other factors can also play a role.

It can be seen from these data that the intrinsic activity of a ligand depends upon the ligand itself, the assay used and the receptor density in the tissue used. The expression of different levels of receptor density may lead to variations in receptor and coupling reserves and consequently to variations in measured efficacy. Hence relative values change with receptor expression. If intrinsic activity were to be useful as a comparison of ligand efficacy in a sense of rank order it may be said that N/OFQ(1-13)-NH_2 is more efficacious than [F/G] but it would not be possible to infer such molecular properties of an agonist as intrinsic efficacy (the response per unit pharmacon/molecule), from comparison of tissue maxima (Kenakin, 1997). However, in cases where fractional occupancy-response curves are of a more linear nature, in the absence of a receptor reserve or when the maximal tissue response has not been saturated, comparison of intrinsic activity (maximal tissue response) may represent a good measure of intrinsic efficacy, this would need rigorous experimental validation (Kenakin, 2002b).

Since GTPγ[^{35}S] binding appears to show neither excess of receptor numbers nor saturation in response at any receptor density (suggested by the fairly consistent value of relative intrinsic activity), [F/G] can be said to have relative intrinsic activity of 0.37-0.55. Given that little change is seen in the intrinsic activity of [F/G] relative to N/OFQ(1-13)-NH_2, it may be suggested that the latter ligand is not achieving maximal response for the system, with regard to GTPγ[^{35}S] binding. Given a high density of available guanine nucleotide binding sites (Albrecht *et al.*, 1998) and promiscuity in receptor coupling (Yung *et al.*, 1999) it is not surprising that in this tissue, under these assay conditions (high GDP, moderate Mg^{2+}), GTPγ[^{35}S] binding appeared not to be saturating. Hence no clear receptor reserve is evident and static relative intrinsic activity is seen. Where the maximal tissue response has not even been reached by the reference agonist (N/OFQ(1-13)NH_2), such as in cAMP measurements at an induction of 2μM Pon A, relative intrinsic activity is 0.48, in line with that for GTPγ[^{35}S] binding. For progressively higher levels of receptor density, in cAMP assays, the activity of [F/G] 'catches up' with that for the reference agonist as a response 'ceiling' is reached. Therefore it could be suggested that the intrinsic **efficacy** of [F/G] is $\approx$ 0.4-0.5, relating the data for GTPγ[^{35}S] and cAMP assays, based upon the lower level of receptor expression.

Finally, the issue that for a partial agonist the pEC_{50} should predict the values for pA_2 and pK_B may be addressed. Using the lowest induction concentration (1μM Pon A), the ability of N/OFQ(1-13)-NH_2 to stimulate GTPγ[^{35}S] binding was competitively antagonised by [F/G] with a pK_B of 7.62, which is essentially identical to the pEC_{50} for [F/G] of 7.68 at 5μM Pon A. This was also true for NalBzOH which antagonised N/OFQ(1-13)-NH_2-stimulated GTPγ[^{35}S] binding with a pK_B of 7.02 ($pEC_{50} \approx 7.00$ (Bigoni *et al.*, 2002)). NalBzOH was devoid of agonist activity and is therefore classed as a very-low efficacy partial agonist.

In conclusion, the ecdysone-inducible system would seem to offer an elegant solution for the study of receptor-mediated signalling at varying levels of receptor density. In particular, the role of receptor expression level in receptor desensitisation may be investigated.

4 Desensitisation.

4.1 Introduction

The term desensitisation (or adaptation) refers to a loss of sensitivity of a receptor to its ligand through prolonged exposure to a stimulus. The effect is reversible and may be achieved by various means, which govern the mode of desensitisation referred to, whether homologous or heterologous (Alberts *et al.*, 1994). Since a change in ligand concentration in the cell's external environment is the main controlling factor of the final regulatory output, there is a need for the cell to adjust its response appropriately over a range of prevailing ligand concentrations. Thus, the effect of desensitisation in the GPCR family is of fundamental importance in the regulation of cellular response to the environment.

The time course for desensitisation of a GPCR can be simply described as follows

1. Receptor/G-protein uncoupling (seconds to minutes)
2. Internalisation (minutes to hours)
3. Degradation (hours to days)
4. Genomic effects - regulation of messenger RNA (hours to days)

When receptors are desensitised they may either be recycled or degraded, depending upon the nature of the desensitisation and the amount of desensitisation is a function of agonist concentration and duration of exposure. Figure 4.1 gives a simple overview of the modes of GPCR desensitisation.

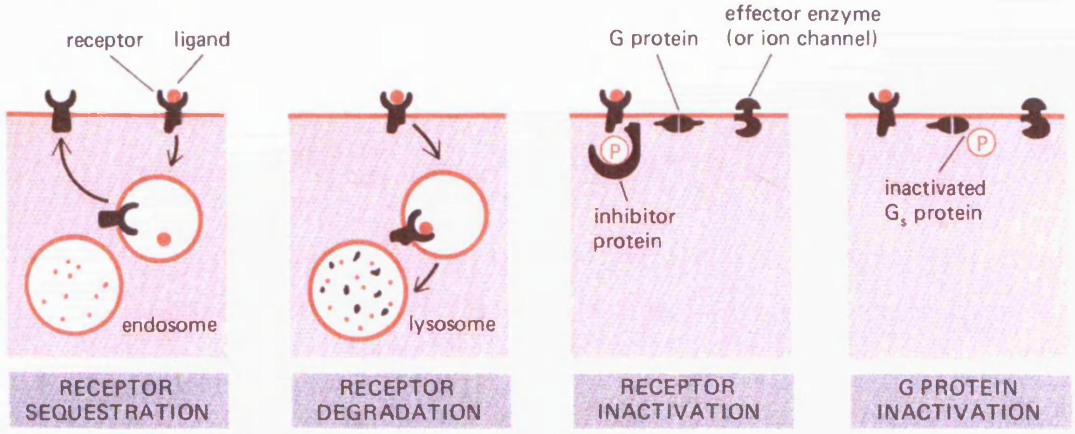

Figure 4.1 Schematic representation of the modes of GPCR desensitisation.
The first two modes (left and left-centre) involve the ligand-bound receptor being internalised by endocytosis into endosomes and either recycled back to the cell surface (if the receptor separates from the ligand in the endosome) or degraded in lysosomes (if the receptor and ligand do not separate). The second two modes (right-centre and right) involve phosphorylation events. Either the activated receptor can be phosphorylated and then bound by inhibitor proteins such as arrestin, or the G-protein can itself be phosphorylated, either mode results in the receptor uncoupling from the G-protein (Alberts *et al.*, 1992).

4.1.1 Homologous Desensitisation

Desensitisation mediated by the activation of the receptor itself, such as inactivation due to phosphorylation or the loss of receptors from the cell surface (internalisation), is classed as homologous desensitisation. The initial step in homologous desensitisation of a GPCR involves the recruitment of G-protein receptor kinases (GRKs) that recognise the active state of a receptor and phosphorylate it. Seven types of GRK are known, grouped into three subfamilies, of these seven GRKs, two (1 and 7) are involved in the sensation of light in retinal cells, another (GRK 4) is predominantly expressed in the testes, thus the remaining four (GRKs 2, 3, 5 and 6) are responsible for the majority of GPCR regulation (Gainetdinov *et al.*, 2004). For clarity, Table 4.1 shows the GRK family with an outline of their expression in mammalian tissue.

Table 4.1 The members of the GRK family and their expression in mammals.

GRK type	Alternative names	Expression in mammals	References
1	Rhodopsion kinase	Retinal rod and cone cells	(Wieland *et al.*, 1999)
2	β-adrenergic receptor kinase 1, βARK1	Throughout, especially in brain	(Benovic *et al.*, 1987)
3	β-adrenergic receptor kinase 2, βARK2	Throughout, lower in brain than βARK1	(Benovic *et al.*, 1991)
4	IT11	Testes, low expression in brain	(Premont *et al.*, 1996)
5	-	Throughout, especially in brain	(Kunapuli *et al.*, 1994; Premont *et al.*, 1994)
6	-	Throughout, especially in brain	(Benovic *et al.*, 1993)
7	Iodopsin kinase	Retinal cone cells	(Pitcher *et al.*, 1998)

The GRK-mediated phosphorylation of a GPCR causes a further protein, from the family of arrestins, to bind the receptor and prevent interaction with the G-protein. In the vertebrates, this family of arrestins comprises four members, of which 1 and 4 are primarily involved in vision, although arrestin 1 is also found in the brain in areas such as the amygdala, superior colliculus and ventral tegmental area and in the pineal gland. The other arrestins (2 and 3) are termed the β-arrestins and are usually denoted βarrestin-1 and βarrestin-2, respectively. These latter have a major role in the regulation of signalling as they are found at high levels of expression throughout the body. For clarity, Table 4.2 shows the members of the arrestin family, with an outline of their

location. Of interest to note is that the two visual arrestins are only implicated in desensitisation of receptors on the retinal cells and not endocytosis (Ferguson, 2001).

Table 4.2 The arrestin family of proteins and their expression in vertebrates.

Arrestin type	Alternative name/s	Expression in vertebrates	References
1	Rod arrestin, S-antigen	Retinal rod cells	(Chen *et al.*, 1999)
2	βarrestin-1	Throughout, especially in brain	(Parruti *et al.*, 1993)
3	βarrestin-2	Throughout, lower in brain than βarrestin-1	(Attramadal *et al.*, 1992)
4	Cone arrestin, X-arrestin	Retinal cone cells, pineal gland	(Chen *et al.*, 1999)

Additionally, the binding of an arrestin to a GPCR facilitates the internalisation of the receptor as the arrestin also binds to clathrin and the clathrin adaptor protein, AP2, in clathrin-coated pits that form at the cell surface. This promotes receptor-mediated endocytosis, in which the receptor, together with its bound ligand, is taken from the cell surface, via the clathrin-coated pits, into vesicles (endosomes) within the cytoplasm (Goodman *et al.*, 1996).

As both GRKs and arrestins recognise the active state of the GPCR, they also play a role in signal transduction through recruitment of molecules involved in other signal transduction pathways, such as PI3-kinases and MAP kinase (Ferguson, 2001; Gainetdinov *et al.*, 2004). Some of the endocytosed receptors release their ligands within the endosomes and are then returned directly to the plasma membrane via the endoplasmic reticulum. These receptors have been sequestered. The ligands are retained within the endosome, moved to lysosomes and are broken down by enzymes in the acidic environment there, along with any receptors and ligands that do not separate following endocytosis. Where a receptor is degraded, this process is termed down-regulation.

If a continuously high level of extracellular ligand is present, it follows from the law of mass action that there will be a consequently higher number of receptors involved in these processes and therefore a larger number will retain the ligand and be degraded, thus reducing the total number of receptors at the cell surface. The half life (turn over) of some receptors may be changed from half a day to one hour by prolonged exposure

to a ligand. The process of down regulation is comparatively slow, whereas more rapid adaptation in homologous desensitisation occurs through the phosphorylation of activated receptors.

4.1.2 Receptor/G-protein Uncoupling

The most immediate desensitisation event following receptor activation is the uncoupling of the receptor from its associated G-protein. This effect occurs over a period of seconds to minutes and may be mediated by phosphorylation of either the receptor or activated G-protein.

Regulation may also occur at the G-protein associated with the GPCR, via regulatory G-protein signalling (RGS) proteins. This is a family of accessory proteins acting as GTPase-activating proteins (GAP), responsible for promoting the GTPase activity of the G-protein α-subunit, thereby causing inactivation of the downstream effects in the system. The role of these proteins is not well understood, but some studies implicate action in the control of brain function in mice (Gainetdinov *et al.*, 2004; Rahman *et al.*, 1999; Rahman *et al.*, 2003; Zachariou *et al.*, 2003). All GRKs have a RGS-like domain and whilst members of GRK2 are known to bind $G\alpha_q$ via this domain, the GTPase activity of the subunit does not increase and it is thought that this GRK acts to dampen the signal. The function of this domain in other GRKs is not understood as there is no evidence of their binding to G-proteins (Pitcher *et al.*, 1998).

Uncoupling of receptor from G-protein may be simply demonstrated in a displacement binding assay. When membranes are prepared for this assay, any guanine nucleotides present in the cells are removed by the washing process, leaving a mixed population of receptors in both high (coupled) and low (free) states of affinity for ligand. In the presence of GTPγS, the G-proteins are irreversibly activated and remain dissociated from the receptor. This forces the receptors into the low affinity state, showing as a rightward shift in the concentration response curve for displacement of radiolabel, as a higher concentration of ligand is needed to occupy the receptors.

In membranes from CHO_{hMOP} cells not pre-treated, or pre-treated only for a short duration ($\leq$ 30min) with endomorphin-1, assays conducted in the presence and absence

of GTPγS showed a concentration response with GTPγS present as a rightward shift of the curve with respect to that for the GTPγS-free control. With pre-treatment for a longer time, up to 18h, if receptor uncoupling is occurring, there will be a predominance of activated G-proteins in the cells. This will result in a majority of the receptors being in the lower affinity state prior to commencement of the assay. The resultant concentration response curves will not show the same shift for those membranes in the presence of GTPγS, as the control curve would effectively be 'pre-shifted' to the right by the effect of uncoupling (Harrison *et al.*, 2000b). This effect is illustrated in Figure 4.2.

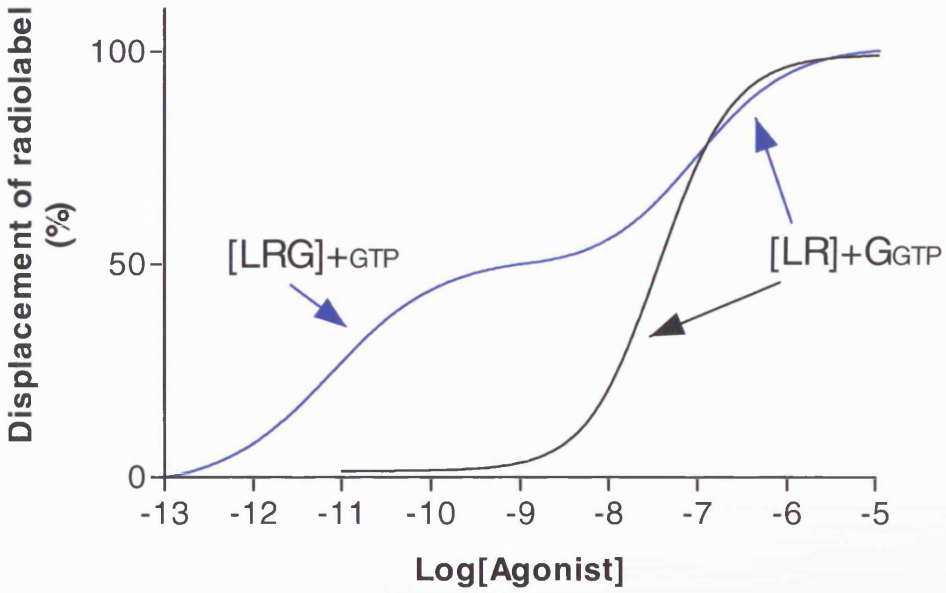

Figure 4.2 Schematic representing the 'G-protein shift' in a displacement binding assay system.
L = ligand; R = receptor; G = G-protein.
The blue curve represents the normal, non pre-treated, situation where receptors are in a mixture of high ([LRG]) and low ([LR]+G)affinity states for the ligand. At the middle plateau there are equal numbers of G-proteins in each state. In the presence of GTP, the receptors are all forced into the lower affinity state, resulting in a rightward shift in the concentration response curve, shown by the black curve. Here the slope of the curve is unity, indicating a single population of receptor states. The pK_i for this curve is the same as that for the upper part of the blue curve, corresponding to the low affinity state.

4.1.3 Heterologous desensitisation

Effects further down the transduction cascade or mediated other than from the activated receptor/ligand complex that reduce responsiveness are termed heterologous desensitisation. The fact that over 700 GPCRs have been cloned whereas only 7 GRKs and 4 arrestins have been discovered to date would seem to imply a level of degeneracy in GPCR signalling that allows for heterologous desensitisation (Gainetdinov *et al.*, 2004).

The most detailed studies into receptor down-regulation have been made using the β_2-adrenoceptor and it is the β-adrenergic receptor system that forms the basis of interpretation for the other GPCRs. In the case of β_2-adrenergic receptors, the activated receptor may be phosphorylated by a cAMP-dependent protein kinase (A-kinase, thought to be responsible for the effects of cAMP in most animal cells) that has been activated due to an increase in cAMP produced by the binding of adrenaline to the receptor. An inhibitory protein, a β-arrestin, may bind to multiple sites that have been phosphorylated by a β-adrenergic kinase, GRK2/3, a more specific enzyme, thereby blocking any interaction with the coupled G-protein (Alberts *et al.*, 1994).

4.1.4 Desensitisation of NOP

Rapid internalisation of human NOP has been reported in a low-expressing, transgenic CHO cell line. A loss of approximately 78% of the cell surface receptors was seen after 2min exposure to 1μM N/OFQ. This was more rapid than in a previously reported study on a neuroblastoma line, SK-N-BE, in which the β_2-arrestin was implicated (Spampinato *et al.*, 2001). Partial recovery, 30% of those internalised, was seen in 60min, in the continued presence of N/OFQ. The process of internalisation was energy-dependent.

A study of CHO cells expressing human NOP at a high level (2fmol.mg^{-1} protein) reported the effect of N/OFQ exposure as a time-dependent decrease in both cell surface receptors and a decrease in potency of subsequent N/OFQ challenge with pre-treatment. Short-term exposure did not seem to desensitise the receptors, but prolonged exposure (24-48 hrs) produced a reduction in potency. Antagonist co-exposure negated these effects. N/OFQ pre-treatment also caused an increase in basal and forskolin-stimulated

activity for cAMP formation, indicating the possibility of constitutive activity of NOP (Hashimoto *et al.*, 2002).

Homologous desensitisation of endogenous NOP has been reported, separate samples of a human neuroblastoma cell line (SK-N-SH) pre-treated with N/OFQ and the DOP agonist DPDPE showed effects that seemed to be agonist-specific (Cheng *et al.*, 1997). Desensitisation of response to 10μM N/OFQ was significantly affected after 10min exposure and restored over the course of 1h. Interestingly, the cells did not show evidence of heterologous desensitisation via DOP.

In the previous chapter, expression-dependent coupling was described and this will be likely to have pronounced effects upon desensitisation. In the high expressing cells a receptor/coupling reserve would be created, such that the downstream effects would be more likely to show resistance to the effects of desensitisation. This coupling reserve would, up to a point, compensate for uncoupling effects generated by pre-treatment and also for a degree of receptor loss at the cell surface. These effects make it advantageous and, indeed necessary, to define desensitisation in terms of different steps in the signal transduction cascade.

4.2 Aims

The aims of this chapter are to investigate the desensitisation of human NOP in a transgenic cell system with controllable expression level, continuing from previous experiments conducted in these laboratories (Hashimoto *et al.*, 2002).

Specifically, at different levels of expression encompassing physiological to supraphysiological (and hence the likely production of a receptor reserve) levels, to assess:

- GTPγ[^{35}S] binding
- cAMP formation
- Cell surface receptor numbers

4.3 Materials and Methods

For the desensitisation studies, methods of cell culture, harvesting, cell/membrane preparation and assays were essentially identical to those described in Chapters 2 and 3, all cells being cultured in flasks.The following amendments apply:

For pre-treating cells prior to assaying for effect of N/OFQ pre-treatment, at induction, cells were given fresh medium containing the appropriate amount of Pon A, 30μM peptidase inhibitor cocktail (as described earlier, but higher concentration to allow for the extended contact time) and, where appropriate, N/OFQ was added to the media to a concentration of 1μM. Desensitisation using 1nM N/OFQ has previously been shown (Hashimoto et al, 2002) but it was decided to use an increased concentration in line with the study of Spampinato (Spampinato *et al.*, 2002) in order to ensure a reproducible desensitising challenge.

After 20h, cells were harvested, washed and their response to N/OFQ re-challenge determined. As an assessment of receptor uncoupling, a comparison of cAMP production in cells, with and without pre-treatment with N/OFQ, from differing levels of induction was made. Assays of cAMP inhibition were performed, as described in Section 2.2.8, under basal and forskolin-stimulated conditions, for incubations in the presence and absence of PTx. Total protein was determined as outlined in Appendix 7.2 (Lowry *et al.*, 1951). From this cAMP formation was expressed as $pmol.mg^{-1}$ protein.
All cAMP assays used cells cultured and, where appropriate, induced and pre-treated in flasks (this is a protocol modification related to 3.3.6), such that N/OFQ re-challenge was performed upon cell suspensions.

4.4 Results

4.4.1 GTPγ[^{35}S] Binding Assays

Induction at 10μM Pon A.

Where cells were induced at 10μM PonA, both with and without (control) 1μM N/OFQ pre-treatment, subsequent N/OFQ challenge stimulated the binding of GTPγ[^{35}S] in a concentration dependent and saturable manner, as shown in Figure 4.3. Values obtained for pEC_{50} and E_{max} are shown in Table 4.3. The concentration response curve for the desensitised cells was shifted to the right compared to the N/OFQ naïve controls such that there was a statistically significant decrease in potency (pEC_{50}). This reduction in potency amounted to approximately a 5-fold change. Maximum stimulation (E_{max}) was also decreased, by 33% compared to control.

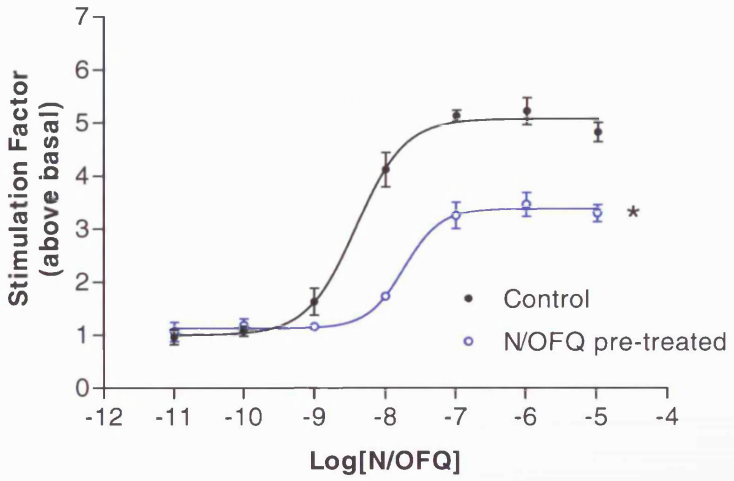

Figure 4.3 N/OFQ stimulation of GTPγ[^{35}S] binding in $CHO_{INDhNOP}$ cell membranes without (Control) and with 1μM N/OFQ pre-treatment, cells induced at 10μM Pon A.
Data are for n=3 experiments, * denotes significant difference from control ($p<0.05$).

Table 4.3 Results of N/OFQ-stimulated Binding of GTPγ[^{35}S] in $CHO_{INDhNOP}$ cell membranes without (Control) and with 1μM N/OFQ pre-treatment, cells induced at 10μM Pon A.
Data are mean ± s.e.mean for n=3 experiments. * denotes significant difference ($p<0.05$) from control. ** denotes significant difference ($p<0.001$) from control.

Treatment	pEC_{50}	E_{max}
Control	8.41±0.18	5.07±0.17
+1μM N/OFQ	7.76±0.03*	3.38±0.19**

Induction at 5μM Pon A.

Where cells were induced at 5μM PonA, both without (control) and with 1μM N/OFQ pre-treatment, subsequent N/OFQ challenge stimulated the binding of GTPγ[^{35}S] in a concentration dependent and saturable manner, as shown in Figure 4.4. Values obtained for pEC_{50} and E_{max} are shown in Table 4.4. As with 10μM induction, the concentration response curve for the desensitised cells was shifted to the right compared to the N/OFQ naïve controls. There was a statistically significant decrease in potency (pEC_{50}). This reduction in potency amounted to approximately a 5-fold change. Maximum stimulation also decreased compared to control, as for the higher induction.

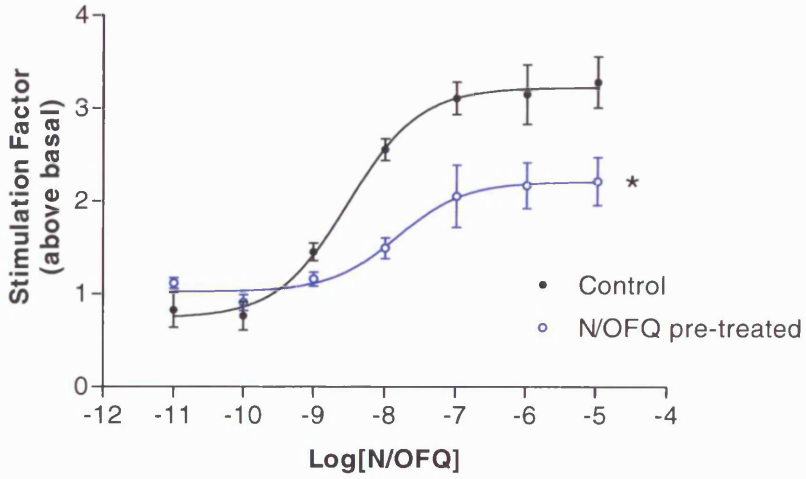

Figure 4.4 N/OFQ stimulation of GTPγ[^{35}S] binding in $CHO_{INDhNOP}$ cell membranes without (Control) and with 1μM N/OFQ pre-treatment, cells induced at 5μM Pon A.
Data are for n=4 experiments, * denotes significant difference from control ($p<0.05$).

Table 4.4 Results for N/OFQ-stimulated binding of GTPγ[^{35}S] in $CHO_{INDhNOP}$ cell membranes without (Control) and with 1μM N/OFQ pre-treatment, cells induced at 5μM Pon A.
Data are mean s.e.mean for n=4 experiments. *denotes significant difference ($p<0.05$) from control. ** denotes significant difference ($p<0.001$) from control.

Treatment	pEC_{50}	E_{max}
Control	8.55±0.06	3.52±0.43
+1μM N/OFQ	7.88±0.07**	2.48±0.10*

4.4.2 Absolute cAMP level and N/OFQ pre-treatment

Initial studies were conducted to compare the absolute level of cAMP production, relative to total protein, in control and N/OFQ pre-treated cells. At high levels of expression, some degree of constitutive activity might be anticipated, revealed as an increase in cAMP levels following receptor uncoupling from G-proteins in pre-treated cells (the G_i-coupled "brakes" on the system would have been released).

Basal

Increasing receptor expression did not appear to reduce basal cAMP formation, although cAMP mass tended to be lower at the higher induction concentrations. Pre-treatment with N/OFQ appeared to increase basal cAMP formation at 5 and 10μM Pon A, shown in Figure 4.5 and Table 4.5, but this was not statistically significant.

Forskolin-stimulated

At all induction concentrations forskolin markedly enhanced cAMP formation by at least 14-fold. Increasing receptor expression did not appear to reduce forskolin stimulated cAMP formation. Pre-treatment with N/OFQ appeared to increase basal cAMP formation at 2, 5 and 10μM Pon A, but this was statistically significant only at the 10μM induction. Results are shown in Figure 4.6 and Table 4.5.

Table 4.5 Results of cAMP production assays without (control) and with 1μM N/OFQ pre-incubation.
Values are pmol cAMP produced per mg protein for each condition and four incubation concentrations of Pon A.
*denotes significant difference from control in paired t-test ($p<0.05$).
Data are mean±s.e.mean for n=5 experiments.

[PonA] μM	Basal		Forskolin	
	Control	+1μM N/OFQ	Control	+1μM N/OFQ
1	76.6±16.5	83.2±12.9	1221.0±199.9	1496.4±188.5
2	95.9±17.3	99.8±17.9	1364.0±216.5	1908.2±326.6
5	52.1±19.6	100.6±16.2	979.9±91.3	1656.8±210.3
10	78.1±17.8	118.2±17.8	1337.3±225.4	2188.7±286.7*

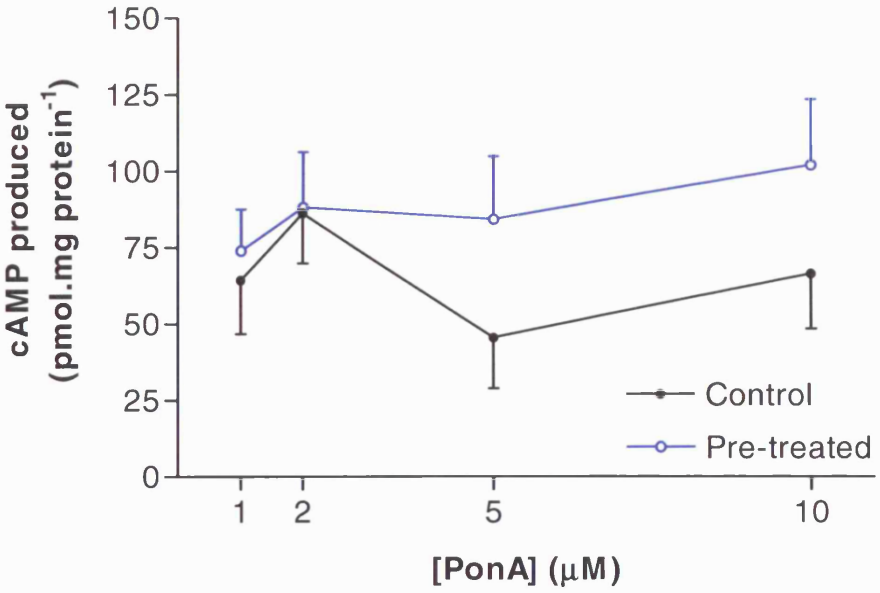

Figure 4.5 Absolute basal levels of cAMP produced in whole $CHO_{INDhNOP}$ cells induced at four concentrations of Pon A in the absence (Control) and presence of 1μM N/OFQ pre-treatment. Data are for n=5 experiments.

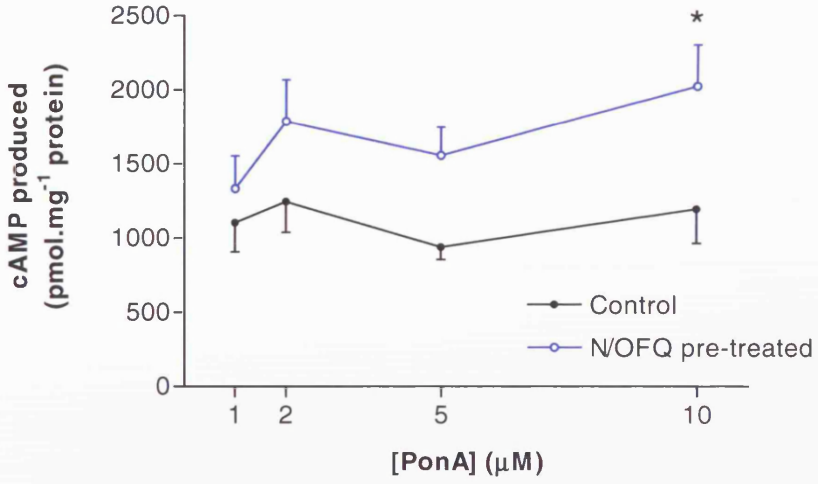

Figure 4.6 Absolute forskolin-stimulated levels of cAMP produced in whole $CHO_{INDhNOP}$ cells induced at four concentrations of Pon A in the absence (Control) and presence of 1μM N/OFQ pre-treatment.
Data are for n=5 experiments. * indicates significant difference ($p<0.05$) from Control.

4.4.3 Inhibition of cAMP formation and PTx sensitivity

The experiments to determine the effect of N/OFQ pre-treatment upon absolute levels of cAMP formation also included an assessment of sensitivity of the induced NOP to PTx. At all induction concentrations 1μM N/OFQ produced a significant reduction in forskolin-stimulated cAMP formation with the degree of reduction dependent upon receptor density (inferred from Pon A concentration), Figure 4.7.

Absolute % inhibition is at variance with Chapter 3 due in part to some variation inherent to the system (see Section *4.4.5*, saturation binding) but also to the use of adherent cells and cell suspensions. In cells pretreated with 100ng.ml^{-1} PTx there was a reduction in absolute cAMP formation but, more importantly, a loss of N/OFQ inhibition as shown in Figure 4.8, further confirming findings in Chapter 3.

In N/OFQ pre-treated cells (desensitised) at all induction concentrations 1μM N/OFQ produced a significant reduction in forskolin stimulated cAMP formation with the degree being dependent on receptor number (Pon A concentration), Figure 4.9. Interestingly the degree of inhibition produced by N/OFQ rechallenge was similar to that seen in naive cells and this is interpreted as no change in maximal responsiveness. This would be consistent with the previous work of Hashimoto *et al.*, 2002, in the stable CHO_{hNOP} clone. Again in cells pretreated with 100ng.ml^{-1} PTx there was a reduction in absolute cAMP formation but more importantly a loss of N/OFQ inhibition, Figure 4.10.

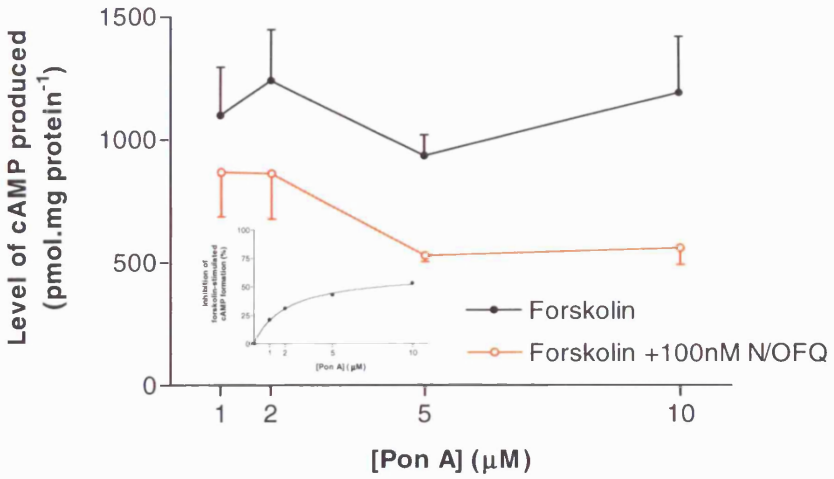

Figure 4.7 Effect of N/OFQ challenge upon absolute levels of forskolin-stimulated cAMP formation in whole $CHO_{INDhNOP}$ cells induced at four concentrations of Pon A.
Inset shows percent inhibition of cAMP formation with increase in inducing concentration of Pon A. Data are from n=5 experiments.

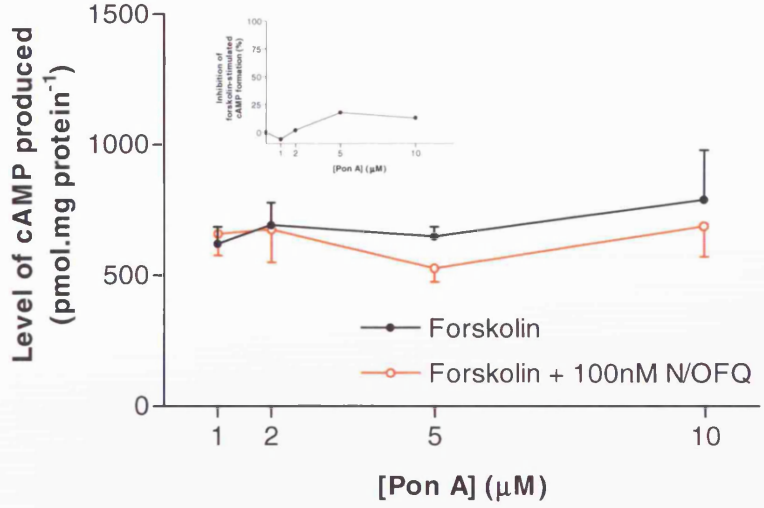

Figure 4.8 Effect of N/OFQ challenge upon absolute levels of forskolin-stimulated cAMP formation in whole $CHO_{INDhNOP}$ cells induced at four concentrations of Pon A in the presence of 100ng.ml^{-1} PTx.
Inset shows percent inhibition of cAMP formation with increase in inducing concentration of Pon A. Data are from n=5 experiments.

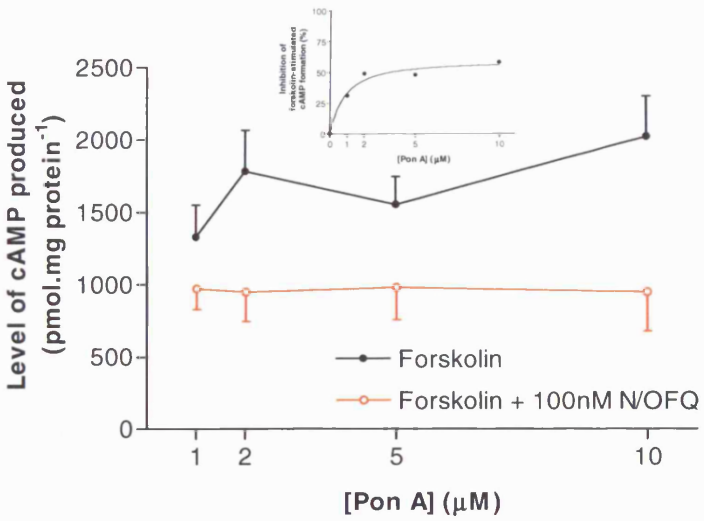

Figure 4.9 Effect of N/OFQ re-challenge upon absolute levels of forskolin-stimulated cAMP formation in whole $CHO_{INDhNOP}$ cells induced at four concentrations of Pon A in the presence of 1μM N/OFQ.
Inset shows percent inhibition of cAMP formation with increase in inducing concentration of Pon A. Data are from n=5 experiments.

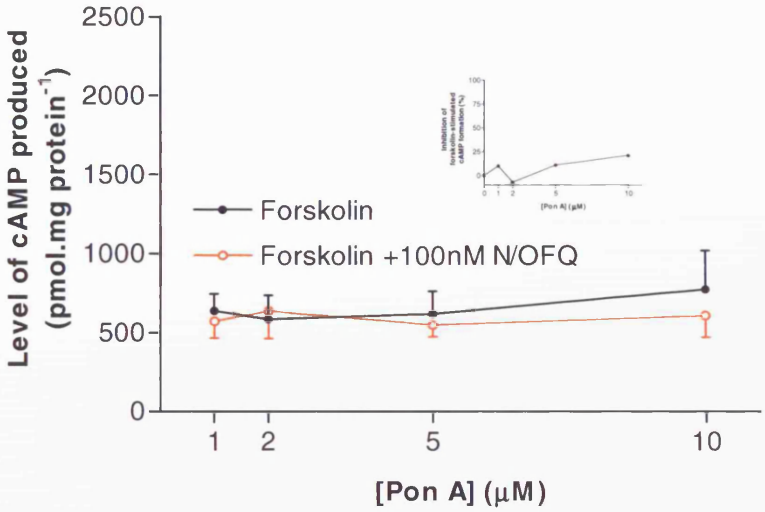

Figure 4.10 Effect of N/OFQ re-challenge upon absolute levels of forskolin-stimulated cAMP formation in whole $CHO_{INDhNOP}$ cells induced at four concentrations of Pon A in the presence of 1μM N/OFQ and 100ng.ml^{-1} PTx.
Inset shows percent inhibition of cAMP formation with increase in inducing concentration of Pon A. Data are from n=5 experiments.

4.4.4 N/OFQ concentration response studies in naïve and pre-treated cells

Data shown in Figures 4.7 and 4.9 (insets) imply that maximal responsiveness does not change following desensitisation, such that there is no change in efficacy. In order to probe this further and to estimate any changes in functional potency full concentration response curves were constructed in suspensions of cells at 10, 5 and 2μM Pon A induction.

Induction at 10μM Pon A.

At an induction concentration of 10μM Pon A, the effect of post-incubation challenge with N/OFQ was concentration-dependent and saturable in both absence (control) and presence of 1μM N/OFQ. Figure 4.11 shows the concentration response curves for this set of experiments. Values for pEC_{50} and E_{max} are shown in Table 4.6. The pEC_{50} for the pre-incubated cells was significantly different to that for the control (≈ 8 fold rightward shift), whilst there was no significant difference between the maximum inhibition (E_{max}) values.

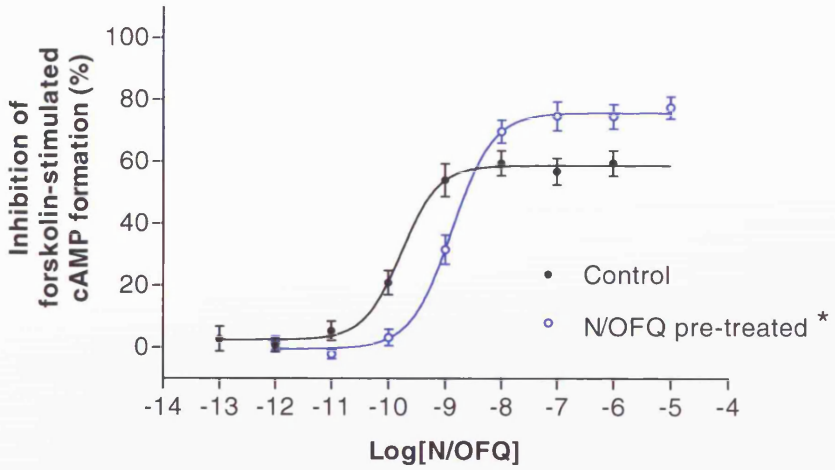

Figure 4.11 Concentration response curves for whole $CHO_{INDhNOP}$ cells incubated without (control) and with 1μM N/OFQ. Cells were induced at 10μM Pon A.

Table 4.6 Results of cAMP inhibition assays for whole $CHO_{INDhNOP}$ cells induced at 10μM Pon A without (control) and with 1μM N/OFQ pre-treatment.
Data are mean ± s.e.mean (n=5). *denotes significant difference ($p<0.05$) from control, paired t-test.

Treatment	pEC_{50}	E_{max}
Control	9.94±0.08	64.4±5.4
+1mM N/OFQ	9.05±0.20*	74.0±5.6

Induction at 5μM Pon A.

At an induction concentration of 5μM Pon A, the effect of post-incubation challenge with N/OFQ was concentration-dependent and saturable in both absence (control) and presence of 1μM N/OFQ. Figure 4.12 shows the concentration response curves for this set of experiments. Values for pEC_{50} and E_{max} are shown in Table 4.7. Both the pEC_{50} (≈ 8-fold rightward shift) and maximum inhibition (E_{max}) values for the cells pre-incubated with N/OFQ were significantly different to those for the control, i.e., there was a small but significant *increase* in E_{max} following pre-treatment.

A small but significant increase in maximum inhibition was seen for both control and pre-treated cells compared to that for the incubation at 10μM Pon A.

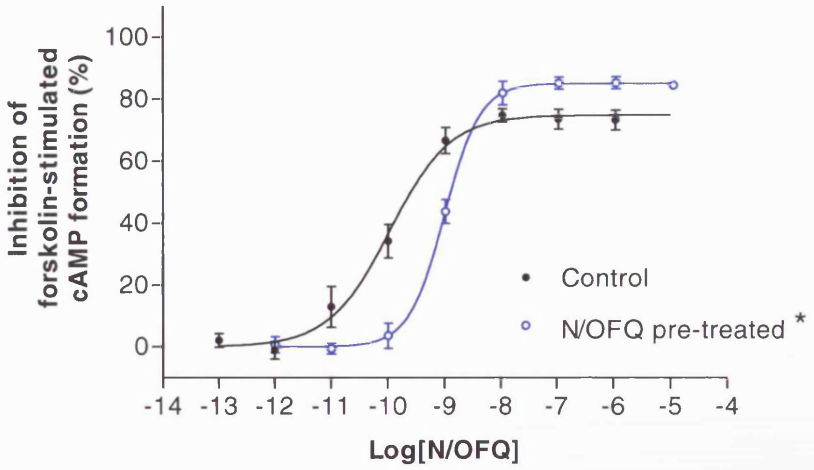

Figure 4.12 Concentration response curves for whole $CHO_{INDhNOP}$ cells incubated without (control) and with 1μM N/OFQ. Cells were induced at 5μM Pon A.
Data are for n=5 experiments.

Table 4.7 Results for inhibition of cAMP formation in whole $CHO_{INDhNOP}$ cells without (control) and with 1μM N/OFQ pre-treatment. Cells were induced at 5μM Pon A.
Data are mean ± s.e.mean for n=5 experiments. * indicates significant difference ($p<0.05$) from control.

Treatment	pEC_{50}	E_{max}
Control	9.96±0.17	75.5±3.7
+1μM N/OFQ	9.03±0.05*	85.2±1.6*

Induction at 2μM PonA.

At an induction concentration of 2μM Pon A, the effect of post-incubation challenge with N/OFQ was concentration-dependent and saturable in both absence (control) and presence of 1μM N/OFQ. Figure 4.13 shows the concentration response curves for this set of experiments, giving values for pEC_{50} and E_{max} shown in Table 4.8.

The pEC_{50} for the pre-incubated cells was significantly different to that for the control (≈ 14-fold rightward shift), whilst there was no significant difference between the maximum inhibition (E_{max}) values. The reduction in N/OFQ potency at lower expression was greater than that observed at the two higher induction concentrations (14- vs 8-fold).

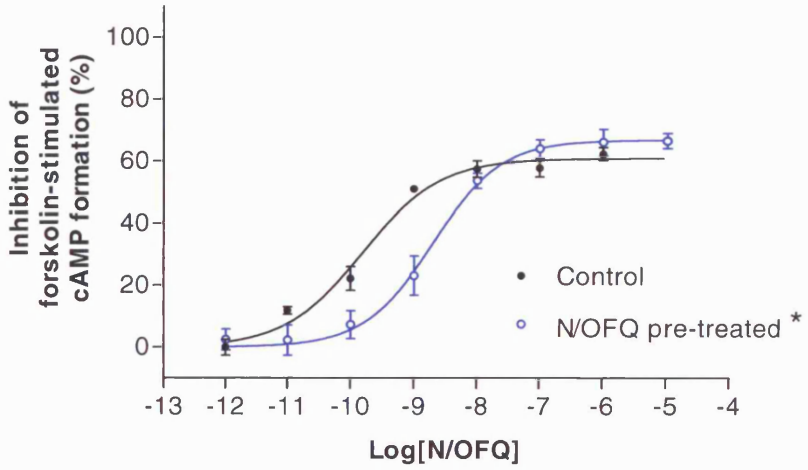

Figure 4.13 Concentration response curves for whole $CHO_{INDhNOP}$ cells incubated without (control) and with 1μM N/OFQ, cells induced at 2μM Pon A.
Data are from n=5 experiments. * indicates significant difference ($p<0.05$) from control.

Table 4.8 Results for inhibition of cAMP formation in whole $CHO_{INDhNOP}$ cells without (control) and with 1μM N/OFQ pre-treatment, cells induced at 2μM Pon A.
Data are mean ± s.e.mean for n=5.
* indicates significant difference ($p<0.05$) from control.

Treatment	pEC_{50}	E_{max}
Control	9.78±0.12	60.6±1.4
+1mM N/OFQ	8.61±0.07*	63.0±2.5

4.4.5 Saturation Binding Assays

In saturation binding assays following 20h induction, both with and without 1μM N/OFQ pre-treatment, $CHO_{INDhNOP}$ cell membranes showed concentration-dependent and saturable binding of [*leucyl*-^{3}H]N/OFQ at both 10μM and 5μM Pon A induction. It is important to note that, as referred to earlier, there was variation in the maximum levels of expression at the different induction levels for this set of experiments, compared to those for the characterisation of the inducible system (see Chapter 3). The most marked difference was at the highest expression level (induction at 10μM Pon A).

The results of these experiments are shown in Table 4.9. Figure 4.14 shows specimen saturation binding curves for control and 1μM N/OFQ pre-treatment and semi-logarithmic transformed sigmoid curves for cells induced at 10μM, for both conditions. Figure 4.15 shows equivalent curves at 5μM induction.

Table 4.9 Results for saturation assays using $CHO_{INDhNOP}$ cell membranes incubated without (Control) and with 1μM N/OFQ.
† significantly higher (p=0.032) than B_{max} for Control at 5μM induction;
* significant difference (p=0.0037, n=5) from corresponding Control value;
** significant difference (p=0.032, n=3) from corresponding Control value.

[Pon A] (μM)	Treatment	pK_D	B_{max}
10	Control	9.87±0.07	477±56†
	+1μM N/OFQ	9.76±0.12	198±41*
5	Control	9.67±0.25	265±23
	+1μM N/OFQ	9.58±0.14	148±28**

Pre-treatment with N/OFQ had no effect upon affinity as there was no significant change in pK_D at either induction concentration and with or without pre-treatment. These data indicate that the (remaining) desensitised receptors recognise N/OFQ in a manner identical to the N/OFQ naïve receptors in control tissue. There was a significant reduction in maximum binding at 5μM Pon A induction compared to that at 10μM Pon A for the control groups, implying that at the lower induction concentration there were fewer binding sites and, hence, fewer receptors as in Chapter 3. A significant reduction in maximum binding (B_{max}) compared to control was seen for cells pre-treated with 1μM N/OFQ at both induction levels, which would indicate that there was a N/OFQ-mediated reduction in receptor numbers with pre-treatment.

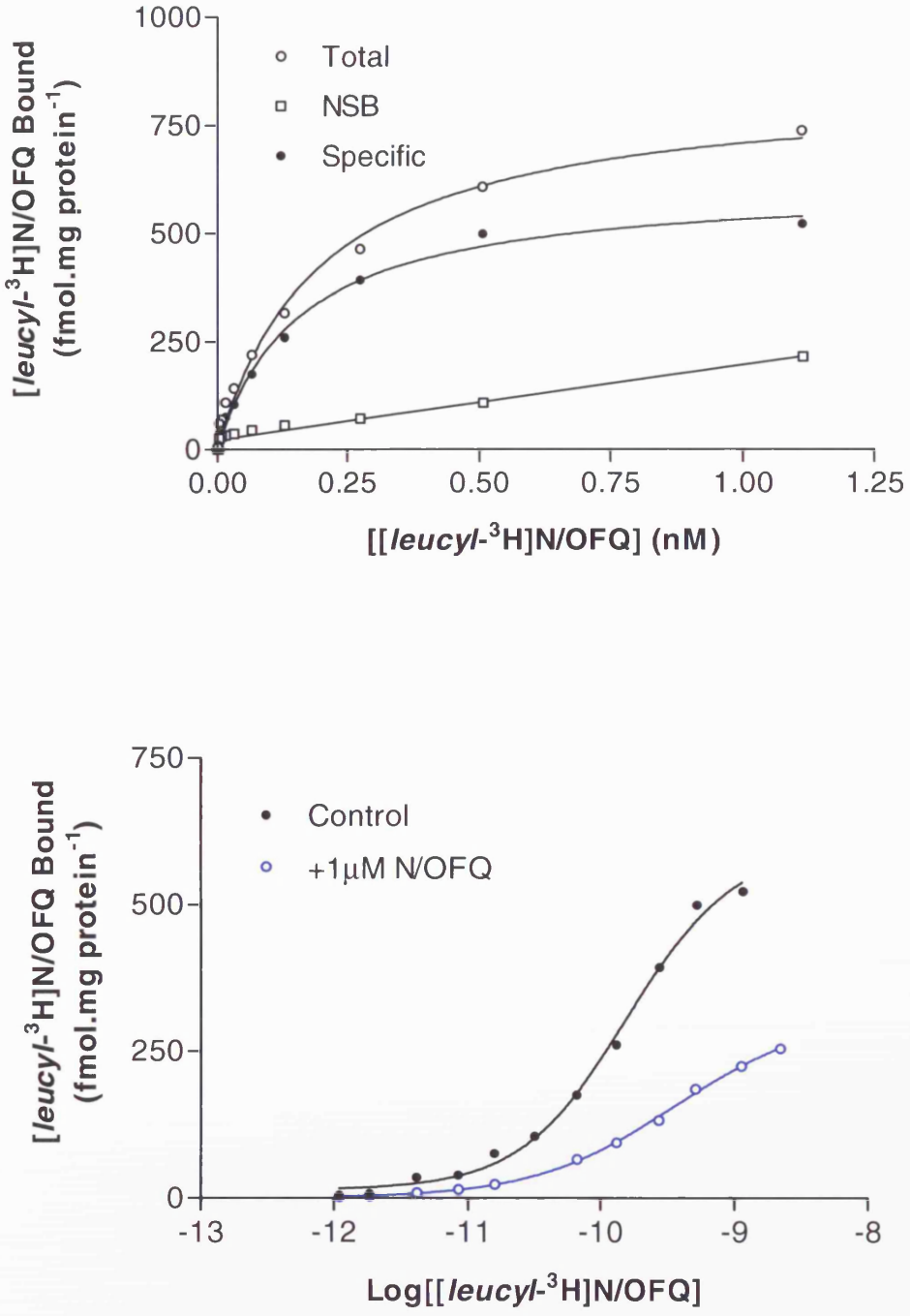

Figure 4.14 Specimen [*leucyl*-^{3}H]N/OFQ saturation binding curves, 10μM Pon A.
Raw data (upper) for cell membranes from Control group of cells and sigmoid transformed semi-logarithmic plot (lower) for binding to $CHO_{INDhNOP}$ cell membranes incubated without (Control) and with 1μM N/OFQ pre-treatment, cells were induced for 20h at a concentration of 10μM Pon A.

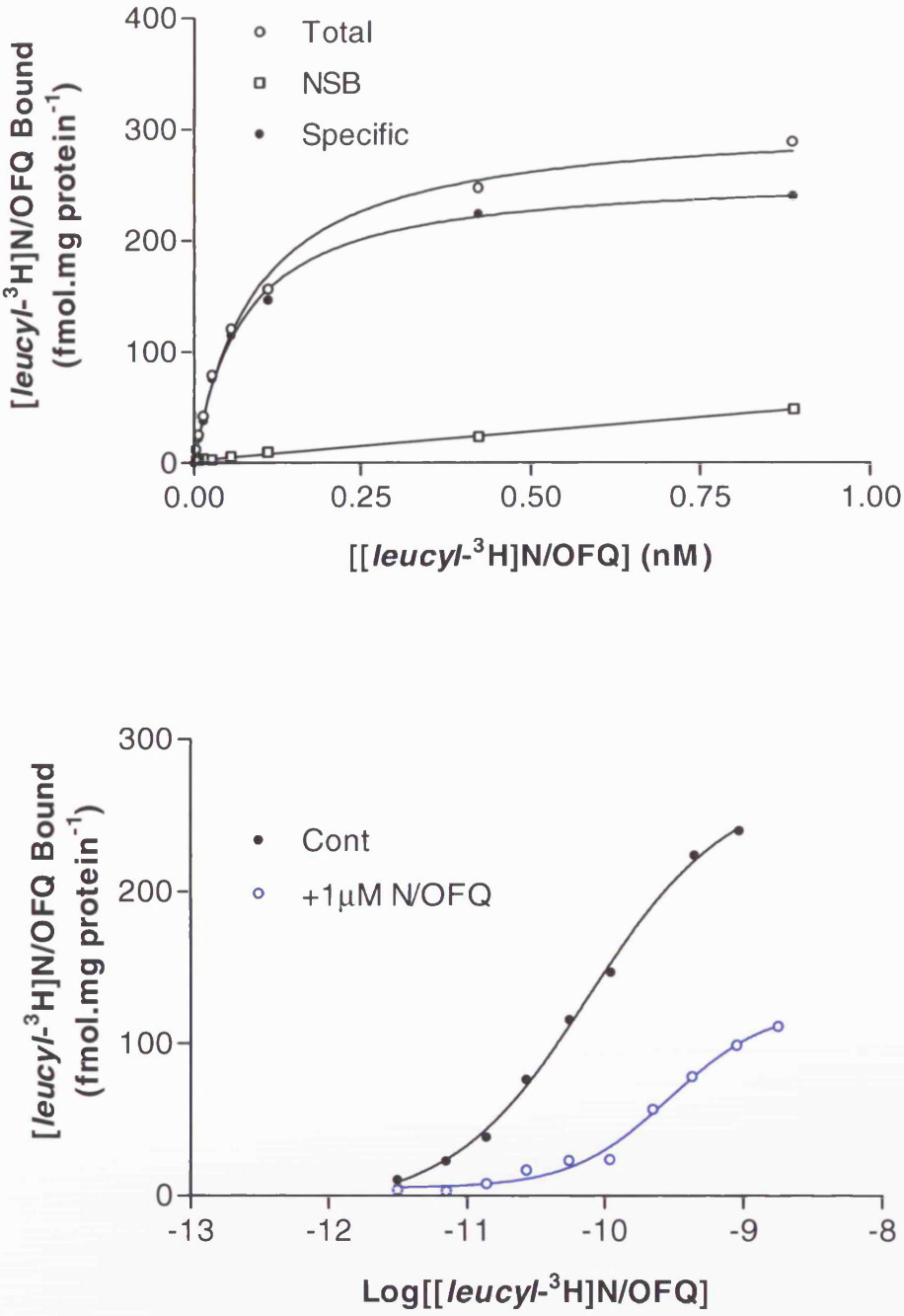

Figure 4.15 Specimen [*leucyl*-^{3}H]N/OFQ saturation binding curves, 5µM Pon A.
Raw data (upper) for cell membranes from Control group of cells and sigmoid transformed semi-logarithmic plot (lower) for binding to $CHO_{INDhNOP}$ cell membranes incubated without (Control) and with 1µM N/OFQ pre-treatment, cells were induced for 20h at a concentration of 5µM Pon A.

4.5 Discussion

Saturation binding studies showed that the effect of increasing the inducing concentration of Pon A gave an increase in density of NOP, consistent with data in Chapter 3. The addition of N/OFQ at induction (pre-treatment) caused a decrease in maximum binding (B_{max}) of labelled N/OFQ, implying that the receptor density was reduced. This was accompanied by no apparent change in the affinity of N/OFQ, as seen by the same value for pK_d for control and pre-treatment at both induction levels, in agreement with the structure activity studies presented earlier in this thesis.

Receptor density was affected by the pre-treatment during the incubation time and could result from a reduction in transfer of new receptors to the cell surface, the down-regulation of mature receptors by endocytosis following phosphorylation or a reduction of transcriptional activity in the nucleus. Table 4.10 shows a comparison of the data from this thesis with that of previously reported studies.

Table 4.10 Comparison of studies into effects of N/OFQ pre-treatment upon cell surface receptor numbers.

Model	B_{max}	N/OFQ challenge	Effect of Pre-treatment upon		Reference
			K_D	B_{max}	
$CHO_{INDhNOP}$	10μM Pon A 477fmol.mg^{-1}	1μM, 20h	None	-58%	This thesis
	5μM Pon A 265 fmol.mg^{-1}		None	-44%	
CHO_{hNOP}	2pmol.mg^{-1}	1nM, 48h	None	-47%	(Hashimoto *et al.*, 2002)
	110fmol.mg^{-1}	1μM, 2min	N/a	-78%	(Spampinato *et al.*, 2002)
HEK293	1205fmol.mg^{-1}	100nM, 30min	incr. 4-fold	-28%	(Dautzenberg *et al.*, 2001)

In the GTPγ[^{35}S] binding assays, N/OFQ showed consistent potency (pEC_{50}) in control samples between 5μM and 10μM Pon A inductions, with lower maximum stimulation (E_{max}) for 5μM compared to 10μM. This would imply that a decrease in receptor density had occurred, leading to a decrease in coupling to the endogenous pool of G-proteins (effectively in excess compared to receptor numbers) and consequent reduction in stimulation, in agreement with saturation studies. The potency was significantly decreased with pre-treatment for both levels of induction and the implication of this may be that uncoupling of receptors from their associated G-proteins was occurring (see

cAMP studies). There was a significant decrease in maximum stimulation with N/OFQ pre-treatment at both 5μM and 10μM Pon A inductions. This would again imply that there was a reduction in receptor density due to the pre-treatment, which might also have been expected at the lower induction concentrations, comparable to endogenous expression levels (Cheng *et al.*, 1997; Connor *et al.*, 2004).

In the cAMP assays, the absolute level of cAMP produced relative to protein in the cells showed a disinhibition of cAMP formation with N/OFQ pre-treatment for both 5μM and 10μM Pon A inductions at basal level and evidence of the same effect for forskolin-stimulation. In agreement with the GTPγS experiments, this would also seem to imply that uncoupling of receptor from G-protein may well be occurring, as an increase in both the basal and forskolin-stimulated levels of cAMP production with pre-treatment could possibly indicate constitutive activity of the receptors in the control (non pre-treated) condition and receptor uncoupling with N/OFQ pre-treatment, leading to the increase in cAMP formation. If this occurs *in vivo*, this increase in cAMP would act via PKA to cause activation of cyclic AMP response element binding protein (CREB) (Montminy, 1997). This in turn may affect transcription of the receptor gene. The consensus sites for phosphorylation in the NOP sequence are a single threonine residue located in the third intracellular loop (PKA) and two serine residues, one in the second intracellular loop and the other in the intracellular tail (PKC) (Mollereau *et al.*, 1994). If cAMP concentration increases and PKA is activated, the receptor may be directly phosphorylated. The consequences of this are unclear, but may be linked to loss of receptors at the cell surface. As effects seen upon cAMP levels lie downstream of G-protein activation, then similar effects upon GTPγ[^{35}S] binding would seem unlikely, although no experimental evidence is available to corroborate this supposition. Although a growing body of evidence implicating the PI-PKC pathway in opioid tolerance exists (Smart *et al.*, 1996), there is little evidence for NOP coupling to PLC (Hawes *et al.*, 2000).

The mechanism of this uncoupling may be phosphorylation of the receptors, thereby losing their effect upon the G-protein. This may lead to endocytosis, reducing the number of receptors at the cell surface and this would be seen as a decrease in the receptor density, shown in saturation assays. These effects could be confirmed with the

use of an inverse agonist for NOP, unfortunately such is not currently known. Other methods of detection may include radiolabelled phosphorylation and immunoprecipitation studies.

For the cAMP concentration response curves, it was seen that at an induction concentration of 2μM Pon A, the maximum inhibition of forskolin-stimulated cAMP formation was reduced compared to that for the two higher levels of induction. This was not accompanied by a reduction in potency from the higher inductions and would seem to imply that the higher levels of receptor density produce a receptor reserve such that, with the effect of downstream amplification at the point of sampling, apparent potency of N/OFQ is not affected by the pre-treatment. The presence of a receptor reserve would also contribute to the effects of any constitutive activity exhibited by the receptor.

Homologous desensitisation of NOP has been reported extensively, in both endogenously and heterologously expressed NOP, in a variety of cell lines (Cheng *et al.*, 1997; Connor *et al.*, 1996a; Hashimoto *et al.*, 2002; Ma *et al.*, 1997; Mandyam *et al.*, 2002; Morikawa *et al.*, 1998; Pu *et al.*, 1999; Spampinato *et al.*, 2002). Where the effect of heterologous desensitisation is mediated by cAMP produced via the action of other receptors, this is presumably only valid for GPCRs coupled to G_s, as an inhibitory protein would decrease the level of cAMP and not cause the second messenger mediated effects associated with this mode of desensitisation. This applies in the case of N/OFQ as it acts via G_i, therefore decreasing the level of cAMP, so presumably this is not what determines the level of desensitisation.

Effects of homologous desensitisation in NOP have been reported that were sensitive to protein kinase C (PKC) and not affected by protein kinase A (PKA) inhibitors ((Pei *et al.*, 1997). The implication here is that the effects of N/OFQ stimulation upon the cAMP part of the pathway are not responsible, as cAMP activates PKA, whereas the increase in intracellular Ca^{2+}, brought about by NOP stimulation, would activate PKC, which would in turn enable regulation of NOP. However, N/OFQ decreases cAMP and a consequent reduction in PKA activity may then be anticipated. In the desensitised state, an increase may be expected. This view is, however, somewhat controversial as few studies are currently published in this area.

Of further consideration is the formation of receptor dimers as both NOP and MOP are reported to form homo-dimers *in vivo*, with an accompanying change in response to stimulation, when expressed in certain cell cultures (Pan *et al.*, 2002). It is possible that the receptor expressed in the CHO cells used here, whilst transgenic, may be able to form such structures, causing a reduction in response.

Evidence exists for differing effects at NOP, dependent upon the agonist concerned. Saturation binding experiments in HEK cells expressing NOP showed that pre-treatment with N/OFQ caused desensitisation, shown by reduced subsequent N/OFQ inhibition of cAMP formation, but with no accompanying loss of receptor numbers or affinity. Pre-treatment with the synthetic agonist Ro64-6198 had the same effect upon cAMP inhibition with re-challenge by the same compound, but this was accompanied by a halving of the receptor density and a four-fold decrease in affinity (Dautzenberg *et al.*, 2001). The effects may be the result of differential recycling, possibly due to slower intracellular release and degradation of the synthetic ligand. The same research team saw a similar effect for Ro64-6198 in experiments using rat brain.

The level of receptor density seems to be a factor in desensitisation as, for responses mediated by downstream effectors such as cAMP, the variety of effects seen in previous chapters for full and partial agonists may also be reflected in the results of desensitisation assays, hence the use of a receptor system with controllable receptor level, such as the inducible system described in this thesis.

5 Genomic studies on the desensitisation of NOP

5.1 Introduction

5.1.1 Rationale for Genomic Studies

From the previous chapter, pre-treatment of cells with N/OFQ for 20h has been shown to cause a decrease in receptor density accompanied by loss of functional potency and reduction in maximal effect. Whilst these effects have been demonstrated at the level of cell surface receptors, the implications for genomic effects of pre-treatment for this length of time have yet to be investigated in this system.

In order to study any genomic effects, the level of mRNA transcription, leading to the formation of functional receptors, must be assessed under the differing conditions of pre-treatment. This may be accomplished by use of the technique of Polymerase Chain Reaction (Saiki *et al.*, 1986), which can be used to amplify DNA copies from the mRNA in the cells. A method is available enabling comparative measurement of this copied DNA, thereby inferring the relative levels of mRNA initially produced under the differing conditions.

5.1.2 Theory of Polymerase Chain Reaction

Since its discovery in 1988, the technique of Polymerase Chain Reaction (PCR) has become a very powerful tool in the field of molecular biology (Saiki *et al.*, 1986). The principle relies upon the 'unzippable' nature of the double strand of DNA in replication and involves the use of a heat-stable DNA polymerase to produce clones of specific regions of template DNA. The action of this polymerase produces short strands of copy, or complementary, DNA (cDNA) from pairs of smaller strands of DNA (termed primers) chosen to encompass an area of the gene of interest. Each of these primers binds to a site on either the sense or anti-sense strand of the cDNA, flanking the region of interest, chosen for specificity within the gene to be studied. The procedure is conducted in specialised reaction tubes, held in a thermal cycler in which the contents of the tube (including template cDNA, polymerase, primers, free nucleotides and buffer) are then subjected to several cycles of predetermined heating and cooling, within specified limits, depending upon the reaction conditions required. As the components are warmed (usually to 95°C), the template cDNA 'unzips', forming single stranded DNA (melting phase). Gradual cooling allows each of the primers to bind the cDNA sequence complementary to its own (annealing phase). As the primers are of

comparatively small size, this occurs in preference to the complementary strand of the template cDNA. With the temperature held at a predetermined value for a given time, the polymerase is allowed to produce new cDNA, by extending the primers using free nucleotides (extension phase). After this, the temperature is raised and the strands separate again, the procedure then being repeated. An exponential increase is seen in the target cDNA as each new strand produced may act as a template for further elongation, with an approximate doubling of cDNA at each step. After a set number of cycles (typically 40) there is an excess of the target cDNA over all else and the reaction may be terminated by a final heating step, followed by cooling to allow the complementary strands of cDNA to re-associate. Following electrophoresis in an agarose or polyacrylamide gel, the results are visualised by staining with a fluorescent dye, such as ethidium bromide, which binds to double stranded DNA and fluoresces when illuminated by UV light.

Although this technique requires DNA as the template, use of PCR has been expanded to include analysis of RNA, a molecule that by its very nature is short lived and labile. A sample containing messenger RNA (mRNA) is first converted by reverse-transcription into a cDNA strand complementary to its sequence. The cDNA so produced may be amplified as described and the RNA template analysed indirectly.
Certain viruses, known as the reverse transcriptase (RT) viruses (an example of which is HIV, the causative agent of AIDS), possess enzymes with such abilities. The use of HIV and similar viruses would not be acceptable for laboratory work, so it is fortunate that a family of RT-viruses exists, the enzymes from some of which are available for use in molecular biology.

Further developments in the technique of PCR have included the ability to quantitatively analyse the products of a reaction and the ability to monitor the progress of a reaction in real time. Such a method in the PCR inventory is quantitative real time PCR (Q-RT PCR), which uses the same principle as PCR but measurement of the cDNA produced is made as the reaction progresses, using a fluorescent marker. Such a marker is SYBR Green, a fluorescent compound which binds to the minor groove of double stranded DNA in much the same way as ethidium bromide (Bustin, 2000).
In quantitative analysis of cDNA the use of a gene for which the level of mRNA is unchanged (termed a 'housekeeping' gene) is essential. This is usually a gene native to

the type of cell used in the transfection and is chosen due to its expression being constant under all conditions associated with the experiment (for the purposes of this work, does not alter significantly in the course of the induction and desensitisation of the cells). With reference to such a gene, the quantification of cDNA from the gene of interest may be used to infer relative levels of original mRNA from that gene in a sample according to the experimental conditions.

5.2 Aims

The aim of this chapter is:

- To measure the levels of NOP mRNA transcribed in $CHO_{INDhNOP}$ cells at different receptor densities with and without N/OFQ pre-treatment.

By means of:

- Designing primers, suitable for use in Q-RT PCR, for the NOP and a housekeeping gene expressed in these cells.
- Quantitatively investigating the effects that induction and N/OFQ pre-treatment have upon the levels of mRNA produced.

5.3 Materials and Methods – RNA extraction, RT, PCR and Q-RT PCR

5.3.1 Reagents

Molecular Biology Grade Water, Phosphate Buffered Saline Tablets – Sigma or Fisher

RNA Extraction – Sigma

Tri-Reagent, Chloroform, Isopropanol, Absolute Ethanol

DNase treatment – Ambion TURBO DNA-*free* Kit

DNase ($2U.ml^{-1}$), 10x Turbo DNase Buffer, DNase Inactivation Reagent,

Nuclease free Water

Reverse Transcription – Applied Biosystems GeneAmp RNA PCR Kit

Murine Leukaemia Virus Reverse Transcriptase ($50U.\mu l^{-1}$),

10x Reverse Transcriptase Buffer, RNase Inhibitor ($20U.\mu l^{-1}$),

Oligo $d(T)_{16}$ (50μM), dNTP's (10mM), 25mM $MgCl_2$,

Standard PCR

2x JumpStart Taq Readymix – Sigma

Q-RT PCR

2x SYBR Green Jumpstart Taq Readymix – Sigma

100x (1mM) Reference Dye (ROX) – Stratagene

Primers – Proligo, France

Primers supplied as 100μM, stock stored as 50μM aliquots at -20°C

Gel Electrophoresis

Agarose – BioPur

50x TAE Buffer (2M Tris-Acetate, 50mM EDTA, pH8.3), Ethidium Bromide – Fisher

5.3.2 Equipment

Microcentrifuge (as previous) – Eppendorf 1541D

Spectrophotometer – Eppendorf BioPhotometer 5131

RNA Integrity Bioanalyser – Agilent Technologies RNA 6000 Nano

Standard PCR Thermocycler – Eppendorf Mastercycler Gradient

Q-RT PCR Thermocycler – StrataGene MX4000 master

UV transilluminator – Chromato-vue transilluminator TM-40, UVP Inc, San Gabriel, Ca, USA.

CCD Camera – UVP Inc., Model No. 4912-5110/0000

5.3.3 RNA Extraction, amended from (Chomczynski, 1993).

Following induction at 5μM and 10μM Pon A with and without N/OFQ pre-treatment (1μM, 20h, see Section 4.3) as appropriate, confluent cultures of $CHO_{INDhNOP}$ cells were harvested as described previously and washed twice by centrifugation (420xg, 2min, room temp.) with PBS to clean cells ready for RNA extraction.

Tri-Reagent was added to the final cell pellet (1ml per sample), mixed, the suspension transferred to a "PCR-clean" tube and allowed to stand at room temperature for 5min before the addition of 200μl chloroform. This was mixed, allowed to stand at room temperature for a minimum of 3min then centrifuged (16000xg, 15min, 4°C) to separate the aqueous and hydrophobic layers. The resultant, aqueous, top layer was removed to a fresh, "PCR-clean" tube and a further 500μl Tri-Reagent added, followed immediately by 100μl chloroform. This was mixed, allowed to stand at room temperature for 5min and again centrifuged (as previous).

The aqueous layer was again removed to a further "PCR-clean" tube, 500μl isopropanol added, the whole then mixed and allowed to stand at room temperature for 10min before being centrifuged (16000xg, 10min, 4°C). The isopropanol was removed from above the pellet of nucleic acids, 1ml 75% ethanol added to wash by resuspension and the tube then centrifuged (16000xg, 15min, 4°C). The resultant, cleaned pellet may then be stored in ethanol at -70°C for up to 1 year pending further use. For quantification and reverse transcription, the ethanol was removed and the pellet dried in air in a laminar flow cabinet, before being dissolved in an appropriate volume of molecular biology grade water.

Quantification of RNA recovered was made from absorbance at 260nm (Eppendorf biophotometer) and an estimate of purity made from the absorbance ratio at 260 and 280nm with 1.7 or greater taken as acceptable.

5.3.4 RNA Integrity Analysis

A further technique for assessing the purity and integrity of RNA yield was the use of an Agilent bioanalyser Nano chip. This takes the form of a gel contained in a microwell plate in which up to 12 samples of RNA may be analysed at a time. The length of time

to elute the sample depends upon the size and the purity of sample and is shown by the duration over which the sample elutes. After filtration of gel matrix, RNA dye was added and the mixture pipetted into the wells of a Nano chip as appropriate. Nano marker was added to wells for sample and ladder. After heat denaturation, RNA ladder was added to the ladder well and 1µl RNA sample (up to 500ng.ml^{-1}) were added to sample wells as appropriate. The Nano chip was then vortexed and loaded onto the analyser to run. Results (not shown) were displayed as electropherograms in similar style to standard gel electrophoresis. (Method according to SOP217.1, Genome Stability Group, Department of Cancer Studies and Molecular Medicine, University of Leicester, see Appendix 7.6)

5.3.5 Removal of DNA Contamination

Prior to reverse transcription, for samples to be used in both PCR and Q-RT PCR, DNA contamination was removed with a proprietary kit (TURBO DNA-*free*, Ambion). From each sample, the RNA was treated with DNase in a reaction comprising 1µl TURBO DNA-*free* reagent, 5µl Reagent Buffer, sample volume containing approximately 10µg RNA and molecular biology grade water to a total reaction volume of 50µl. This was mixed and incubated at 37°C for 20-30min, depending upon purity measured. A 5µl volume of inactivation reagent was then added, the whole mixed and stood at room temperature for 2min with occasional agitation. This was then centrifuged (10000xg, 1.5min, room temperature) to precipitate the inactivation reagent and the supernatant removed to a fresh "PCR clean" tube. Reverse transcription of each sample was performed immediately and the remainder stored at –70°C for possible future use.

5.3.6 Reverse transcription

From the total RNA extracted, cDNA was produced using reverse transcriptase from a murine leukaemia virus (MuLV, Applied BioSystems). A 16-mer Oligo(dT) was used as a primer to select for the polyadenylation tail of mRNA. The reaction tube contents are shown in Table 5.1.

Protocol - Samples were incubated for 10min at 25°C, 30min at 44°C and 2min at 99°C, followed by a holding temperature of 4°C, before storage at –20°C. The final incubation

temperature of 99°C ensures the inactivation of the reverse transcriptase, which, if left intact, can have inhibitory effects upon PCR through its cDNA-binding properties.

Table 5.1 Reaction contents used for reverse transcription.

Reaction Components	Volume (µl)	
	Sample	RT- control
Magnesium Chloride	4	4
10x Reverse Transcriptase Buffer	2	2
DeoxyNucleotideTriPhosphates (dNTP)	8	8
$Oligo(dT)_{16}$	1	1
RNase Inhibitor	1	1
MuLV Reverse Transcriptase	1	-
Molecular Biology Grade Water	-	1
RNA Sample	3	3
Total	20	20

5.3.7 Polymerase Chain Reaction (PCR)

Following production of cDNA by reverse transcription, the specific region of the cDNA transcript corresponding to the gene for NOP could then be selectively amplified to observe any difference in transcription level between treatments.

Primer Design

The choice and design of primers are fundamental to the success of PCR as they must be specific to the region to be studied, without being so large as to be impossible to use, and must encompass a manageable product with as few secondary structures as possible. Primers for all PCR were chosen using the following computer program:

Primer 3, (Rozen *et al.*, 2000):
http://frodo.wi.mit.edu/primer3/primer3_code.html
and accepted after analysis for parameters such as homologous sequences, primer dimers, secondary structures and self-complementarity using:
Blast NCBI http://www.ncbi.nlm.nih.gov/BLAST/
M-fold, (Zuker, 2003):
http://www.bioinfo.rpi.edu/applications/mfold/old/dna/form1.cgi and
Vector NTI (InforMax) programs.

An initial attempt at design of primers for PCR of the NOP gene (primer set designated NOP1) proved to be unsuccessful as the target site chosen by the Primer3 design program was located in a non-coding region of the complete human NOP gene (Mollereau *et al.*, 1994). The sequences for this set of primers are shown in Figure 5.1.

NOP1 Forward	5'-ATGTGGCAAGCGTTACTTCCTGTG-3'
NOP1 Reverse	5'-GCCAGTGAGCAGGTGTTTATTAGGG-3'

Figure 5.1 Sequences of forward and reverse primers in primer set NOP1 for Q-RT PCR in CHO cells. Predicted product size was 93 bp.

Since reverse transcription of mRNA uses the polyadenylated tail to initiate production of cDNA, PCR primers usually give better amplification if designed with the target sequence towards the 3' end of the gene, hence the initial choice of site. This primer set gave no amplification in routine PCR (see Results section), showing that the construct used to transform the CHO cells was lacking this region. This would imply that cDNA had originally been used for the transfection, rather than gDNA.

A second set of NOP primers was designed (designated NOP2/3), overlapping the region coding for the second extracellular loop in the human NOP sequence (see Appendices 7.3-7.5), corresponding to two separate exons in the gene. These primers were denoted NOP2/3 forward and reverse. The use of a primer set overlapping the boundary between two exons is of further benefit in that discrimination may be made between gDNA and cDNA (derived from transgenic mRNA) in human-derived transgenic cells, since mRNA is free of introns whereas gDNA will contain the entire genetic sequence and either give a much longer transcript or none at all.

The housekeeping gene used for these experiments was a rodent (chinese hamster) glyceraldehyde 3-phosphate dehydrogenase (GAPDH) gene, which is associated with the energy turnover of the cell. The primers for the GAPDH gene were designed using the same programs as for the NOP primers. The sequences for these sets of primers are shown in Figure 5.2.

NOP2/3 Forward	5'-ACAGGTCGAGGATGAAGAGATCGAG-3'
NOP2/3 Reverse	5'-GAAGAGGAAGATGCAGATGGCAAAC-3'
GAPDH Forward	5'-GACTCCCACTCTTCCACCTTTGATG-3'
GAPDH Reverse	5'-ACCACTCTGTTGCTGTAGCCAAATTC-3'

Figure 5.2 Sequences of primer sets NOP2/3 and GAPDH gene in transgenic CHO cells.

The PCR products of these primers were calculated to be 94bp for NOP2/3 and 110bp for GAPDH. Optimal size for product in Q-RT PCR is approximately 100bp, giving a good balance between specificity and efficiency (Bustin, 2000).

Optimisation of PCR

To ensure the most efficient use of these primers, PCR optimisation was performed in a standard cycler.

There are two main areas for optimisation:

1) Temperature profile for the reaction must be optimised to enable the separation of cDNA strands, primer annealing and extension of cDNA strands by polymerase. The number of cycles, their duration and temperature may be adjusted.
2) Concentrations of primers may be optimised, as may the concentration of such reaction components as magnesium and DNA template in the reaction.

The melting temperature used was standard to PCR and not altered, first of the optimisation procedures was performed by using a gradient of annealing temperature across the heating block of the PCR-cycler to define a temperature suitable for all primers used. Extension temperature was left unchanged.

Optimisation of the second aspect normally entails the use of dilutions of all possible components in separate reactions to ascertain the best combination for the most efficient outcome. The reaction mixture used for these experiments was an all-in-one kit and already optimised for PCR, so only the optimisation of the primers was required. This was carried out by adding each of the primers at different concentrations in a grid of reaction tubes, providing for all combinations of three dilutions of each.

PCR and Q-RT PCR

The enzyme used in the PCR experiments was a *Taq* polymerase supplied in a complete reaction mixture (at 2x concentration) to which only the primers, reference dye and sample cDNA need be added. This reaction mixture was a 'hot-start' mixture, with the enzyme bound in an inactive state by an antibody until the heat of the first melting step in the reaction dissociated this complex, allowing the polymerase to work. The protocol used for preparation of reactions in this procedure is shown in Table 5.2.

Table 5.2 Protocol for PCR.

Components		Sample Tube (µl)	Negative Control Tube (µl)
Molecular Biology Grade H_2O		21	23
Jumpstart Taq Readymix (2x)		25	25
Primers (10µM)	Forward	1	1
	Reverse	1	1
Sample cDNA		2	-
Total		50	50

For the Q-RT PCR experiments, a similar reaction mixture was used again containing all necessary components as a 2x premixed solution, with SYBR Green dye added to allow fluorescent monitoring of reaction progress. Protocol used for preparing reactions in this procedure is shown in Table 5.3.

Table 5.3 Protocol for Q-RT PCR.

Components		Sample Tube (µl)	Non-template Control (NTC) Tube (µl)
Molecular Biology Grade H_2O		10.375	11.375
SYBR Green Jumpstart Taq Readymix (2x)		12.5	12.5
Reference Dye (1mM, diluted 1/500)		0.375	0.375
Primers (10µM)	Forward	0.375	0.375
	Reverse	0.375	0.375
Sample cDNA		1	-
Total		25	25

In every set of samples, a standard curve (consisting of 10-fold dilutions from the sample with highest cDNA content, the 10μM control induction) was generated for each gene. This was used both to measure the relative quantities of cDNA produced and to show the efficiency of the reaction. The efficiency of a PCR is a measure of the linearity of amplification with decreasing amount of template cDNA. From the standard curves, the relative amounts of mRNA originally in the sample cells are inferred, with reference to the housekeeping gene as a measure of total mRNA content.

The thermal profile used for the Q-RT PCR in these experiments is shown in Figure 5.3 and layout of samples in the machine is shown in Figure 5.4, with an overview shown in Figure 5.5 for clarity.

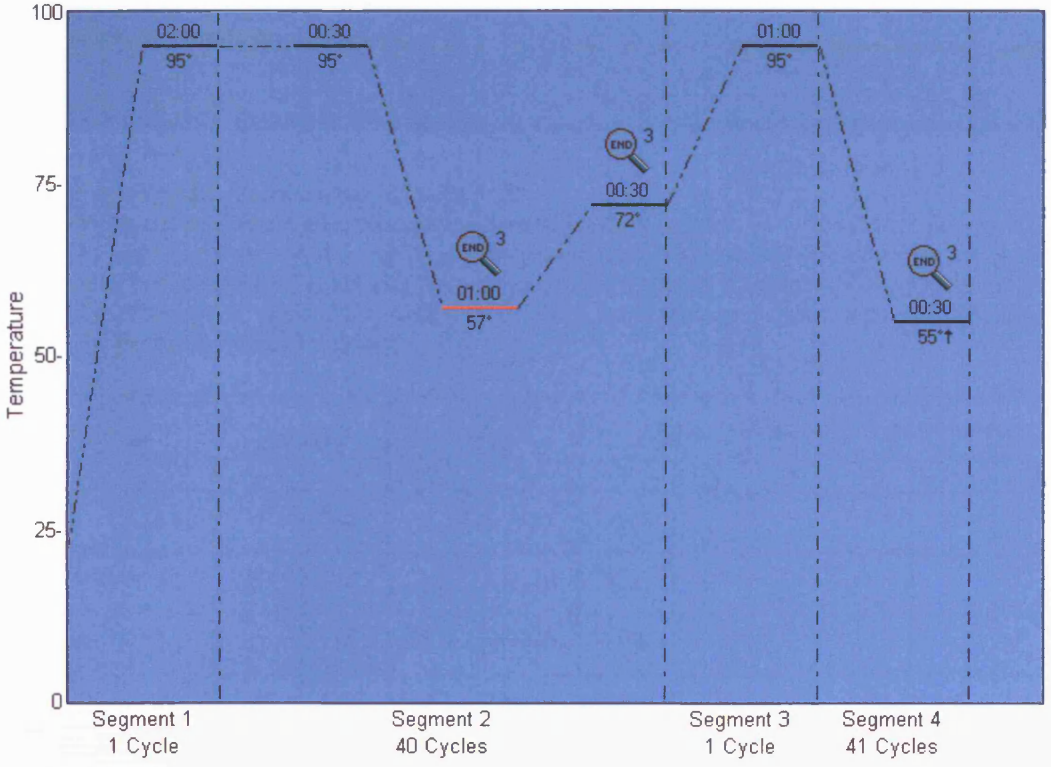

Figure 5.3 Profile of Q-RT PCR.
Thermal profile shows steps in the reaction:
Segment 1 is the initial melting phase of 2min at 95°C;
Segment 2 has a melting step of 30s at 95°C, followed by 1min annealing at 57°C and extension for 30s at 72°C. This segment is repeated for 40 cycles to amplify the cDNA;
Segment 3 is a final melting step of 1min at 95°C to separate all strands of cDNA;
Segment 4 is an annealing phase for 20min 30s at an initial temperature of 55°C, increasing by 1°C increments, to produce the dissociation curves for the PCR products, shown in Figures 5.11 and 5.12.

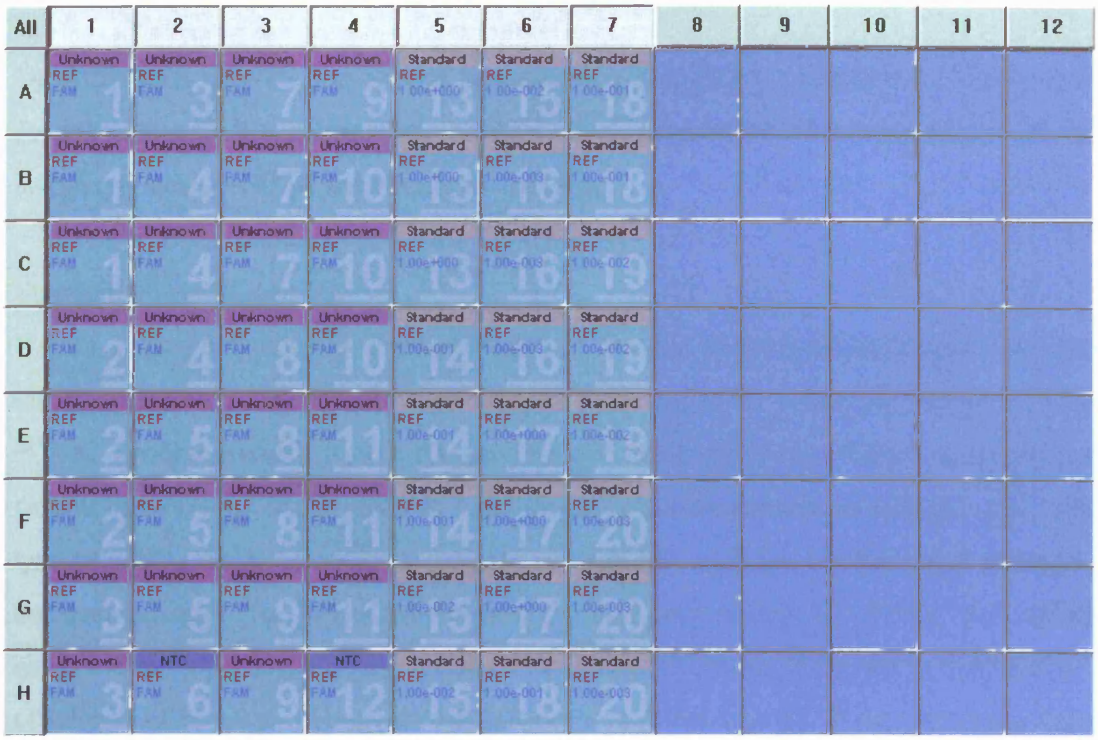

Figure 5.4 Layout of the reaction tubes in Q-RT PCR.
Picture is as appears on computer attached to the PCR cycler.
Tubes 1A-2G and 3A-4G represent tubes containing sample cDNA with primers for NOP and GAPDH, respectively; H2 and H4 represent Non-Template Controls (NTC) for the NOP and GAPDH genes, respectively; tubes in columns 5-7 represent standard curve cDNA dilutions for the two genes as indicated.

	Gene				Standard Curves			Empty positions - unused				
	NOP		GAPDH		NOP							
Grid	1	2	3	4	5	6	7	8	9	10	11	12
A	0	5+	0	5+	1.0	0.01	0.1					
B	0	10	0	10	1.0	0.001	0.1					
C	0	10	0	10	1.0	0.001	0.01					
D	5	10	5	10	0.1	0.001	0.01					
E	5	10+	5	10+	0.1	1.0	0.01					
F	5	10+	5	10+	0.1	1.0	0.001					
G	5+	10+	5+	10+	0.01	1.0	0.001					
H	5+	NTC	5+	NTC	0.01	0.1	0.001					
						GAPDH						

Figure 5.5 The layout for a Q-RT PCR reaction.
0 – Control, cDNA from non-induced cell mRNA; 5 – cDNA from mRNA in cells induced at 5μM Pon A; 10 - cDNA from mRNA in cells induced at 10μM Pon A; + denotes cells were pre-treated with 1μM N/OFQ; NTC, Non-Template Control. Standard curves show relative concentration in a dilution series of cDNA from mRNA in cells of 10μM Pon A Control.

5.3.8 Quantification of Q-RT PCR results.

Quantification of cDNA produced was made by comparing cycle threshold (C_T) values for samples with the appropriate standard curve, calculation of relative levels of cDNA and, from these, mRNA were made as follows.

Standard Curve Method

Use of a standard curve is a precise method, but has consequentially high cost due to use of more tubes and greater demand on what might be a limited supply of sample cDNA. From a standard curve for each gene, constructed from the serial dilution of a sample previously determined to contain the greatest amount of cDNA, the relative quantity of cDNA in each sample is calculated and the fold-change derived by comparison with the sample containing the smallest amount of cDNA, the calibrator sample (Rutledge *et al.*, 2003). A check on linearity of amplification as a gauge of the efficiency of reaction is inherent to this method. A reaction of 100% efficiency ensures that each unit change in cycle threshold value represents a two-fold increase in cDNA level for the gene studied (Rutledge *et al.*, 2003). The design of primers giving amplicons of less than 150bp usually gives reaction efficiencies of approximately 100% (Livak *et al.*, 2001) (Applied Biosystems User Bulletin N°.2, 2001). The quantity of cDNA produced corresponding to a particular gene is determined from the cycle threshold number, a value based upon the number of PCR cycles at which fluorescence from a sample becomes significantly greater than that of the background. The relative quantity of cDNA for each sample is based upon that from standard curves for each gene. The calibrator sample is usually that with lowest amount of cDNA, such that fold-changes are expressed .

viii) Calculation of Fold-change by Standard Curve Method.

$$\frac{Quantity_{GeneofInterest}}{\left(Quantity_{HousekeepingGene} \times Quantity_{Calibrator}\right)}$$

5.4 Results

5.4.1 Test for primer specificity

Following standard PCR, an agarose gel electrophoresis was run to test all three primer sets in both types of CHO cells used, plus a positive control for the NOP1 primers from a human-derived neuroblastoma (SH-SY5Y) cell line endogenously expressing NOP. The resultant gel, shown in Figure 5.6, reveals that amplification for the first set of primers to be designed (NOP1) was seen in neither CHO_{hNOP} (lane 2) nor $CHO_{INDhNOP}$ cells (lane 5), whereas endogenously expressed NOP was amplified (SH-SY5Y cells, lane 11). From this it may be concluded that only the DNA for the functional receptor was used to transfect the CHO cells. The NOP1 primers were designed to anneal to a section of the receptor at the 3' end of the sequence for maximising efficiency in Q-RT PCR (Appendices 7.3 and 7.4 show the sequences used, the lengths of these differing considerably). Amplification was seen for the second set of NOP primers (NOP2/3) in both cell lines (lanes 3 and 6), so these could be used. Primers for the housekeeping gene (GAPDH) were seen to work for both cell lines (lanes 4 and 7). All primers showed no amplification in negative controls (lanes 8-10).

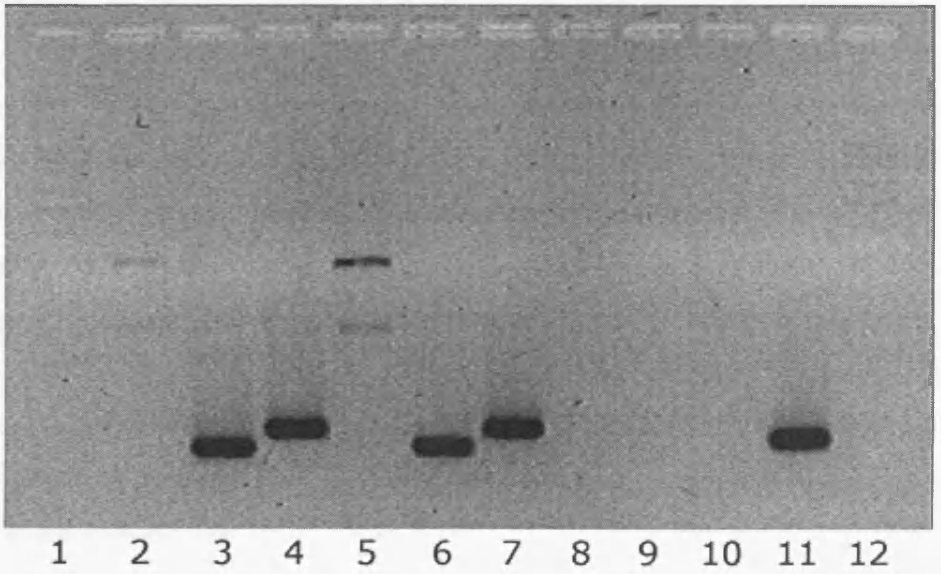

Figure 5.6 Agarose gel electrophoresis of PCR results using the primers designed for Q-RT PCR.
Lanes were loaded as follows:
1 and 12, 100bp ladder; 2-4, $CHO_{INDhNOP}$ using primer sets NOP1, NOP2/3 and GAPDH, respectively; 5-7, CHO_{hNOP} with same primers; 8-10, negative controls for all primer sets; 11, positive control using NOP1 primers on extract from a human neuroblastoma cell line.

Further optimisation

Optimisation of primers was carried out in the Q-RT PCR cycler and the optimal concentration of primers found to be 10μM. $MgCl_2$ concentration was set at 7mM (3.5mM at working concentration) within the reaction mixture and this was found to work adequately, no adjustments being made.

5.4.2 Q-RT PCR

The results of the Q-RT PCR were analysed for each gene and the relative amounts of cDNA (from which are inferred the starting amounts of mRNA) calculated. Standard curves were included with all experimental runs. A typical set of amplification curves for NOP is shown in Figure 5.7, together with their transformation to a log scale on the Y-axis in Figure 5.8. Corresponding curves for GAPDH are shown in Figures 5.9 and 5.10. These show the growth curves of cDNA for the samples tested. The blue horizontal line denotes the threshold at which fluorescence was taken to be significantly above baseline (determined internally by the cycler). This is the derivation of the C_T value and is taken at a point where the growth curves are parallel in the exponential phase of the curve, such that components of the reaction are not limiting the replication of cDNA.

Figures 5.11 and 5.12 show typical dissociation curves for NOP and GAPDH, respectively. This acts as a gauge of product purity and a single peak, at the melting temperature (T_m) of the product, should be seen. If smaller peaks are seen to the right and left of the product peak in samples, these would represent genomic DNA contamination and primer dimer formation respectively. A standard curve for NOP is shown in Figure 5.13. This is derived from the dilution series of the sample with the highest level of cDNA and, by inference, the largest amount of mRNA from which the relative amounts in each of the other samples may be derived. It is also possible to quantify the absolute amount of cDNA by this method but for the purposes of this study the relative amounts were sufficient to compare the effect of desensitisation. The standard curve for GAPDH, Figure 5.14, is used in the same manner to calculate the relative amounts of cDNA for GAPDH. Use of a standard curve enables the efficiency of the reaction to be gauged, such that a difference in C_T value corresponds to an actual difference in relative amounts of cDNA. From this mRNA quantity, rather than a reduction in the total level of cDNA replication, may be inferred.

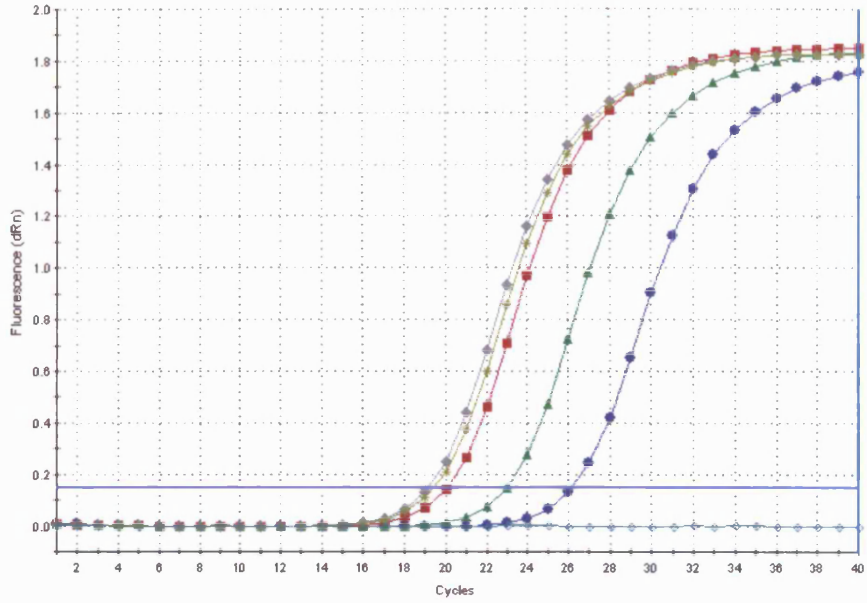

Figure 5.7 Sample Q-RT PCR amplification curves for hNOP.

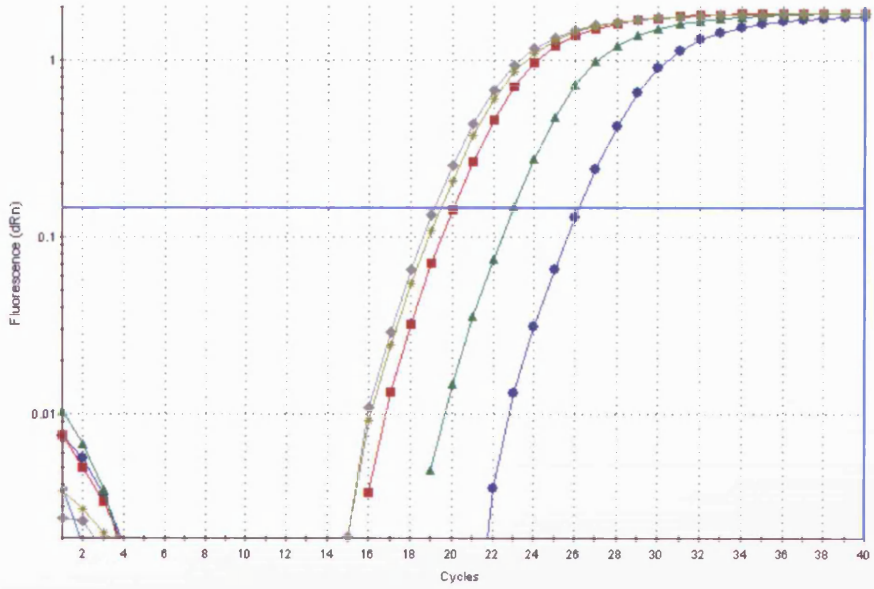

Figure 5.8 Log-transformed Q-RT PCR amplification curves for hNOP.

Figures 5.6 and 5.7 show growth curves of cDNA for the samples tested with the second set of primers for the human NOP gene. Cycle number is along the x-axis and the y-axis represents fluorescence intensity. Each individual set of points relates to a sample tube with curves at left of graph having more initial cDNA template and consequently a lower cycle number to reach exponential amplification.

The blue horizontal line denotes the threshold at which fluorescence was taken to be significantly above baseline (determined internally by the cycler) and is the derivation of the C_T value used for fold-change calculations. Logarithmic transformation of the y-axis allows easier visualisation of the reaction to check for linearity of growth curves.

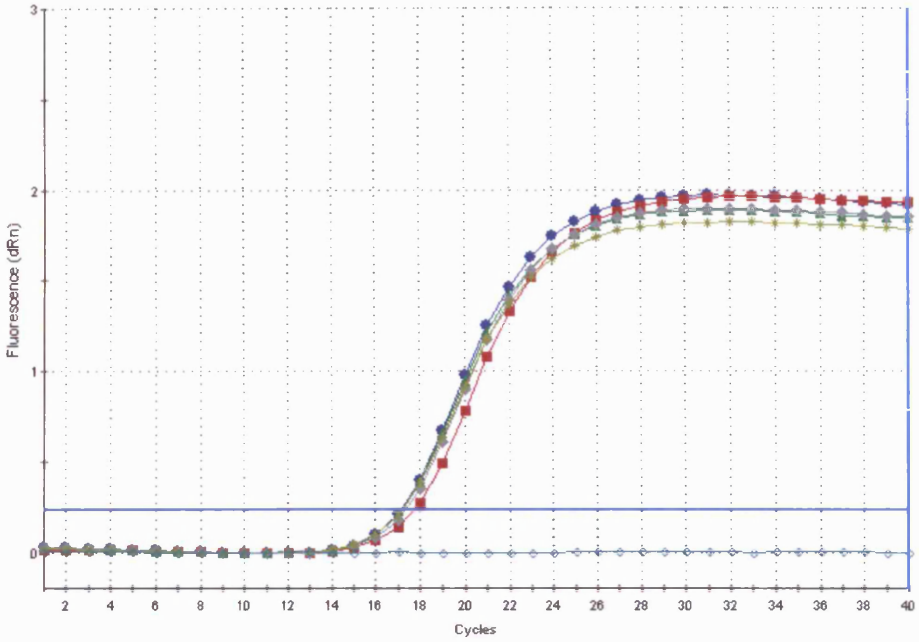

Figure 5.9 Sample Q-RT PCR amplification curves for GAPDH.

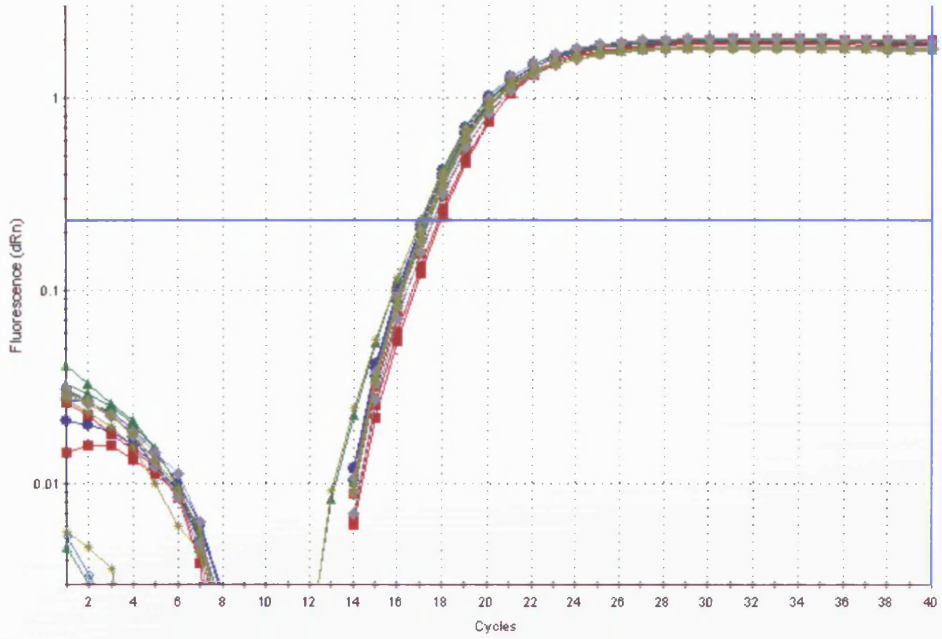

Figure 5.10 Log-transformed Q-RT PCR amplification curves for GAPDH.

Figures 5.8 and 5.9 show growth curves of cDNA for the samples tested with primers for the GAPDH housekeeping gene. Cycle number is along the x-axis and the y-axis represents fluorescence intensity. Each individual set of points relates to a sample tube with curves at left of graph having more initial cDNA template and consequently a lower cycle number to reach exponential amplification.

The blue horizontal line denotes the threshold at which fluorescence was taken to be significantly above baseline (determined internally by the cycler) and is the derivation of the C_T value used for fold-change calculations. Logarithmic transformation of the y-axis allows easier visualisation of the reaction to check for linearity of growth curves.

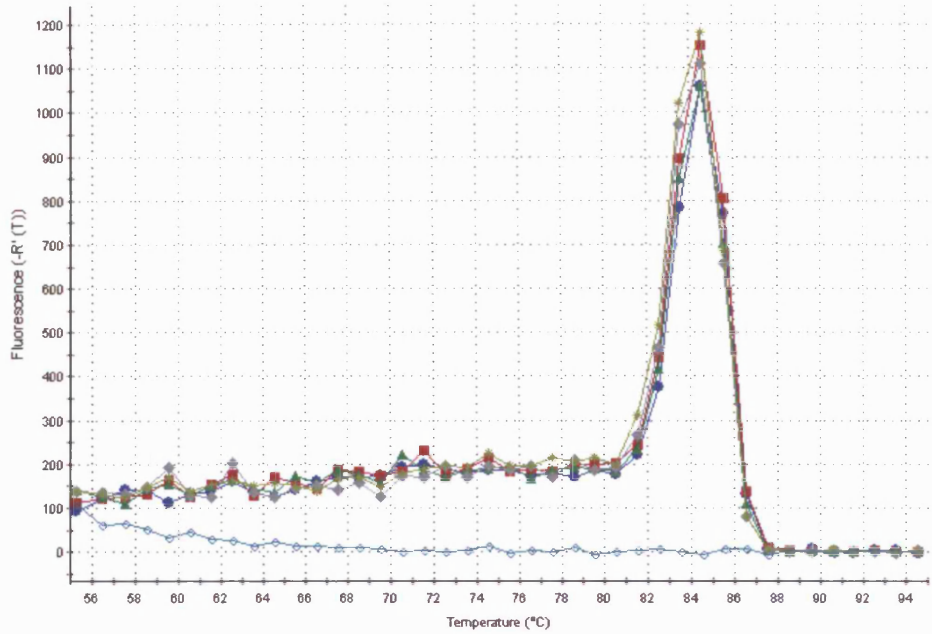

Figure 5.11 Sample dissociation curves for hNOP Q-RT PCR product.

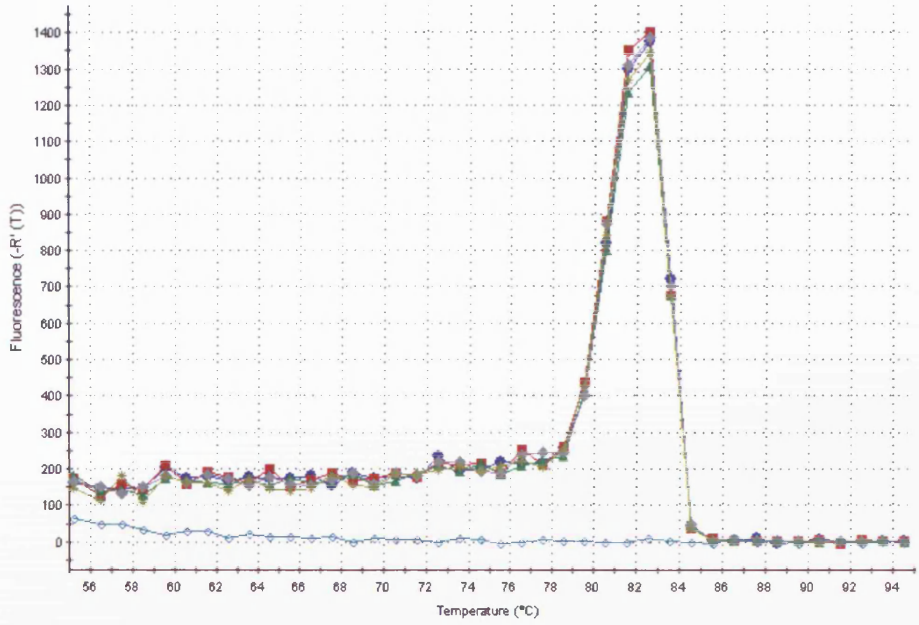

Figure 5.12 Sample dissociation curves for GAPDH Q-RT PCR product.

For all dissociation curves in Figures 5.10 and 5.11, there should be a single peak for all samples, seen at a position corresponding to a single melting temperature for the amplification product, according to the primers used. This indicates the purity of the product, with no contamination from genomic DNA or primer dimer formation. Non-template control shows as the flat line along the base, indicating no non-specific amplification or primer-dimer formation.

5.4.3 Calculations Using Standard Curve Method

Sample Standard curves for NOP and GAPDH are shown in Figures 5.12 and 5.13.

The results for the fold-change calculations are shown in Table 5.4. At 5μM Pon A induction there was an approximately twenty-fold increase in mRNA compared to control. For induction at 10μM Pon A, a thirty-fold increase over control was seen. These results reached statistically significant difference from control levels. There was also significant difference between the levels of mRNA for the two inductions.

Following pre-treatment with 1μM N/OFQ, at either induction level there was a significant down-regulation of NOP mRNA. These reductions, of approximately a third at 10μM Pon A and half at 5μM Pon A, when compared to the reduction in receptor numbers (two thirds at 10μM Pon A and half at 5μM Pon A) seen previously in saturation binding studies in these cells (Chapter 4) show good agreement at the lower induction but differ at the higher level.

Table 5.4 Results of calculations using the standard curve method.
* shows significant difference ($p<0.001$) from non-induced Calibrator; † shows significant difference ($p<0.001$) from corresponding Control; ** shows significant difference ($p<0.001$) from non-induced Calibrator and lower induction control. (n=6).

Induction [Pon A] (μM)	'Quantity Ratio' NOP/GAPDH	Ave. Fold-change (Ratio/Calibrator)
0 (Calibrator)	0.035±0.003	1
5 Control	0.700±0.043*	20.7
5 +1μM N/OFQ	0.403±0.041†	12.2
10 Control	1.059±0.036**	31.5
10 +1μM N/OFQ	0.713±0.047†	21.5

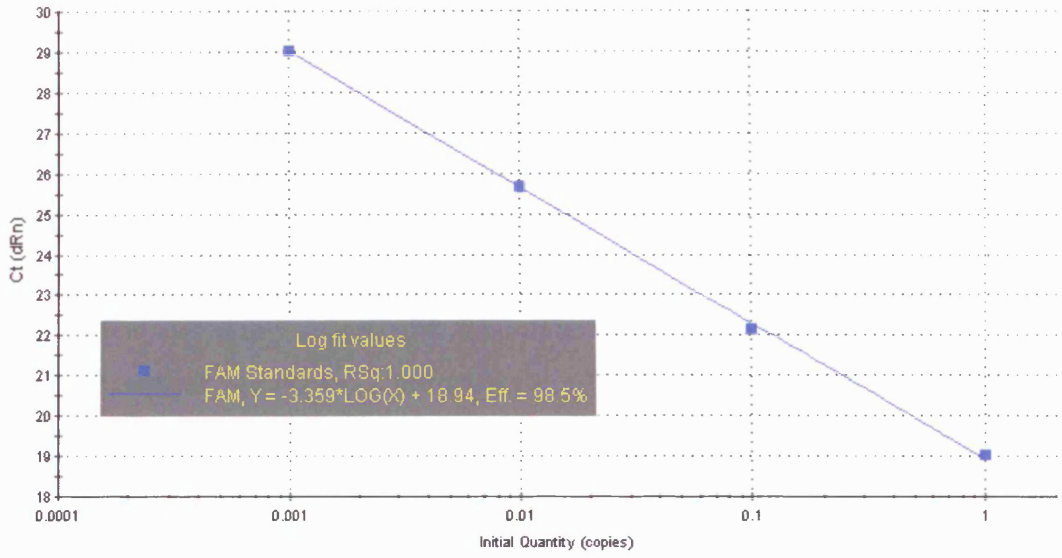

Figure 5.13 Sample standard curve for hNOP.
Inset shows R^2 value for linear regression and calculated efficiency for reaction.

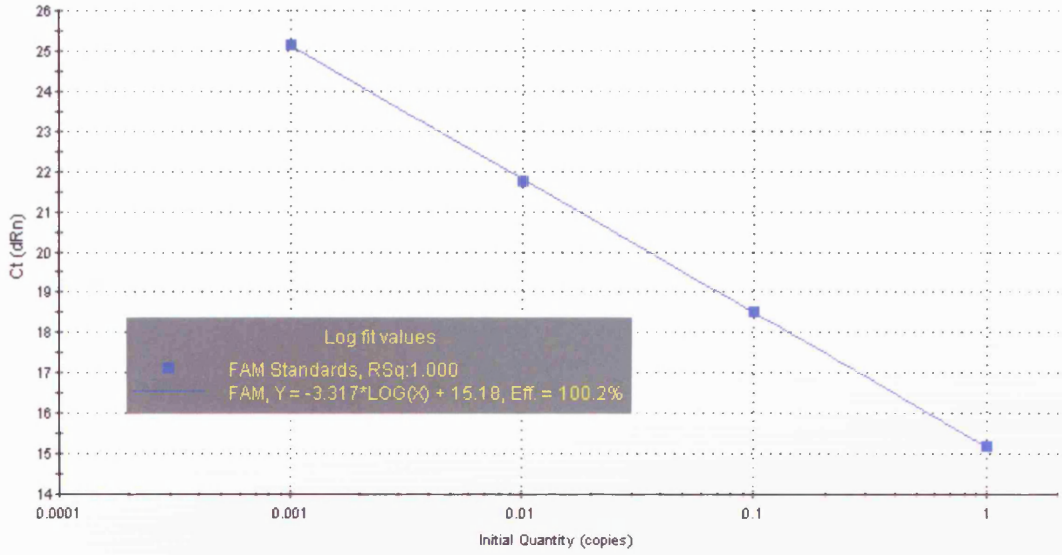

Figure 5.14 Sample standard curve for GAPDH.
Inset shows R^2 value for linear regression and calculated efficiency for reaction

5.5 Discussion

In CHO cells induced to express differing levels of human NOP by varying the concentration of Pon A, an investigation of the effects of pre-treatment with N/OFQ upon the level of mRNA was made using Q-RT PCR. The results of the reactions were transformed into fold-changes, derived from standard curves of cDNA for both NOP and GAPDH (the housekeeping gene used) with relative levels calculated by comparison with non-induced cells. By inference from good reaction efficiency, levels of cDNA seen in the reactions reflected the effect of Pon A concentration and N/OFQ pre-treatment upon mRNA produced in these cells.

The effect of Pon A induction was an increase in the level of mRNA produced in line with induction level (controlled by concentration of Pon A), from a basal value of unity (by definition) at zero Pon A through twenty times basal at 5μM Pon A to approximately thirty times basal at the highest induction of 10μM Pon A. These values cannot be compared statistically due to the basal level being defined as unity, so the intermediate calculation of cDNA levels for NOP relative to those for GAPDH (the 'Quantity Ratio') in each case was used. Using these values, a significant increase was seen for both the induction levels compared to the non-induced control and for the higher (10μM Pon A) induction compared to the lower (5μM Pon A) induction, corroborating the results inferred from the fold changes. This is the first study to show desensitisation of NOP at the genomic level.

With 1μM N/OFQ pre-treatment, the fold change results showed that mRNA produced by the cells in this system was decreased, for both induction levels, by approximately a third with respect to the corresponding control induction. Again, calculated from the 'Quantity ratio' values, the results showed a statistically significant decrease in mRNA for hNOP in these cases. This is broadly in keeping with the results for the Saturation binding assays from the previous chapter as receptor numbers showed a significant increase in receptor density with increased induction and decreased significantly with N/OFQ pre-treatment at the two induction levels used here.

Use of Housekeeping Genes in Q-RT PCR

There is much debate in literature as to the validity of using GAPDH as a housekeeper gene, indeed all genes used as such are potentially susceptible to effects upon the cell/tissue system being examined. Ultimately one particular gene must be relied upon to represent the underlying cellular state. Most studies currently reported are for native populations of endogenously expressed genes where pathological condition of the subject may elicit global effects (Bustin *et al.*, 2004; Dheda *et al.*, 2004; Thellin *et al.*, 1999; Tricarico *et al.*, 2002). This problem is perhaps of greater consequence than in transgenic systems where the endogenous genetic situation should not be as susceptible to treatments affecting heterologously expressed genes.

Other Methods of Calculation

Several alternative methods of calculation, such as the $\Delta\Delta C_T$ method and Relative Expression Software Tool (REST©), have been proposed in the literature, but all ultimately rely upon good sample preparation and reaction efficiency (Pfaffl, 2001; Pfaffl *et al.*, 2002). Again the conclusion must be that a method be adopted appropriate to the assay system and conditions.

6 Discussion

6.1 Summary of Main Findings

6.1.1 Structure Activity Relationship (SAR) Studies

In this thesis it has been shown that various modifications on the natural sequence of nociceptin can generate a spectrum of effects. These included the simple agonist with increased protection from enzymatic degradation by amidation of the carboxyl terminus, to agonists with enhanced affinity and/or increased efficacy using amino acid substitution within the sequence and alterations to the side chains of residues in positions 1 and 4. Partial agonists of varying efficacy and high affinity antagonists with no residual activity may also be generated in this manner (Calo *et al.*, 2000c; Guerrini *et al.*, 1997).

6.1.2 Ecdysone Inducible Expression System

An inducible expression system in which the receptor density may be varied was characterised using the assay systems described for the structure activity relationship studies. A series of induction levels was used to investigate the effect of this variation upon the efficacy of partial agonists. At high receptor density, the N/OFQ analogue [F/G] behaved as a partial agonist in GTPγS assays but showed full agonist activity for cAMP inhibition, a comparable effect seen in a stably transfected, high expressing cell line (CHO_{hNOP}). Where lower levels of receptor density were induced, comparable to those reported in native tissue, cAMP assays showed this compound to be, in effect, a partial agonist with antagonism observed in GTPγ[^{35}S] assays.

6.1.3 Desensitisation

Studies using the inducible cell system described previously investigated the effect of desensitisation of NOP by pre-treatment with N/OFQ, previously shown in the stable expressing cell line. With pre-treatment, the receptor density decreased at all levels of induction and this was accompanied by a decrease in stimulation of GTPγ[^{35}S] binding upon re-challenge with N/OFQ. In both GTPγ[^{35}S] binding and cAMP inhibition assays, the potency of N/OFQ decreased. Additionally, the cAMP assays revealed that pre-treatment increased cAMP production. This may have been a result of receptor uncoupling from associated G-proteins implying constitutive activity of the receptor in this system.

6.1.4 Genomic Effects

To further investigate desensitisation, the same cell line was analysed by Q-RT PCR to detect genomic effects of pre-treatment with N/OFQ. The levels of mRNA relative to a housekeeping gene were seen to increase with induction. A decrease in mRNA was clearly seen with pre-treatment of cells, implying that the decrease in receptor density seen in the previous chapter was likely due to a down-regulation of mRNA levels.

6.2 Structure/Activity Relationships

For descriptive purposes, the seventeen amino acid sequence of N/OFQ may be regarded as composed of two motifs, message and address. The sequence may be truncated to the initial thirteen residues without loss of function. Amidation of the carboxyl terminus, where the address motif is located, resulted in an increase in affinity (pK_i), with no loss of potency (pEC_{50}) in either of the functional assays. As such this modification was used in all subsequent analogues of the peptide.

For the purposes of this thesis, further analogues were described as amendments to the two motifs in three templates, the agonist sequence and those generated by alterations to either the initial residue (phenylalanine) or to the bond between this residue and the second (glycine). Relocation of the sidechain of the initial phenylalanine residue from the α-carbon atom to the terminal nitrogen creates an antagonist ([Nphe^1]N/OFQ-NH_2) and modification of the bond between the first two residues creates a partial agonist ([F/G]N/OFQ-NH_2) (Guerrini *et al.*, 2000a; Guerrini *et al.*, 1998).

The affinity for NOP was seen to increase with addition of the amino acids arginine and lysine to the address motif, forming a third repeat of this pair of basic residues within the sequence. This modification had the same effect upon affinity in all templates used but was not sufficient to counteract antagonism in the antagonist template, implying that this motif is involved in receptor recognition.

The substitution of fluorine into the *para*-position of the fourth residue, phenylalanine, enhanced the affinity of the peptide in each template to a lesser extent than the previous modification and was also able to elicit partial agonist activity in the antagonist template. This corroborates the idea that the initial four residues form the message motif, responsible for receptor activation.

The substitution of the first phenylalanine with tyrosine, the N-terminal amino acid in several opioid receptor peptides, such as the endomorphins, enkephalins, DAMGO, DPDPE and dynorphin, causes N/OFQ to exhibit slightly higher affinity for the opioid receptors KOP and MOP, with an accompanying loss of affinity for NOP (Calo *et al.*, 2000c). This initial tyrosine is essential for activity in the opioid peptides and the phenylalanine at the fourth position would seem to play an analogous role in N/OFQ as substitution of this residue with tyrosine (equivalent to *para*-hydroxy substitution in the phenylalanine normally seen there) results in a dramatic loss of potency for this analogue of N/OFQ (Reinscheid *et al.*, 1996). In the partial agonist template, a further modification of the peptide bond between the initial two residues gave the analogue [F/G-O]. This showed an increase in binding affinity and both potency and efficacy in GTPγ[^{35}S] assays compared to the equivalent template.

Substitution of cystine at two positions within the address motif, forming a cyclised peptide resulted in an agonist with decreased binding affinity and decreased potency in GTPγ[^{35}S] assays. This analogue behaved as a full agonist in cAMP inhibition assays but, at high concentration (10μM) in GTPγ[^{35}S] binding, showed a decrease in stimulation from a maximum at 1μM. This modification in the antagonist template created a low potency agonist.

Figure 6.1 illustrates the relative positions in the full sequence of the various modifications used in this work. A comparison of the results for potency in the two functional assays with binding affinity of the analogues tested, shown in Figure 6.2, reveals that affinity is in all cases less than the observed potency (shown by all points lying to the right of the line of identity). Good correlation of results was seen, with the exception of the antagonist template analogues, having residual agonist activity for cAMP inhibition. These three form a small outlying group with reasonable linearity, showing proportionate increase in both affinity and potency of cAMP inhibition.

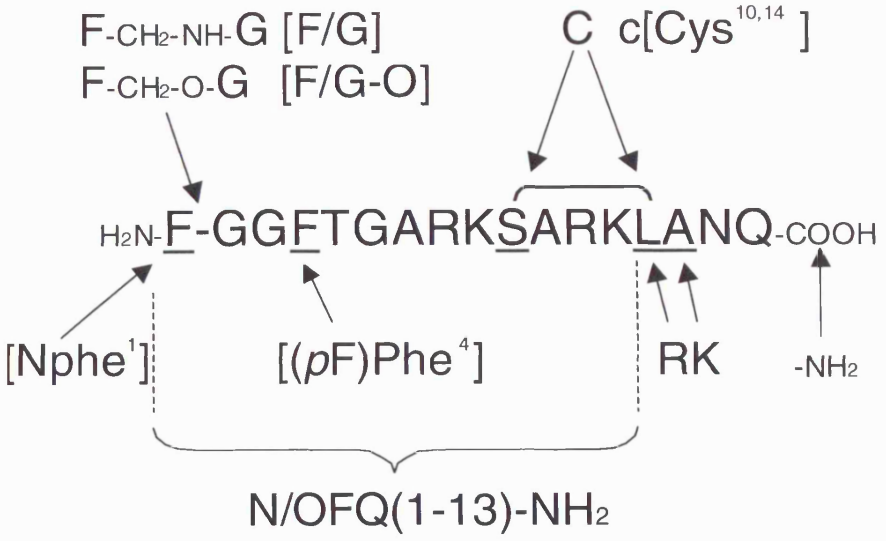

Figure 6.1 Schematic representing the relative positions of the modifications to the sequence of N/OFQ used in this thesis.
Clockwise from top left, the analogues [F/G] and [F/G-O] have altered peptide bonds between the first and second residues; in c[Cys^{10,14}] the serine and leucine in the native peptide are each replaced by cystine, forming a disulphide bridge, resulting in a cyclised peptide; amidation of the carboxyl terminus protects from enzymatic degradation; substitution of arginine and lysine for leucine and alanine in the address motif; *para*-fluoro substitution on phenylalanine (residue 4) in the message motif; translocation of the sidechain of the N-terminal phenylalanine to give an antagonist; at bottom is the truncated peptide, the minimum sequence necessary for full activity at NOP.

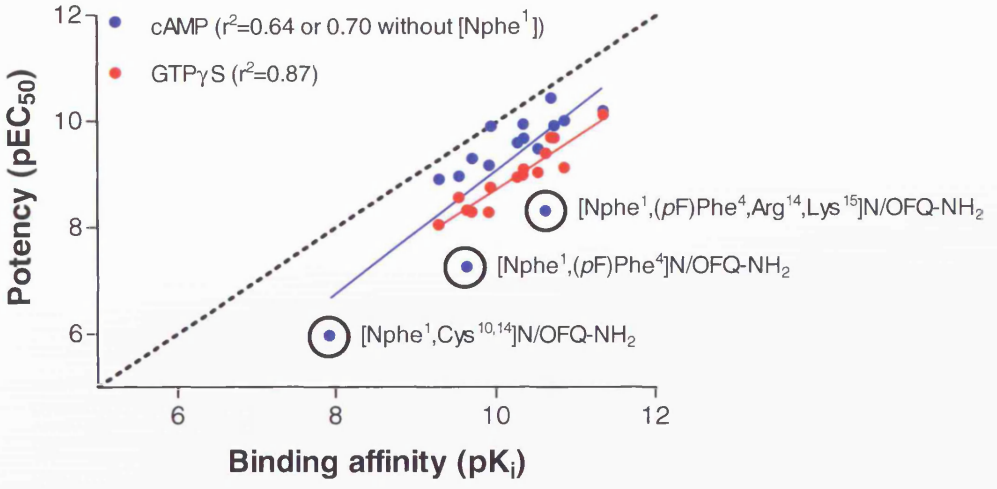

Figure 6.2 Comparison of binding affinity and functional potency in GTPγ[^{35}S] and cAMP inhibition assays in CHO_{hNOP} cells.
In general binding affinity is higher than corresponding functional potency and potency in the cAMP assay is higher than in the GTPγ[^{35}S] assay. The three outliers from the cAMP assay (circled) are [Nphe^1] derivatives in which there was a quantifiable agonist response. Dotted line is the line of identity.

Tables 6.1 and 6.2 show a summary of the data from [*leucyl*-^{3}H]N/OFQ binding, GTPγ[^{35}S] binding using CHO_{hNOP} membranes and cAMP inhibition assays in whole cells with the natural peptide and different combinations of the possible modifications to the sequence of N/OFQ.

For a partial agonist pEC_{50} should predict pA_2/pK_B and, in general, pK_i should also predict pA_2/pK_B. In binding experiments some of the variations upon the antagonist template showed partial agonist activity. Of these analogues, [Nphe^1,(*p*F)Phe^4] displayed $pK_i \approx$ 9.6 with $pK_B \approx$ 8.3 in GTPγ[^{35}S] and $pEC_{50} \approx$ 7.3 in cAMP; [Nphe^1,(*p*F)Phe^4,Arg^{14},Lys^{15}] $pK_i \approx$ 10.6, $pA_2 \approx$ 9.7 in GTPγ[^{35}S], $pEC_{50} \approx$ 8.3 in cAMP; c[Nphe^1,Cys^{10,14}] $pK_i \approx$ 8, $pA_2 \approx$ 7 in GTPγ[^{35}S], with an estimated $pEC_{50} \approx$ 5.8 obtained in cAMP studies. This latter, measured downstream in whole cells, agrees well with the value for pK_B (5.7) obtained in mVD. These discrepancies with and differences from accepted theory are common to this system and likely result from differences in sensitivity for buffer and assay (Calo *et al.*, 2000c). For example, presence of Na^+ would reduce affinity in saturation binding (Dooley *et al.*, 2000) but is necessary for GTPγ[^{35}S] binding and cAMP/mVD assays use whole cells/tissues with (relatively high) native concentrations of guanine nucleotides. Thus in comparison with the Na^+-free receptor binding assay, a reduction in pA_2 from GTPγ[^{35}S] assays might be predicted with further reductions in binding affinity for whole cells also anticipated. This has been discussed previously (Calo *et al.*, 2000c).

In inhibiting forskolin-stimulated cAMP formation, the high residual agonist activity with these analogues is worthy of further note. As cAMP formation is downstream in the signal transduction cascade, this functional assay involves significant amplification of signal. The net result of this is the creation of a receptor reserve, with partial agonists behaving as full agonists (Kenakin, 2002a; McDonald *et al.*, 2003a). Indeed, it has been reported that the partial agonists Ac-RYYRIK-NH_2 (Berger *et al.*, 2000a) as well as [F/G]N/OFQ(1-13)NH_2 (present data), behave as full agonists in this assay system. Again these studies underscore the need for caution in defining pharmacology based on a single functional end point.

Short peptides with activity at NOP – the Dooley peptides

In an investigation of a combinatorial library of approximately 150 million hexapeptides, twenty were synthesised individually after bulk screening. Of these, five were found to have affinity for NOP (Dooley *et al.*, 1997). These compounds have become known as 'Dooley peptides'. Although their potency was seen to be similar to that of N/OFQ, efficacy was reduced by comparison, hence their grouping as partial agonists in this report. They each consist of six amino acids with acetylated N-termini and amidated C-termini (effectively reversed-terminus peptides). Acetylation is known to reduce the degradative effects of amino-peptidases upon the terminal amino acid (Phe^1) shown to be essential for receptor activation (Yu *et al.*, 1996). In addition these compounds have the protection afforded by amidation at the normal C-terminus. Both of these effects are especially important *in vivo*. It is interesting to note that these hexapeptides possess arginine and lysine, separated by tryptophan, at the C-terminus of their sequence showing similarity to the address domain of N/OFQ (Mason *et al.*, 2001). seemingly anomalous to the message address concept with activity at NOP that would not theoretically be predicted.

Table 6.1 Summary of results for Displacement binding and GTPγ^{35}S binding in CHO_{hNOP} membranes and cAMP inhibition assays in CHO_{hNOP} cells. Data in italics courtesy of J. McDonald, 2003.

Ligand	Displacement of [*leucyl*-^{3}H]N/OFQ binding	GTPγ[^{35}S] Binding		cAMP Inhibition	
	(pK_i)	pEC_{50}	E_{max}	pEC_{50}	E_{max} (%)
N/OFQ	9.91±0.04	*8.75±0.11*	*10.20±0.79*	9.90±0.13	103.0±0.6
N/OFQ-NH_2	*10.31±0.04*	*8.98±0.08*	*10.98±1.30*	9.94±0.04	102.7±1.4
N/OFQ(1-13)-NH_2	10.24±0.09	*8.94±0.01*	*11.19±0.48*	9.59±0.04	102.8±1.0
[(*p*F)Phe^4]N/OFQ-NH_2	10.66±0.09	*9.51±0.04*	*11.42±0.72*	10.18±0.19	101.0±1.3
[(*p*F)Phe^4]N/OFQ(1-13)-NH_2	10.81±0.10	*9.55±0.01*	*11.94±0.34*	10.25±0.06	101.4±2.0
[Arg^{14},Lys^{15}]N/OFQ-NH_2	11.16±0.05	*9.85±0.11*	*9.70±0.69*	10.00±0.10	102.3±1.0
[(*p*F)Phe^4,Arg^{14},Lys^{15}]N/OFQ-NH_2	*11.32±0.08*	*10.12±0.04*	*12.26±0.39*	10.17±0.09	103.8±1.1
[Nphe^1]N/OFQ-NH_2	9.38±0.01	*pA_2=7.54*	Inactive	6.78±0.47	26.3±3.0
[Nphe^1]N/OFQ(1-13)-NH_2	8.08±0.07	*pA_2=7.33*±0.08	Inactive	pA_2=5.96	Inactive
[Nphe^1,(*p*F)Phe^4]N/OFQ-NH_2	*9.62±0.02*	*8.23±0.30*	*1.36±0.11*	7.26±0.61	28.1±9.9
[Nphe^1,Arg^{14},Lys^{15}]N/OFQ-NH_2 (UFP-101)	9.89±0.09	*pA_2=8.85±0.12*	Inactive	pA_2=7.11	Inactive
[Nphe^1,(*p*F)Phe^4,Arg^{14},Lys^{15}]N/OFQ-NH_2	*10.60±0.10*	*9.39±0.20*	*2.03±0.01*	8.31±0.15	91.3±9.6
[F/G]N/OFQ-NH_2	*9.89±0.08*	*8.28±0.57*	*4.58±0.52*	9.12±0.06	97.0±8.6
[F/G]N/OFQ(1-13)-NH_2	*9.27±0.06*	*8.05±0.21*	*7.75±1.02*	8.90±0.24	97.5±2.6
[F/G,(*p*F)Phe^4]N/OFQ-NH_2	*10.32±0.04*	*9.09±0.29*	*4.30±0.28*	9.32±0.52	104.0±4.1
[F/G,Arg^{14},Lys^{15}]N/OFQ-NH_2	*10.50±0.03*	*9.03±0.09*	*5.29±0.27*	9.62±0.33	89.0±9.4
[F/G,(*p*F)Phe^4,Arg^{14},Lys^{15}]N/OFQ-NH_2	*10.70±0.03*	*9.68±0.10*	*4.20±0.07*	9.52±0.44	92.0±2.3

Table 6.2 Summary of results for Displacement binding and GTPγ^{35}S binding in CHO_{hNOP} membranes and cAMP inhibition assays in whole CHO_{hNOP} cells.

Ligand	Displacement of [*leucyl*-^{3}H]N/OFQ binding	GTPγ[^{35}S] Binding		cAMP Inhibition	
	(pK_i)	pK_B	E_{max}	pEC_{50}	E_{max} (%)
[F/G-O]N/OFQ(1-13)NH_2	9.52±0.06	8.56±0.17	10.17±1.88	8.96±0.18	103.1±2.3
[Cys^{10,14}]N/OFQ-NH_2	9.68±0.27	8.29±0.08	5.67±0.46**	9.29±0.11	102.4±0.61
[Nphe^1,Cys^{10,14}]N/OFQ-NH_2	7.92±0.23	pA_2=7.05±0.05	Inactive	5.97±0.21	101.7±4.9
JTC-801*	7.35±0.15	-	-	pK_B=7.77±0.19*	Inactive
J113397	8.82±0.02	pK_B=8.34±0.02	Inactive	pA_2=7.98±0.50	Inactive
III-BTD	8.74±0.08	pA_2=7.89±0.17	Inactive	pK_B=7.27±0.15	Inactive
* After 90 min pre-incubation, not at equilibrium; ** decreased E_{max} at 10μM					

6.3 Ecdysone Inducible System

In this expression system, the hNOP expressed in CHO cells not only displayed the same pharmacology observed in other cell lines and tissues, but also allowed titration of receptor density. For comparison with data from Chapter 2 and reported studies (Hashiba *et al.*, 2002; Johnson *et al.*, 2002), Figure 6.3 shows correlation of values for pK_i derived for compounds used with CHO_{hNOP} cells and native tissue extracts from rat and dog with those presented here from $CHO_{INDhNOP}$. In general, there was good agreement. PTx-sensitivity, confirming $G_{i/o}$ coupling, was seen in both transgenic cell lines.

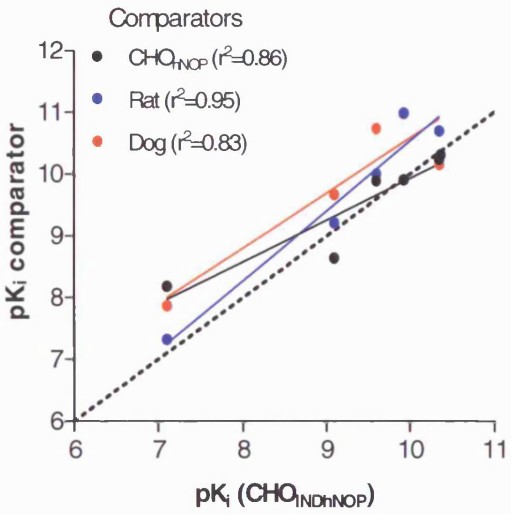

	INDhNOP	hNOP
PTx sensitivity	✓	✓
GTPγS pEC_{50}	8.92	8.94
GTPγS E_{max}	4.1 fold	11.2 fold
cAMP pEC_{50}	9.72	9.59
cAMP E_{max}	80%	103%

Figure 6.3 Induced NOP behaves in a manner analogous to NOP in stable expression system and that endogenously expressed in rat and dog brain.
Correlation between displacement pK_i values (left) for 5-6 NOP ligands determined in $CHO_{INDhNOP}$ (induced at 5μM Pon A) and CHO_{hNOP} (see Chapter 3 and Hashiba et al, 2002), rat and dog brain membranes (Johnson *et al.*, 2002). Data for N/OFQ(1-13)NH_2 are form saturation studies with the [*leucyl*-^{3}H]-labelled form of this peptide). Dotted line is the line of identity.
Comparison of pertussis toxin (PTx) sensitivity, potency and efficacy (right) for GTPγ[^{35}S] and cAMP inhibition in $CHO_{INDhNOP}$ (induced at 5μM Pon A)and CHO_{hNOP}.

Investigation of the effect of receptor density upon partial agonist activity was made for [F/G] in the inducible cell line. In GTPγ[^{35}S] assays this analogue behaved as a low efficacy partial agonist but as an agonist for cAMP inhibition. With a reduction in receptor density, this compound behaved as a partial agonist at cAMP inhibition, implicating a receptor/coupling reserve at higher levels of expression.

6.4 Desensitisation

The phenomenon of receptor desensitisation is another factor of particular relevance in the clinical situation as prolonged exposure to a pharmacologically active compound will result in a loss of response. Desensitisation may be the result of a loss in receptor numbers or a loss of responsiveness in the signal generated by the system. This can be due to down regulation of response via a number of mechanisms such as receptor uncoupling, phosphorylation effects and receptor internalisation and degradation. Conflicting theories exist as to whether cells may increase or reduce the level of receptor DNA transcribed, ultimately affecting the balance of the pain response and possibly removing response to stimuli entirely, again an issue of importance in cells with very low levels of expression (Bilecki *et al.*, 2000; Buzas *et al.*, 2002; Nestler, 2004).

Desensitisation may be mediated by any of four main processes. Fast effects occur via receptor uncoupling from G-protein and phosphorylation of either the receptor or G-protein; internalisation of the receptor occurs over an intermediate time period and leads to either or degradation and receptor down-regulation. Of these latter phenomena, sequestration is a relatively fast effect with a time course of minutes, the receptors being returned to the cell surface intact after release of bound ligand. Degradation is slower than sequestration and leads to permanent loss of receptor numbers, seen as down-regulation. Finally the slowest effect and that of longest duration occurs at the molecular level in the cell nucleus where the amount of mRNA produced coding for the receptor is diminished.

The range of expression levels used in this study enabled a comparison of the effects of N/OFQ pre-treatment upon cells expressing NOP at high density with these effects at a lower level, mimicking levels seen in native tissue. The higher level of expression used was similar to that seen for the stable transgenic cell line used in previous work (Hashimoto *et al.*, 2002). In that study, cells were treated with 1nM N/OFQ for up to 48h in the absence and presence of antagonist (1μM [Nphe^1]N/OFQ(1-13)-NH_2). A reduction in potency for cAMP inhibition was seen that was dependent upon duration of pre-treatment (control $pEC_{50} \approx 9.5$, after 48h, $pEC_{50} \approx 8.7$) and this was prevented by co-exposure to the antagonist. This reduction only reached significance after 24h pre-treatment with N/OFQ. A 35% loss of binding to cell surface receptors was seen at 48h

exposure, again reversed by co-exposure to antagonist, that correlated with the reduction in cAMP inhibition. Absolute levels of cAMP production increased 2.5-fold with pre-treatment longer than 24h.

In this thesis, the effect of pre-treatment with N/OFQ was seen to decrease receptor density at both levels of expression used. This decrease was 58% at 10μM Pon A and 44% at 5μM Pon A induction. In the functional assays, decreases in both potency and maximum stimulation in GTPγ[^{35}S] were seen at both of these induction levels. This decrease in potency was also seen for cAMP inhibition but there was an increase in maximum inhibition in this assay, implying that some constitutive activity was present. The effect of pre-treatment was to remove this activity, resulting in an increase in basal level of cAMP in these cells.

A detailed study of the effects that differential expression and phosphorylation have upon desensitisation in another receptor system has previously been reported (Law *et al.*, 2000b). Here, the internalisation of DOP expressed in HEK293 cells using the ecdysone-inducible system, was dependent upon receptor density, showing rapid desensitisation at low levels of expression (up to 90fmol.mg^{-1} protein) with pre-treatment by deltorphin II. The desensitisation was mediated by other cellular mechanisms than phosphorylation alone, since site directed mutagenesis of the DOP intracellular carboxyl tail removed agonist-induced phosphorylation with only a reduction in the rate of internalisation. This internalisation was dependent upon the formation of clathrin-coated pits. Similar effects have been reported for MOP in a stable transfection cell line (Law *et al.*, 2000a).

An issue requiring further comment is that of the initial washing, at cell harvest, to remove the original (pre-treatment) N/OFQ and its effect on subsequent challenge. In a previous study (Hashimoto *et al.*, 2002) a lower concentration of N/OFQ was used and it was determined that only 3% remained (equivalent to 30pM), well below the K_D (70pM) in a binding experiment. In this study the 'spiking' studies were not repeated due to the lack of availability of radiolabelled iodinated N/OFQ. However, application of the 3% estimate from Hashimoto *et al* to the 1μM N/OFQ used for pre-treatment in this study would, in this case, yield a residual concentration of 30nM, sufficient to

saturate both cAMP and GTPγ[^{35}S] protocols. This was clearly not the case as the subsequent rechallenge produced a full concentration response curve.

It must be stated that the percentage calculated by Hashimoto *et al* may only apply to the pre-treatment concentration used then and that this represents the residual amount of N/OFQ. This amount is then not a simple percentage of the applied N/OFQ. In addition, if there was significant residual stimulation, total GTPγ[^{35}S] binding would be markedly elevated and basal cAMP formation would be inhibited (compared to non-treated controls). Whilst there was some elevation in GTPγ[^{35}S] experiments, the increase was small (~100 counts over naïve cells at 10μM Pon A).
As an estimate of residual N/OFQ carried forward to the assay, a simple calculation of ligand washout, based upon the cell preparation protocol, may be made:
Remove medium from flask (13ml) and assume 1ml remains. Rinse with ≈20ml harvest buffer, discard and add further harvest buffer to detach cells. Make to 25ml with Krebs'/HEPES buffer, spin, discard and again assume 1ml carry over. Wash twice more with 25ml Krebs'/HEPES buffer and assume the same carryover. Finally make up into volume for assay (≈2.5ml). From a pre-treatment concentration of 1μM, this yields a final carry over concentration of ≈30pM. This is "worst case" as in the GTPγ[^{35}S] protocol there are further washing and homogenisation steps. In summary, a 'spiking' protocol may have been useful but it is unlikely that significant amounts of N/OFQ remained from the incubation.

6.5 Interaction of NOP and Opioid Receptors

It has been reported that endogenous NOP is not affected by desensitisation of DOP with DPDPE in more than one cell line (Cheng *et al.*, 1997; Ma *et al.*, 1997), but the effects of pre-treatment with the DOP agonist Met-enkephalin in rat locus coeruleus neurones did show a reduction in N/OFQ activation of potassium channels (Connor *et al.*, 1996b). The desensitising effect of N/OFQ pre-treatment upon NOP has caused heterologous desensitisation of MOP (Pan *et al.*, 2000). The mediator for this latter effect would seem to be PKC as the desensitisation was phorbol ester-sensitive and GRKs 2 and 3 were increased with N/OFQ pre-treatment, all of which are involved in MOP desensitisation. Both PKA and MAP kinase were also excluded as mediators for MOP desensitisation (Mandyam *et al.*, 2002). PKC-sensitive desensitisation of NOP-

mediated effects upon $GABA_B$ receptor calcium channel inhibition in rat hippocampal neurones has also been reported (Pu *et al.*, 1999). The action of N-methyl-D-aspartate (NMDA) upon its receptor, prior to NOP and opioid receptor activation, in neuronal cells reduces the effects of both N/OFQ and opioids in one cell line (NG108-15) but only the effects of NOP stimulation in another (SK-N-SH), leading to the conclusion that differences in regulation may be seen for heterologous desensitisation via another receptor (Zhao *et al.*, 1998).

6.6 PCR and Genomic Effects

To form a more complete picture of the desensitisation process in these cells, the effects of pre-treatment were assessed at the genomic level by analysis of mRNA extracted after incubation and induction of the cells. This was reverse transcribed into cDNA and part of the transcript for NOP selectively amplified using Q-RT PCR. With 1μM N/OFQ pre-treatment, the fold change results showed that mRNA produced by the cells in this system was decreased for both induction levels, by comparison with the expression of a protein native to the cells. The level of mRNA decreased with pre-treatment by 41% at 10μM and 32% at 5μM Pon A. This is the first study to show genomic desensitisation effects at NOP.

The Q-RT PCR data are broadly in keeping with the results for the saturation binding assays from the previous chapter. Receptor numbers showed a significant increase in receptor density with increasing induction and decreased significantly with N/OFQ pre-treatment at the two induction levels used. Functional assays of desensitisation (GTPγ[^{35}S] binding, cAMP inhibition) are correlated with receptor numbers but do not necessarily reflect the prevailing conditions within the cell. The effects of pre-treatment with N/OFQ upon mRNA levels from this results chapter are shown in Table 6.3 with the results from the pharmacological studies of desensitisation as comparison.

Table 6.3 Changes in $CHO_{INDhNOP}$ cells pre-treated with 1μM N/OFQ, relative to control, measured for induction at 5 and 10μM Pon A, in the assays used for this study.

Site of Assay		Change (from control) following 1μM N/OFQ pre-treatment (%)	
		5μM Pon A	10μM Pon A
Receptor Density		-44.2	-58.5
GTPγ[^{35}S] Binding	E_{max}	-29.5	-33.3
cAMP Inhibition	E_{max}	+12.8	+14.9
NOP mRNA		-41.1	-31.7

A potential problem must be addressed, in that the inducible system used in these studies is transgenic and, as was seen from the primers first used for this section of experiments, the sequence used for transfection was not the whole gene but only that coding for the functional receptor. Thus the native environment for this gene, consisting of promoter, regulatory regions and any introns, is not present and the mediation of the desensitising effect cannot be assumed to reflect the whole situation *in vivo*. It may be suggested that such regulatory proteins as cAMP response element binding protein (CREB) may be involved in this process in native tissue. In a transgenic system these elements may not necessarily be present and the absence of this response element (the binding site for CREB) would infer that other, perhaps cytoplasmic, mechanisms are involved.

In the presence of complete, functional gene complexes an increase in cAMP levels may allow, following prolonged activation of G_i-coupled receptors, an elevation in transcriptional activity, since CREB is thought to act as an enhancer of this process (Nestler, 2004). The transgenic system examined showed a significant down-regulation of mRNA, the inference of which for a native system is not clear. An illustration of the possible mode of transduction for a desensitising signal is depicted in Figure 6.4.

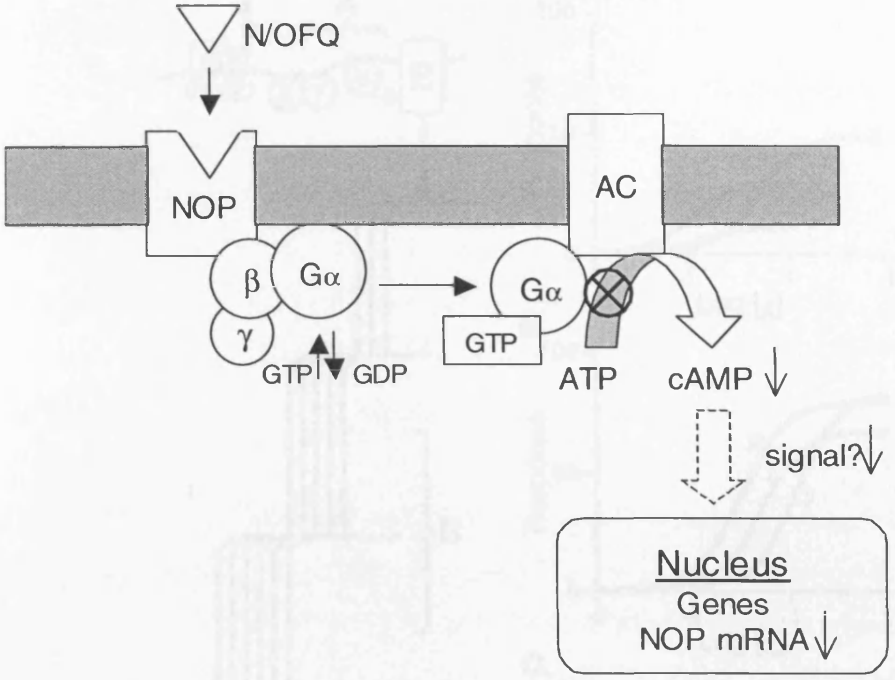

Figure 6.4 Representation of the possible transduction process involved in receptor desensitisation, resulting from N/OFQ pre-treatment of a transgenic human NOP.
N/OFQ binding to NOP causes dissociation of the G-protein through GTP/GDP exchange. The GTP-bound $G_{\alpha i}$ subunit inhibits adenylyl cyclase, causing a decrease in cAMP production. This may perhaps generate a signal to the nucleus resulting in a decrease in transcription of the NOP gene. However, in the desensitised situation NOP uncouples, thereby allowing an increase in cAMP, potentially having the opposite effect.

6.7 Advantages and Limitations of Individual Assay Systems.

The use of functional assays in addition to binding assays gives an overall view of the process from ligand binding, through receptor activation, G-protein activation and finally to second messenger generation, which results in the final output of the cell in the signalling process.

The amplification occurring using a downstream assay such as that for cAMP can mask small/subtle differences in potency of modified ligands which may be shown in binding assays or other functional assays, such as GTPγ[^{35}S], that work immediately downstream of the activated receptor (Dooley *et al.*, 1997). This effect is extremely important in the case of partial agonists as the discrimination between full and partial activity needs to be very fine. An illustration of the reason for this lack of discrimination is given in Figure 6.5.

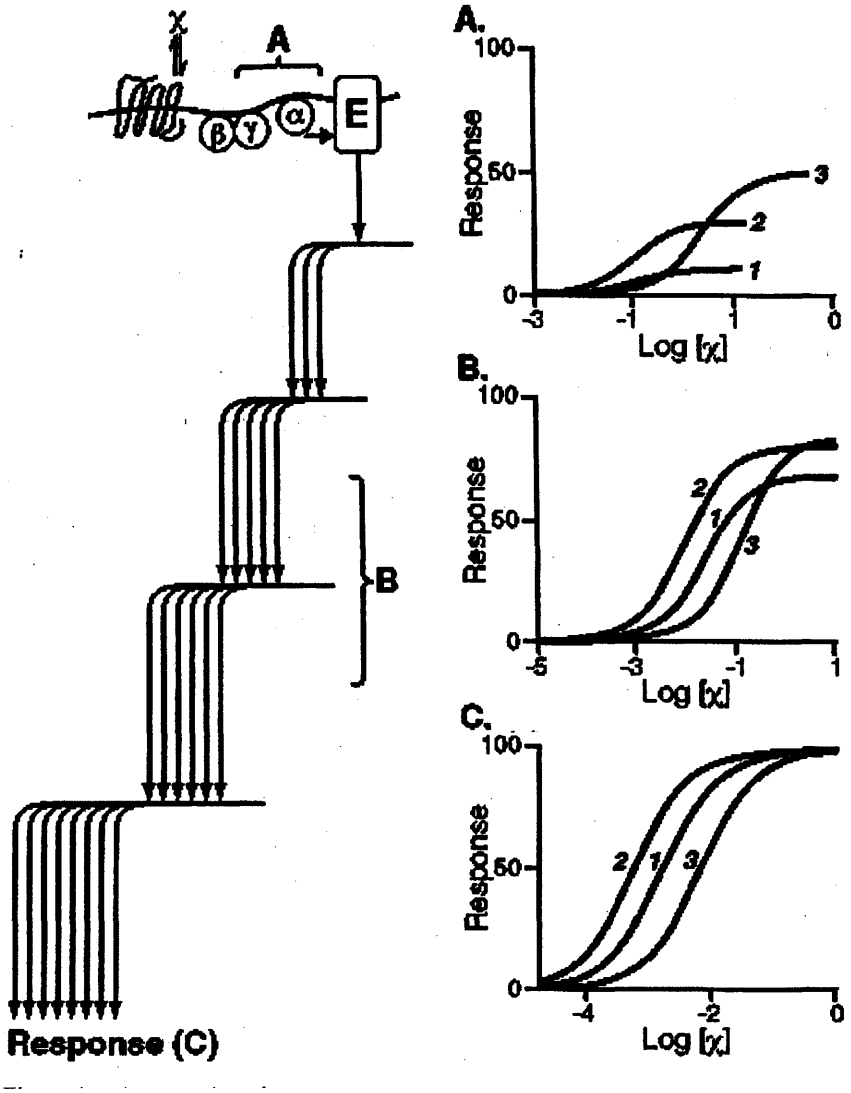

Figure 6.5 The effect of amplification upon measurement of stimulus-response in a saturable system. Ligands 1 and 2 have, respectively, 0.2 and 0.6 times the efficacy of ligand 3. Upstream measurement (at A in the diagram) allows discrimination between the efficacy of these ligands. Measurement at B begins to mask the differences due to amplification as in, for example, a G-protein which interacts with more than one effector enzyme. When the final response is measured at C, as with measurement of cAMP where many messenger molecules may be produced by each effector enzyme, the degree of amplification is so great as to saturate the system and remove any discrimination between the ligands (Kenakin, 2002b).

Of further note is the lack of need for peptidase inhibitors in whole cell assays (Okawa *et al.*, 1999), whereas membrane-based assays require the addition of a cocktail of inhibitors due to the release of peptidases from the cytoplasmic environment (Terenius *et al.*, 2000).

The cAMP inhibition assays using the inducible cells described in Chapter 3 were performed using adherent cell cultures in 24-well plates. All cAMP assays described

elsewhere in this thesis used cell suspensions harvested from flask cultures, after treatment where appropriate. The choice of the well-plate method enabled the use of both N/OFQ(1-13)-NH_2 and [F/G]N/OFQ(1-13)-NH_2, with replicates, at a range of induction levels in the same plate. Desensitisation experiments used a single ligand (N/OFQ) for pre-treatment at each induction concentration and therefore used suspended cells. Whilst there was some variation between the actual values measured for the two ligands using the different methods, at 10μM induction the intrinsic activity of [F/G](1-13)-NH_2 (relative to N/OFQ(1-13)-NH_2) was 0.97. This compares favourably with the equivalent value from the stable expression system of 0.95.

Studies *in vivo* show that N/OFQ exhibits a variety of effects, dependent upon route and area of administration. When applied to the CNS, the effects of nociceptin are generally to enhance pain perception, whereas application to peripheral sites appears to give pain relief (Hara *et al.*, 1997; Tian *et al.*, 1997; Xu *et al.*, 1996). These are effects that may be sensitive to receptor expression level. Additionally, receptor numbers and receptor reserve can have a significant effect upon activity of a ligand.

One theory proposes that these effects may depend upon the level of receptors presented at the cell surface (Berger *et al.*, 1999). This is of particular interest in the case of partial agonists such as F/G, where high levels of receptor expression evoke full agonist behaviour, lower levels showing only partial or no activity (antagonism).

6.8 Concluding Statement

This thesis has made a significant contribution to the N/OFQ-NOP field in that:

- Several novel molecules have been characterised and are now becoming available to other researchers in this field;
- A system in which pharmacological behaviour (agonist, partial agonist and desensitisation) can be defined accurately, namely the ecdysone-inducible system, has been characterised;
- The first example of genomic desensitisation of NOP has been described.

The N/OFQ-NOP system is now leaving the pre-clinical laboratory and full evaluation of clinical potential is eagerly awaited.

7 Appendices

7.1 Amino-acids and their Abbreviations

A = Ala, alanine

C = Cys, cysteine

D = Asp, aspartate

E = Glu, glutamate

F = Phe, phenylalanine

G = Gly, glycine

H = Hist, histidine

I = Ile, isoleucine

K = Lys, lysine

L = Leu, leucine

M = Met, methionine

N = Asn, asparagine

P = Pro, proline

Q = Gln, glutamine

R = Arg, arginine

S = Ser, serine

T = Thr, threonine

V = Val, valine

W = Trp, tryptophan

Y = Tyr, tyrosine

7.2 Modification of Protein Assay, after Lowry *(Lowry et al., 1951).*

Standards (0, 50, 100, 150, 200 and 250 $\mu g.ml^{-1}$ BSA in 0.1M NaOH) were used with samples simultaneously.

Samples were diluted as appropriate (1/5, 1/10, 1/20) in 0.1M NaOH.

To 0.5ml standard or diluted sample, 2.5ml reducing solution was added, the whole mixed and incubated (10min, room temperature).

250µl Folin and Ciocalteu's phenol reagent was added, the whole mixed and incubated (30min, room temperature).

Absorbance was read in a spectrophotometer at 750nm and the results analysed using linear regression to produce standard curve with fixed origin. Valid results for each sample were averaged and used to analyse the binding results.

A typical standard curve for this assay is shown in Figure 7.1.

Reducing solution comprised 100:1:1 solutions A:B:C (A – 2% Na_2CO_3 in 0.1M NaOH; B – 1% $CuSO_4$ in H_2O; C – 2% Na/K tartrate in H_2O).

Folin and Ciocalteu's phenol reagent (stock diluted 1:3 in H_2O).

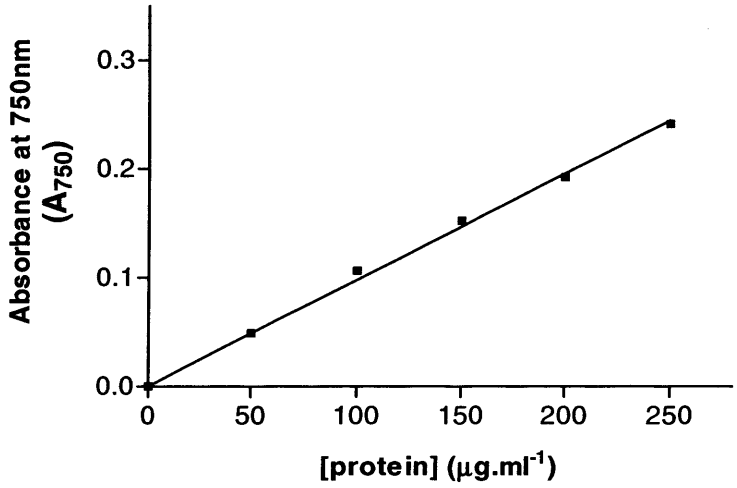

Figure 7.1 Sample standard curve for protein assay by Lowry method.

7.3 Primer Design – NOP1

```
LEFT PRIMER  - atgtggcaagcgttacttcctgtg
RIGHT PRIMER - gccagtgagcaggtgtttattaggg
SEQUENCE SIZE: 3208, PRODUCT SIZE: 93.

    1 gtcgaggtgctcatagtggagccctggctcccgggcggacggagccgcacggtagtagat
      X------------------------------------------------------------
   61 gggggtgtggccgtggcccccgactctgctcggcggggccgttcctgctttgccatccgt
      ------------------------------------------------------------
  121 gtgggacttccacgacagtggaggcacgagagctgggccccatatgctgcttgcccagct
      ------------------------------------------------------------
  181 tgggaaagaggaggctgctgcaaaggaccgatcggcgggtaccgtacagagtggatttgc
      ------------------------------------------------------------
  241 agggcagtggcatggagcccctcttccccgcgccgttctgggaggttatctacggcagcc
      ------------M-----------------------------------------------
  301 accttcagggcaacctgtccctcctgagccccaaccacagtctgctgcccccgcatctgc
      ------------------------------------------------------------
  361 tgctcaatgccagccacggcgccttcctgcccctcgggctcaaggtcaccatcgtggggc
      ------------------------------------------------------------
  421 tctacctggccgtgtgtgtcggagggctcctggggaactgccttgtcatgtacgtcatcc
      ------------------------------------------------------------
  481 tcaggcacaccaaaatgaagacagccaccaatatttacatctttaacctggccctggccg
      ------------------------------------------------------------
  541 acactctggtcctgctgacgctgcccttccagggcacggacatcctcctgggcttctggc
      ------------------------------------------------------------
  601 cgtttgggaatgcgctgtgcaagacagtcattgccattgactactacaacatgttcacca
      ------------------------------------------------------------
  661 gcaccttcaccctaactgccatgagtgtggatcgctatgtagccatctgccaccccatcc
      ------------------------------------------------------------
  721 gtgccctcgacgtccgcacgtccagcaaagcccaggctgtcaatgtggccatctgggccc
      ------------------------------------------------------------
  781 tggcctctgttgtcggtgttcccgttgccatcatgggctcggcacaggtcgaggatgaag
      ------------------------------------------------------------
  841 agatcgagtgcctggtggagatccctacccctcaggattactggggcccggtgtttgcca
      ------------------------------------------------------------
  901 tctgcatcttcctcttctccttcatcgtccccgtgctcgtcatctctgtctgctacagcc
      ------------------------------------------------------------
  961 tcatgatccggcggctccgtggagtccgcctgctctcgggctcccgagagaaggaccgga
      ------------------------------------------------------------X
 1021 acctgcggcgcatcactcggctggtgctggtggtagtggctgtgttcgtgggctgctgga

 1081 cgcctgtccaggtcttcgtgctggcccaagggctgggggttcagccgagcagcgagactg

 1141 ccgtggccattctgcgcttctgcacggccctgggctacgtcaacagctgcctcaacccca

 1201 tcctctacgccttcctggatgagaacttcaaggcctgcttccgcaagttctgctgtgcat

 1261 ctgccctgcgccgggacgtgcaggtgtctgaccgcgtgcgcagcattgccaaggacgtgg

 1321 ccctggcctgcaagacctctgagacggtaccgcggcccgcatgactaggcgtggacctgc

 1381 ccatggtgcctgtcagcccgcagagcccatctacgcccaacacagagctcacacaggtca

 1441 ctgctctctaggcggacacaccctgggccctgagcatccagagcctgggatgggcttttc

 1501 cctgtgggccagggatgctcggtcccagaggaggacctagtgacatcatgggacaggtca

 1561 aagcattagggccacctccatggccccagacagactaaagctgccctcctggtgcagggc

 1621 cgaggggacacaaggacctacctggaagcagctgacatgctggtggacggccgtgactgg
```

```
 1681 agcccgtgcccctccctccccgtgcttcatgtgactcttggcctctctgctgctgcgttg

 1741 gcagaaccctgggtgggcaggcacccggaggaggagcagctgtgtcatcctgtgccc

 1801 cccatgtgctgtgtgctgtttgcatggcagggctccagctgccttcagccctgtgacgtc

 1861 tcctcagggcagctggacaggcttggcactgcccgggaagtgcagcaggcagcttttctt

 1921 tggggtgggacttgccctgagcttggagctgccacctggaggacttgcctgttccgactc

 1981 cacctgtgcagccggggccaccccaggagaaagtgtccaggtgggggctggcagtccctg

 2041 gctgcagaccccgagctggccctgggccagccgcacctctgaaggttttctgtgtgctgc

 2101 acggtgcaggcctcatccctgactgcagcttgactctgggcccaacccccatttcccttc

 2161 aggagaccagcgagaggccctggcccattccctccagcggtgcaatgaactatcatgctg
      X----------------------------------------------------------
 2221 tggaccgtcaacccagccctgcttctcagtgtggggcaggtgtctcaggacgaaggcgcc
      ----------------------------------------------------------
 2281 gcgtgaccacatgggcagctctgttcacaaagtggaggcctcgttttcctggtcttgact
      ----------------------------------------------------------
 2341 gctctgtttgggtgggagaagattctctgggggtccccacatcctcccaaggctcccctc
      ----------------------------------------------------------
 2401 acagcctctcctttgcttgaagccagaggtcagtggccgtgctgtgttgcgggggaagct
      ----------------------------------------------------------
 2461 gtgtggaaggagaagctggtggccacagcagagtcctgctctggggacgcctgcttcatt
      ----------------------------------------------------------
 2521 tacaagcctcaagatggctctgtgtagggcctgagcttgctgcccaacgggaggatggct
      ----------------------------------------------------------
 2581 tcacagcagagccagcatgaggggtggggcctggcagggcttgcttgagccaaactgcaa
      ----------------------------------------------------------
 2641 aggctgtggtggctgtgaggacactgcgggggttgggggggggcgtctgtacctcaggg
      ----------------------------------------------------------
 2701 gatgccccgctgtggtcacccagagaatcacccttcctggtctacagatggaagctgcag
      ----------------------------------------------------------
 2761 gttggtgactttgcaaatgcacttcctacagatgaactattaaaagacctgcaacattga
      ----------------------------------------------------------
 2821 aaaaactcatttttccaccaaaaccttggccaggtaacctaccttaggcacctgcaaag
      X
 2881 aacaggaagtgatggctgtctcgcaacagagcctgggctgctcctcctgctctggggagt

 2941 ctaggccgtggggactgttctggggaggctcatgctgtctccatgacgtctgtggcagga

 3001 gtccctgaggacgggagctgcctagctacagttttcttgccaaggcgaggtgttttgtga

 3061 atctgtgctgatgtaatgtgcaccttcacgtatttatgcatgtggcaagcgttacttcct
                                              >>>>>>>>>>>>>>>>>>>>

 3121 gtgcacgtagccagccctgggtctgtctctggggtaatgaaaaaggaccctaataaacac
      >>>                                              <<<<<<<<<<<<

 3181 ctgctcactggctgggtattcttcgtaa
      <<<<<<<<<<<<

KEYS (in order of precedence):
X----X excluded region; >>>>>> left primer; <<<<<< right primer
```

7.4 Primer Design – NOP2/3

```
LEFT PRIMER  - acaggtcgaggatgaagagatcgag
RIGHT PRIMER - gaagaggaagatgcagatggcaaac
SEQUENCE SIZE: 1113; PRODUCT SIZE: 94.

    1 atggagcccctcttccccgcgccgttctgggaggttatctacggcagccaccttcagggc
       M
   61 aacctgtccctcctgagccccaaccacagtctgctgcccccgcatctgctgctcaatgcc

  121 agccacggcgccttcctgcccctcgggctcaaggtcaccatcgtggggctctacctggcc

  181 gtgtgtgtcggagggctcctggggaactgccttgtcatgtacgtcatcctcaggcacacc

  241 aaaatgaagacagccaccaatatttacatctttaacctggccctggccgacactctggtc

  301 ctgctgacgctgcccttccagggcacggacatcctcctgggcttctggccgtttgggaat

  361 gcgctgtgcaagacagtcattgccattgactactacaacatgttcaccagcaccttcacc

  421 ctaactgccatgagtgtggatcgctatgtagccatctgccaccccatccgtgccctcgac

  481 gtccgcacgtccagcaaagcccaggctgtcaatgtggccatctgggccctggcctctgtt

  541 gtcggtgttcccgttgccatcatgggctcggcacaggtcgaggatgaagagatcgagtgc
                                     >>>>>>>>>>>>>>>>>>>>>>>>
  601 ctggtggagatccctacccctcaggattactggggcccggtgtttgccatctgcatcttc
                                                  <<<<<<<<<<<<<<<<<<
  661 ctcttctccttcatcgtccccgtgctcgtcatctctgtctgctacagcctcatgatccgg
      <<<<<<
  721 cggctccgtggagtccgcctgctctcgggctcccgagagaaggaccggaacctgcggcgc

  781 atcactcggctggtgctggtggtagtggctgtgttcgtgggctgctggacgcctgtccag

  841 gtcttcgtgctggccaagggctgggggttcagccgagcagcgagactgccgtggccatt

  901 ctgcgcttctgcacggccctgggctacgtcaacagctgcctcaaccccatcctctacgcc

  961 ttcctggatgagaacttcaaggcctgcttccgcaagttctgctgtgcatctgccctgcgc

 1021 cgggacgtgcaggtgtctgaccgcgtgcgcagcattgccaaggacgtggccctggcctgc

 1081 aagacctctgagacggtaccgcggcccgcatga

KEYS (in order of precedence):
>>>>>> left primer; <<<<<< right primer
```

7.5 Primer Design – Chinese Hamster GAPDH

```
DEFINITION  Cricetus cricetus mRNA for glyceraldehyde-3-
phosphate dehydrogenase
Source sequence:X52123. 1266 bp mRNA    linear   ROD 12-SEP-1993
translation="MVKVGVNGFGRIGRLVTRAAFTSGKVEVVAINDPFIDLNYMVYMFQYDSTHGKFKGT
VKAENGKLVINGKAITIFQERDPANIKWGDAGAEYVVESTGVFTTMEKAGAHLKGGAKRVIISAPSADAP
MFVMGVNQDKYDNSLKIVSNASCTTNCLAPLAKVIHDNFGIVEGLMTTVHAITATQKTVDGPSGKLWRDG
RGAAQNIIPASTGAAKAVGKVIPELNGKLTGMAFRVPTPNVSVVDLTCRLEKPAKYEDIKKVVKQASEGP
LKGILGYTEDQVVSCDFNSDSHSSTFDAGAGIALNDNFVKLISWYDNEFGYSNRVVDLMAYMASKE"
PRIMER 3 OUTPUT:
LEFT PRIMER  - gactcccactcttccacctttgatg
RIGHT PRIMER - accactctgttgctgtagccaaattc
PRODUCT SIZE: 110

1  ggctctctgctcctccctgttctagagacagccgcatctttccgtgcagtgccagcctcg
61 ctccggagacgcaatggtgaaggtcggcgtgaacggatttggccgtattggacgcctggt
121 taccagggctgccttcacttctggcaaagtggaagttgttgccatcaatgacccttcat
181 tgacctcaactacatggtctacatgttccagtatgactctacccatggcaagttcaaagg
241 cacagtcaaggctgagaatggaaagcttgtcatcaacgggaaggccatcaccatcttcca
301 ggagcgagatcccgccaacatcaaatggggtgatgctggcgccgagtatgttgtggaatc

361 tactggcgtcttcaccaccatggagaaggctggggcccacttgaagggcggggccaagag

421 ggtcatcatctccgccccttctgctgatgcccccatgtttgtgatgggtgtgaaccaaga

481 caagtatgacaactccctcaagattgtcagcaatgcgtcctgcaccaccaactgcttagc

541 ccccctggccaaggtcatccatgacaactttggcattgtggaaggactcatgaccacggt

601 ccatgccatcactgccacccagaagactgtggatggcccctccggaaagctgtggcgtga

661 tggccgtggggctgcccagaacatcatccctgcatccactggcgctgccaaggctgtggg

721 caaagtcatcccagagctgaacgggaagctgactggcatggccttccgtgttcctacccc

781 caacgtgtccgttgtggatctgacatgtcgcctggagaaacctgccaagtatgaggacat

841 caagaaggtggtgaagcaggcatctgagggcccactgaagggcatcctgggctacaccga
      XXXXXXXXXX
901 ggaccaggttgtctcctgcgacttcaacagtgactcccactcttccacctttgatgctgg
                                    >>>>>>>>>>>>>>>>>>>>>>>>
961 ggctggcattgctctcaatgacaactttgtaaagctcatttcctggtatgacaatgaatt
                                                          <<<<<
1021 tggctacagcaacagagtggtggacctcatggcctacatggcctccaaggagtaagaagc
      <<<<<<<<<<<<<<<<<<<
1081 ccaccctggaccatccaccccagcaaggactcgagcaagagggaggccctggctgctgag

1141 cagtccctgtccaataacccccacaccgatcatctccctcacagtttccatcccagaccc

1201 ccagaataaggaggggcttagggagccctactctcttgaataccatcaataaagttcact

1261 gcaccc

KEYS (in order of precedence):
XXXXXX excluded region; >>>>>> left primer; <<<<<< right primer
```

7.6 Procedure for RNA Integrity Analysis

Materials and Equipment

RNA 6000 Nano Assay Kit:

RNA 6000 Dye concentrate (blue top); RNA 6000 Nano Marker (green top); RNA 6000 Nano Gel Matrix (red top); Spin Filters; 1ml Disposable Syringe.

RNA 6000 Nano Chip; Electrode Cleaners; Chip Priming Station – Agilent Technologies

Rnase-free Water

RNA Ladder – Invitrogen

'Rnase Zap' – Ambion

Sample Preparation

Remove RNA 6000 Nano assay kit from storage (4°C) and allow to equilibrate for 30min, protected from light.

RNA samples should be <500ng.ml^{-1} and kept on ice when not in storage (-80°C).

Equipment Preparation

Set chip selector in Bioanalyzer to position 1

Fill electrode cleaners:

350µl 'RNase Zap' in that labelled 'RNase Zap'

350µl RNase-free water in that labelled 'RNase-free water'

Load 'RNase Zap' electrode cleaner into Bioanalyzer, close lid and leave for 1min.

Exchange for 'RNase-free water' electrode cleaner, close lid and leave for 10s.

Open lid and allow 10s for water to evaporate from electrodes.

Remove electrode cleaner from machine and empty both electrode cleaners before storage.

Chip Preparation

NB - The following steps, up until loading the chip into the Bioanalyzer, must be performed protected from direct light.

Prepare 550µl gel matrix by spin filtration (1500xg, 10min, 4°C) using a spin filter from the kit.

Transfer 65µl into a clean RNase-free tube and add 1µl dye concentrate and mix.

Place RNA 6000 Nano Chip into chip priming station (base plate in position C, syringe clip set at top notch).

With syringe set at 1ml, pipette 9µl gel-dye mix into chip well marked '**G**', close priming station and press syringe plunger until held by clip.

After 30s, release plunger and return to 1ml position.

Open priming station and pipette 9µl gel-dye mix into each of the two wells marked 'G'.

Pipette 5µl Nano Marker each into the well marked with a ladder symbol and 12 sample wells (6µl into sample wells not to receive sample).

Heat denature (70°C, 2min) sample aliquots, at appropriate working concentration, plus 1µl RNA Ladder solution for each Nano Chip to be used.

Pipette 1µl denatured ladder solution into ladder well and 1µl of each sample into corresponding sample well.

Vortex chip (2400rpm, 1min, IKA vortexer) and load into Bioanalyser.

NB - Prepared chips must be analysed within 5min of sample loading.

Running Procedure

With Agilent 2100 Bio Sizing software loaded, select assay type ('Eukaryote Total RNA Nano' for this work), name file and press 'Start' to commence run.

After a run is completed, approximately 20min, remove chip immediately and either load the next for analysis or carry out cleaning procedure.

Cleaning Procedure

After final chip has been analysed, fill electrode cleaner labelled 'RNase-free water' with 350µl RNase-free water, load into Bioanalyzer, close lid and leave for 10s.

Open lid and allow 10s for water to evaporate from electrodes.

Remove electrode cleaner from machine and empty before storage.

Analysis of Results

Results are presented as an elution profile electropherogram and may also be shown pictorially as for a conventional electrophoretic gel.

7.7 Publications arising from this thesis.

7.7.1 Full Papers

1. McDonald J, **Barnes TA**, Calo' G, Guerrini R, Rowbotham DJ and Lambert DG (2002) Effects of [(pF)Phe^4]Nociceptin/orphanin FQ(1-13)NH_2 on GTPγ^{35}S binding and cAMP formation in Chinese hamster ovary cells expressing the human nociceptin/orphanin FQ receptor. Eur. J. Pharmacol. 443:7-12.
2. Marti M, Stocchi S, Paganini F, Mela F, De Risi C, Calo' G, Guerrini R, **Barnes TA**, Lambert DG, Beani L, Bianchi C and Morari M. (2003) Pharmacological profiles of presynaptic nociceptin/orphanin FQ receptors modulating 5-hydroxytryptamine and noradrenaline release in the rat neocortex. Brit. J. Pharmacol. 138:91-98.
3. Wright KE, McDonald J, **Barnes TA**, Rowbotham DJ, Guerrini R, Calo' G and Lambert DG. (2003) Assessment of the activity of a novel nociceptin/orphanin FQ analogue at recombinant human nociceptin/orphanin FQ receptors expressed in Chinese hamster ovary cells. Neuroscience Letters 346:145-148.
4. McDonald J, **Barnes TA**, Okawa H, Williams J, Calo'G, Rowbotham DJ and Lambert DG (2003) Partial agonist behaviour depends upon the level of nociceptin/orphanin FQ receptor expression. Studies using the ecdysone inducible mammalian expression system. Brit. J. Pharmacol. 140:61-70.
5. Kitayama M, **Barnes TA**, Carra G, McDonald J, Calo' G, Guerrini R, Rowbotham DJ, Smith G and Lambert DG (2003) Pharmacological Profile of the Cyclic Nociceptin/Orphanin FQ Analogues c[Cys^{10,14}]N/OFQ(1-14)NH_2 and c[Nphe^1,Cys^{10,14}]N/OFQ(1-14)NH_2. Naunyn-Schmiedebergs Arch. Pharmacol. 368:528-537.
6. Carra' G, Rizzi A, Guerrini R, **Barnes TA**, Mc Donald J, Hebbes CP, Mela F, Kenigs VA, Marzola G, Rizzi D, Gavioli E, Zucchini S, Regoli D, Morari M, Salvadori S, Rowbotham DJ, Lambert DG, Kapusta DR and Calo G (2005) [(pF)Phe4,Arg14,Lys15]N/OFQ-NH2 (UFP-102), a highly potent and selective agonist of the nociceptin/orphanin FQ receptor. J Pharmacol Exp Ther. 2004 Oct 27; [Epub ahead of print]
7. Guerrini R, Calo' G, Lambert DG, Carra' G, Arduin M, **Barnes TA**, McDonald J, Rizzi D, Trapella C, Marzola E, Rowbotham DJ, Regoli D, and Salvatori S (2005) N- and C-Terminal Modifications of Nociceptin / Orphanin FQ Generate Highly Potent NOP Receptor Ligands. J. Med. Chem (in press).
8. **Barnes TA**, Rowbotham DJ and Lambert DG. Nociceptin receptor desensitisation. Studies using the ecdysone inducible mammalian expression system. Manuscript in preparation for Molecular Pharmacology.

7.7.2 Reviews and Editorials

Barnes TA and Lambert DG (2004) Nociceptin/orphanin FQ peptide-receptor system: are we any nearer the clinic? Br. J. Anaesthesia. 93:626-628.

7.7.3 Abstracts

British Pharmacological Society.

Imperial College, University of London, London, Dec 2001:

- McDonald J, **Barnes TA**, Guerrini R, Calo G, Rowbotham DJ and Lambert DG. (2002). *In vitro* characterisation of [(pF)Phe^4]nociceptin(1-13)NH_2 a novel agonist for the NOP receptor. Brit. J. Pharmacol. 135:258P.

Brighton, Hosted by William Harvey Research Institute, Jan 2003:

- McDonald J, **Barnes TA**, Williams J, Calo G, Rowbotham DJ and Lambert DG (2003) Studies of [Phe$^1\Psi(CH_2\text{-}NH)$Gly^2]N/OFQ(1-13)NH_2 at the recombinant human nociceptin receptor using the ecdysone inducible expression system. Brit. J. Pharmacol. 138:26P.
- Kitayama M, **Barnes TA**, McDonald J, Calo G, Guerrini R, Smith G, Rowbotham DJ and Lambert DG (2003) Pharmacological profile of the cyclic nociceptin/orphanin FQ analogues c[Cys^{10,14}]N/OFQ(1-14)NH_2 and c[Nphe^1,Cys^{10,14}]N/OFQ(1-14)NH_2. Brit. J. Pharmacol. 138:223P.

Guy's Hospital, Hosted by Kings College, University of London, London, Dec 2003:

- **Barnes TA**, Rowbotham DJ and Lambert DG (2004) Studies on the desensitisation of the human nociceptin receptor (NOP). use of the ecdysone inducible expression system. Brit. J. Pharmacol. 141:121P.
- Carra G, McDonald J, Rizzi D, **Barnes TA**, Zucchini S, Guerrini R, Lambert DG and Calo G (2004) *In vitro* characterisation of a novel, highly potent nociceptin/orphanin FQ receptor agonist Brit. J. Pharmacol. 141:117P.

7.7.4 Presentations

Leicester-Ferrara collaboration meetings:

- **Barnes TA**. UFP-101, the story so far. Ferrara (2004)
- **Barnes TA**. Desensitisation of NOP-Genomic effects. Leicester (2005)

8 Bibliography

ALBERTS, B., BRAY, D., LEWIS, J., RAFF, M., ROBERTS, K. & WATSON J.D. (1994, 3rd ed.). *Molecular Biology of the Cell*. New York: Garland Publishing.

ALBRECHT, E., SAMOVILOVA, N.N., OSWALD, S., BAEGER, I. & BERGER, H. (1998). Nociceptin (orphanin FQ): high-affinity and high-capacity binding site coupled to low-potency stimulation of guanylyl-5'-O-(gamma-thio)-triphosphate binding in rat brain membranes. *J Pharmacol Exp Ther*, **286,** 896-902.

AMBO, A., HAMAZAKI, N., YAMADA, Y., NAKATA, E. & SASAKI, Y. (2001). Structure-activity studies on nociceptin analogues: ORL1 receptor binding and biological activity of cyclic disulfide-containing analogues of nociceptin peptides. *J Med Chem*, **44,** 4015-8.

ANDERBERG, U.M., LIU, Z., BERGLUND, L. & NYBERG, F. (1998). Plasma levels on nociceptin in female fibromyalgia syndrome patients. *Z Rheumatol*, **57 Suppl 2,** 77-80.

ATTRAMADAL, H., ARRIZA, J.L., AOKI, C., DAWSON, T.M., CODINA, J., KWATRA, M.M., SNYDER, S.H., CARON, M.G. & LEFKOWITZ, R.J. (1992). Beta-arrestin2, a novel member of the arrestin/beta-arrestin gene family. *J Biol Chem*, **267,** 17882-90.

BEAR, M.F., CONNORS, B.W. & PARADISO, M.A. (2001). *Neuroscience: exploring the brain*. Philadelphia: Lippincott Williams & Wilkins.

BECKER, J.A., WALLACE, A., GARZON, A., INGALLINELLA, P., BIANCHI, E., CORTESE, R., SIMONIN, F., KIEFFER, B.L. & PESSI, A. (1999). Ligands for kappa-opioid and ORL1 receptors identified from a conformationally constrained peptide combinatorial library. *J Biol Chem*, **274,** 27513-22.

BENOVIC, J.L. & GOMEZ, J. (1993). Molecular cloning and expression of GRK6. A new member of the G protein-coupled receptor kinase family. *J Biol Chem*, **268,** 19521-7.

BENOVIC, J.L., MAYOR, F., JR., STANISZEWSKI, C., LEFKOWITZ, R.J. & CARON, M.G. (1987). Purification and characterization of the beta-adrenergic receptor kinase. *J Biol Chem*, **262,** 9026-32.

BENOVIC, J.L., ONORATO, J.J., ARRIZA, J.L., STONE, W.C., LOHSE, M., JENKINS, N.A., GILBERT, D.J., COPELAND, N.G., CARON, M.G. & LEFKOWITZ, R.J. (1991). Cloning, expression, and chromosomal localization of beta-adrenergic receptor kinase 2. A new member of the receptor kinase family. *J Biol Chem*, **266,** 14939-46.

BERG, K.A., MAAYANI, S., GOLDFARB, J., SCARAMELLINI, C., LEFF, P. & CLARKE, W.P. (1998). Effector pathway-dependent relative efficacy at serotonin type 2A and 2C receptors: evidence for agonist-directed trafficking of receptor stimulus. *Mol Pharmacol*, **54,** 94-104.

BERGER, H., ALBRECHT, E., WALLUKAT, G. & BIENERT, M. (1999). Antagonism by acetyl-RYYRIK-NH2 of G protein activation in rat brain preparations and of chronotropic effect on rat cardiomyocytes evoked by nociceptin/orphanin FQ. *Br J Pharmacol*, **126,** 555-8.

BERGER, H., BIGONI, R., ALBRECHT, E., RICHTER, R.M., KRAUSE, E., BIENERT, M. & CALO, G. (2000a). The nociceptin/orphanin FQ receptor ligand acetyl-RYYRIK-amide exhibits antagonistic and agonistic properties. *Peptides*, **21,** 1131-9.

BERGER, H., CALO, G., ALBRECHT, E., GUERRINI, R. & BIENERT, M. (2000b). [Nphe^1]NC(1-13)NH_2 selectively antagonizes nociceptin/orphanin FQ-stimulated G-protein activation in rat brain. *J Pharmacol Exp Ther*, **294,** 428-33.

BIGONI, R., CALO, G., RIZZI, A., OKAWA, H., REGOLI, D., SMART, D. & LAMBERT, D.G. (2002). Effects of naloxone benzoylhydrazone on native and recombinant nociceptin/orphanin FQ receptors. *Can J Physiol Pharmacol*, **80,** 407-12.

BILECKI, W. & PRZEWLOCKI, R. (2000). Effect of opioids on Ca2+/cAMP responsive element binding protein. *Acta Neurobiol Exp (Wars)*, **60,** 557-67.

BIRNBAUMER, L. (1990). G proteins in signal transduction. *Annu Rev Pharmacol Toxicol*, **30,** 675-705.

BOBROVA, I., VLASKOVSKA, M., KASAKOV, L., SUROVOY, A., EGOROVA, N., JOHANSSON, L., KARSNAS, P. & TERENIUS, L. (2003). A structure-activity study of nociceptin-(1-13)-peptide amide. Synthesis of analogues substituted in positions 0, 1, 3, 4 and 10. *Eur J Med Chem*, **38,** 687-94.

BROOKS, H., ELTON, C.D., SMART, D., ROWBOTHAM, D.J., MCKNIGHT, A.T. & LAMBERT, D.G. (1998). Identification of nociceptin in human cerebrospinal fluid: comparison of levels in pain and non-pain states. *Pain*, **78,** 71-3.

BUNZOW, J.R., SAEZ, C., MORTRUD, M., BOUVIER, C., WILLIAMS, J.T., LOW, M. & GRANDY, D.K. (1994). Molecular cloning and tissue distribution of a putative member of the rat opioid receptor gene family that is not a mu, delta or kappa opioid receptor type. *FEBS Lett*, **347,** 284-8.

BUSTIN, S.A. (2000). Absolute quantification of mRNA using real-time reverse transcription polymerase chain reaction assays. *J Mol Endocrinol*, **25,** 169-93.

BUSTIN, S.A. & NOLAN, T. (2004). Pitfalls of quantitative real-time reverse-transcription polymerase chain reaction. *J Biomol Tech*, **15,** 155-66.

BUTOUR, J.L., MOISAND, C., MAZARGUIL, H., MOLLEREAU, C. & MEUNIER, J.C. (1997). Recognition and activation of the opioid receptor-like ORL 1 receptor by nociceptin, nociceptin analogs and opioids. *Eur J Pharmacol*, **321,** 97-103.

BUZAS, B., ROSENBERGER, J., KIM, K.W. & COX, B.M. (2002). Inflammatory mediators increase the expression of nociceptin/orphanin FQ in rat astrocytes in culture. *Glia*, **39,** 237-46.

BYLUND, D.B. & TOEWS, M.L. (1993). Radioligand binding methods: practical guide and tips. *Am J Physiol*, **265,** L421-9.

CALO, G., BIGONI, R., RIZZI, A., GUERRINI, R., SALVADORI, S. & REGOLI, D. (2000a). Nociceptin/orphanin FQ receptor ligands. *Peptides*, **21,** 935-47.

CALO, G., GUERRINI, R., BIGONI, R., RIZZI, A., BIANCHI, C., REGOLI, D. & SALVADORI, S. (1998). Structure-activity study of the nociceptin(1-13)NH_2 N-terminal tetrapeptide and discovery of a nociceptin receptor antagonist. *J Med Chem*, **41,** 3360-6.

CALO, G., GUERRINI, R., BIGONI, R., RIZZI, A., MARZOLA, G., OKAWA, H., BIANCHI, C., LAMBERT, D.G., SALVADORI, S. & REGOLI, D. (2000b). Characterization of [Nphe^1]nociceptin(1-13)NH_2, a new selective nociceptin receptor antagonist. *Br J Pharmacol*, **129,** 1183-93.

CALO, G., GUERRINI, R., RIZZI, A., SALVADORI, S. & REGOLI, D. (2000c). Pharmacology of nociceptin and its receptor: a novel therapeutic target. *Br J Pharmacol*, **129,** 1261-83.

CALO, G., RIZZI, A., BODIN, M., NEUGEBAUER, W., SALVADORI, S., GUERRINI, R., BIANCHI, C. & REGOLI, D. (1997). Pharmacological characterization of nociceptin receptor: an in vitro study. *Can J Physiol Pharmacol*, **75,** 713-8.

CALO, G., RIZZI, A., BOGONI, G., NEUGEBAUER, V., SALVADORI, S., GUERRINI, R., BIANCHI, C. & REGOLI, D. (1996). The mouse vas deferens: a pharmacological preparation sensitive to nociceptin. *Eur J Pharmacol*, **311,** R3-5.

CALO, G., RIZZI, A., RIZZI, D., BIGONI, R., GUERRINI, R., MARZOLA, G., MARTI, M., MCDONALD, J., MORARI, M., LAMBERT, D.G., SALVADORI, S. & REGOLI, D. (2002). [Nphe^{1},Arg^{14},Lys^{15}]Nociceptin-NH_2, a novel potent and selective antagonist of the nociceptin/orphanin FQ receptor. *Br J Pharmacol*, **136,** 303-311.

CAMARDA, V., RIZZI, A., CALO, G., WIRTH, K. & REGOLI, D. (2002). Pharmacological characterisation of novel kinin B2 receptor ligands. *Can J Physiol Pharmacol*, **80,** 281-6.

CHEN, J., SIMON, M.I., MATTHES, M.T., YASUMURA, D. & LAVAIL, M.M. (1999). Increased susceptibility to light damage in an arrestin knockout mouse model of Oguchi disease (stationary night blindness). *Invest Ophthalmol Vis Sci*, **40,** 2978-82.

CHEN, Y., FAN, Y., LIU, J., MESTEK, A., TIAN, M., KOZAK, C.A. & YU, L. (1994). Molecular cloning, tissue distribution and chromosomal localization of a novel member of the opioid receptor gene family. *FEBS Lett*, **347,** 279-83.

CHENG, Y. & PRUSOFF, W.H. (1973). Relationship between the inhibition constant (K_i) and the concentration of inhibitor which causes 50 per cent inhibition (IC_{50}) of an enzymatic reaction. *Biochem Pharmacol*, **22,** 3099-108.

CHENG, Z.J., FAN, G.H., ZHAO, J., ZHANG, Z., WU, Y.L., JIANG, L.Z., ZHU, Y., PEI, G. & MA, L. (1997). Endogenous opioid receptor-like receptor in human neuroblastoma SK-N-SH cells: activation of inhibitory G protein and homologous desensitization. *Neuroreport*, **8,** 1913-8.

CHIOU, L.C. & FAN, S.H. (2002). CompB (J-113397), selectively and competitively antagonizes nociceptin activation of inwardly rectifying K+ channels in rat periaqueductal gray slices. *Neuropharmacology*, **42,** 987-92.

CHOMCZYNSKI, P. (1993). A reagent for the single-step simultaneous isolation of RNA, DNA and proteins from cell and tissue samples. *Biotechniques*, **15,** 532-4, 536-7.

CIVELLI, O., NOTHACKER, H.P. & REINSCHEID, R. (1998). Reverse physiology: discovery of the novel neuropeptide, orphanin FQ/nociceptin. *Crit Rev Neurobiol*, **12,** 163-76.

CLAPHAM, D.E. & NEER, E.J. (1997). G protein beta gamma subunits. *Annu Rev Pharmacol Toxicol*, **37,** 167-203.

COLE, S.L., SCHINDLER, M., SELLERS, L.A. & HUMPHREY, P.P. (2001). Titrating the expression of a Gi protein-coupled receptor using an ecdysone-inducible system in CHO-K1 cells. *Receptors Channels*, **7,** 289-302.

CONNOR, M. & HENDERSON, G. (1996a). delta- and mu-opioid receptor mobilization of intracellular calcium in SH-SY5Y human neuroblastoma cells. *Br J Pharmacol*, **117,** 333-40.

CONNOR, M., OSBORNE, P.B. & CHRISTIE, M.J. (2004). Tau-opioid receptor desensitization: Is morphine different? *Br J Pharmacol*, **143,** 685-96.

CONNOR, M., VAUGHAN, C.W., CHIENG, B. & CHRISTIE, M.J. (1996b). Nociceptin receptor coupling to a potassium conductance in rat locus coeruleus neurones in vitro. *Br J Pharmacol*, **119,** 1614-8.

CORBETT, A., MCKNIGHT, A. & HENDERSON, G. (2000). *Opioid Receptors*. Tocris Cookson Inc., Life Science Reviews.

CORDEAUX, Y., BRIDDON, S.J., MEGSON, A.E., MCDONNELL, J., DICKENSON, J.M. & HILL, S.J. (2000). Influence of receptor number on functional responses elicited by agonists acting at the human adenosine A_1 receptor: evidence for signaling

pathway-dependent changes in agonist potency and relative intrinsic activity. *Mol Pharmacol*, **58,** 1075-84.

COX, B.M., CHAVKIN, C., CHRISTIE, M.J., CIVELLI, O., EVANS, C., HAMON, M.D., HOELLT, V., KIEFFER, B., KITCHEN, I., MCKNIGHT, A.T., MEUNIER, J.C. & PORTOGHESE, P.S. (2000). Opioid receptors. In *The IUPHAR Compendium of Receptor Characterization.* ed Girdlestone, D. pp. 321-333. London: IUPHAR Media Ltd.

DARLAND, T. & GRANDY, D.K. (1998). The orphanin FQ system: an emerging target for the management of pain? *Br J Anaesth*, **81,** 29-37.

DAUTZENBERG, F.M., WICHMANN, J., HIGELIN, J., PY-LANG, G., KRATZEISEN, C., MALHERBE, P., KILPATRICK, G.J. & JENCK, F. (2001). Pharmacological characterization of the novel nonpeptide orphanin FQ/nociceptin receptor agonist Ro 64-6198: rapid and reversible desensitization of the ORL1 receptor in vitro and lack of tolerance in vivo. *J Pharmacol Exp Ther*, **298,** 812-9.

DESPOPOULOS, A. & SILBERNAGL, S. (1986). *Colour Atlas of Physiology.* New York: Thieme Inc,.

DHAWAN, B.N., CESSELIN, F., RAGHUBIR, R., REISINE, T., BRADLEY, P.B., PORTOGHESE, P.S. & HAMON, M. (1996). International Union of Pharmacology. XII. Classification of opioid receptors. *Pharmacol Rev*, **48,** 567-92.

DHEDA, K., HUGGETT, J.F., BUSTIN, S.A., JOHNSON, M.A., ROOK, G. & ZUMLA, A. (2004). Validation of housekeeping genes for normalizing RNA expression in real-time PCR. *Biotechniques*, **37,** 112-4, 116, 118-9.

DICKENSON, A.H. (2002). Gate control theory of pain stands the test of time. *Br J Anaesth*, **88,** 755-7.

DOOLEY, C.T. & HOUGHTEN, R.A. (2000). Orphanin FQ/nociceptin receptor binding studies. *Peptides*, **21,** 949-60.

DOOLEY, C.T. & HOUGHTEN, R.A. (1996). Orphanin FQ: receptor binding and analog structure activity relationships in rat brain. *Life Sci*, **59,** L23-9.

DOOLEY, C.T., SPAETH, C.G., BERZETEI-GURSKE, I.P., CRAYMER, K., ADAPA, I.D., BRANDT, S.R., HOUGHTEN, R.A. & TOLL, L. (1997). Binding and in vitro activities of peptides with high affinity for the nociceptin/orphanin FQ receptor, ORL1. *J Pharmacol Exp Ther*, **283,** 735-41.

EMONDS-ALT, X., VILAIN, P., GOULAOUIC, P., PROIETTO, V., VAN BROECK, D., ADVENIER, C., NALINE, E., NELIAT, G., LE FUR, G. & BRELIERE, J.C. (1992). A potent and selective non-peptide antagonist of the neurokinin A (NK2) receptor. *Life Sci*, **50,** PL101-6.

ERTSEY, C., HANTOS, M., BOZSIK, G. & TEKES, K. (2004). Circulating nociceptin levels during the cluster headache period. *Cephalalgia*, **24,** 280-3.

FERGUSON, S.S. (2001). Evolving concepts in G protein-coupled receptor endocytosis: the role in receptor desensitization and signaling. *Pharmacol Rev*, **53,** 1-24.

FUKUDA, K., KATO, S., MORI, K., NISHI, M., TAKESHIMA, H., IWABE, N., MIYATA, T., HOUTANI, T. & SUGIMOTO, T. (1994). cDNA cloning and regional distribution of a novel member of the opioid receptor family. *FEBS Lett*, **343,** 42-6.

GAGLIARDI, S., DONDIO, G. & GIARDINA, G.A. (2003). Morphinan derivatives--A review of the recent patent literature. *IDrugs*, **6,** 129-37.

GAINETDINOV, R.R., PREMONT, R.T., BOHN, L.M., LEFKOWITZ, R.J. & CARON, M.G. (2004). Desensitization of G protein-coupled receptors and neuronal functions. *Annu Rev Neurosci*, **27,** 107-44.

GOODMAN, O.B., JR., KRUPNICK, J.G., SANTINI, F., GUREVICH, V.V., PENN, R.B., GAGNON, A.W., KEEN, J.H. & BENOVIC, J.L. (1996). Beta-arrestin acts as a

clathrin adaptor in endocytosis of the beta2-adrenergic receptor. *Nature*, **383,** 447-50.

GRISEL, J.E., FARRIER, D.E., WILSON, S.G. & MOGIL, J.S. (1998). [Phe1psi(CH2-NH)Gly2]nociceptin-(1-13)-NH2 acts as an agonist of the orphanin FQ/nociceptin receptor in vivo. *Eur J Pharmacol*, **357,** R1-3.

GUERRINI, R., CALO, G., BIGONI, R., RIZZI, A., VARANI, K., TOTH, G., GESSI, S., HASHIBA, E., HASHIMOTO, Y., LAMBERT, D.G., BOREA, P.A., TOMATIS, R., SALVADORI, S. & REGOLI, D. (2000a). Further studies on nociceptin-related peptides: discovery of a new chemical template with antagonist activity on the nociceptin receptor. *J Med Chem*, **43,** 2805-13.

GUERRINI, R., CALO, G., BIGONI, R., RIZZI, D., REGOLI, D. & SALVADORI, S. (2001a). Structure-activity relationship of [Nphe^1]-NC-(1-13)-NH_2, a pure and selective nociceptin/orphanin FQ receptor antagonist. *J Pept Res*, **57,** 215-22.

GUERRINI, R., CALO, G., BIGONI, R., RIZZI, D., RIZZI, A., ZUCCHINI, M., VARANI, K., HASHIBA, E., LAMBERT, D.G., TOTH, G., BOREA, P.A., SALVADORI, S. & REGOLI, D. (2001b). Structure-activity studies of the Phe^4 residue of nociceptin(1-13)NH_2: identification of highly potent agonists of the nociceptin/orphanin FQ receptor. *J Med Chem*, **44,** 3956-64.

GUERRINI, R., CALO, G., RIZZI, A., BIANCHI, C., LAZARUS, L.H., SALVADORI, S., TEMUSSI, P.A. & REGOLI, D. (1997). Address and message sequences for the nociceptin receptor: a structure-activity study of nociceptin-(1-13)-peptide amide. *J Med Chem*, **40,** 1789-93.

GUERRINI, R., CALO, G., RIZZI, A., BIGONI, R., BIANCHI, C., SALVADORI, S. & REGOLI, D. (1998). A new selective antagonist of the nociceptin receptor. *Br J Pharmacol*, **123,** 163-5.

GUERRINI, R., CALO, G., RIZZI, A., BIGONI, R., RIZZI, D., REGOLI, D. & SALVADORI, S. (2000b). Structure-activity relationships of nociceptin and related peptides: comparison with dynorphin A. *Peptides*, **21,** 923-33.

GUERRINI, R., RIZZI, D., ZUCCHINI, M., TOMATIS, R., REGOLI, D., CALO, G. & SALVADORI, S. (2003). Nociceptin/Orphanin FQ(1-13)NH2 analogues modified in the Phe1-Gly2 peptide bond. *Bioorg Med Chem Lett*, **13,** 365-8.

HANTOS, M.B., SZALAY, F., LAKATOS, P.L., HEGEDUS, D., FIRNEISZ, G., REICZIGEL, J., TOROK, T. & TEKES, K. (2002). Elevated plasma nociceptin level in patients with Wilson disease. *Brain Res Bull*, **58,** 311-3.

HARA, N., MINAMI, T., OKUDA-ASHITAKA, E., SUGIMOTO, T., SAKAI, M., ONAKA, M., MORI, H., IMANISHI, T., SHINGU, K. & ITO, S. (1997). Characterization of nociceptin hyperalgesia and allodynia in conscious mice. *Br J Pharmacol*, **121,** 401-8.

HARRISON, C. & LAMBERT, D.G. (2000a). Opioid Pharmacology. In *Anaesthesia, Pain and Intensive Care Medicine*. ed Gullo, A. pp. 387-394: Springer.

HARRISON, C., ROWBOTHAM, D.J., GRANDY, D.K. & LAMBERT, D.G. (2000b). Endomorphin-1 induced desensitization and down-regulation of the recombinant mu-opioid receptor. *Br J Pharmacol*, **131,** 1220-6.

HARRISON, L.M. & GRANDY, D.K. (2000c). Opiate modulating properties of nociceptin/orphanin FQ. *Peptides*, **21,** 151-72.

HASHIBA, E., HARRISON, C., CALO, G., GUERRINI, R., ROWBOTHAM, D.J., SMITH, G. & LAMBERT, D.G. (2001). Characterisation and comparison of novel ligands for the nociceptin/orphanin FQ receptor. *Naunyn Schmiedebergs Arch Pharmacol*, **363,** 28-33.

HASHIBA, E., LAMBERT, D.G., FARKAS, J., TOTH, G. & SMITH, G. (2002). Comparison of the binding of [^{3}H]nociceptin/orphaninFQ(1-13)NH_2, [^{3}H]nociceptin/orphaninFQ(1-17)OH and [^{125}I]Tyr^{14}nociceptin/orphaninFQ(1-17)OH to recombinant human and native rat cerebrocortical nociceptin/orphanin FQ receptors. *Neurosci Lett*, **328,** 5-8.

HASHIMOTO, Y., CALO, G., GUERRINI, R., SMITH, G. & LAMBERT, D.G. (2000). Antagonistic effects of [Nphe1]nociceptin(1-13)NH2 on nociceptin receptor mediated inhibition of cAMP formation in Chinese hamster ovary cells stably expressing the recombinant human nociceptin receptor. *Neurosci Lett*, **278,** 109-12.

HASHIMOTO, Y., CALO, G., GUERRINI, R., SMITH, G. & LAMBERT, D.G. (2002). Effects of chronic nociceptin/orphanin FQ exposure on cAMP accumulation and receptor density in Chinese hamster ovary cells expressing human nociceptin/orphanin FQ receptors. *Eur J Pharmacol*, **449,** 17-22.

HAWES, B.E., GRAZIANO, M.P. & LAMBERT, D.G. (2000). Cellular actions of nociceptin: transduction mechanisms. *Peptides*, **21,** 961-7.

HEBBES, C. P., (2004). Identification and characterisation of small peptoid opioid receptor ligands. *Intercalated B.Sc. Dissertation*: University of Leicester.

HENDERSON, G. & MCKNIGHT, A.T. (1997). The orphan opioid receptor and its endogenous ligand-- nociceptin/orphanin FQ. *Trends Pharmacol Sci*, **18,** 293-300.

HORVATH, A., FOLHOFFER, A., LAKATOS, P.L., HALOSZ, J., ILLYES, G., SCHAFF, Z., HANTOS, M.B., TEKES, K. & SZALAY, F. (2004). Rising plasma nociceptin level during development of HCC: a case report. *World J Gastroenterol*, **10,** 152-4.

JENCK, F., WICHMANN, J., DAUTZENBERG, F.M., MOREAU, J.L., OUAGAZZAL, A.M., MARTIN, J.R., LUNDSTROM, K., CESURA, A.M., POLI, S.M., ROEVER, S., KOLCZEWSKI, S., ADAM, G. & KILPATRICK, G. (2000). A synthetic agonist at the orphanin FQ/nociceptin receptor ORL1: anxiolytic profile in the rat. *Proc Natl Acad Sci U S A*, **97,** 4938-43.

JOHNSON, E.E. & LAMBERT, D.G. (2002). Characterisation of the nociceptin receptor in dog brain membranes. *Br J Pharmacol*, **135,** 257P.

KATADA, T. & UI, M. (1981). Islet-activating protein. A modifier of receptor-mediated regulation of rat islet adenylate cyclase. *J Biol Chem*, **256,** 8310-7.

KAWAMOTO, H., OZAKI, S., ITOH, Y., MIYAJI, M., ARAI, S., NAKASHIMA, H., KATO, T., OHTA, H. & IWASAWA, Y. (1999). Discovery of the first potent and selective small molecule opioid receptor-like (ORL1) antagonist: 1-[(3R,4R)-1-cyclooctylmethyl-3- hydroxymethyl-4-piperidyl]-3-ethyl-1, 3-dihydro-2H-benzimidazol-2-one (J-113397). *J Med Chem*, **42,** 5061-3.

KEEN, M. (1997). Radioligand-binding methods for membrane preparations and intact cells. *Methods Mol Biol*, **83,** 1-24.

KENAKIN, T. (2002a). Drug efficacy at G protein-coupled receptors. *Annu Rev Pharmacol Toxicol*, **42,** 349-79.

KENAKIN, T. (2002b). Efficacy at G-protein-coupled receptors. *Nat Rev Drug Discov*, **1,** 103-10.

KENAKIN, T. (1997). *Pharmacologic Analysis of Drug-Receptor Interaction*. New York: Lippincott-Raven.

KITAYAMA, M., BARNES, T.A., CARRA, G., MCDONALD, J., CALO, G., GUERRINI, R., ROWBOTHAM, D.J., SMITH, G. & LAMBERT, D.G. (2003). Pharmacological profile of the cyclic nociceptin/orphanin FQ analogues c[Cys(10,14)]N/OFQ(1-

14)NH(2) and c[Nphe(1),Cys(10,14)]N/OFQ(1-14)NH(2). *Naunyn Schmiedebergs Arch Pharmacol.*

KO, M.H., KIM, Y.H., WOO, R.S. & KIM, K.W. (2002). Quantitative analysis of nociceptin in blood of patients with acute and chronic pain. *Neuroreport*, **13,** 1631-3.

KUMAR, N., SMART, D., MASON, S., MCKNIGHT, A.T., ROWBOTHAM, D.J. & LAMBERT, D.G. (1999). Neither nociceptin nor its receptor are present in human synovial fluid or tissue. *Br J Anaesth*, **83,** 470-1.

KUNAPULI, P., ONORATO, J.J., HOSEY, M.M. & BENOVIC, J.L. (1994). Expression, purification, and characterization of the G protein-coupled receptor kinase GRK5. *J Biol Chem*, **269,** 1099-105.

LACHOWICZ, J.E., SHEN, Y., MONSMA, F.J., JR. & SIBLEY, D.R. (1995). Molecular cloning of a novel G protein-coupled receptor related to the opiate receptor family. *J Neurochem*, **64,** 34-40.

LAW, P.Y., ERICKSON, L.J., EL-KOUHEN, R., DICKER, L., SOLBERG, J., WANG, W., MILLER, E., BURD, A.L. & LOH, H.H. (2000a). Receptor density and recycling affect the rate of agonist-induced desensitization of mu-opioid receptor. *Mol Pharmacol*, **58,** 388-98.

LAW, P.Y., KOUHEN, O.M., SOLBERG, J., WANG, W., ERICKSON, L.J. & LOH, H.H. (2000b). Deltorphin II-induced rapid desensitization of delta-opioid receptor requires both phosphorylation and internalization of the receptor. *J Biol Chem*, **275,** 32057-65.

LAZARENO, S. (1997). Measurement of agonist-stimulated [35S]GTP gamma S binding to cell membranes. *Methods Mol Biol*, **83,** 107-16.

LAZARENO, S. & BIRDSALL, N.J. (1993). Estimation of competitive antagonist affinity from functional inhibition curves using the Gaddum, Schild and Cheng-Prusoff equations. *Br J Pharmacol*, **109,** 1110-9.

LAZZERI, M., CALO, G., SPINELLI, M., GUERRINI, R., BENEFORTI, P., SANDRI, S., ZANOLLO, A., REGOLI, D. & TURINI, D. (2001). Urodynamic and clinical evidence of acute inhibitory effects of intravesical nociceptin/orphanin FQ on detrusor overactivity in humans: a pilot study. *J Urol*, **166,** 2237-40.

LAZZERI, M., CALO, G., SPINELLI, M., GUERRINI, R., SALVADORI, S., BENEFORTI, P., SANDRI, S., REGOLI, D. & TURINI, D. (2003). Urodynamic effects of intravesical nociceptin/orphanin FQ in neurogenic detrusor overactivity: a randomized, placebo-controlled, double-blind study. *Urology*, **61,** 946-950.

LEFKOWITZ, R.J. (1996). G protein-coupled receptors and receptor kinases: from molecular biology to potential therapeutic applications. *Nat Biotechnol*, **14,** 283-6.

LIVAK, K.J. & SCHMITTGEN, T.D. (2001). Analysis of relative gene expression data using real-time quantitative PCR and the 2(-Delta Delta C(T)) Method. *Methods*, **25,** 402-8.

LOWRY, O.H., ROSEBROUGH, N.J., LEWIS FARR, A. & RANDALL, R.J. (1951). Protein measurement with the Folin phenol reagent. *J Biol Chem*, **193,** 265-275.

MA, L., CHENG, Z.J., FAN, G.H., CAI, Y.C., JIANG, L.Z. & PEI, G. (1997). Functional expression, activation and desensitization of opioid receptor-like receptor ORL1 in neuroblastoma x glioma NG108-15 hybrid cells. *FEBS Lett*, **403,** 91-4.

MANDYAM, C.D., THAKKER, D.R., CHRISTENSEN, J.L. & STANDIFER, K.M. (2002). Orphanin FQ/nociceptin-mediated desensitization of opioid receptor-like 1 receptor and mu opioid receptors involves protein kinase C: a molecular mechanism for heterologous cross-talk. *J Pharmacol Exp Ther*, **302,** 502-9.

MARTI, M., STOCCHI, S., PAGANINI, F., MELA, F., DE RISI, C., CALO, G., GUERRINI, R., BARNES, T.A., LAMBERT, D.G., BEANI, L., BIANCHI, C. & MORARI, M. (2003). Pharmacological profiles of presynaptic nociceptin/orphanin FQ receptors modulating 5-hydroxytryptamine and noradrenaline release in the rat neocortex. *Br J Pharmacol*, **138,** 91-8.

MASON, S.L., HO, M., NICHOLSON, J. & MCKNIGHT, A.T. (2001). In vitro characterization of Ac-RYYRWK-NH(2), Ac-RYYRIK-NH(2) and [Phe1Psi(CH(2)-NH)Gly2] nociceptin(1-13)NH(2) at rat native and recombinant ORL(1) receptors. *Neuropeptides*, **35,** 244-56.

MCDONALD, J., BARNES, T.A., CALO, G., GUERRINI, R., ROWBOTHAM, D.J. & LAMBERT, D.G. (2002). Effects of [(pF)Phe(4)]nociceptin/orphanin FQ-(1-13)NH(2) on GTPgamma35S binding and cAMP formation in Chinese hamster ovary cells expressing the human nociceptin/orphanin FQ receptor. *Eur J Pharmacol*, **443,** 7-12.

MCDONALD, J., BARNES, T.A., OKAWA, H., WILLIAMS, J., CALO, G., ROWBOTHAM, D.J. & LAMBERT, D.G. (2003a). Partial agonist behaviour depends upon the level of nociceptin/orphanin FQ receptor expression: studies using the ecdysone-inducible mammalian expression system. *Br J Pharmacol*, **140,** 61-70.

MCDONALD, J., CALO, G., GUERRINI, R. & LAMBERT, D.G. (2003b). UFP-101, a high affinity antagonist for the nociceptin/orphanin FQ receptor: radioligand and GTPgamma(35)S binding studies. *Naunyn Schmiedebergs Arch Pharmacol*, **367,** 183-7.

MEIS, S. & PAPE, H.C. (1998). Postsynaptic mechanisms underlying responsiveness of amygdaloid neurons to nociceptin/orphanin FQ. *J Neurosci*, **18,** 8133-44.

MELZACK, R. & WALL, P.D. (1965). Pain mechanisms: a new theory. *Science*, **150,** 971-9.

MENZIES, J.R., GLEN, T., DAVIES, M.R., PATERSON, S.J. & CORBETT, A.D. (1999). In vitro agonist effects of nociceptin and [Phe(1)psi(CH(2)-NH)Gly(2)]nociceptin(1-13)NH(2) in the mouse and rat colon and the mouse vas deferens. *Eur J Pharmacol*, **385,** 217-23.

MERSKEY, H. (1994). Logic, truth and language in concepts of pain. *Qual Life Res*, **3 Suppl 1,** S69-76.

MEUNIER, J.C. (1997). Nociceptin/orphanin FQ and the opioid receptor-like ORL1 receptor. *Eur J Pharmacol*, **340,** 1-15.

MEUNIER, J.C., MOLLEREAU, C., TOLL, L., SUAUDEAU, C., MOISAND, C., ALVINERIE, P., BUTOUR, J.L., GUILLEMOT, J.C., FERRARA, P., MONSARRAT, B. & AL., E. (1995). Isolation and structure of the endogenous agonist of opioid receptor-like ORL1 receptor. *Nature*, **377,** 532-5.

MEUNIER, J.C., MOULEDOUS, L. & TOPHAM, C.M. (2000). The nociceptin (ORL1) receptor: molecular cloning and functional architecture. *Peptides*, **21,** 893-900.

MOGIL, J.S. & PASTERNAK, G.W. (2001). The molecular and behavioral pharmacology of the orphanin FQ/nociceptin peptide and receptor family. *Pharmacol Rev*, **53,** 381-415.

MOLLEREAU, C. & MOULEDOUS, L. (2000). Tissue distribution of the opioid receptor-like (ORL1) receptor. *Peptides*, **21,** 907-17.

MOLLEREAU, C., PARMENTIER, M., MAILLEUX, P., BUTOUR, J.L., MOISAND, C., CHALON, P., CAPUT, D., VASSART, G. & MEUNIER, J.C. (1994). ORL1, a novel member of the opioid receptor family. Cloning, functional expression and localization. *FEBS Lett*, **341,** 33-8.

MONTIEL, J.L., CORNILLE, F., ROQUES, B.P. & NOBLE, F. (1997). Nociceptin/orphanin FQ metabolism: role of aminopeptidase and endopeptidase 24.15. *J Neurochem*, **68,** 354-61.

MONTMINY, M. (1997). Transcriptional regulation by cyclic AMP. *Annu Rev Biochem*, **66,** 807-22.

MORIKAWA, H., FUKUDA, K., MIMA, H., SHODA, T., KATO, S. & MORI, K. (1998). Desensitization and resensitization of delta-opioid receptor-mediated Ca2+ channel inhibition in NG108-15 cells. *Br J Pharmacol*, **123,** 1111-8.

MORK, H., HOMMEL, K., UDDMAN, R., EDVINSSON, L. & JENSEN, R. (2002). Does nociceptin play a role in pain disorders in man? *Peptides*, **23,** 1581-7.

NAITO, T., ITOH, H. & TAKEYAMA, M. (2003). Application of an enzyme immunoassay for nociceptin(orphaninFQ)-like immunoreactive substances to determination of the human plasma levels. *J Health Sci.* **49(5).** 353-358.

NAKANISHI, K. (1992). Past and present studies with ponasterones, the first insect molting hormones from plants. *Steroids*, **57,** 649-57.

NESTLER, E.J. (2004). Molecular mechanisms of drug addiction. *Neuropharmacology*, **47 Suppl 1,** 24-32.

NISHI, M., TAKESHIMA, H., MORI, M., NAKAGAWARA, K. & TAKEUCHI, T. (1994). Structure and chromosomal mapping of genes for the mouse kappa-opioid receptor and an opioid receptor homologue (MOR-C). *Biochem Biophys Res Commun*, **205,** 1353-7.

NO, D., YAO, T.P. & EVANS, R.M. (1996). Ecdysone-inducible gene expression in mammalian cells and transgenic mice. *Proc Natl Acad Sci U S A*, **93,** 3346-51.

NOBLE, F. & ROQUES, B.P. (1997). Association of aminopeptidase N and endopeptidase 24.15 inhibitors potentiate behavioral effects mediated by nociceptin/orphanin FQ in mice. *FEBS Lett*, **401,** 227-9.

OKADA, K., SUJAKU, T., CHUMAN, Y., NAKASHIMA, R., NOSE, T., COSTA, T., YAMADA, Y., YOKOYAMA, M., NAGAHISA, A. & SHIMOHIGASHI, Y. (2000). Highly potent nociceptin analog containing the Arg-Lys triple repeat. *Biochem Biophys Res Commun*, **278,** 493-8.

OKAWA, H., HIRST, R.A., SMART, D., MCKNIGHT, A.T. & LAMBERT, D.G. (1998). Rat central ORL-1 receptor uncouples from adenylyl cyclase during membrane preparation. *Neurosci Lett*, **246,** 49-52.

OKAWA, H., NICOL, B., BIGONI, R., HIRST, R.A., CALO, G., GUERRINI, R., ROWBOTHAM, D.J., SMART, D., MCKNIGHT, A.T. & LAMBERT, D.G. (1999). Comparison of the effects of [Phe^{1}psi(CH_2-NH)Gly^2]nociceptin(1-13)NH_2 in rat brain, rat vas deferens and CHO cells expressing recombinant human nociceptin receptors. *Br J Pharmacol*, **127,** 123-30.

OKUDA-ASHITAKA, E. & ITO, S. (2000). Nocistatin: a novel neuropeptide encoded by the gene for the nociceptin/orphanin FQ precursor. *Peptides*, **21,** 1101-9.

OLIANAS, M.C., MAULLU, C., INGIANNI, A. & ONALI, P. (1999). [Phe1phi(CH2-NH)Gly2]nociceptin-(1-13)-NH2 acts as a partial agonist at ORL1 receptor endogenously expressed in mouse N1E-115 neuroblastoma cells. *Neuroreport*, **10,** 1127-31.

OSINSKI, M.A., PAMPUSCH, M.S., MURTAUGH, M.P. & BROWN, D.R. (1999). Cloning, expression and functional role of a nociceptin/orphanin FQ receptor in the porcine gastrointestinal tract. *Eur J Pharmacol*, **365,** 281-9.

OZAKI, S., KAWAMOTO, H., ITOH, Y., MIYAJI, M., IWASAWA, Y. & OHTA, H. (2000). A potent and highly selective nonpeptidyl nociceptin/orphanin FQ receptor (ORL1) antagonist: J-113397. *Eur J Pharmacol*, **387,** R17-8.

PAN, Y.X., BOLAN, E. & PASTERNAK, G.W. (2002). Dimerization of morphine and orphanin FQ/nociceptin receptors: generation of a novel opioid receptor subtype. *Biochem Biophys Res Commun*, **297,** 659-63.

PAN, Y.X., CHENG, J., XU, J., ROSSI, G., JACOBSON, E., RYAN-MORO, J., BROOKS, A.I., DEAN, G.E., STANDIFER, K.M. & PASTERNAK, G.W. (1995). Cloning and functional characterization through antisense mapping of a kappa 3-related opioid receptor. *Mol Pharmacol*, **47,** 1180-8.

PAN, Z., HIRAKAWA, N. & FIELDS, H.L. (2000). A cellular mechanism for the bidirectional pain-modulating actions of orphanin FQ/nociceptin. *Neuron*, **26,** 515-22.

PARRUTI, G., AMBROSINI, G., SALLESE, M. & DE BLASI, A. (1993). Molecular cloning, functional expression and mRNA analysis of human beta-adrenergic receptor kinase 2. *Biochem Biophys Res Commun*, **190,** 475-81.

PATERLINI, G., PORTOGHESE, P.S. & FERGUSON, D.M. (1997). Molecular simulation of dynorphin A-(1-10) binding to extracellular loop 2 of the kappa-opioid receptor. A model for receptor activation. *J Med Chem*, **40,** 3254-62.

PATNEAU, D.K. & MAYER, M.L. (1990). Structure-activity relationships for amino acid transmitter candidates acting at N-methyl-D-aspartate and quisqualate receptors. *J Neurosci*, **10,** 2385-99.

PEI, G., LING, K., PU, L., CUNNINGHAM, M.D. & MA, L. (1997). Nociceptin/orphanin FQ stimulates extracellular acidification and desensitization of the response involves protein kinase C. *FEBS Lett*, **412,** 253-6.

PFAFFL, M.W. (2001). A new mathematical model for relative quantification in real-time RT-PCR. *Nucleic Acids Res*, **29,** e45.

PFAFFL, M.W., HORGAN, G.W. & DEMPFLE, L. (2002). Relative expression software tool (REST) for group-wise comparison and statistical analysis of relative expression results in real-time PCR. *Nucleic Acids Res*, **30,** e36.

PIERCE, K.L., PREMONT, R.T. & LEFKOWITZ, R.J. (2002). Seven-transmembrane receptors. *Nat Rev Mol Cell Biol*, **3,** 639-50.

PITCHER, J.A., FREEDMAN, N.J. & LEFKOWITZ, R.J. (1998). G protein-coupled receptor kinases. *Annu Rev Biochem*, **67,** 653-92.

PREMONT, R.T., KOCH, W.J., INGLESE, J. & LEFKOWITZ, R.J. (1994). Identification, purification, and characterization of GRK5, a member of the family of G protein-coupled receptor kinases. *J Biol Chem*, **269,** 6832-41.

PREMONT, R.T., MACRAE, A.D., STOFFEL, R.H., CHUNG, N., PITCHER, J.A., AMBROSE, C., INGLESE, J., MACDONALD, M.E. & LEFKOWITZ, R.J. (1996). Characterization of the G protein-coupled receptor kinase GRK4. Identification of four splice variants. *J Biol Chem*, **271,** 6403-10.

PRICE, D.D. (1999). *Psychological mechanisms of pain and analgesia.* IASP Press: ISBN 0-931092-29-9.

PU, L., BAO, G.B., MA, L. & PEI, G. (1999). Acute desensitization of nociceptin/orphanin FQ inhibition of voltage- gated calcium channels in freshly dissociated hippocampal neurons. *Eur J Neurosci*, **11,** 3610-6.

RAHMAN, Z., GOLD, S.J., POTENZA, M.N., COWAN, C.W., NI, Y.G., HE, W., WENSEL, T.G. & NESTLER, E.J. (1999). Cloning and characterization of RGS9-2: a striatal-enriched alternatively spliced product of the RGS9 gene. *J Neurosci*, **19,** 2016-26.

RAHMAN, Z., SCHWARZ, J., GOLD, S.J., ZACHARIOU, V., WEIN, M.N., CHOI, K.H., KOVOOR, A., CHEN, C.K., DILEONE, R.J., SCHWARZ, S.C., SELLEY, D.E., SIM-SELLEY, L.J., BARROT, M., LUEDTKE, R.R., SELF, D., NEVE, R.L., LESTER, H.A.,

SIMON, M.I. & NESTLER, E.J. (2003). RGS9 modulates dopamine signaling in the basal ganglia. *Neuron*, **38,** 941-52.

RANG, H.P., DALE, M.M. & RITTER, J.M. (1995). *Pharmacology*. Edinburgh: Churchill Livingstone.

REINSCHEID, R.K., ARDATI, A., MONSMA, F.J., JR. & CIVELLI, O. (1996). Structure-activity relationship studies on the novel neuropeptide orphanin FQ. *J Biol Chem*, **271,** 14163-8.

REINSCHEID, R.K., HIGELIN, J., HENNINGSEN, R.A., MONSMA, F.J., JR. & CIVELLI, O. (1998). Structures that delineate orphanin FQ and dynorphin A pharmacological selectivities. *J Biol Chem*, **273,** 1490-5.

REINSCHEID, R.K., NOTHACKER, H.P., BOURSON, A., ARDATI, A., HENNINGSEN, R.A., BUNZOW, J.R., GRANDY, D.K., LANGEN, H., MONSMA, F.J., JR. & CIVELLI, O. (1995). Orphanin FQ: a neuropeptide that activates an opioidlike G protein-coupled receptor. *Science*, **270,** 792-4.

REYNOLDS, D.V. (1969). Surgery in the rat during electrical analgesia induced by focal brain stimulation. *Science.*, **164,** 444-5.

RIEDEL, W. & NEECK, G. (2001). Nociception, pain, and antinociception: current concepts. *Z Rheumatol*, **60,** 404-15.

RIZZI, A., BIGONI, R., CALO, G., GUERRINI, R., SALVADORI, S. & REGOLI, D. (1999). [Nphe(1)]nociceptin-(1-13)-NH(2) antagonizes nociceptin effects in the mouse colon. *Eur J Pharmacol*, **385,** R3-5.

RIZZI, D., BIGONI, R., RIZZI, A., JENCK, F., WICHMANN, J., GUERRINI, R., REGOLI, D. & CALO, G. (2001). Effects of Ro 64-6198 in nociceptin/orphanin FQ-sensitive isolated tissues. *Naunyn Schmiedebergs Arch Pharmacol*, **363,** 551-5.

RIZZI, D., RIZZI, A., BIGONI, R., CAMARDA, V., MARZOLA, G., GUERRINI, R., DE RISI, C., REGOLI, D. & CALO, G. (2002). [Arg(14),Lys(15)]nociceptin, a highly potent agonist of the nociceptin/orphanin FQ receptor: in vitro and in vivo studies. *J Pharmacol Exp Ther*, **300,** 57-63.

ROZEN, S. & SKALETSKY, H. (2000). Primer3 on the WWW for general users and for biologist programmers. *Methods Mol Biol*, **132,** 365-86.

RUTLEDGE, R.G. & COTE, C. (2003). Mathematics of quantitative kinetic PCR and the application of standard curves. *Nucleic Acids Res*, **31,** e93.

SAIKI, R.K., BUGAWAN, T.L., HORN, G.T., MULLIS, K.B. & ERLICH, H.A. (1986). Analysis of enzymatically amplified beta-globin and HLA-DQ alpha DNA with allele-specific oligonucleotide probes. *Nature*, **324,** 163-6.

SALVADORI, S., GUERRINI, R., CALO, G. & REGOLI, D. (1999). Structure-activity studies on nociceptin/orphanin FQ: from full agonist, to partial agonist, to pure antagonist. *Farmaco*, **54,** 810-25.

SANDIN, J., GEORGIEVA, J., SILBERRING, J. & TERENIUS, L. (1999). In vivo metabolism of nociceptin/orphanin FQ in rat hippocampus. *Neuroreport*, **10,** 71-6.

SHINKAI, H., ITO, T., IIDA, T., KITAO, Y., YAMADA, H. & UCHIDA, I. (2000). 4-Aminoquinolines: novel nociceptin antagonists with analgesic activity. *J Med Chem*, **43,** 4667-77.

SIMONDS, W.F. (1999). G protein regulation of adenylate cyclase. *Trends Pharmacol Sci*, **20,** 66-73.

SMART, D. & LAMBERT, D.G. (1996). The stimulatory effects of opioids and their possible role in the development of tolerance. *Trends Pharmacol Sci*, **17,** 264-9.

SMITH, P.A. & MORAN, T.D. (2001). The nociceptin receptor as a potential target in drug design. *Drug News Perspect*, **14,** 335-45.

SPAMPINATO, S., DI TORO, R., ALESSANDRI, M. & MURARI, G. (2002). Agonist-induced internalization and desensitization of the human nociceptin receptor expressed in CHO cells. *Cell Mol Life Sci*, **59,** 2172-83.

SPAMPINATO, S., DI TORO, R. & QASEM, A.R. (2001). Nociceptin-induced internalization of the ORL1 receptor in human neuroblastoma cells. *Neuroreport*, **12,** 3159-63.

SUTHERLAND, E.W. & RALL, T.W. (1958). Fractionation and characterization of a cyclic adenine ribonucleotide formed by tissue particles. *J Biol Chem*, **232,** 1077-91.

SZALAY, F., HANTOS, M.B., HORVATH, A., LAKATOS, P.L., FOLHOFFER, A., DUNKEL, K., HEGEDUS, D. & TEKES, K. (2004). Increased nociceptin/orphanin FQ plasma levels in hepatocellular carcinoma. *World J Gastroenterol*, **10,** 42-5.

TERENIUS, L., SANDIN, J. & SAKURADA, T. (2000). Nociceptin/orphanin FQ metabolism and bioactive metabolites. *Peptides*, **21,** 919-22.

THEILADE, J., HAUNSO, S. & SHEIKH, S.P. (2001). G protein-coupled receptor kinase 2--a feedback regulator of Gq pathway signalling. *Curr Drug Targets Immune Endocr Metabol Disord*, **1,** 139-51.

THELLIN, O., ZORZI, W., LAKAYE, B., DE BORMAN, B., COUMANS, B., HENNEN, G., GRISAR, T., IGOUT, A. & HEINEN, E. (1999). Housekeeping genes as internal standards: use and limits. *J Biotechnol*, **75,** 291-5.

TIAN, J.H., XU, W., FANG, Y., MOGIL, J.S., GRISEL, J.E., GRANDY, D.K. & HAN, J.S. (1997). Bidirectional modulatory effect of orphanin FQ on morphine-induced analgesia: antagonism in brain and potentiation in spinal cord of the rat. *Br J Pharmacol*, **120,** 676-80.

TOPHAM, C.M., MOULEDOUS, L., PODA, G., MAIGRET, B. & MEUNIER, J.C. (1998). Molecular modelling of the ORL1 receptor and its complex with nociceptin. *Protein Eng*, **11,** 1163-79.

TORTORA, G.J. & ANAGNOSTAKOS, N.P. (1990). *Principles of Anatomy and Physiology.* London: Harper Collins.

TRICARICO, C., PINZANI, P., BIANCHI, S., PAGLIERANI, M., DISTANTE, V., PAZZAGLI, M., BUSTIN, S.A. & ORLANDO, C. (2002). Quantitative real-time reverse transcription polymerase chain reaction: normalization to rRNA or single housekeeping genes is inappropriate for human tissue biopsies. *Anal Biochem*, **309,** 293-300.

VAN CRAENENBROECK, K., VANHOENACKER, P., LEYSEN, J.E. & HAEGEMAN, G. (2001). Evaluation of the tetracycline- and ecdysone-inducible systems for expression of neurotransmitter receptors in mammalian cells. *Eur J Neurosci*, **14,** 968-76.

WANG, J.B., JOHNSON, P.S., IMAI, Y., PERSICO, A.M., OZENBERGER, B.A., EPPLER, C.M. & UHL, G.R. (1994). cDNA cloning of an orphan opiate receptor gene family member and its splice variant. *FEBS Lett*, **348,** 75-9.

WATKINS, J.C., DAVIES, J., EVANS, R.H., FRANCIS, A.A. & JONES, A.W. (1981). Pharmacology of receptors for excitatory amino acids. *Adv Biochem Psychopharmacol*, **27,** 263-73.

WICK, M.J., MINNERATH, S.R., LIN, X., ELDE, R., LAW, P.Y. & LOH, H.H. (1994). Isolation of a novel cDNA encoding a putative membrane receptor with high homology to the cloned mu, delta, and kappa opioid receptors. *Brain Res Mol Brain Res*, **27,** 37-44.

WIELAND, T. & CHEN, C.K. (1999). Regulators of G-protein signalling: a novel protein family involved in timely deactivation and desensitization of signalling via heterotrimeric G proteins. *Naunyn Schmiedebergs Arch Pharmacol*, **360,** 14-26.

XU, X.J., HAO, J.X. & WIESENFELD-HALLIN, Z. (1996). Nociceptin or antinociceptin: potent spinal antinociceptive effect of orphanin FQ/nociceptin in the rat. *Neuroreport*, **7,** 2092-4.

YAMADA, H., NAKAMOTO, H., SUZUKI, Y., ITO, T. & AISAKA, K. (2002). Pharmacological profiles of a novel opioid receptor-like1 (ORL1) receptor antagonist, JTC-801. *Br J Pharmacol*, **135,** 323-32.

YU, J., CHAIT, B.T., TOLL, L. & KREEK, M.J. (1996). Nociceptin in vitro biotransformation in human blood. *Peptides*, **17,** 873-6.

YUNG, L.Y., JOSHI, S.A., CHAN, R.Y., CHAN, J.S., PEI, G. & WONG, Y.H. (1999). GalphaL1 (Galpha14) couples the opioid receptor-like1 receptor to stimulation of phospholipase C. *J Pharmacol Exp Ther*, **288,** 232-8.

ZACHARIOU, V., GEORGESCU, D., SANCHEZ, N., RAHMAN, Z., DILEONE, R., BERTON, O., NEVE, R.L., SIM-SELLEY, L.J., SELLEY, D.E., GOLD, S.J. & NESTLER, E.J. (2003). Essential role for RGS9 in opiate action. *Proc Natl Acad Sci U S A*, **100,** 13656-61.

ZEILHOFER, H.U. & CALO, G. (2003). Nociceptin/orphanin FQ and its receptor--potential targets for pain therapy? *J Pharmacol Exp Ther*, **306,** 423-9.

ZHANG, C., MILLER, W., VALENZANO, K.J. & KYLE, D.J. (2002). Novel, potent ORL-1 receptor agonist peptides containing alpha-Helix-promoting conformational constraints. *J Med Chem*, **45,** 5280-6.

ZHAO, J., ZHANG, Y., XIN, S.M., MA, L. & PEI, G. (1998). Attenuation of nociceptin/orphanin FQ-induced signaling by N-methyl-D- aspartate in neuronal cells. *Neuroreport*, **9,** 631-6.

ZUKER, M. (2003). Mfold web server for nucleic acid folding and hybridization prediction. *Nucleic Acids Res*, **31,** 3406-15.